Meristem regulation in the early divergent land plant *Marchantia polymorpha*

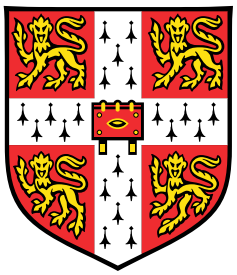

Marius Rebmann

Department of Plant Sciences
University of Cambridge

This dissertation is submitted for the degree of
Doctor of Philosophy

King's College December 2021

Declaration

This thesis is the result of my own work and includes nothing which is the outcome of work done in collaboration except as declared in the Preface and specified in the text. I further state that no substantial part of my thesis has already been submitted, or, is being concurrently submitted for any such degree, diploma or other qualification at the University of Cambridge or any other University or similar institution except as declared in the Preface and specified in the text. It does not exceed the prescribed word limit for the relevant Degree Committee.

Marius Rebmann
December 2021

Abstract

Name: Marius Rebmann
Thesis title: Meristem regulation in the early divergent land plant *Marchantia polymorpha*

Meristems are key features of land plant development, enabling post-embryonic organogenesis through precise spatial patterning of cell division and differentiation. Extensive work on flowering plant meristems has revealed gene circuits driving meristem patterning, which are increasingly targeted to engineer crop development. However, genetic redundancy and morphological complexity present powerful obstacles to explore engineering of meristem regulation. *Marchantia polymorpha* is an early divergent land plant which has received re-surging interest as a model plant, following the publication of its genome which revealed extraordinarily low levels of genetic redundancy. Marchantia's genetic simplicity is mirrored by a simple body plan. Asexual propagules called gemma are a particularly attractive model to study meristem regulation owing to their small size, disc shaped morphology and open development. This permits facile live imaging of early development of whole plants at cellular resolution. Despite these benefits, our understanding of the Marchantia meristem remains rudimentary compared to other plant models.

This dissertation describes the use of single cell RNA-sequencing and novel marker lines to define the cell composition of the Marchantia meristem and the use of genetic and experimental perturbation to interrogate the gene networks and phytohormone patterning systems governing meristem maintenance and initiation.

I describe the use of a proximal promoter library comprising a near complete collection of promoter elements for all Marchantia transcription factors, to identify novel meristem markers. Fluorescent reporters for approximately 20% of all Marchantia transcription factors were screened in gemma, identifying novel cell type markers.

I present the analysis of a single cell RNA-sequencing dataset comprising approximately 7'000 cells from developing gemmalings. I characterise Marchantia cell types based on their transcriptomic profiles and identify corresponding cell identities *in vivo* using marker genes. The data captured broad developmental gradients of proximal-distal and dorsal-ventral

patterning as well as resolving specific cell lineages such as rhizoid cells at unprecedented resolution.

I define central stem cells as tissue organisers of the Marchantia meristem. I show that central stem cells are auxin sources and develop novel markers to study auxin response in gemma. I identify a ERF/AP2 transcription factor Mp *ERF20* as a positive regulator of central stem cell fate.

I interrogate the regulation of the division zone by cytokinins and identify Mp *CYCD1* as a key regulator of cell division rates in the Marchantia meristem. I show that Mp *CYCD1* overexpression can be leveraged as a tool to induce ectopic cell divisions.

I characterise meristem regeneration in Marchantia explants using marker lines and precise surgical manipulation. I observe the activation of proliferation markers and establish auxin transport reorganisation as a critical driver of meristem regeneration. Using this data I propose a model for meristem maintenance and regeneration in Marchantia which will form an important framework for future attempts to engineer growth in this simple morphogenic system.

Acknowledgements

My PhD experience has been shaped by many people throughout my four years in Cambridge, whom I would like to thank for their support, help and contributions.

To my supervisor Prof. Jim Haseloff for his support and guidance throughout this project and for introducing me to the potential of plant growth engineering and the unique advantages of Marchantia as a model system.

To the Biotechnology and Biological Sciences Research Council for funding my research and keeping a roof over my head.

To Susanna Sauret-Güeto for all her support in helping me define my project and her tireless efforts to maintain organisation in the lab.

To Alan Marron for many exciting discussions on the nature of growth regulation in Marchantia, advice on laser dissection in Marchantia and many entertaining lab meetings.

To Eftychios Frangedakis for advice on molecular biology, careers and life.

To Alex Ting, Marta Tomaselli and Owen Male for making the start of my PhD such an enjoyable time.

To Julian Hibberd and Alexander Jones for excellent feedback, advice and encouragement throughout the project.

To all other past and present members of the Haseloff lab for always providing a great source for inspiring conversations: Fernando Guzman-Chavez, Lukas Muller, Natasha Elina, Emma Talbot, Harriet Kempson, Jenna Rever, Jay Devlin, Linda Silvestri, Jenny Molloy, Antonio Ruiz, Gemma Swan, Camillo Moschner, Mihails Delmans, William Boxall, Ignacy Bonter, Owen Male, Kasey Markel, Nicolas Larus-Stone, Liat Adler, Marc Bal, Massimo Guazzini, Alicja Szalapak, Emanuele Orsini and Stephanie Norwood.

To Satoshi Naramoto for sharing Marchantia resources and helpful discussions on meristem regulation in Marchantia.

To Alistair Blackmoore for giving me a truly enjoyable glimpse of the corporate world and reassuring me that there is a world outside of academia.

To my parents for inspiring me to pursue my own path in life and always providing unconditional support in the process.

Finally, to my partner Rasa, thank you for your never ending love and support. You have helped me through many dark times and made the good times shine brightest.

Table of contents

List of figures

List of tables

Chapter 1

Introduction

1.1 Plant trait engineering

Plants are by far the most abundant life form on earth when measured by biomass, representing >80% of all living matter on earth [13]. Plants are essential for the global human food supply, either directly through human consumption, or indirectly through feedstock feeding. Approximately 100 plant species account for >90% of human calorie consumption [246], The four most abundant crops: rice, wheat, soy and maize alone may account for as much as 60% of human calorie consumption [217]. The domestication of plants is consequently considered one of the most important developments in human history [59]. Humans have shaped plant growth to boost yields, improve nutrition and adapt plants to diverse environments through thousands of years of selection [94]. The modern economic importance of different crops is in large part explained by when humans first started domesticated them [217]. In the face of a rapidly changing climate, crops will need to be modified quickly to adapt to new environments in order to sustain or even expand agronomic productivity [158]. While modern breeding techniques have accelerated the development of new traits, breeding alone may not be able to deliver changes rapidly enough. The development of CRISPR/Cas9 gene editing [102, 164] and its successful adoption in crop plants [287, 311, 163] has opened up the possibility of directly editing genes to boost crop yields and modify other traits. Indeed, recent work has demonstrated how CRISPR/Cas9 can be used to engineer trait variation in tomato fruit size and plant architecture, by modifying the regulatory regions of known gene modules [262]. This approach was rapidly expanded to other species such as maize [194]. It can also be used to overcome negative epistatic interactions [300], rapidly improve species for new environments such as urban agriculture [181] and even catalyse *de novo* domestication of new crops [184]. While these results demonstrated that rational plant trait engineering is feasible and likely will play a major role for the future of agriculture, these

modification build on detailed characterisation of growth regulation in model plant species to select appropriate targets. So far, studies have focused on small modifications to a limited number of key regulatory genes. However, there are likely many more pathways that could be exploited, but currently lack sufficient characterisation. The addition of new interactions or completely orthogonal regulation could expand the possibilities of plant growth engineering even further, but such approaches remain very challenging even in well established model systems, due to their morphological and genetic complexity. A minimally complex plant model system could fulfill this niche, providing a simple platform to explore more extensive re-coding of growth regulation.

1.2 The synthetic biology paradigm

Efforts to genetically engineer organisms have been catalysed by the increasing abundance of sequencing information for diverse organisms and advanced molecular biology and gene editing tools available today. However, genetic engineering remains a notoriously unpredictable, slow and iterative process, owing to the complexity of living systems, lack of orthogonality and frequent unintended emergent behaviours. The field of synthetic biology aims to improve our ability to predictably engineer living systems by applying principles from classical engineering to the life sciences. While the historical root of the field has been in the predictable engineering of dynamic gene circuits such as the repressilator [73], the field has diversified into areas like metabolic engineering, synthetic genomics and more recently synthetic developmental biology [283, 68] or synthetic morphogenesis [318]. The unifying theme of synthetic biology is an emphasis on concepts of standardisation, modularity, and abstraction, the use of mathematical modelling and computer aided design and the utilisation of simple systems to enable predictable behaviour in the face of biological complexity. The complexity of multicellular eukaryotic systems has so far precluded the widespread application of these methods outside narrow projects. However, the abundance of plants, their autotrophic growth and ability to sequester carbon, make plants increasingly attractive targets for synthetic biology applications. The development of simpler plant model systems with rapid experimental cycles will be critical to promote the development of plant synthetic biology and *Marchantia polymorpha* has been suggested as an ideal candidate to fill this niche [279].

1.3 Marchantia as a minimal plant model

Marchantia polymorpha is a thalloid liverwort which is a prostrate and grows as a branching sheet of tissue [290]. Marchantia has a long and rich history as a model plant in plant sciences, owing to its rapid growth in laboratory conditions and simple body plan [28]. Liverworts, hornworts and mosses form the monophyletic bryophyte clade which comprise the earliest diverging land plant lineages, diverging from all other land plants approximately 500 million year ago [120, 307]. Their ancestral position in the phylogeny of land plants makes plants from these lineages powerful models for evolutionary developmental biology. Marchantia in particular has attracted increasing interest as a model plant following the publication of its genome [29]. Marchantia has a very streamlined genome displaying near minimal genetic complexity for many important regulatory pathways such as auxin signaling. This is in stark contrast to the high levels of genetic redundancy observed in angiosperm models [29]. The number of transcription factors in Marchantia is exceptionally low compared to other plant species and more similar to numbers found in algae [343]. This is not the result of widespread loss of transcription factor families, although some families are absent from Marchantia [358], rather it is the result of many families containing only a single gene in Marchantia. This makes Marchantia an excellent model system to study transcription factor function, as the function of individual gene is unlikely to be obscured by the presence of partially redundant orthologs [29].

In addition to the streamlined genome, fast growth and simple morphology, Marchantia has many practical advantages which make it ideally suited as a chassis for plant synthetic biology. Highly efficient nuclear transformation methods have been reported for cultured cells [225], sporelings [151, 327], gemma [328] and thallus [179]. Spore based methods in particular, enable high throughput transformation in multi-well plates [279] and may be suitable for fully automated transformation in the future. Efficient plastid transformation has also been reported [41, 279]. Highly efficient type-IIs DNA assembly methods have been developed for Marchantia to facilitate high throughput DNA assembly [245, 279]. Large collections of characterised DNA parts are available for these DNA assembly frameworks, permitting rapid assembly of complex DNA constructs. CRISPR/Cas9 mediated gene editing has been demonstrated in Marchantia [308] and subsequent improvements have enabled highly efficient gene editing [279] which benefits from the haploid nature of the Marchantia genome during most of the life cycle. Methods for the inducible expression of transgenes have also been characterised, including a heat shock inducible promoter [227], nuclear translocation via the dexamethasone inducible GR-domain [242, 227], an estrogen-inducible XVE chimeric transcription factor [87], the GAL4-VP16 transactivation system [169] and CRE-loxP mediated recombination [227].

The Marchantia life cycle contains a short sporophyte stage and a dominant gametophyte stage (Figure 1.1). This is in contrast to angiosperms, where the sporophyte forms the dominant stage of the life cycle. The gametophyte stage starts with spore germination (Figure 1.1). Germinating spores form multi cellular sporelings which develop into mature thallus tissue within three to four weeks. Thalli of female and male plants are indistinguishable at this stage. Mature thalli form gemma cups to facilitate asexual reproduction (Figure 1.1). Each cup is filled with disk shaped propagules called gemmae which are dormant while residing inside the cup [71]. Once transferred from the cup, gemma rapidly initiate tissue growth and form a full dorso-ventral patterned thallus within a week. New gemma cups form within two to three weeks of germination, completing the asexual reproductive cycle. Mature thalli transition to reproductive growth in response to far-red light . Male and female plants will initiate antheridiophore and archegoniophore development respectively when exposed to high levels of far red light [142]. Antheridiophores generate motile sperm cells which are naturally released by rain fall. Archegoniophores form egg cells, which develop into a diploid sporophyte when fertilised by sperm. The sporophyte undergoes mitotic divisions to form a tissue comprising hundreds of cells, before meiotic divisions generate thousands of new haploid spores, completing the sexual reproduction cycle (Figure 1.1).

The Marchantia gametophyte is comprised of multiple distinct cell types which emerge at different stages of thallus development (Figure 1.2). The first division of germinating spores is asymmetric (Figure 1.2 B), with the smaller cell differentiating into a rhizoid cell (Figure 1.2 C) [230]. The larger cell initiates rapid divisions which are initially apparently random, generating a small callus like tissue (Figure 1.2 D). Divisions become progressively restricted to an emerging meristem, which can be identified by a characteristic notch in the tissue (Figure 1.2 E). The centre of this prothallus meristem contains lenticular-shaped cells, with the centremost cell commonly labeled as the apical initial cell of the meristem (Figure 1.2 F). The prothallus initially grows as a two dimensional tissue mat and the two dimensional prothallus meristem is morphologically similar to the gemmae meristem at germination. The transition to mature thallus growth is marked by dorso-ventral thallus patterning. During gemma development, this is marked by a dorso-ventral split of the gemma meristem which can typically be observed by day two or three of gemma growth. While the upper meristem lobes will not continue to divide, the bottom lobes will continue to grow and generate air pore complexes on the new dorsal surface by day 4-5 [299], marking the onset of full dorso-ventral patterning. Air pore complexes are comprised of pore cells (Figure 1.2 L-O), which cannot close or open to but are thought to mediate gas exchange. The air chamber also contains roof and wall cells which form the structural components of the pore. At the pore floor, chlorophyll rich assimiliatory filaments and sub-epidermal cells

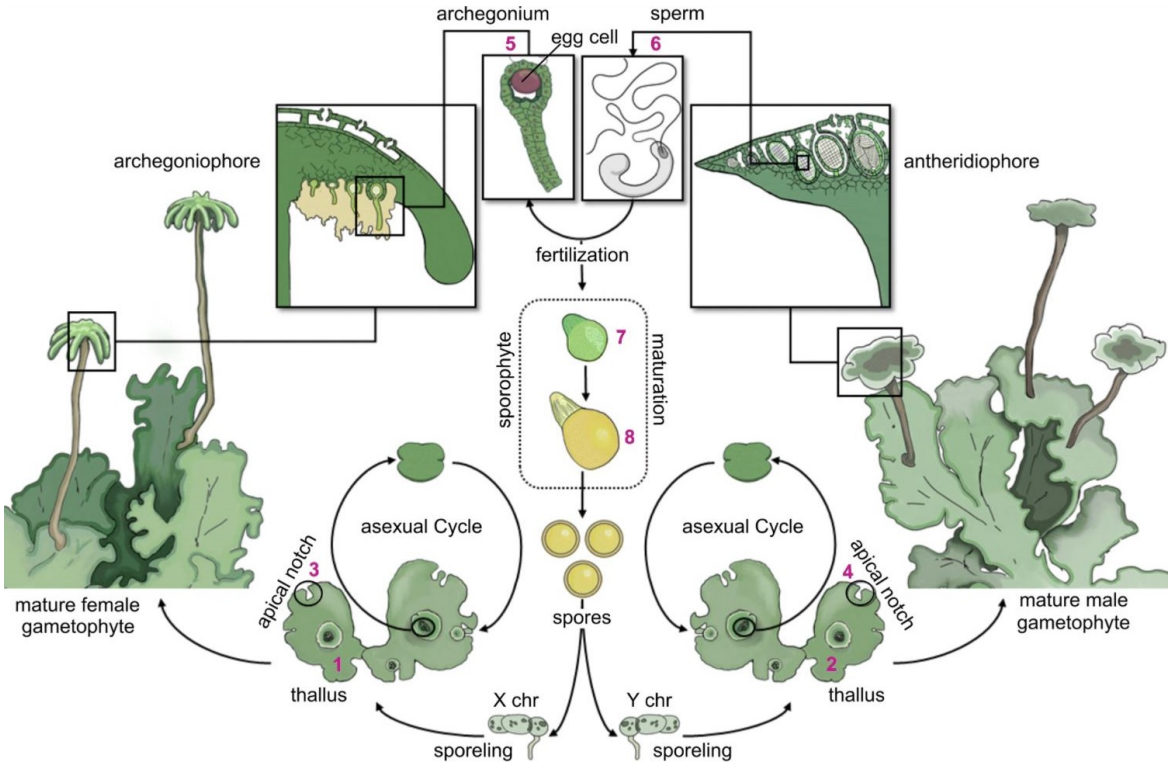

Fig. 1.1 **Marchantia life cycle** Adapted from [284]. During the asexual phase of the life cycle Marchantia grows as a flat, sheet-like thallus. Thallus growth can be initiated from spores as well as gemma which develop ectopically on mature thalli to facilitate asexual reproduction. Marchantia is dioecious and exposure to far red light triggers development of distinct male (antheridiophore) or female (archegoniophore) reproductive organs. Mobile sperm cells develop in the antheridiophore and can be released by water. Sperm cells can fertilise egg cells on archegoniophores triggering devlopment of a diploid sporophyte. The sporophyte generates thousands of new haploid spores thorugh meiosis completing the sexual reproduction cycle.

are thought to facilitate high rates of photosynthesis (Figure 1.2 O). The central portion of the thallus contains parenchyma cells which contain few chloroplasts and are thought to be primarily involved in nutrient storage [290]. On the ventral side of thalli, rhizoid cells and ventral scales form (Figure 1.2 O). Rhizoids are tip growing cells which facilitate water and nutrient exchange with the substrate, similar to root hair cells in angiosperms [165], Indeed, root hairs and rhizoids share common genetic regulators suggesting they may represent homologous cell types [249]. Ventral scales are thought to also facilitate water and nutrient exchange as well as protecting apical cells and bundles of rhizoids. Ventral scales share genetic regulators with lateral organ formation in angiosperms [224]. The mature thallus meristem is notch like and contains a U-shaped population of lenticular-shaped cells (Figure 1.2 H). The centre most cell is commonly labeled as the apical initial cell of the meristem (Figure 1.2 H). Current models of the thallus meristem assume distinct identities for lateral or dorso-ventral derivatives of this central apical cell, which are labelled as lateral, dorsal or ventral merophytes. However, this model is largely based on morphological analysis of cells and cell lineages rather than genetic analysis of cell function [295, 9, 290]. I propose the use of the term "central stem cells" to refer to the U-shaped population of lenticular shaped cells in the centre of the Marchantia meristem. This population comprises the central apical cell, sub-apical cells and the first few lateral derivatives. A distinct identity for this population of cells is supported by transcriptomic data presented in Chapter 4, marker gene expression presented in Chapter 5 and surgical manipulation in Chapter 7.

In summary, Marchantia has many advantages over more established model plants including: rapid growth in isogenic conditions, a dominantly haploid life cycle, a highly streamline genome with minimal genetic redundancy and an open form of development permitting facile live imaging, particularly with respect to gemma development. All of these aspects make Marchantia poised to fill the niche of a minimally complex plant model system to explore synthetic morphogenesis, which may eventually lead to the development of design principles that improve our ability to engineer plant growth in general.

1.4 Meristem regulation in angiosperms and beyond

Meristems are a key feature of land plants, enabling continuous tissue growth and organ formation by maintaining a dynamic balance of stem cell proliferation and differentiation into mature cell types. Meristems can typically be divided into several functionally and genetically distinct regions that maintain this balance through complex signaling between domains. In both the shoot and root apical meristem of vascular plants a slowly dividing population of cells at the centre of the tissue orchestrates meristem organisation via hormone

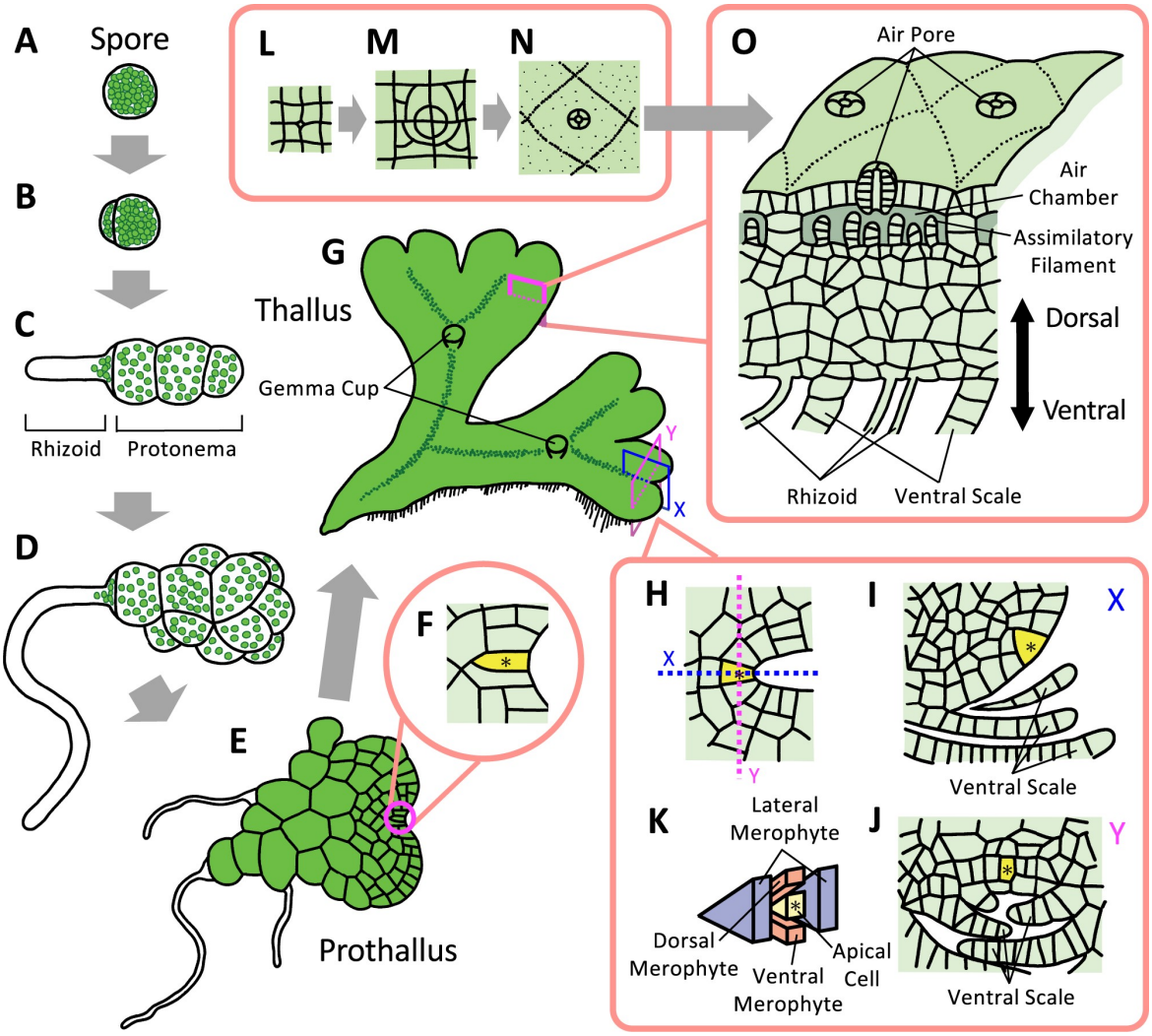

Fig. 1.2 **Marchantia gametophyte development and anatomy** Adapted from [223]. (**A**) Spores initiate chlorophyll biosynthesis within the first 24h of germination. (**B**) The first division in sporeling development is asymmetric. (**C**) The smaller cell develops into a rhizoid cell while the larger cell divides, generating a undifferentiated green cell mass (**D**). (**E**) Approximately 1 week after germination a two dimensional notch shaped meristem emerges with a central apical initial cell (**F**). (**G**) The prothallus subsequently matures into a three dimensional, dorsal ventral patterned thallus. (**L-N**) Air pores develop on the dorsal surface marked by a characteristic cell cross. (**O**) Air chambers form the dorsal surface of thalli and are comprised of air pore cells, epidermal cells, sub-epidermal cells, assimilatory filaments and chamber wall cells. On the ventral surface, rhizoids and ventral scales develop. (**H-J**) The centre of the thallus meristem contains a U-shaped population of cells. The central apical initial cell is highlighted in yellow.

gradients, signaling peptides and other signals. The central organising cell population is typically flanked by domains of rapidly dividing cells which subsequently differentiate into distinct cell fates. Most research on plant meristems has focused on the Arabidopsis shoot apical meristems (SAM) and root apical meristems (RAM) which consequently are by far the most well studied plant meristem systems.

1.4.1 Arabidopsis embryogenesis

The SAM and RAM are specified gradually during Arabidopsis embryogenesis. The first signs of distinct meristem cell identities appear in the globular stage of embryogenesis (Figure 1.3). Auxin and cytokinin play a central role in patterning the emerging embryo from the very first division. The first asymmetric division of the zygote creates an embryo and suspensor cell and the polar auxin transport into the embryo creates a transient auxin maxima in the embryo apex [92]. At the octant stage, differential expression of *WOX2* and *WOX8/9* define the upper and lower tier of the embryo [32]. The transient auxin accumulation at the apex activates the auxin-dependent transcription factor *MONOPTEROS* (*MP*) which drives hypophysis specification by promoting transport of the hormone auxin from the embryo to the hypophysis precursor [20, 119, 338]. This promotes expression of *PLETHORA* (*PLT*) genes in the basal domain which orchestrate RAM development [2]. In the upper embryo, WOX2 proteins induce expression of class III-HD ZIP transcription factors [365]. Class II-HD ZIP genes activate expression of *WUSCHEL* (*WUS*) [248] and promote the expression of cytokinin biosynthesis genes [144, 365]. The class I KNOTTED-like homeobox (KNOX1) protein SHOOT MERISTEMLESS (STM) additionally promotes establishment of the SAM, in part through upregulation of cytokinin [200, 159]. The reorientation of auxin transport creates local auxin maxima at the sides of the apical region, which will form the cotelydons, while the central apical portion becomes an auxin response minima, promoting SAM formation in this domain [92, 16]. At the transition stage, *CUP-SHAPED COTYLEDON* (*CUC2*) starts to be expressed between the developing cotyledons, defining the boundary zone between developing leaves and the emerging SAM [3].

1.4.2 Arabidopsis shoot meristem

The shoot apical meristem (SAM) is located at the dome of the shoot apex (Figure 1.4 A). The SAM can be divided into distinct cell layers (Figure 1.4 B). Cells in the two uppermost cell layers, L1 and L2, divide anticlinally, i.e perpendicular to the outer surface (Figure). As a result, they form clonally distinct monolayers. All cells below form the L3 layer, where division orientations are less constrained. The SAM is also commonly divided into four tissue

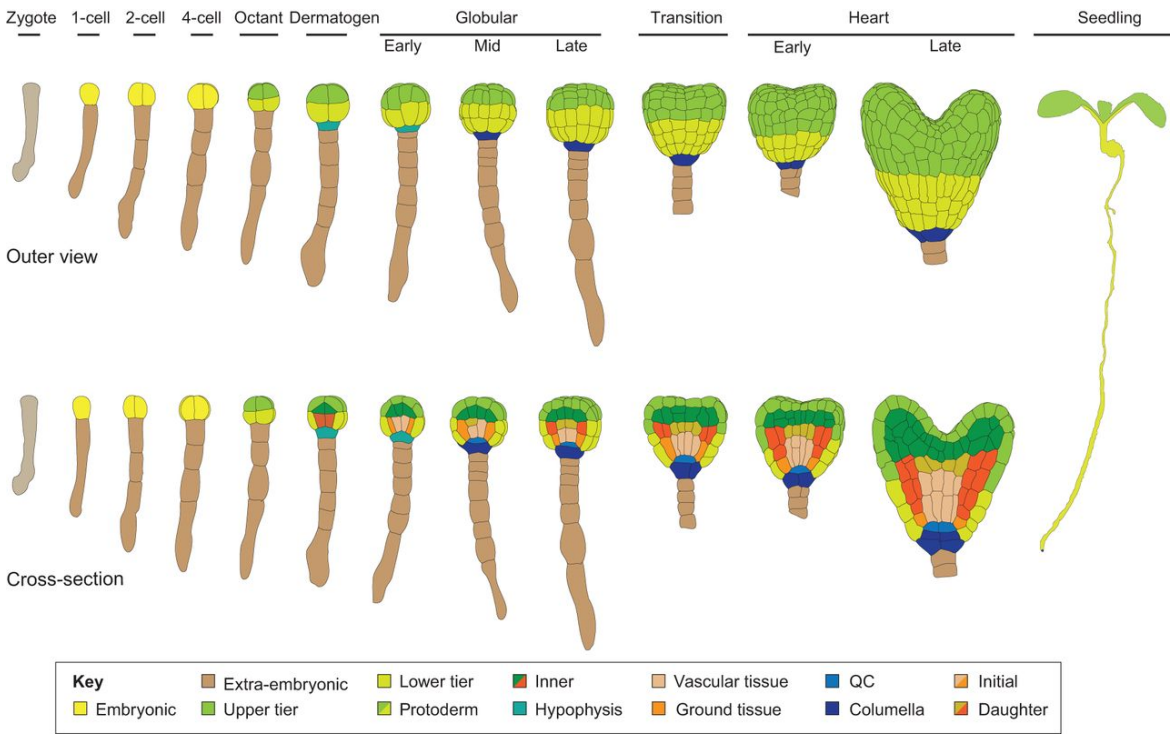

Fig. 1.3 **Arabidopsis embryogenesis** Adapted from [319]. Key stages of embryogenesis in *Arabidopsis thaliana*. The first asymmetric division defines the extra-embryonic suspensor which supports the embryo. In the octant stage the embryo is divided into upper and lower tier. The dermatogen stage delimits the internal tissue from the epidermis and defines the hypothesis which develops into the QC and columella of the emerging RAM at the globular stage. Further expansion of the embryo defines distinct internal cell layers and results in the emergence of cotyledons at the heart stage.

domains (Figure 1.4 B). The central zone (CZ) contains a population of slowly dividing stem cells which gradually displace distal daughter cells into the peripheral zone (PZ) where cells divide rapidly and new organ are initiated. CZ cells can also undergo transition into the rib zone (RZ) which is located below the CZ and provides cells for the internal tissues of the stem. A small population of cells located above the RZ, but below the CZ, forms the organising centre (OC). Clonal analysis of cells in the SAM demonstrated that cell identity is a result of positional information rather than cell lineage [244, 305, 110], suggesting that cell-cell communication and patterning of signaling molecules drive SAM organisation. Unlike the cell layers, cell zones in the SAM do not have clear sharp boundaries and are commonly defined by the expression of a small number of important shoot meristem regulators. The CZ and OC in particular are defined by *CLAVATA3* (*CLV3*) [86] and *WUSCHEL* (*WUS*) [211] expression respectively.

Current models of SAM organisation are centred on a negative feedback loop between WUS and CLV3 signaling. OC cells express WUS protein which can move to surrounding cells, where it promotes stem cell identity and antagonise cell differentiation [211, 286, 350, 50]. WUS directly activates expression of the CLV3 peptide in cells of the CZ [350]. CLV3 is secreted from CZ cells [263] and inhibits stem cell fate in surrounding cells by activating multiple receptor like kinases, including CLV1 [161, 30, 220]. This negative feedback loop spatially separates and balances *WUS* and *CLV3* expression domains in the SAM. However, WUS paradoxically does not induce stem cell fate in the OC where it is expressed. This paradox was solved by identifying the function of a family of GRAS transcription factors called HAIRY MERISTEM (HAM). *HAM* genes are expressed basally overlapping with WUS expression in the OC but not reaching the CZ of the SAM [369]. HAM proteins form complexes with WUS to prevent CLV3 induction in OC cells [370]. The HAM expression gradient is in turn established by the expression of a family of HAM repressing micro-RNAs from the L1 layer of cells, mediated by the epidermis specific transcription factor ATML1 [116]. The WUS expression domain is further tuned by a second incoherent negative feedback loop with cells of the PZ [282]. WUS represses expression of CLE40 peptides which show complementary expression to WUS in the PZ [282]. In the PZ CLE40 is perceived by BAM1 and BAM1 mediated signaling appears to promote WUS expression in the OC via a unknown mobile signal [282]. The CLV3-CLV1-WUS and CLE40-BAM1-WUS feedback loops are thought to tune the balance of growth between the apical-basal axis and the meristem periphery, with weaker CLV3 signaling promoting apical-basal growth, while weaker CLE40 signaling promotes peripheral growth, flattening the meristem.

Hormone gradients are also critical for SAM function. Cytokinin signaling is essential for SAM function, with overexpression of cytokinin oxidases arresting SAM activity, similar

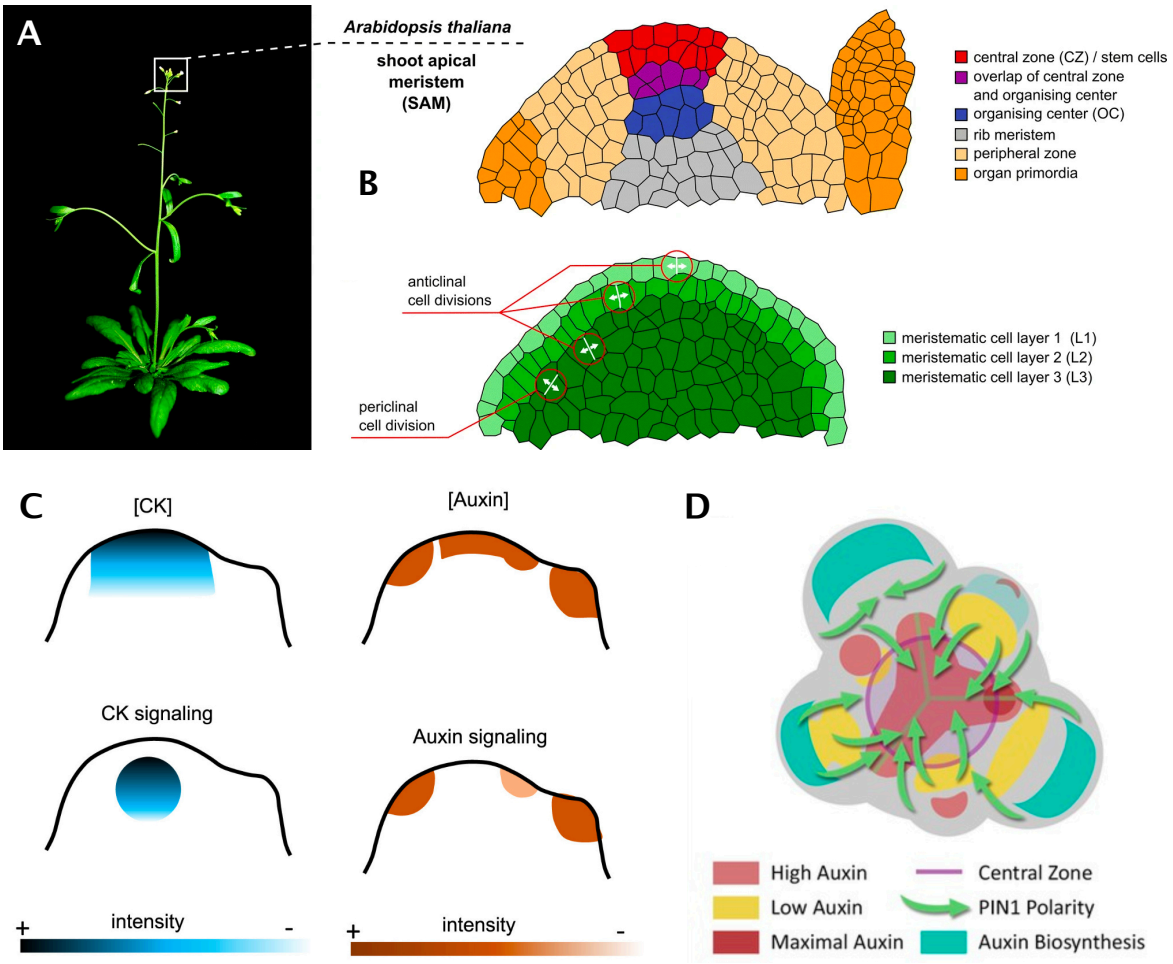

Fig. 1.4 **Arabidopsis shoot apical meristem organisation** Adapted from [93, 98, 289]. (**A**) *A. thaliana* morphology, white box indicates the location of the shoot apical mersitem (SAM). (**B**) Schematic representation of SAM cross-section, cell layers and cell zones are indicated. (**C**) Approximate levels of cytokinin concentration ([CK]) cytokinin signaling (CK signaling) auxin concentration and auxin signaling in the SAM. (**D**) Diagrammatic top view of the SAM, illustrating patterns of auxin flow.

to *WUS* loss of function alleles [341]. Cytokinin signaling is tightly spatially controlled in the SAM (Figure 1.4 C). *LOG* genes which catalyse the last step in cytokinin biosynthesis are specifically expressed in the L1 layer of the shoot meristem while *AHK* cytokinin receptor expression is restricted to the OC and RZ [40, 107]. Cytokinin signaling and WUS activity re-enforce each other to stabilise OC identity. Cytokinin directly induces WUS expression and represses CLV1 expression [105] while WUS represses A-type ARABIDOPSIS RESPONSE REGULATOR (ARR) proteins, which are negative regulators of cytokinin signaling [183]. Cytokinin is also important for antagonising cell differentiation outside the OC. The SHOOT MERISTEMLESS (STM) class I KNOTTED-like homeobox (KNOX1) protein is required to suppress differentiation throughout the meristem dome and acts independently of WUS [76, 185]. STM is broadly expressed in the SAM and induces expression of *IPT* genes which perform the first step in cytokinin biosynthesis, elevating cytokinin concentration across the SAM [159, 352]. STM is indispensable for meristem maintenance, but *stm* mutants can be partially complemented by exogenous cytokinin treatment [159, 352]. Apart from the intimate association of cytokinin with key meristem regulators, cytokinin also directly promotes cell proliferation [218] by promoting cell cycle progression through both the G1/S and G2/M phase transitions [280]. At the G1/S transition, cytokinin activates expression of D-type cyclins [260] promoting entry into the cell cycle [43]. At the G2/M phase transition, cytokinin promotes MYB3R4 nuclear localization to activate mitosis [353]. Both of these mechanisms directly link cytokinin to cell division rates.

Auxin also plays a critical role in the SAM (reviewed in [276]). Classical studies characterised auxin as a mobile morphogen which emanates from the SAM and confers apical dominance of the SAM over lateral buds [321, 297]. Subsequent studies have demonstrated that auxin is transported from the shoot to the root, refluxing in the root tip [99, 24]. While auxin broadly inhibits shoot growth and promotes root growth, auxin plays multifaceted role during plant growth and is also an important signal during SAM maintenance. Auxin in the SAM is best known for the important role of auxin in the regulation of phyllotaxis. Auxin transport in the SAM is mostly restricted to the L1 layer and the pro-vasculature [331, 124]. Expression patterns of auxin response reporters and auxin transport polarity align with emerging organ primordia [255, 16, 124] (Figure 1.4 C). Recent work demonstrates that auxin signaling in emerging primordia involves temporal integration of auxin concentration in cells as they are displaced from the centre of the SAM [98] (Figure 1.4 D). Auxin is thought to promote stem cell differentiation and cell expansion in primordia, driving outgrowth of leaf tissue. Inhibition of auxin transport generates column shaped shoot growth with disrupted organ formation and local auxin application alone is sufficient to initiate outgrowths in these plants [254]. Expansins are a family of genes which have been shown to loosen cell wall

stiffness of plant cells [46]. Local induction of expansin genes also triggers outgrowths [85, 243] and natural expansin expression is restricted to primordia [256], suggesting that local cell wall loosening is critical to permit organ outgrowth. Auxin treatment indeed induces the expression of several expansin genes [234]. Classically, auxin-mediated growth has been described by the acid growth hypothesis, which proposes a non-transcriptional mechanism for the loosening of the cell wall based on apoplast acidification [266, 252] (reviewed in [11]). The activity of expansin proteins is modulated by pH, with acidic environments increasing activity [214]. Initially, auxin was postulated to directly decrease apoplastic pH, as IAA is a weak acid [266, 252]. While this theory was later invalidated [11], molecular mechanisms for both rapid and sustained auxin mediated apoplast acidification have been identified since. Auxin signaling has been shown to stabilise H+ pump activity through downstream transcriptional regulation via SAUR proteins, to acidify the apoplast and promote cell elongation, providing a mechanisms for sustained acidification [302, 82]. However, this mechanism requires prior activation of H+ pumps through phosphorylation. More recently, membrane localized TMK-receptor-like kinases have been shown to directly phosphorylate H+ pumps within seconds of auxin treatment, providing a direct molecular mechanism for auxin mediated apoplast acidification independent of transcriptional signaling [192, 189]. While these results strongly suggest that the primary role of auxin in the SAM is to antagonise stem cell fate and promote cell expansion and differentiation, auxin has complex effects on cells in different contexts. Auxin has for instance been reported to repress *ARR* genes via the *AUXIN RESPONSE FACTOR5/MONOPTEROS* (*MP*), thereby promoting cytokinin signaling in the central zone [367]. Detailed characterisation of auxin flux in the SAM suggests that auxin is not only channelled into organ primordia, but also more broadly into the centre of the SAM, including stem cells of the central zone [98]. Recent results suggest that a low level of auxin signaling is required to maintain stem cell fate in the CZ [204]. WUS appears to acts as an auxin response rheostat, permitting low levels of auxin signaling in stem cells, but preventing high levels of auxin signaling, even in the presence of high levels of auxin, by repressing transcription of auxin response regulators via recruitment of the transcriptional co-repressor TOPLESS (TPL) [204, 196].

1.4.3 Arabidopsis root meristems

The root apical meristem (RAM) is located at the tip of the primary root. Similarly to the SAM, the RAM can be divided into cell layers, which are radially patterned in the RAM, and different functional zones along the proximal distal axis. The RAM contains a small population of slowly dividing cells at the centre, which are termed the quiescent centre [42, 63]. The tip of the root is formed by columella and lateral root cap cells which protect

the central stem cell population. Above the QC, the root is radially patterned into cell layers with distinct functions, starting with xylem, cambium and phloem at the centre, followed by layers of pericycle, endodermis, cortex and epidermis cells [63]. The stem cell niche of the RAM is commonly defined as the QC and the immediately surrounding cells, which form the progenitors for the distinct lineages of the root [240]. Along the longitudinal axis, the root is commonly further divided into a meristematic or division zone, which is positioned above the stem cell niche and includes rapidly dividing cells, an elongation zone where cells start to elongate, and a differentiation zone that is marked by root hair emergence. However, cell proliferation and differentiation gradually change along the longitudinal axis and many important genetic regulators also show smooth gradients [340].

RAM organisation is driven by auxin patterning and auxin generally promotes root growth and root cell division, in contrast to the effects of auxin in the shoot. The refluxing auxin transport in the root [24] establishes an auxin concentration gradient with a maximum in the QC and a proximal distal gradient [106, 239]. Auxin induces the expression of PLETHORA (PLT) AP2/ERF transcription factors which induce stem cell fate and are indispensable for QC specification [97, 2, 206]. *PLT* genes also reinforce the auxin transport gradient by maintaining PIN transcription [24]. The GRAS-transcription factors SHORTROOT (SHR) and SCARECROW (SCR) are also essential for QC fate [15, 58]. SHR is expressed in the stele and moves into the adjacent cell layers to activate SCR transcription in the QC [125, 222]. SCR expression is required for QC identity and maintenance of stem cell identity in surrounding cells [269]. SHR activates expression of the WUSCHEL-related HOMEOBOX5 (WOX5) transcription factor which exclusively marks the QC [275, 356]. WOX5 promotes stem cell fate in columella stem cells [275, 241] and is also required for PLT activity in the QC, providing a point of convergence for the auxin-PLT and SCR regulatory pathways [62]. PLT and SCR are also able to directly form protein complexes with TCP20 and this complex is critical for QC specification [292]. WOX5 expression outside of the QC is restricted by the (CLE) peptide CLE40 which is expressed in columella cells and signals through the receptor-like kinase ARABIDOPSIS CRINKLY4 (ACR4) and CLV1 to repress WOX5 expression [304, 303].

Similarly to auxin, cytokinin generally displays opposite effects in the RAM compared to the SAM [145]. In the RAM, cytokinin antagonises meristem activity in part through repressing PIN expression and auxin signaling which in turn inhibits PLT [268, 146].

Relatively little is known about RAM regulation outside of angiosperms. Roots are thought to have evolved multiple times independently in vascular plants [128]. In the fern *Azolla filiculoides*, root growth is inhibited by auxin application and promoted by cytokinin treatment which is the opposite effect observed in angiosperms [51]. This suggests that

a pre-existing set of hormonal interactions may have been recruited in different ways in different lineages of root evolution.

1.4.4 Meristem regulation beyond the SAM and RAM

The RAM is thought to have evolved after the SAM, potentially through co-option of pre-existing meristem regulatory modules. While there are many differences between the SAM and the RAM, the expression of WOX genes in the organising centres of both meristems and the presence of feedback loops with CLE peptides are striking similarities between both systems. Another WOX CLE signaling network also regulates the cambial stem cell niche. WOX4 is regulated by a CLE peptide (CLE41/TDIF) emanating from the phloem side of the cambium, which is sensed by a receptor kinase (PXY/TDR) in the cambium [79]. Furthermore, experiments in Arabidopsis have demonstrated that *wus* mutants can be complemented by WOX5 expression from the *WUS* promoter and *vice versa* suggesting that WUS and WOX5 are fully interchangeable [275]. However, ectopic expression of WUS in the root outside of the QC can induce expression of shoot stem cell markers [226] while ectopic expression of PLT in the shoot can induce root formation [97]. These results suggest that while there are common components of angiosperm meristems, the function of root and shoot meristem regulators is highly dependent on the tissue context.

1.4.5 Bryophyte meristem regulation

Unlike vascular plants where the life cycle is dominated by the sporophyte generation, bryophyte life-cycles are dominated by the gametophyte generation. There are two classical theories to attempt to explain the evolution of the sporophyte SAM from an ancestral gametophyte SAM [114]. The homologous theory postulates that the sporophyte SAM evolved by acquiring the regulatory network of the gametophyte SAM, while the antithetic theory suggests that the sporophytes SAM evolved *de novo* by acquiring a novel SAM system between embryonic growth and reproductive growth [114]. While the origin of the sporophytic SAM is still under debate [172], many genetic regulators of the Angiosperm sporophyte SAM have been implicated in gametophyte SAM regulation, suggesting common features in SAM regulation of land plants (Figure 1.5).

Gametophyte SAM regulation has been most extensively studied in the moss *Physcomitrium patens*. Early research in Physcomitrium characterised the role of auxin and cytokinin in moss SAM regulation. In Physcomitrium, auxin represses stem cell identity and promotes organ formation [12, 247] and auxin transport is important for correct organ patterning [18, 332], while cytokinin promotes stem cell identity, similarly to the function of both

hormones in Angiosperms [12, 258, 48]. The signaling pathways for auxin and cytokinin were also found to be broadly conserved [257, 333, 320], suggesting that both hormones are involved in similar processes in the gametophyte and sporophyte SAM. Homologues of *AINTEGUMENTA*, *PLETHORA* and *BABY BOOM* (*APB*) in Physcomitrium are regulated by auxin and indispensable for gametophyte SAM formation [8] while CLE peptide signaling inhibits stem cell activity [342] similarly to the function of CLV3 in Angiosperms. These results point to a conserved role of many core elements of SAM regulation (Figure 1.5), however some central angiosperm SAM regulators are not conserved. WOX proteins are involved in tissue regeneration in Physcomitrium, but are not required for the maintenance of the SAM [273]. This is consistent with interspecies complementation analysis which suggests that WOX function in stem cell maintenance evolved in vascular plants [364]. Similarly, even though class I KNOTTED1-LIKE HOMEOBOX (KNOXI) proteins activate cytokinin biosynthesis in Physcomitrium, they do not play a role in gametophyte SAM regulation, but are important for sporophyte development [272, 47].

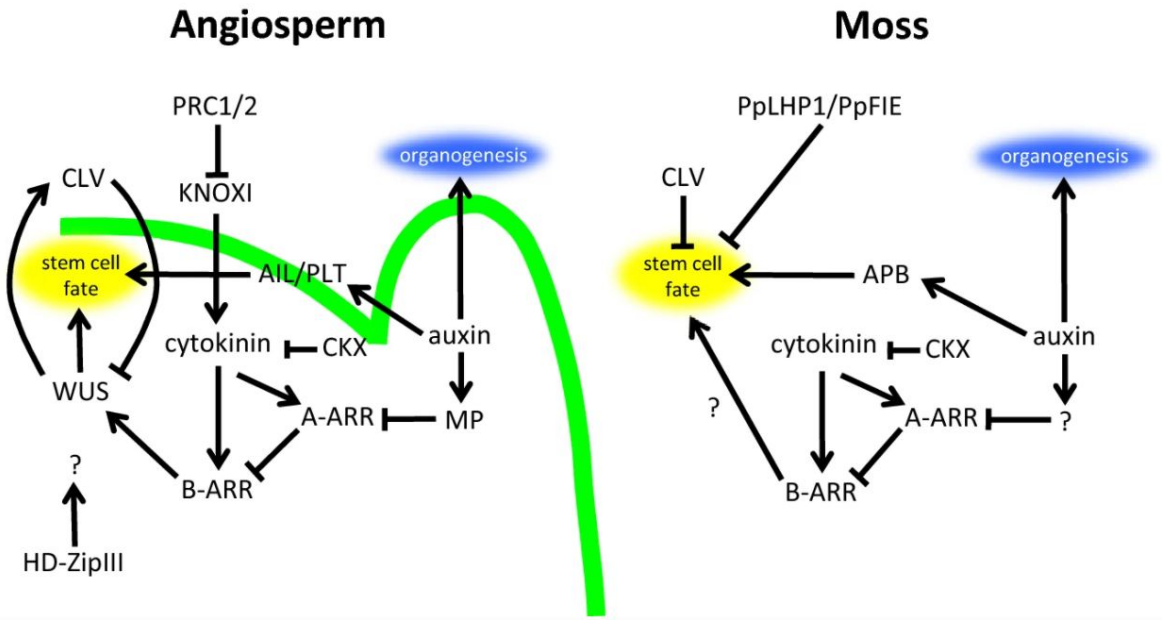

Fig. 1.5 **Conserved meristem regulators in Angiosperms and Mosses** Adapted from [122]. Left: Interactions between key meristem regulators in Arabidopsis, position of genes indicates their spatial distribution in the SAM. Right: Stem cell regulators in Physcomitrium, spatial location of labels is used to emphasise similarities between Angiosperms and Physcomitrium.

1.4.6 Growth in Marchantia gemmae

Growth in Marchantia gemmae is localised to the notch regions at either end of the gemmae tissue (Figure 1.6). Mapping of cell divisions and tissue expansion rates in gemmae showed increasing rates of tissue expansion with closer proximity to the centre of the notch (Figure 1.6 C) [250, 25]. Solly et al. [299] further characterised tissue expansion in Marchantia and developed computational models to investigate the growth rate distributions that give rise to the characteristic notch shaped thallus morphology. Consistent with previous results, Solly et al. [299] showed thalli growth is characterised by increasing tissue expansion rates with decreasing proximity to the centre of the notch, however the tissue in the centre of the notch itself displayed very low rates of tissue expansion, driving notch formation. These tissue expansion distributions combined with previous observations on the distinct morphology of apical cells and their derivatives Shimamura [290] and apical cell emergence at the onset of notch formation during sporeling development [223], suggest that reduced tissue expansion in central stem cells compared to the surrounding tissue may drive notch formation. The Marchantia meristem may therefore be divided into two distinct zones, a central zone of low proliferation which comprises the central stem cells and a surrounding proliferation zone which displays high rates of tissue expansion.

Meristem regulation in Marchantia is poorly understood, but some regulators have been identified. Auxin has long been known as an important signal for establishing apical dominance of the Marchantia meristem [208]. Auxin is thought to be synthesized in the Marchantia apex and transported basipetally [23]. Exogenous auxin treatment promoted cell expansion, differentiation and rhizoid elongation, [70] and auxin signaling is thought to be restricted to the central portion of Marchantia plants [154, 170]. This suggests that auxin may act as a mobile signal which promotes cell differentiation, similar to the role of auxin in the angiosperm SAM. Loss of function alleles of cytokinin signaling components in Marchantia caused defects in thallus development, generating smaller thalli with serrated margins and fewer gemma cups [87], Conversely increased cytokinin signaling resulted in more gemma cups and epinastic thallus growth [4]. These results suggest that the roles of auxin and cytokinin may be broadly similar in Marchantia compared to angiosperm SAM regulation, with auxin promoting cell differentiation and cytokinin signaling contributing to cell proliferation.

CLE peptide signaling also plays an important role in regulating cell proliferation in the Marchantia meristem, but the role of different CLE families is distinct compared to angiosperms [134, 133]. The Marchantia genome contains two CLE genes, Mp *CLE1* a homologue of *CLE41/TDIF* which positively regulates cambium stem cells in Arabidopsis [79] and Mp *CLE2*, a homologue of *CLV3* which negatively regulators stem cells in the SAM

of Arabidopsis. MpCLE1 was found to be expressed in the centre of the meristem, with evidence for expression of the MpCLE1 receptor MpTDR in surrounding cells. However, unlike CLE41/TDIF, MpCLE1 is a negative regulator of cell proliferation in the proliferation zone Hirakawa et al. [134]. In contrast exogenous MpCLE2 treatment expands the central stem cell population, resulting in a widened meristem without notch morphology [133]. The expression of MpCLE2 is localised to cells surrounding the central stem cell population and cells in the centre of the notch show expression of the MpCLE2 receptor MpCLV1 [133] and the co-receptor MpCIK [314]. Loss of function of Mp *CLE2*, Mp *CLV1* [133] or Mp *CIK* [314] results in a reduced size of the apical cell population suggesting that Mp *CLE2* is a positive regulator of the central stem cell population, in contrast to the function of *CLV3* in the Arabidopsis SAM. Loss of function alleles of the only *WUSCHEL-related HOMEOBOX* (*WOX*) homologue Mp *WOX* did not disrupt meristem architecture or CLE signaling, [133] suggesting CLE signaling in Marchantia is independent of Mp *WOX*.

1.5 Thesis aims

The morphological and genetic simplicity of Marchantia make it an attractive model system to study the regulation of growth and establish frameworks for rational engineering of plant growth. However, the function of genetic and cellular processes in the Marchantia meristem remain poorly characterised. Integrated models of cellular interactions and signaling pathways that govern meristem maintenance and initiation are needed to unlock the potential of Marchantia as a simple morphogenetic system. This dissertation describes the use of single cell RNA-sequencing and novel marker lines to define the cell composition of the Marchantia meristem and the use of genetic and experimental perturbation to interrogate the gene networks and phytohormone patterning systems governing meristem maintenance and initiation.

The key objectives of this work are:

1. **Screening of a proximal promoter library for novel meristem marker genes.** Meristem domains in Marchantia remain poorly defined owing to a lack of genetic markers for distinct cell domains. Transcription factors (TF) play a critical role in the regulation of cell fate and the small number of transcription factors in Marchantia represents a unique opportunity to attempt comprehensive screening of TF expression. Promoter elements with specific expression are also expected to be valuable tools for targeted missexpression of cell fate regulators in the future.

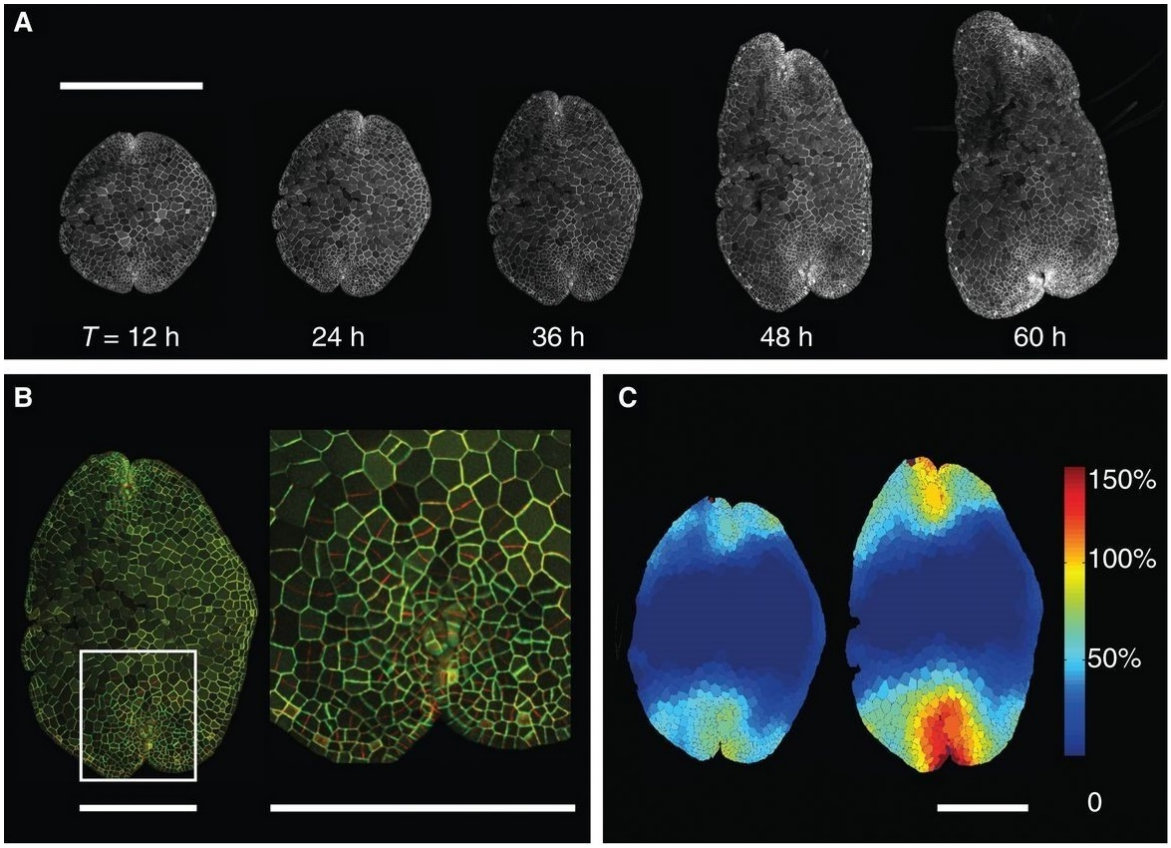

Fig. 1.6 **Early gemma growth** Adapted from [25]. (**A**) Confocal imaging of transgenic Marchantia gemma containing green fluorescent protein localized to the plasma membrane. Plants were imaged at indicated time-points. Scale bars 500µm. (**B**) Composite image of the 24h (green channel) and 36h image (red channel) overlaid onto each other using warp-registration image-processing. Red plasma membrane signal indicate new cell cell walls. Scale bars 200µm. (**C**) Measurements of percent clonal sector expansion per 12h are shown as a color map: left 12h-24h, right 24h-36h. Scale bars 200µm.

2. **Cell type mapping of gemmalings using single cell RNA-sequencing** Single cell RNA-seqeuncing enables unbiased cell type characterisation at scale. The genetic identity of cell types in Marchantia gemmalings are still largely undefined and single cell RNA-seq could be a powerful tool to map the cellular diversity of Marchantia.

3. **Investigate the function of central stem cells and their relationship with auxin signaling in the Marchantia meristem** Central stem cells form a distinct population of cells in the centre of the gemma meristem including the central apical cell. The apical cell has been proposed to play an important role for auxin signaling in gemmae. However, studies so far have lacked the necessary resolution to characterise which cells in the meristem control auxin patterning as well as the necessary reporter systems to analyse auxin response in the tissue with cellular resolution. High resolution imaging of auxin marker genes and the development of auxin response markers could shed light on the organisation of the gemma meristem. The identification of cell fate regulators of central stem cells could further help to clarify cell identities in the centre of the gemma meristem.

4. **Dissect the regulation of cell divisions in the division zone** Cell divisions are largely restricted to the gemma meristem, but little is known about cell division regulation in Marchantia. Genetic markers and functional analysis of cell cycle regulators could shed light on the regulators of cell division and clarify the role of phytohormones in the regulation of division rates. Once characterised cell cycle regulators could also be used as powerful tools to induce ectopic divisions in tissues of interest.

5. **Characterise the regeneration of meristems in gemma explants** Marchantia explants without meristems rapidly regenerate new meristems without the application of exogenous hormones, but little is known about the regulation of this process. Precise surgical manipulation and the use of cell fate, hormone signaling and cell cycle markers could help shed light on the regeneration process and elucidate the dynamics of meristem establishment. By exploiting this dynamic process, improved models of meristem maintenance and regeneration may be build which would establish an important framework for future attempts to rationally engineer growth in Marchantia.

Chapter 2

Methods

Online supplementary information and files can be found at the GitHub repository:
https://github.com/HaseloffLab/MariusRebmannThesis
Plasmid maps are additionally avaliable at:
https://benchling.com/mariusrebmann/f_/aVSKR2za-thesis_marius_rebmann/
Most methods used in this thesis are also included in the OpenPlant project on at:
https://www.protocols.io/workspaces/openplant-project/publications.

2.1 Molecular Biology

2.1.1 *Escherichia coli* transformation

The *E. coli* strain TOP10 (Thermo Fisher Scientific) was used for all cloning. Chemically competent TOP10 cells were generated using the CCMB80 buffer method [118]. For transformation, 50µL aliquots were removed from -80°C storage and thawed on ice. Once thawed, 1µL of 50ng/µL plasmid DNA or 1µL of Loop reaction (see chapter 2.1.2) was added and incubated on ice for 10 minutes. Tubes were placed into a 42°C water bath for 45 seconds and returned to ice for 2 minutes. 500µL of LB media, Miller's Broth Base (invitrogen), was added and cells were moved to a shaking incubator at 37°C and 200rpm for 1 hour. 100µL of the cell suspension was plated on 1% v/w agar (Melford A20021) LB media petri dishes with antibiotics for selection and X-gal (Thermo Fisher Scientific R0404) for blue white screening where appropriate. Plates were incubated at 37°C overnight.

2.1.2 Plasmid assembly

DNA parts were assembled into transcription units using Loop assembly [245, 279] a variant of type IIS assembly [77]. Loop assembly enables recursive assembly of DNA parts by employing two sets of four plasmids (pCk1-4 or pCsA-D) with restriction sites that facilitate joining four parts from one set into a backbone of the other set. Reactions into pCK backbones are catalysed by BsaI and reactions into pCs backbones by SapI. Since the product of each reaction is again compatible with assembly into the other plasmid set, large DNA parts can be assembled recursively by looping through the sets repeatedly. Assemblies are labelled based on the level of the reaction.

2.1.3 DNA part design and L0 parts

Since Loop assembly reactions are catalysed by BsaI and SapI, restrictions sites for these two enzymes have to be removed from DNA sequences to be compatible with assembly. This process is called part domestication and is typically achieved by introducing a single silent point mutations for each restriction site. Most novel parts introduced in this work were generated by DNA synthesis, with mutations introduced computationally prior to synthesis. L0 parts contain fusion sites flanking the DNA part to specify their position in the resulting transcription unit. Most parts used in this thesis have been described previously [245, 279] and novel parts are listed in Table 2.1 and Table 2.2.

2.1.4 Plasmid verification

Plasmid DNA was extracted from *E. coli* either manually using the QIAprep Spin Miniprep Kit (Qiagen) or using the QIAcube® platform (Qiagen), following manufacturer instructions. Plasmids were eluted in 40µL nuclease free water and DNA concentration was measured using a Nanodrop® spectrophotometer (Thermo Fisher Scientific). All L0 and L1 plasmids were Sanger sequenced with Genewiz® using pairs of inward facing primers binding the backbones. Additional sequencing was done for some L1 constructs, typically using reverse facing primers binding the start of fluorescent proteins to validate the promoter-CDS junction. L2 constructs were typically validated by restriction digests, because of the large insert size. 500ng of plasmid DNA was digested in 10µL final reaction volume, using either FastDigest enzymes (Thermo Fisher Scientific) in a FastDigest Green Buffer (Thermo Fisher Scientific) or High-Fidelity enzymes (New England BioLabs) in CutSmart buffer (New England BioLabs) according to manufacturer instructions. Restriction enzymes were selected to cut each plasmids 3-10 times and virtual restriction enzyme digests (Benchling) were used

Table 2.1 New DNA parts

Part ID	Gene	Part	Source	Start
p0_1121	Mp3g20570	5UTR	This work	GAAGGAAGCAGATGTGGCTC
p0_1122	MpIPT1	5UTR	This work	CGAGTGCTACCACTGGTGTG
p0_1123	MpCKX2	CDS12	This work	ATGATGCTGCAATTACTGAA
p0_1124	MpCYCD;1	CDS12	This work	ATGGCTCCCAGTATCGATTG
p0_1125	MpCYCD;2	CDS12	This work	ATGTGCGTGCGCTACTTTAG
p0_1126	MpERF20	CDS12	This work	ATGGTGGGGAGGAAGCTGGG
p0_1127	MpIPT2	CDS12	This work	ATGATGCTGGGCGGGCACGC
p0_1128	Mp1g13170	PROM5	This work	AATTTACATTTATAAGCAAG
p0_1129	Mp1g15580	PROM5	This work	GCTCTAATAAATCCCACGTA
p0_1130	Mp3g11280	PROM5	This work	TACTGTAATTGAGTTTTCAA
p0_1131	Mp3g20970	PROM5	This work	TGAGATGATTAATAATCAAT
p0_1132	Mp4g01930	PROM5	This work	AAAAATATATTTATTTTGTA
p0_1133	Mp4g09230	PROM5	This work	TGCAATGTCGTACTGCCCAG
p0_1134	Mp4g17680	PROM5	This work	TATCATCGTGTAGGATGATG
p0_1135	Mp5g13870	PROM5	This work	GTTCTTTAGTCCGATCTATG
p0_1136	Mp6g10160	PROM5	This work	GAAAGCAATCTGGGACTCTC
p0_1137	Mp8g13430	PROM5	This work	ATTGCTTTTTCGACAGCAGG
p0_1138	Mp8g17780	PROM5	This work	CCTTGTGTTCTTGTGGCGTT
p0_1139	MpCHK1	PROM5	This work	TTTATCAGAGACACCAAAAA
p0_1140	MpCHK2	PROM5	This work	ATTTGATCATTAAGATATCA
p0_1141	MpCKX1	PROM5	This work	GTTCTGTTGGAATCACACGA
p0_1142	MpCKX2	PROM5	This work	GAAAACTAGATTGCACTGTT
p0_1143	MpCYCD;1	PROM5	This work	AATCGACAAAATCCGAATTA
p0_1144	MpCYCD;2	PROM5	This work	TGATCATCGTCTTCGAGTTA
p0_1145	MpCYP707A	PROM5	This work	ATCCACGCTAATATATGGTT
p0_1146	MpIPT2	PROM5	This work	TTCTCTTCAATATCTCCGTC
p0_1147	MpLOG	PROM5	This work	AATCTCGCACACACCGATGA
p0_1148	Mp3g20570	PROM	This work	CTTCATCCTGTACAAGCTAC
p0_1149	MpIPT1	PROM	This work	TCTTCAAATTTTTTTGATA
p0_1028	MpPIN1	PROM5	This work	TGAATGCGGTCGAGGACGGG
p0_1004	DR5v2	PROM5	[191]	GTTGGAATAGGATTTCGAAT
p0_o949	GH3	PROM5	[198, 190]	GAGTTCACGAATAAAGAAAA
p0_o966	MpYUC2	PROM5	[52]	TACCTCGGACGGGTTCTGTT
-	MpYUC2	PROM5	Satoshi Naramoto	GTGGTTCCGCTCTCTCGTCG

Table 2.2 Promoter screening parts

Part ID	Gene	Part	Start
p0_o544	MpARF1	PROM	AAAACATCATACACCGGAGG
p0_o515	MpARF1	5UTR	CAGCGAATGTTGTCGTCATT
p0_o139	MpARF2	PROM	TGCTCCCAGCTTCCCGGCCG
p0_o125	MpARF2	5UTR	GCTCGCCTCTCGGCCCCCGC
p0_o276	MpBHLH42	PROM5	TGGTAGTTCATCTTGTCTAA
p0_o408	MpBZR1	PROM	ATATTGATATACATTATGTG
p0_o153	MpBZR1	5UTR	ACAAAGGCATGCAGTAAGAG
p0_o514	MpWRKY11	PROM	TGAGAGACGAACCGTTGTGA
p0_o259	MpWRKY11	5UTR	CAGTTTTACTAGACGGAGCT
p0_o267	MpBHLH29	PROM5	TATAAGCATGAGGAGACGAA
p0_o357	MpNAC1	PROM5	CCGATAGACGGTGCGCATCG
p0_o275	MpBHLH13	PROM5	TGGTTCGTTAGACGCTGAAA
p0_o319	MpGRAS1	PROM5	AGTATTAGGCTAATGAGGAA
p0_o852	MpWOX	PROM	GCCTTAGTTCATACGTAGCC
p0_o716	MpWOX	5UTR	GCTCTGTCGTCCTCGGGTGC
p0_o847	MpAPB	PROM	GGAACGGGGAATGTTGACAA
p0_o711	MpAPB	5UTR	GAGCGACGTCGACTGTCATT
p0_o476	MpASLBD24	PROM	CATGTGGAAAGTAATTTGCT
p0_o221	MpASLBD24	5UTR	ACTCTTGCACCCTCCAAACA
p0_o358	MpNAC4	PROM5	AGCGGTGGTAATAAGGAGGA
p0_o870	MpNAC2	PROM	GTCGGCGGTCGGGCGAGGTT
p0_o734	MpNAC2	5UTR	AGCTGAGCGCTGCTTGTTTG
p0_o419	MpRSL2	PROM	GTCCATCATCCCAAGAATGT
p0_o164	MpRSL2	5UTR	GACGCTTCCCTGCAAACGGA
p0_o482	Mp3R-MYB1	PROM	CGAAGTGCGCAAGCTGCAAC
p0_o227	Mp3R-MYB1	5UTR	CCCGAGGCAAGCGCGAGCCA
p0_o674	MpTUBA	PROM5	GCATGTACCGCGCTCTTATG
p0_o668	p35S	PROM5	AGATTAGCCTTTTCAATTTC

to ensure clear diagnostic digestion patterns. After digestion, the DNA was subjected to gel electrophoresis.

2.1.5 List of L1 and L2 constructs

All plasmids maps for plasmids generated in this work are available in the online supplementary information. Table A.1 details the constructs used for each figure in this thesis.

2.1.6 Gel electrophoresis

Agarose gels, 1.2% w/v agarose (Sigma Aldrich) in 1x Tris-acetate-EDTA with SybrSafe DNA gel stain were prepared according to manufacturer instructions and placed in a horizontal gel tank. Samples were mixed with Gel Loading Dye Purple (6X) (New England Biolabs) where necessary and loaded into the gel wells. Gels were run at 100 V for 45 minutes and inspected using a blue light transilluminator. Where appropriate DNA fragments of expected size were extracted from the gel using a scalpel and purified using the MinElute kit (Qiagen) following manufacturer instructions. Gel images were acquired on a GelDoc Go imaging system (Bio-Rad).

2.1.7 Polymerase Chain Reaction (PCR)

Phusion High-Fidelity DNA polymerase (Thermo Fisher Scientific) was used for all PCR reactions, following manufacturer instructions.

2.2 Marchantia methods

2.2.1 Tissue culture

All Marchantia experiments were performed using the Cam accessions (male *Cam-1*, female *Cam-2*), isolated in Cambridge, UK by Prof. Jim Haseloff. Tissue culture methods are based on Ishizaki et al. [153]. Marchantia plants were grown on 1.2% w/v agar (Melford A20021) plates of Gamborg B5 media with vitamins (Duchefa Biochemie G0210) prepared at half the manufacturer's recommended concentration and adjusted to a pH=5.8 (referred to as 0.5 Gamborg media in the remaining text). Plants were propagated by transferring gemmae using sterile inoculation loops, or placing cuttings of plants on agar plates. Plates were sealed with Micropore tape (3M) to enable gas exchange while preventing moisture loss. Plants were grown at 21°C under continuous light (150mol/m/s). For short term

storage (3 months) plants were moved to 14°C with the same light conditions. For intermediate term storage (1 year) 1.5mL Ependorf tubes were half filled with 0.5 Gamborg agar, fresh gemmae were placed on top and stored at 4°C in the dark. For long term storage at −80°C we used a simplified protocol, based on Tanaka et al. [315] available at dx.doi.org/10.17504/protocols.io.9vxh67n.

2.2.2 Sporeling transformation

Sporeling transformation was based on of Ishizaki et al. [151] following modifications described in Sauret-Gueto et al. [279]. Sterile Marchantia sporangia were generated as described by Sauret-Gueto et al. [279] and stored at −80°C until use.

2.3 Microscopy

2.3.1 Sample preparation

Where appropriate, Marchantia samples were prepared for microscopy using plates, slides or slide based imaging chambers. Irrespective of the method, all samples imaged in this thesis were gemmae transferred from gemma cups at the start of the experiment, imaged at various time points afterwards. The initial day of the experiment was always labelled as Day 0, with Day 1 corresponding to samples 24h after gemmae germination.

For single time-point or short term (>24h) time-lapse imaging, gemmae were mounted on microscopy glass slides. 65µL Geneframes (ThermoFisher) were placed on glass slides and filled with sterile water. Gemmae were transferred from gemma cups using sterile inoculation loops and placed on the water. 22x22mm No. 0 coverslips were carefully placed on top to seal samples, taking care to remove air bubbles where possible. For extended time-lapse imaging (up to 3 days), five gene frames were stacked on a glass slide generating a chamber. The chamber was filled almost to the top with 0.5 Gamborg agar media by carefully pipetting 300µL of molten 0.5 Gamborg media in the chamber. Once the media solidified gemmae were placed on the agar and the chamber was sealed with a coverslip as above.

For time course imaging, gemma were placed on 50mm 0.5 Gamborg agar plates and grown as described above. When imaging, plates were unsealed and lids removed to image gemmae directly on the agar surface. Samples prepared using this method were imaged at most once every 24h and for up to 1h at a time to prevent excessive moisture loss, which may impair gemmae growth.

2.3.2 Epifluorescence microscopy

Transformed Marchantia plantlets and plants expressing fluorescent proteins were screened for positive transformants and highly fluorescent lines inside sealed 0.5 Gamborg plates using a Leica M205 FA fluorescence stereo microscope, with filter settings summarized in table 2.3.

Table 2.3 Leica M205 FA filters

Channel	Part No.	Excitation	Collection
CFP	10 447 409	426-446nm	460-500nm
GFP	10 447 408	450-490nm	500-550nm
YFP	10 447 410	490-510nm	520-550nm
Chlorophyll LP	10 447 407	460-500nm	510nm LP

2.3.3 Confocal microscopy

All fluorescence imaging shown in this thesis was performed on a upright Leica SP8 confocal system equipped with: a super continuum white light laser (WLL), 405nm and 405nm diode lasers and four high sensitivity hybrid detectors (HyD). Typically, images of gemmae at day 0 or 1 were acquired using a HC PL APO 20x/0.75 CS2 dry objective while older plants were imaged with a HC PL APO 10x 0.40 CS2 dry objective. The HC PL APO 40x/1.10 W CORR CS2 water immersion objective was used for higher magnification imaging. Confocal imaging settings are summarised in table 2.4. Typically, 1024x1024px images were acquired using bidirectional scanning with scan speeds of 200-600kHZ and z-stacks with 3-10µm step size. HyD detectors were used in standard mode, but all fluorophores except chlorophyll were imaged using temporal gating, collecting signal from 1-10ns to reduce noise and artifacts from light reflection. For multispectral imaging, separate sequential scans were used for each fluorophore, except chlorophyll which was acquired in the same scan with mturquoise2 or EGFP if present.

2.3.4 Light microscopy

Marchantia plants were imaged in 0.5 Gamborg plates using a Keyence VHX 5000 digital microscope equipped with a VH-Z20T lens (20x-200x).

Table 2.4 Leica SP8 imaging settings

Fluorophore	Excitation	Collection
mTurqouise2	442nm (Diode)	465-485nm
EGFP	488nm (WLL)	500-520nm
mVenus	515nm (WLL)	520-540nm
mScarlet	570nm (WLL)	580-620nm
Chlorophyll	442nm (Diode)	650-700nm

2.3.5 Image processing

All images were processed using Fiji [281] an ImageJ [1] distribution. Leica lif files were imported using the Bioformat Importer plugin. For z-stacks, maximum intensity projections were generated for each channel. Unless signal intensity was quantified or compared across conditions, each channel was adjusted to cover the full 8-bit range by using the enhance contrast method (histogram stretching) to saturate 0.1% of pixels. Multispectral images were generated using the merge colors function, assigning each greyscale channel image to the indicated color lookup tables. Scale bars were added using the Set Scale tool. Processed images were saved as jpeg files (compression level = 85) before being displayed in this theses to reduce file sizes.

2.3.6 Laser microdissection

Cell ablation was performed using a Leica LMD6000 laser microdissection microscope equipped with a solid state 355nm cutting laser. Gemmae were placed on 50mm 0.5 Gamborg agar plates and cut without further sample handling. Ablation of large regions was performed using the draw and cut function at 10x magnification using maximum laser power, aperture set to 50 and speed set to 40. Ablation of individual cells was also performed with the draw and cut function but using 40x magnification and the following settings: laser power = 10, aperture = 5, speed = 10. Samples were typically imaged using confocal microscopy without further sample preparation.

2.4 Bioinformatics

Scripts used for data analysis are available in the online supplementary information.

2.4.1 Gene orthologs

Marchantia gene orthologs were identified using Orthofinder [74, 75]. Protein sequences of primary transcripts were obtained from Phytozome [104]. The Orthofinder pipeline was run with default settings. Gene trees of specific orthogroups were visualised using Dendroscope [139, 140].

2.4.2 Analysis of public bulk RNA-sequencing data

Fastq files for the following BioProject study accessions: PRJDB4420 [131], PRJDB5890 [178], PRJDB6579 [351], PRJDB7023 [29], PRJNA218052 [288], PRJNA265205 [91], PRJNA350270 [29], PRJNA397394 [221], PRJNA433456 [89], and PRJNA251267 [29] were obtained from the European Nucleotide Archive. TrimGalore was used to inspect read quality and trim low-quality reads and sequencing adapters. Reads were pseudo-aligned using kallisto [31] to the Tak1 reference genome v5.1 (available at marchantia.info). This collection of bulk-RNA sequencing data is available in the supplementary information of Sauret-Gueto et al. [279]

2.4.3 Single cell data generation

Marchantia protoplasts were generated by Mihails Delmans and sequencing libraries were generated by Mihails Delmans and the Cancer Research UK Cambridge Institute Genomics core facility (CRUK).

Approximately 150 CAM-1 (male) Marchantia gemmae were grown on a 0.5 Gamborg agar plate for 4 days. 10mL 0.6M Mannitol solution was pipetted to the plate, submerging plants. The plate was placed on a platform shaker at 50rpm at room temperature for 20min. Driselase solution was prepared by adding 2% Driselase (Sigma-Aldrich, D9515) to 0.6M mannitol solution, mixing for 15min on a platform shaker at 100rpm. Once dissolved, the mixture was centrifuged at 2500rpm for 5min and the supernatant filter sterilised using a 0.2µm syringe filter. Mannitol solution was removed from the plate by pipetting and replaced with 10mL of Driselase solution. The plate was incubated at room temperature on a platform shaker at 30rpm for 4h. After digestion, the protoplast containing liquid was transferred to a 50mL Falcon tube and passed through a 70µm cell strainer. Protoplasts were centrifuged for 10min at 50g with minimal acceleration and deceleration. The supernatant was removed and protoplast were resuspended in 200µL 0.6M mannitol. Cell count and viability were accessed using fluorescein diacetate (FDA, Thermo Fisher Scientific, F1303) staining. 5 mg/mL FDA was dissolved in acetone and 20µL added to 1mL of 0.6M mannitol

solution to generate a working stock. 10µL protoplast solution was mixed with 10µL FDA working stock, loaded on a haemocytometer and imaged using the ET YFP on the Leica M205 FA epifluorescence microscope. Single cell RNA-seq libraries were generated from the protoplast sample using the Single Cell 3' Reagent Kit v2 (10x Genomics) according to manufacturers instructions. The total time from removing plants from the growth room to cell lysis during library preparation was approximately 6 hours. Libraries were sequenced to a depth of approximately 300 million reads.

2.4.4 Count matrix generation

Reads were processed using the kallisto-bustools pipeline (kb-python v0.24.4) [216] mapping against the Marchantia Tak1 reference genome v5.1 (available at marchantia.info). To separate cells from empty droplets, the raw count matrix was loaded using anndata (v0.7.6) and a kneeplot was generated using NumPy (v1.19.5) [121], pandas (v1.1.5) [213] and matplotlib (v3.4.3) [138] in python (v3.6.9). Based on the kneeplot a UMI threshold of 2000 was chosen to filter the count matrix. After removing barcodes with fewer than 2000 UMI, we also removed barcodes with fewer than 200 detected genes and genes expressed in fewer than two cells. The filtered count matrix contained measurements of 16682 genes across 7456 cells.

2.4.5 Dimensionality reduction and clustering

Downstream analysis was performed in Scanpy (v1.8.1) [344]. For clustering and dimensionality reduction a normalised count matrix was generated. Gene expression for each cell was normalised to 10,000 UMI per cell and log transformed using the Scanpy functions sc.pp.normalize_total() and sc.pp.log1p(). Next, highly variable genes were identified using sc.pp.highly_variable_genes() with flavor="seurat". Genes were scaled to unit variance using sc.pp.scale() with max_value=10 to clip values exceeding 10 standard deviations. Principal components were calculated for a subset of the normalised expression matrix that contains only the highly variable genes identified prior, using sc.tl.pca() with svd_solver='arpack' and use_highly_variable=True. The top 20 principal components by variance ratio were used to compute neighbours and a UMAP projection [212] using sc.pp.neighbors() with n_neighbors = 50 and n_pcs=20 and sc.tl.umap() with min_dist=0.1. Leiden clustering [326] was used to assign cell clusters by running sc.tl.leiden() with resolution=0.95. Diffusion pseudotime [113, 344] was calculated using sc.tl.diffmap() and sc.tl.dpt() with default settings. All plots were generated using Scanpy plotting functions or matplotlib.

2.4.6 Marker gene identification

Marker genes for cell clusters were identified using the sc.tl.rank_genes_groups() function in scanpy using leiden clusters and the wilcoxon rank-sum test. This function returns a list of genes for each cluster ranked by the test-statistic. We selected candidates for validation from the 20 highest ranked genes. Marker genes should ideally display binary expression in clusters. However, statistical tests often assign high scores to abundant genes with small but consistent difference in expression between clusters. Expression patterns for top 20 candidate genes were manually examined to prioritise genes with maximal specificity of expression. Gene annotations were also manually checked to avoid very short genes or genes with poor annotation, to avoid potential pseudogenes. Promoter sequences for candidate genes were obtained from the Tak1 reference genome v5.1 (available at marchantia.info). The DNA sequence 1.8kb upstream of the putative transcription start site and the 5' untranslated region where present, were synthesised. The sequence length was chosen to be consistent with parts obtained from the promoter screening library (Chapter 3), which was constrained by the requirements of the DNA synthesis provider (Twist Biosciences). The first nucleotides of these sequences can be found in table 2.1.

2.4.7 Gene set scoring

For figures showing expression of gene collections, sc.tl.score_genes() was used to calculate a gene expression score which was calculated as the average gene expression of a list of genes minus the average expression of a reference gene set which was randomly sampled from a gene pool with similar expression levels [277]. Gene lists were obtained from functional annotation of the Marchantia genome v6.1 (available at marchantia.info) or previously published work as indicated in table 2.5

Table 2.5 Gene sets for expression scores

Set name	Term/Source
Photosynthesis	GO:0015979
Cell Wall	GO:0042546, GO:0030244
Expansin	PR01226
Auxin response	PF02519
ABA response	Eklund et al. [71]

2.4.8 Rhizoid subset

The rhizoid cluster was re-analysed separately from the remaining data to identify rhizoid sub-clusters. First, the count matrix was filtered for barcodes that were previously identified as rhizoid cells by leiden clustering. This subset of the matrix was processed as described in 2.4.5 except UMAP projection and leiden clustering, where n_neighbors = 20, n_pcs=8, min_dist=0.01 and resolution=1 was used instead.

2.4.9 RNA velocity analysis

RNA velocity was introduced by La Manno et al. [182] and we used Scvelo [19] to perform RNA velocity analysis. RNA velocity analysis was restricted to rhizoid cells as the fraction of unspliced reads was generally very low (4%), requiring high expression to get reliable velocity estimates and rhizoids had higher average UMI counts than other cells.

Chapter 3

Identifying novel cell markers by screening a proximal promoter library

3.1 Introduction

Part of the work presented in this chapter has been published in:
Susana Sauret-Güeto, Eftychios Frangedakis, Linda Silvestri, Marius Rebmann, Marta Tomaselli, Kasey Markel, Mihails Delmans, Anthony West, Nicola J. Patron, and Jim Haselof *"Systematic tools for reprogramming plant gene expression in a simple model, marchantia polymorpha"*. (2020) ACS Synthetic Biology, 9(4):864–882 [279].

Since the advent of microscopy, cell types have been categorised based on their morphology, lineage relationships and cell responses to experimental perturbations. However, while cell morphology can be diagnostic of distinct cell function, cell morphology can be very plastic and populations of morphologically indistinguishable cells may perform different functions in a tissue. Cell functions are determined by the combination of genes expressed in a cell at any given time. Consequently, cell type definitions would ideally be based on live measurements of the complete set of genes expressed in a cell at any given moment. While no such method has been developed so far, advancements in molecular biology tools have enabled a shift towards defining cell types based on the expression of genes. The development of reporter genes such as green fluorescent protein (GFP) [36] enabled the construction of reporter constructs where the reporter genes is expressed from a promoter sequence, comprising binding sites for RNA-polymerase as well as upstream regulatory sequences. This can be used to obtain a proxy measurement of gene expression in living cells. By combining the expression of different marker genes, robust cell type classification

can be obtained. In combination with transcriptomic measurements and functional validation of gene function, this underpins our modern understanding of plant cell types, particularly in well studied model systems such as the Arabidopsis shoot and root meristems.

Once characterised, promoters can also be valuable tools for driving expression of genes of interest in specific cell types or tissues. These can be used to further probe the function of cells and the gene networks that drive their identity and can also be used to add novel interactions which may drive new functionality.

The field of synthetic biology has catalysed the development of fast, efficient and modular DNA assembly techniques such as type IIs assembly [77], greatly expanding the throughput of DNA assembly. At the same time, DNA synthesis has emerged as an economical and highly scalable method to obtain genetic parts, owing to continuous improvements in lowering cost and error rates [136]. In combination, these developments permit the assembly of large collections of reporter constructs to screen the function of genetic elements such as promoter sequences.

The sequencing of the Marchantia genome revealed remarkably low genetic redundancy in regulatory genes for hormone signaling pathways and transcription factor families [29]. Comprehensive comparisons with other plant genomes suggest that the number of transcription factors in Marchantia is low compared to other land plants and more similar to numbers found in algae [343]. Figure 3.1 illustrates this, showing the number of transcription factors across common algal and plant model species using data from PlantRegMap [323]. The most abundant transcription factor families in Marchantia are coloured, but clear trends in transcription factor abundance are evident across all families. Recent high quality genome assemblies of *Anthoceros agrestis* [187, 358] suggest that some hornwort genomes may contain even fewer transcription factors. However, some of the differences in TF numbers arise from lineage specific loss or gain of transcription factors. Both Anthoceros and Marchantia have single transcription factors for many transcription factor subfamilies known to be important for plant development, suggesting a close to minimal repertoire of transcription factors [358].

In this chapter I present preliminary results of a lab wide effort to generate fluorescent reporter lines for proximal promoter sequences of all 398 transcription factors in Marchantia. Proximal promoters may not fully recapitulate gene expression, but this collection should provide a rich source of DNA parts for tissue specific expression in Marchantia. Results for the first 76 promoters which were successfully cloned into reporter constructs and transformed into Marchantia are presented in this chapter. For each reporter, gemmae were imaged via confocal microscopy for the first seven days of gemma development to obtain a time-course of reporter expression at cellular resolution. 46/76 genes showed expression at some stage of gemma development. We identified novel markers of differentiated cell types, including oil

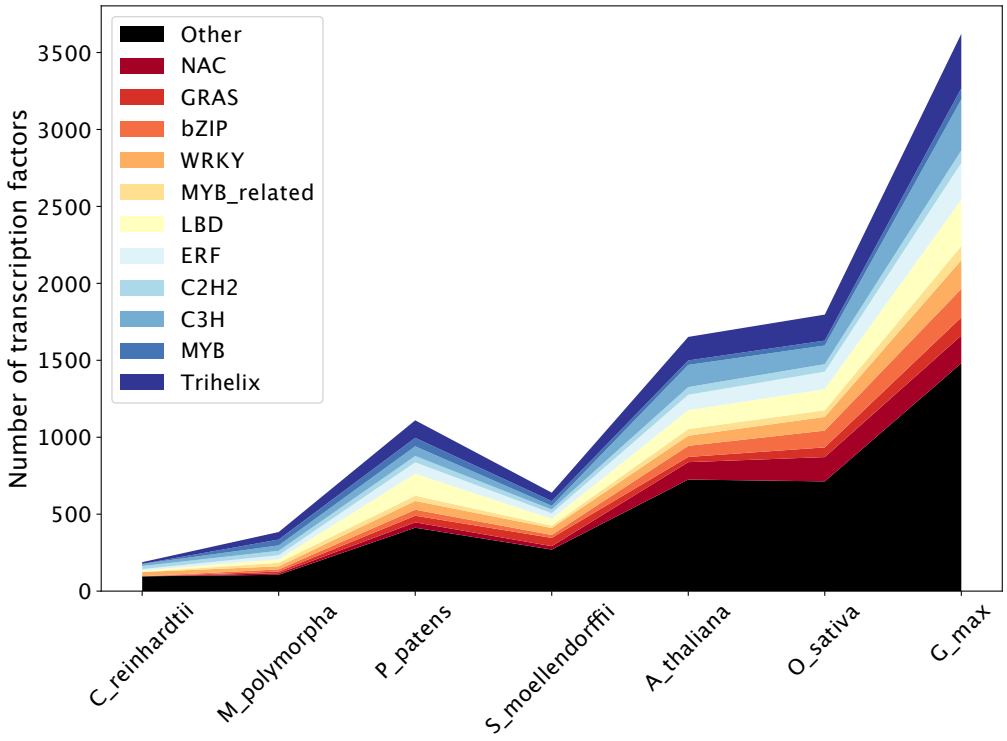

Fig. 3.1 **Number of transcription factors for common model plant species.** Transcription factor numbers were obtained from PlantRegMap [323]. Transcription factor families with the largest number of genes in Marchantia are colored.

bodies, rhizoids and air chamber pore cells. Most genes that showed expression, displayed proximal-distal gradients, either showing highest expression in the meristem or in distal cells. Promoters of Marchantia homologues of the angiosperm core meristem regulators *WUSCHEL* and *PLETHORA* were not expressed in the Marchantia meristem. While the screening of all promoters of transcription factors has not been completed yet, we obtained many new genetic markers which enabled improved annotation of cell types in Marchantia and provided valuable reference markers for the remaining work presented in this thesis.

3.2 Library overview and construct design

Proximal promoter sequences were computationally extracted from the CAM1 genome [53] by Mihails Delmans. If the predicted 5'UTR of a gene was shorter than 500bp, the promoter sequence included the DNA sequence 1.8 kbp upstream of the start codon, otherwise the promoter sequence covered 1.8 kbp upstream of the transcription start and a separate 5'UTR part was synthesised. The length of the regulatory sequence was constrained by size requirements for cost effective DNA synthesis (Twist Biosciences). Susana Sauret-Güeto and Jenna Rever coordinated the project, Linda Silvestri, Emmanuelle Orisini, Alicja Szalapak, Marius Rebmann, Marta Tomaselli performed DNA assembly of reporter constructs and Marchantia transformations. Marius Rebmann and Marta Tomaselli performed confocal the initial imaging of all 76 constructs. All images shown in this work were acquired by the author.

For each promoter part, we assembled a level 1 transcription unit using loop assembly [245, 279] (see chapter 2.1.2). We fused the promoter part to the mVenus coding sequence [177] and added the N7 nuclear localisation tag from Arabidopsis [49]. Nuclear localisation provides several advantages over cytoplasmic fluorescent reporters. Nuclear localised fluorescence concentrates the reporter signal in a small area, improving signal to noise. Nuclei size in plants also scales with DNA content but not cell size, therefore normalising the signal for cells of varying size. We then assembled level 2 constructs which also included a resistance cassette as well as reference markers for the nucleus and the cell membrane (Figure 3.2 A). The aim of the reference markers was to enable ratiometric fluorescence quantification [81] and cell segmentation. However, the promoters we used to drive our reference markers failed to induce ubiquitous expression, limiting their utility. For the remaining work, we therefore only imaged mVenus to capture the expression of our genes of interest and chlorophyll autofluorescence as a counter marker to visualise gemma architecture.

76 reporter constructs were transformed into Marchantia sporelings (Table 3.1). Primary transformants were screened for fluorescence using epifluorescence microscopy and propa-

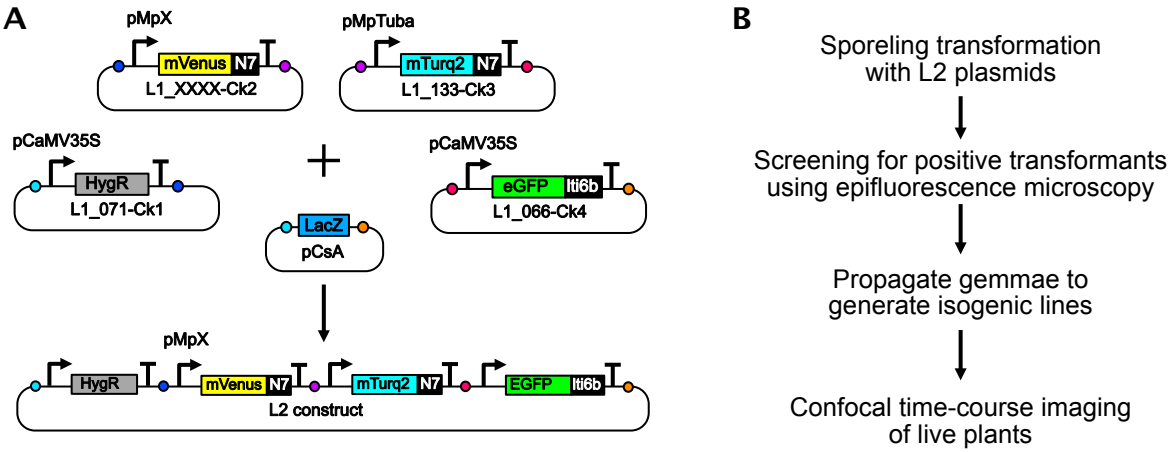

Fig. 3.2 **Construct design and screening strategy** (**A**) Cloning strategy for transcription factor screening. The promoter of interest (pMpX) is assembled into a L1 construct with the mVenus coding sequence, a N7 nuclear localisation signal [49] and a terminator [279]. A L2 loop assembly combines the reporter construct with a hygromycin resistance cassette, a nuclear reference marker expressing nuclear localised mTurq2 from the MpTUBA (Mp4g00550) promoter and a membrane marker expressing eGFP with the lti6b tag [49] from the cauliflower mosaic virus 35S promoter (pCaMV35S). Inserts replace the lacZ coding sequence in the pCsA backbone, permitting blue-white screening on X-Gal plates. Colored circles indicate type IIs fusion sites which determine the position of parts in the final assembly [279]. (**B**) Overview of screening strategy

gated until gemma formed. Gemma form from individual cells at the base of gemma cups [14, 137] providing a simple method to obtain isogenic lines. For each gene, we imaged at least three independent isogenic lines from different transformation events, to avoid artifacts arising from the genomic integration site, which can have profound effects on transgene expression [103]. We performed time course confocal imaging for all plants, imaging live, growing plants directly on 0.5 Gamborg agar at the day of gemma removal from the gemma cup (Day 0), two days after germination (Day 2), on Day 4 or 5 after germination and on Day 7. For simplicity, I only show images from Day 0 and Day 4/5 in this Chapter. 46 promoters showed expression at some stage of gemma development, while approximately one third of the promoters showed no detectable fluorescence during early gemma development (Table 3.1). In this chapter I focus on genes with meristematic expression, but examples of marker gene expression for differentiated cell types are shown in Chapter 4 and in previously published studies [279, 325].

3.3 Expression of putative angiosperm meristem gene orthologs

Given the relatively short length of regulatory sequence included for our promoter sequences, our reporters may not perfectly recapitulate native gene expression. However these sequences should nonetheless approximate gene expression patterns and provide a collection of expression patterns that could be used to classify cell types. Our main interest for this work was the identification of marker genes that would define distinct domains of the Marchantia meristem. Gemma meristems are located inside the notches on either side of the tissue (see chapter 1.4.6). The gemma meristem comprises a slowly proliferating centre and a surrounding proliferation zone where rapid rates of cell division are observed [299, 25]. While there is considerable variability between gemma, the proliferation zone typically extends to approximately a third of the distance between the centre of the notch and the centre of the gemmae. Novel marker genes could help to establish clearer boundaries of meristem domains, providing a framework for cell classification which may reveal insights into gemma meristem regulation.

In Arabidopsis, the expression of core meristem regulators such as *WUSCHEL* has been used to define distinct cell populations in the shoot apical meristem [286]. The Marchantia genome only contains one *WUSCHEL*-related HOMEOBOX gene, Mp *WOX* (Mp1g11660) [29]. We assembled a transcriptional reporter for Mp *WOX* and observed expression in Marchantia gemma. In contrast to the expression of *WUSCHEL* in the centre of the SAM

Table 3.1 List of genes for which reporters were imaged in Marchantia

Gene name	Gene ID	Expression detected	Notable A. thaliana orthologs
Mp3R-MYB1	Mp1g08640	Yes	MYB3R1, MYB3R4
MpAP2L3	Mp5g10280	No	
MpAP2L4	Mp6g16760	No	
MpAPB/MpAP2L1	Mp8g11450	Yes	PLT1
MpARF1	Mp1g12750	Yes	MP
MpARF2	Mp4g11820	Yes	ARF1-4
MpASLBD10	Mp5g17820	No	
MpASLBD12	Mp5g11460	No	
MpASLBD13	Mp6g05810	No	
MpASLBD14	Mp6g09270	No	
MpASLBD15	Mp1g14500	Yes	
MpASLBD16	Mp6g06850	Yes	
MpASLBD19	Mpzg00130	Yes	
MpASLBD2	Mp8g11560	Yes	
MpASLBD24	Mp3g12980	Yes	
MpASLBD7	Mp5g21080	Yes	
MpBHLH1	Mp5g03020	No	
MpBHLH11	Mp4g15560	Yes	
MpBHLH13/MpFIT	Mp2g20990	Yes	FIT
MpBHLH15	Mp6g18480	No	
MpBHLH16	Mp4g04910	No	
MpBHLH17/MpSCRM2	Mp4g04920	No	SCRM2
MpBHLH18	Mp6g10690	Yes	
MpBHLH2	Mp2g00890	No	
MpBHLH21	Mp3g11900	Yes	
MpBHLH22	Mp8g18080	No	
MpBHLH23	Mp4g06170	Yes	
MpBHLH24	Mp8g04130	Yes	
MpBHLH27	Mp1g19210	Yes	
MpBHLH29	Mp2g07150	Yes	
MpBHLH3	Mp2g00910	No	
MpBHLH36	Mp2g04180	No	
MpBHLH38	Mp4g19650	Yes	
MpBHLH4	Mp2g00930	No	
MpBHLH40	Mp5g18910	Yes	
MpBHLH42	Mp5g09710	Yes	
MpBHLH45	Mp2g19970	Yes	
MpBHLH47	Mp2g00500	Yes	
MpBHLH49	Mp2g26400	No	
MpBHLH7/MpTMO5	Mp3g17260	No	TMO5
MpBHLH8	Mp2g06450	No	
MpBHLH9	Mp2g06460	No	
MpBNB	Mp3g23300	Yes	BNB1/2
MpBZR1	Mp8g07390	Yes	BZR1/BES1
MpERF20/MpLAXR	Mp5g06970	Yes	ESR1
MpGRAS1	Mp1g20490	Yes	
MpGRAS2	Mp7g12630	Yes	
MpGRAS3	Mp1g10440	No	
MpGRAS4	Mp2g03850	No	
MpGRAS5	Mp6g13820	No	
MpGRAS6	Mp5g20660	No	
MpGRAS7	Mp8g01770	Yes	
MpMYCX	MpUg00430	No	
MpNAC1	Mp2g07720	Yes	CUC
MpNAC2/MpCUCA	Mp6g02590	Yes	CUC
MpNAC3	Mp4g11910	Yes	
MpNAC4	Mp4g22890	Yes	
MpNAC5	Mp6g20920	No	
MpNAC6	Mp5g01530	No	
MpNAC7	Mp6g02620	Yes	
MpNAC8	Mp6g02670	No	
MpNAC9	Mp5g08410	Yes	
MpRSL1	Mp3g17930	Yes	RSL1
MpRSL2/MpBHLH28	Mp6g21470	Yes	
MpRSL3/MpBHLH33	Mp1g01110	Yes	
MpTCP2	Mp1g19590	No	
MpWIP	Mp1g09500	Yes	WIP1-6
MpWOX	Mp1g11660	Yes	WOX5
MpWRKY10	Mp7g06550	Yes	
MpWRKY11	Mp1g24950	Yes	
MpWRKY12	Mp4g00200	Yes	
MpWRKY13	Mp4g00180	No	
MpWRKY3	Mp5g05560	Yes	
MpWRKY6	Mp1g08960	Yes	
MpWRKY7	Mp3g17660	Yes	
MpWRKY8	Mp2g20960	No	

dome in angiosperms, we observed a gradient of Mp *WOX* promoter expression which increased with the distance of cells from the meristem, with minimal expression in the centre of the meristem (Figure 3.3). Mp *WOX* reporter expression was also notably absent from rhizoid precursor cells or mature rhizoids. This expression pattern was consistent across developmental stages and different transgenic lines, which indicates that Mp *WOX* may be predominantly present in differentiated cells, potentially arguing against a role as a stem cell promoting factor in Marchantia. Indeed, recent characterisation of CLE peptide signaling in Marchantia suggests that, while CLE peptides are regulators of the Marchantia meristem, they act independently of Mp *WOX* and Mp *WOX* does not have a prominent role in meristem regulation in Marchantia [133]. This is consistent with results in Physcomitrium where *PpWOX13L* has been characterised as a regulator of cell wall loosening and affects cell regeneration, but does not affect meristem function [273].

AINTEGUMENTA, *PLETHORA* and *BABY BOOM* (APB) form another key family of meristem regulators in angiosperms. Physcomitium APB genes are expressed in the gametophore apical cell and required for gametophore development, suggesting that APB function as meristem regulators may be conserved in bryophytes [8]. However, when we imaged a transcriptional reporter for Mp *APB* (Mp8g11450), the only clear APB homologue in Marchantia [358], we also observed reduced expression in the gemma meristem (Figure 3.3). Similar to Mp *WOX* we also observed no expression for the Mp *APB* reporter in rhizoid precursors or mature rhizoids. The exclusion of Mp *APB* reporter expression from the meristem may argue against a role of Mp *APB* in the regulation of the Marchantia meristem, although functional characterisation of Mp *APB* will be needed to verify this. GRAS transcription factors form another important group of meristem regulating transcription factors in Angiosperms which include *HAIRY MERISTEM* (*HAM*) [78, 369, 370], *SHORT-ROOT* (*SHR*) [125] and *SCARECROW* (*SCR*) [58]. While there are no clear orthologs of *HAM* or *SCR* in Marchantia, we did observe expression of one Marchantia GRAS gene promoter Mp *GRAS1* (Mp1g20490) in the gemma meristem (Figure 3.3). Mp *GRAS1* reporter expression was highest in a small population of cells in the centre of the meristem, while surrounding meristematic cells showed reduced expression and distal cells showed increased expression again. The area showing reduced expression roughly corresponds to the proliferation zone of the gemma meristem [25, 299], suggesting that Mp *GRAS1* may be a negative marker of highly proliferating cells.

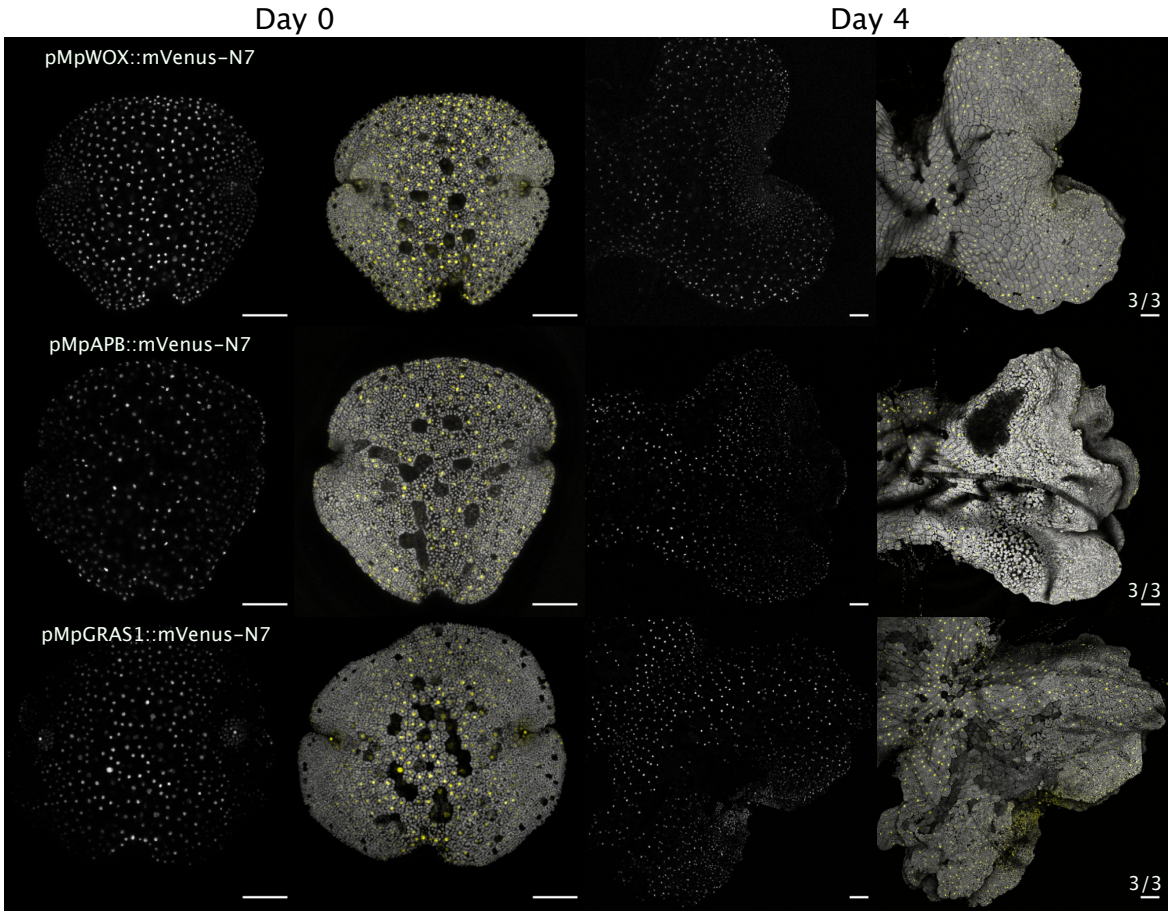

Fig. 3.3 **Expression of Marchantia homologues for Angiosperm meristem marker genes** Maximum intensity projections of confocal z-stack images of transgenic gemma at indicated time-points after germination on 0.5 Gamborg media. Each row shows expression of the indicated construct. First column shows reporter fluorescence in greyscale, second column shows a composite image with reporter expression in yellow and chlorophyll autofluorescence in grey. Third and fourth column are the same as the first and two but show images of the same plant after four days of growth. Numbers above the scale bar indicate the number of independent transgenic lines imaged, which showed comparable expression. All scale bars 100µm.

3.4 New meristem markers

While we were unable to observe meristematic expression for some homologues of core angiosperm meristem genes, we identified a number of uncharacterised genes, whose promoter expression was restricted to the gemma meristem. Images for four of these promoters are shown in Figure 3.4. The Mp *BHLH42* (Mp5g09710) reporter showed very specific and bright expression exclusively in the centre of the meristem. This expression pattern persisted at later stages of development. While the function of this gene has not been characterised so far, co-expression analysis suggests that Mp *BHLH42* is implicated in auxin signaling [90] which is a key driver of meristem regulation in Marchantia [171]. We observed slightly broader, meristematic expression for the promoter of Mp *BZR1* (Mp8g07390) one of three BZR/BES type transcription factors in Marchantia. BZR/BES transcription factors control meristem proliferation in Arabidopsis through brassinosteroid (BR) signaling [37], which suggests that Mp *BZR1* may also play a role in meristem regulation in Marchantia. Indeed, a recent study showed that Mp *BZR1* is the only close homologue to *AtBZR1* [337] and *AtBES1* [355] and characterised Mp *BZR1* function in Marchantia [215]. Mecchia et al. [215] demonstrated that Mp *BZR1* controls cell proliferation in the Marchantia meristem, despite the absence of BR receptors in Marchantia [84, 95]. The authors of this study did not investigate Mp *BZR1* expression, but based on our observations, Mp *BZR1* expression appears to be highest in cells of the proliferation zone [25, 299], consistent with the functional characterisation of Mp *BZR1*. We observed very similar expression for the promoter of another bHLH transcription factor Mp *BHLH29* (Mp2g07150) which was expressed across the meristem in gemma. However, expression for this gene was very dim overall, preventing us from obtaining clear images at later stages of development. The promoter sequence of Mp *WRKY11* (Mp1g24950) showed very specific expression in the centre of the gemma meristem in some lines, however the expression patterns for the Mp *WRKY11* reporter were variable across different transgenic lines and across development for individual lines, making this reporter a relatively unreliable marker to define cell domains.

We also observed a number of reporters which showed meristematic expression as well as expression in specific cell types such as rhizoid precursors. Mp *NAC1* (Mp2g07720) and Mp *BHLH13* (Mp2g20990) are two examples of these expression patterns and are shown in Figure 3.5. Mp *NAC1* is tightly co-expressed with the auxin response regulators Mp *ARF1* and Mp *ARF2* suggesting a potential connection to auxin response [90]. Indeed, Mp *NAC1* is a homologue of CUP-SHAPE COTYLEDON which controls organ separation in Arabidopsis [3] and is intimately linked to auxin signaling [124]. Given its homology and expression in the wider meristem Mp *NAC1* is a promising target for the regulation of meristem boundary formation, but functional validation of Mp *NAC1* will be required to determine if it has a role

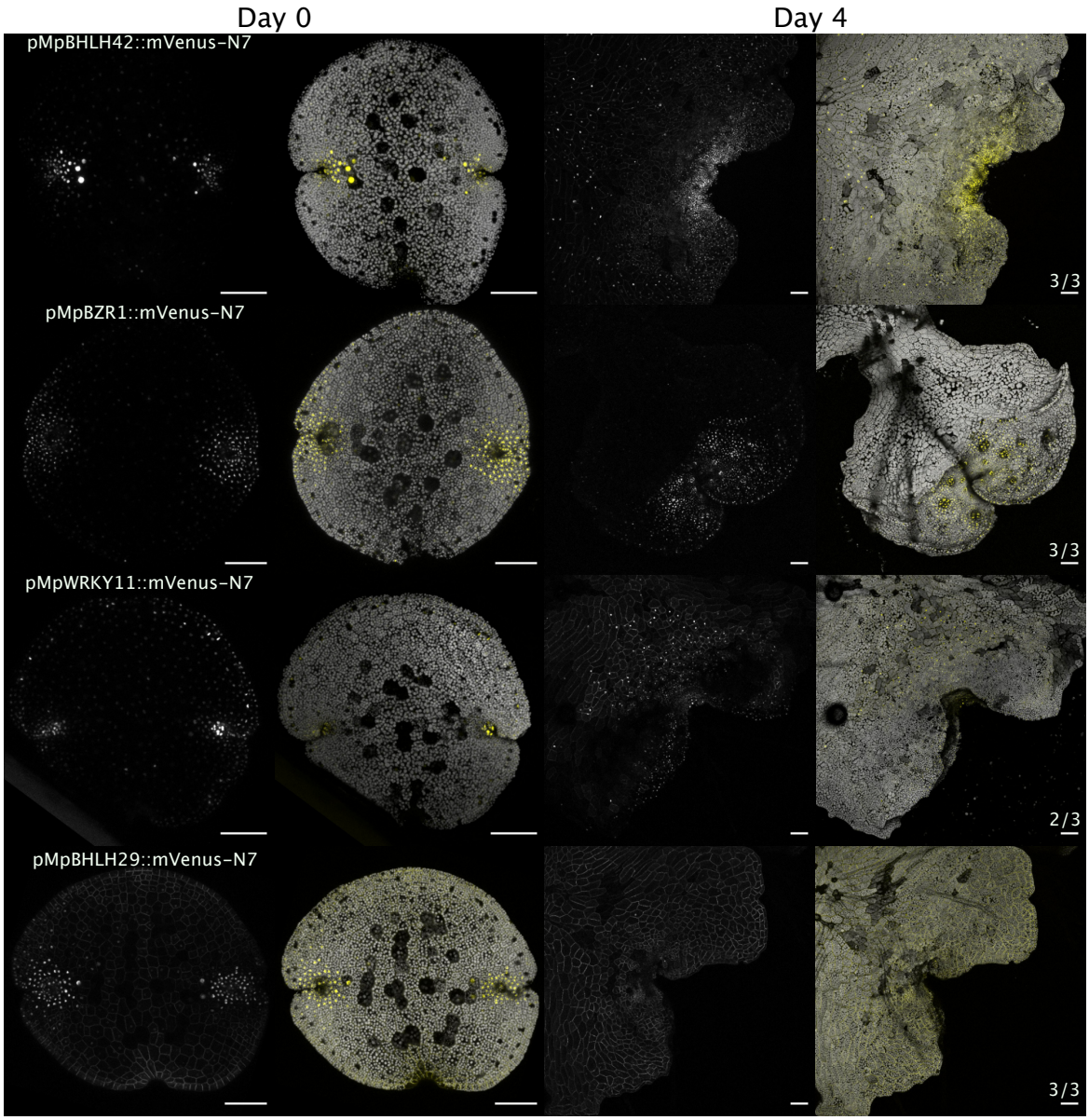

Fig. 3.4 **Expression patterns of new meristem marker genes** Confocal images of transgenic gemma at indicated time-points after germination on 0.5 Gamborg media. Each row shows expression of the indicated construct. First column shows reporter fluorescence in greyscale, second column shows a composite image with reporter expression in yellow and chlorophyll autofluorescence in grey. Third and fourth column are the same as the first and two but show images of the same plant after four days of growth. Numbers above the scale bar indicate the number of independent transgenic lines imaged, which showed comparable expression. All scale bars 100µm.

in regulating the gemma meristem. Mp *BHLH13* has recently been identified as a homolog of *AtFIT* [199]. *AtFIT* regulates iron homeostasis [45], Mp *BHLH13* appears to perform a similar role and has been suggested to be re-named Mp *FIT1* [199].

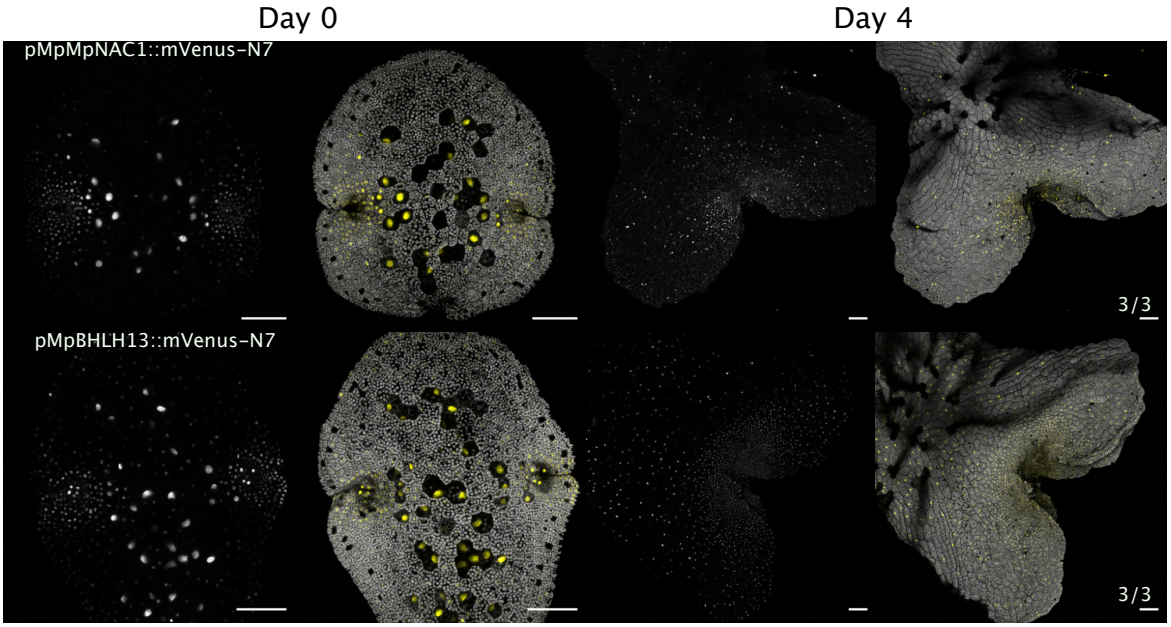

Fig. 3.5 **Expression patterns of genes with complex meristematic expression** Confocal images of transgenic gemma at indicated time-points after germination on 0.5 Gamborg media. Each row shows expression of the indicated construct. First column shows reporter fluorescence in greyscale, second column shows a composite image with reporter expression in yellow and chlorophyll autofluorescence in grey. Third and fourth column are the same as the first and two but show images of the same plant after four days of growth. Numbers above the scale bar indicate the number of independent transgenic lines imaged, which showed comparable expression. All scale bars 100µm.

3.5 Differentiation markers

Finally, we also identified several promoters which showed gradients of increasing expression with increasing distance to the meristem. These promoters represent negative markers of the meristem and displayed a variety of patterns of expression. Mp *NAC2* (Mp6g02590) reporter expression was very clearly and broadly excluded from the meristem at all developmental stages, while Mp *ASLBD24* (Mp3g12980) promoter expression was only reduced but not absent from the meristem (Figure 3.6). The Mp *NAC4* (Mp4g22890) reporter showed an intermediate expression pattern compared to Mp *NAC2* and Mp *ASLBD24* also indicating reduced abundance of this gene in the gemma meristem.

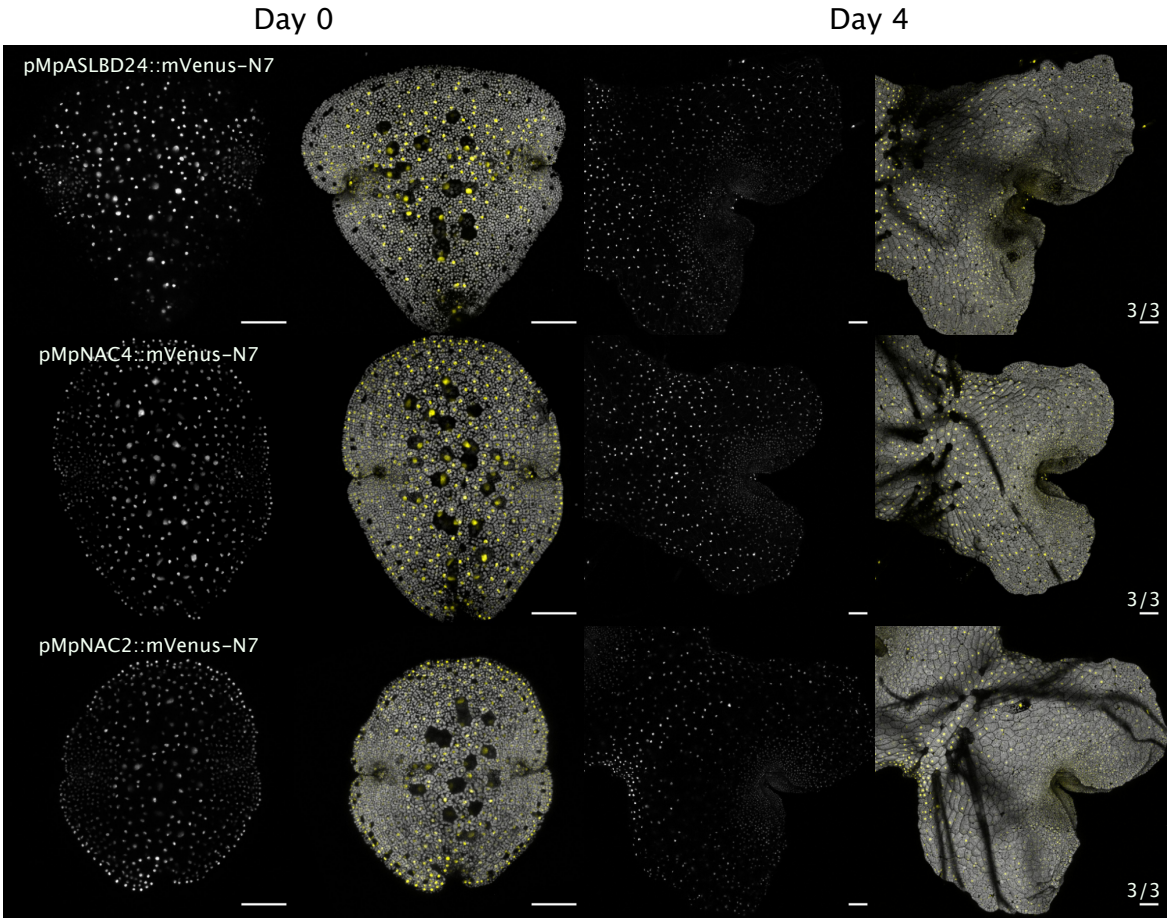

Fig. 3.6 **Expression patterns of genes with reduced expression in the meristem** Confocal images of transgenic gemma at indicated time-points after germination on 0.5 Gamborg media. Each row shows expression of the indicated construct. First column shows reporter fluorescence in greyscale, second column shows a composite image with reporter expression in yellow and chlorophyll autofluorescence in grey. Third and fourth column are the same as the first and two but show images of the same plant after four days of growth. Numbers above the scale bar indicate the number of independent transgenic lines imaged, which showed comparable expression. All scale bars 100µm.

3.6 Discussion

In this chapter I present the initial results of screening the expression patterns of proximal promoter elements for all transcription factors in Marchantia. 76 promoters have been screened so far and 46 promoters showed expression during gemma development, providing a rich source of promoter activities. Most genes displayed ubiquitous expression or gradients of meristematic or non-meristematic expression. We screened homologues of important Arabidopsis shoot and root meristem regulators and identified several new positive and negative regulators of the Marchantia meristem which can be used to define meristem domains.

We observed reduced expression of a reporter for the *WUSCHEL* homologue Mp *WOX* in the gemma meristem, in contrast to the expression of *WUS* in the centre of the SAM in Arabidopsis. Mobility is a critical aspect of WUS protein function and our transcriptional reporter does not rule out the possibility that MpWOX protein could move from surrounding cells into the centre of the Marchantia meristem. However, cross species complementation analysis suggests that the stem cell promoting function of WOX proteins evolved in vascular plants, while WOX cell-cell mobility evolved in the common ancestor of seed plants after divergence from ferns [364]. This is consistent with the function of WOX proteins in Physcomitrium [273] and the characterisation of Mp *WOX* loss of function mutants in Marchantia, which do not show clear meristem defects [133]. These results strongly suggest that WOX genes are not involved in meristem regulation of non-vascular plants and that WOX proteins were likely recruited into a pre-existing CLE signaling network during sporophyte SAM evolution.

We also observed reduced expression in the meristem for a reporter of the only Marchantia *AINTEGUMENTA*,*PLETHORA* and *BABY BOOM* (*APB*) homologue Mp *APB*. However, unlike WOX genes, APB genes are thought to play an important role in gametophyte meristems. *APB* homologues in Physcomitrium are expressed in apical cells and are indispensable for meristem maintenance [8]. Physcomitrium APB genes are induced by auxin, similarly to *PLT* in Arabidopsis [2] suggesting that APB gene induction by auxin is an ancient response. The exclusion of Mp *APB* reporter expression from the Marchantia meristem argues against a direct role of Mp *APB* in the regulation of the gemma meristem, however functional testing will be needed to validate this. It is possible that the short promoter element used in our screen does not accurately reflect Mp *APB* expression. However, in Arabidopsis *PLETHORA* expression is promoted by auxin and in the root, PLT abundance follows a very similar distribution compared to auxin concentration [97]. The high expression of Mp *APB* in the central portion of gemmae would be consistent with auxin mediated induction of Mp *APB*, as the central portion of gemma is thought to be an auxin response maximum in

Marchantia [70, 154]. Indeed, our characterisation of auxin response in chapter 5 suggests that the expression pattern for Mp *APB* closely matches auxin response in gemmae. Genetic perturbations to Mp *APB* should shed light on whether this gene does have a role in gemma meristem maintenance or plays a role in the central portion of gemma instead.

We did observe expression of one GRAS transcription factor promoter, Mp *GRAS1*, in a small population of cells in the centre of the meristem as well as the central portion. While Mp *GRAS1* is not a clear homologue of Angiosperm meristem regulators, many GRAS transcription factors are implicated in meristem maintenance and the expression of MpGRAS1 makes it a promising target for future functional testing.

We also characterised the expression of six new meristem markers, Mp *BHLH42*, Mp *BZR1*, Mp *WRKY11*, Mp *BHLH29*, Mp *NAC1* and Mp *BHLH13*. Of the BHLH transcription factors, only Mp *BHLH13* (Mp *FIT1*) has been implicated in a biological function as a potential regulator of iron homeostasis [199], all other genes have no known function. However, the Mp *BHLH42* promoter in particular is an excellent meristem marker, showing bright, consistent expression in a small number of cells at the centre of the meristem. The Mp *BZR1* reporter was expressed across the meristem, consistent with the recent functional characterisation of Mp *BZR1* as a regulator of cell proliferation in Marchantia [215]. Mp *NAC1* and Mp *NAC2* are the closest homologues of CUC1 in Marchantia, moreover the reporters of these genes showed near perfect complementary expression patterns. The Mp *NAC1* reporter was expressed broadly in the meristem as well as in rhizoid precursors, while Mp *NAC2* was excluded from the meristem and not expressed in rhizoid precursors. In Arabidopsis CUC transcription factors regulate polar auxin transport in boundary domains but are usually excluded from high auxin response zones [210]. It is unknown whether the regulation of boundary domains by NAC transcription factors is conserved in bryophytes, but Mp *NAC1* and Mp *NAC2* represent promising targets to investigate this question in the future.

While incomplete, the screening of proximal promoters in Marchantia has revealed many new cell type markers and important differences to angiosperm meristem regulation. Similar to gene expression patterns in the angiosperm SAM, we observed gradient like expression for many genes, suggesting a possible lack of sharp cell fate boundaries in the Marchantia meristem. Nonetheless, we anticipate that the functional characterisation of meristem regulators will lead to the establishment of functional domains based on the expression of important meristem regulators. In the next chapter we present a complementary approach to cell type classification in Marchantia, based on single cell RNA-sequencing. While we favour basing cell type definition on unbiased data driven methods such scRNA-seq, the collection of promoter elements described in this chapter was instrumental to validate cell identities in tissue, illustrating the benefit of combining both approaches.

Chapter 4

Mapping cell types in Marchantia with scRNA-seq

4.1 Introduction

As mentioned earlier, cell type characterisation would ideally be based on a comprehensive measurement of all molecules within individual cells. While this is not feasible with current technology, measurements of mRNA abundance in individual cells has recently been enabled by the development of single cell RNA sequencing technologies. While the relationship between mRNA abundance and protein abundance is complex, mRNA abundance can be used as an imperfect proxy to categorise cell identities. Single cell RNA-sequencing has seen explosive growth since the first demonstration of whole transcriptome sequencing of a single cell in 2009 [317]. The development of high throughput droplet based single cell RNA-seq [205] has catalysed the widespread adoption of single cell RNA-seq in animal research [310] revolutionizing cell type discovery. Large scale initiatives such as the Human Cell Atlas [253] are now leveraging single cell RNA-seq and other technologies to build comprehensive reference cell atlases. Despite the announcement of a Plant Cell Atlas initiative [259, 162], the adoption of single-cell RNA-seq in plants has lagged behind.

Since 2019, high throughput droplet based single cell RNA-seq has been successfully applied to plant samples starting with the Arabidopsis root [54, 160, 267, 293, 362, 64, 80, 96]. Following the initial demonstration of feasibility, this method has also been applied to the Arabidopsis shoot meristem [361], leafy tissues [197, 173, 201], reproductive tissues [135] and callus [357]. Single cell studies of other angiosperms, including maize [22, 207, 349, 232], rice [195, 361, 336, 335, 346, 335], tomato [322] and poplar [188, 39] have followed, demonstrating the feasibility and utility of single cell profiling for diverse plant species and

tissues. These studies have enriched our understanding of tissue organization in angiosperms adding unprecedented resolution to existing cell lineage models. However, cell diversity in non-angiosperm species remains poorly defined and to date, single cell profiling has not been applied to any non-vascular plant.

In this Chapter, I present the analysis of a single cell RNA-sequencing dataset of four day old gemmalings. I show that the data captures the cellular diversity of gemmalings and validate key cell populations *in planta*. I investigate broad patterning processes such as dorso-ventral fate specification as well as illuminating the key steps of cell fate commitment during rhizoid development. This dataset represents the first application of single cell RNA-seq to non-vascular plants and the first attempt at, genomic cell type classification in Marchantia.

4.2 Data generation, QC and pre-processing

To profile the cellular diversity of the Marchantia gametophyte we generated single cell transcriptomes of protoplasts isolated from gemmalings 4 days after germination on agar plates (Figure 4.1, see Chapter 2.4.3). Mature thallus patterning, including the formation of air chambers, typically emerges around 4 days after gemma germination. We aimed to sample plants as early as possible to maximise the fraction of meristematic cells and facilitate validation via live microscopy. Live imaging in older plants is challenging, as the tissue bends downwards, obscuring the centre of the meristem from view. Protoplasts were isolated via enzymatic cell wall digestion by Mihails Delmans and library preparation and sequencing were performed by the Cancer Research UK Cambridge Institute Genomics Core facility. Sample processing, from removal of plants from the growth room to cell lysis inside the droplet, was completed in > 6 hours. Mihails Delmans also selected Mp *Expansin12* as a marker gene candidate and obtained its promoter sequence for validation. All other data analysis and validation was performed by the author.

The protoplast suspension was processed in a 10X chromium controller microfluidics device (10x Genomics) to produce water-in-oil droplets containing cells, enzymes and 10X barcoded gel beads. The 10X platform uses synchronised encapsulation of tightly packed hydrogel beads resulting in a 80% occupancy rate (droplets that contain a bead) with very few droplets containing two beads [368]. The number of droplets formed by the 10X chromium controller greatly exceeds the number of cells loaded. As a result most droplets will be empty or contain only a bead. A small number of droplets contain both a bead and a cells. The probability of a droplet containing two cells and a bead (doublet) is far lower still, ensuring that most droplets encapsulate single cells [368]. After our protoplast were encapsulated in droplets, cells were lysed to release their mRNA. The 10X gel beads are

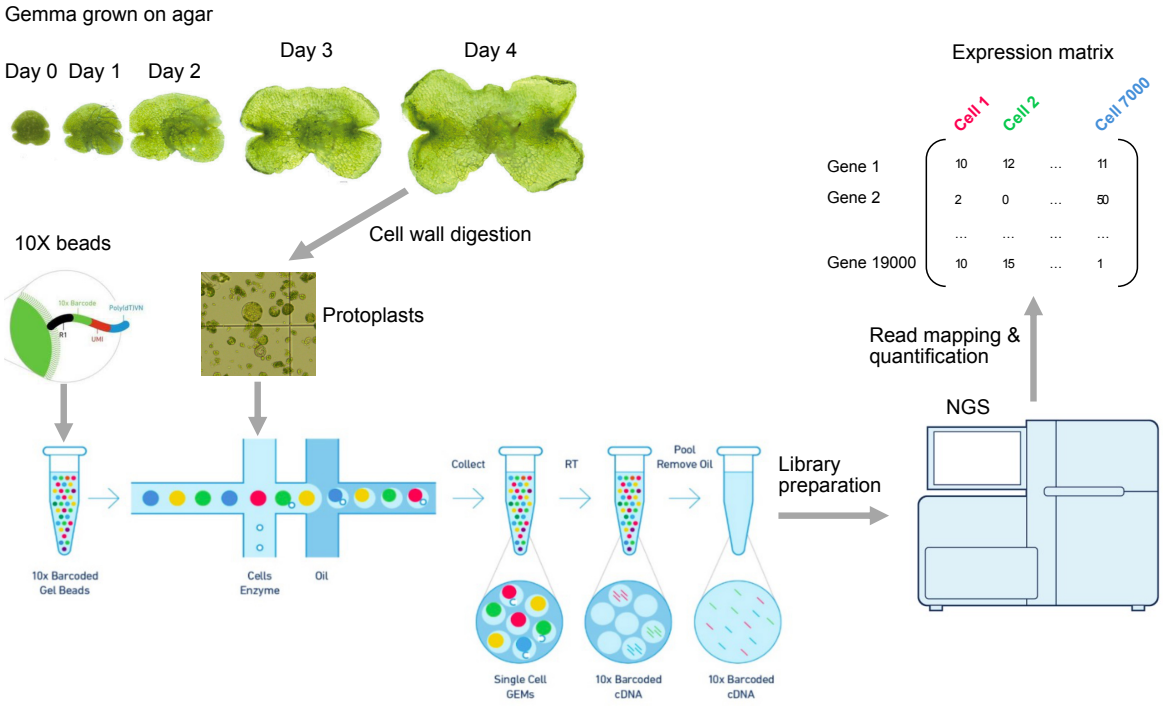

Fig. 4.1 **Single cell RNA-sequencing data generation** Gemmae were grown on agar plates for four days (images adapted from [299]). Protoplasts were isolated using enzymatic cell wall digestion. Protoplasts, enzymes and 10X barcoded gel beads were processed in a 10X chromium controller microfluidics device (10x Genomics) to produce water-in-oil droplets. 10X beads are covered in oligonucleotides with four functional sequences: a poly T-tail on the free end is used to bind the poly-A tail of mRNAs. A unique molecular identifier (UMI) barcode which differs for each oligonucleotide enables detection of PCR duplicates by uniquely labelling each cDNA molecule. A 10x barcode which has a unique sequence for each gel bead, but is identical for each oligonucleotide on a bead, enables assignment of cDNA molecules to their cells of origin. The R1 barcode is bound by a primer to initiate reverse transcription. After cDNA preparation and next generation sequencing (NGS) reads were mapped and quantified. The 10x barcode was used to assign gene counts to cells and reads that share the same UMI barcode were collapsed to a single count, removing PCR duplicates. After read processing a count matrix was obtained which forms the input for downstream analysis.

covered in oligonucleotides with a poly-T tail enabling capture of poly-A tail mRNA inside the droplet. On the other end of the oligonucleotides is a R1 barcode which was used to initiate reverse transcription of the mRNA into cDNA. Each oligonucleotide also contained a unique molecular identifier (UMI) barcode which differed for each oligonucleotide and a 10x barcode which had a unique sequence for each gel bead, but was identical for each oligonucleotide on a bead. These barcodes were incorporated into the cDNA molecule through reverse transcription. The library was amplified for seqeuncing using PCR and sequenced to a depth of 300 million reads. 232 million reads were successfully mapped against the Marchantia genome (see Chapter 2.4.4), for a mapping rate of 76%. Since each original cDNA molecule was uniquely labeled by a UMI barcode, PCR duplicates were computationally removed during read mapping and gene quantification, by collapsing reads that contain the same UMI barcode into a single UMI count [216]. After UMI de-duplication we obtained 149 million UMI counts.

After mapping and UMI quantification, we first investigated library saturation of our data (Figure 4.2A). The number of genes detected per bead barcode is expected to increase with the number of transcripts (UMI) recorded for that bead barcode. Initially, this relationship may be nearly linear, but as more transcripts are recorded the probability of observing expression of a new gene drops. In other words, there are diminishing returns of seqeuncing more reads. At very high sequencing depth, additional UMI counts may not reveal any additional information about which genes were expressed in the sample or the relative abundance of genes. While fully saturating a library would enable capturing all information present in a sample it is generally inadvisable given the diminishing returns of additional sequencing depth and the fact that experiments are typically constrained by cost. In fact for a given budget theoretical work suggests that 0.1-1 reads per cell per gene represent the ideal trade off between sequencing depth and the number of cells sequenced [360]. For our dataset, we did observe a mostly linear relationship between the number of UMI counts and the number of genes recorded for each bead barcode (Figure 4.2A). There were some signs of diminishing returns at high UMI counts indicated by a flatting of the curve, however, there was no plateau, suggesting that the library was not saturated (Figure 4.2A).

At this stage the count matrix contained UMI counts for all 10X barcodes that recorded any counts, most of which likely represent empty droplets where small amounts of ambient RNA was captured. A kneeplot was used to select an appropriate threshold to separate cell transcriptomes from likely empty droplets based on the number of UMI recorded per bead barcode (Figure 4.2B). Cell barcodes with fewer than 2000 UMI counts were removed. Cells with fewer than 200 expressed genes and genes detected in fewer than 2 cells were also removed. After filtering we obtained 7,456 single cell transcriptomes with an average of

15,372 transcripts (UMI) and 2,580 genes detected per cell (Figure 4.2C). The sequencing depth of our filtered dataset was approximately 0.8 transcripts per cell per gene which is at the upper end of the aforementioned most cost effective range. Gene expression dropouts and zero inflation are common concerns with single cell RNA-seq methods. It is often assumed that the large number of zero values observed in a typical single cell RNA-seq count matrix stems from technical issues resulting in the loss of transcripts (dropouts) which inflate the number of zero values observed. However, given the low number of molecules sequenced per cell, zeros are to be expected as a result of random sampling. For instance if 20,000 UMI counts were obtained from a cell where 20,000 genes are perfectly evenly expressed, we would observe an average of 1 UMI count per gene. However, each time a molecule is sequenced it is akin to a random draw and the probability of not obtaining a UMI count for a given gene in this cell is (19,999/20,000)^20,000 = 36.8%. It has been unclear whether technical issues contribute additional zeros beyond this [294]. Recent work demonstrated that data generated using UMI based single cell RNA-seq methods are indeed not zero inflated and the number of zeros observed in such data is consistent with random molecule sampling alone [309, 35]. For the data presented here, Figure 4.2D shows the relationship between the average expression of a gene and the fraction of cells that record no expression for that gene. As expected we observed the typical relationship described by [309], suggesting that the number of zeros we observed in our data arose from random sampling. While expected, this nonetheless limits the ability of single cell RNA-seq data to accurately measure lowly expressed genes. Indeed, when looking only at transcription factor genes Figure 4.2E demonstrates that most transcription factors were not expressed at high enough levels to be detected reliably with the sequencing depth of this dataset. Only 22 transcription factors had a dropout rate of under 50% (Figure 4.2E). Finally, we investigated if the transcriptional profile of our data matches previous RNA-seq experiments in similar tissues. We observed a strong correlation between aggregated expression of our single cell dataset (pseudobulk) and previously published RNA-seq data from gemmalings nine days after germination but not with data from antheridiophores (Figure 4.2F, see Chapter 2.4.2). In summary the dataset comprises >7,000 single cell transcriptomes matching the transcriptional profile of the tissue of origin and sequenced at comparatively high depth.

4.3 Cell type annotation

Next we used dimensionality reduction [212] and leiden clustering [326] to computationally group cells into clusters (see Chapter 2.4.5). We then annotated clusters with putative cell type labels based on the expression of previously published marker genes, transcription

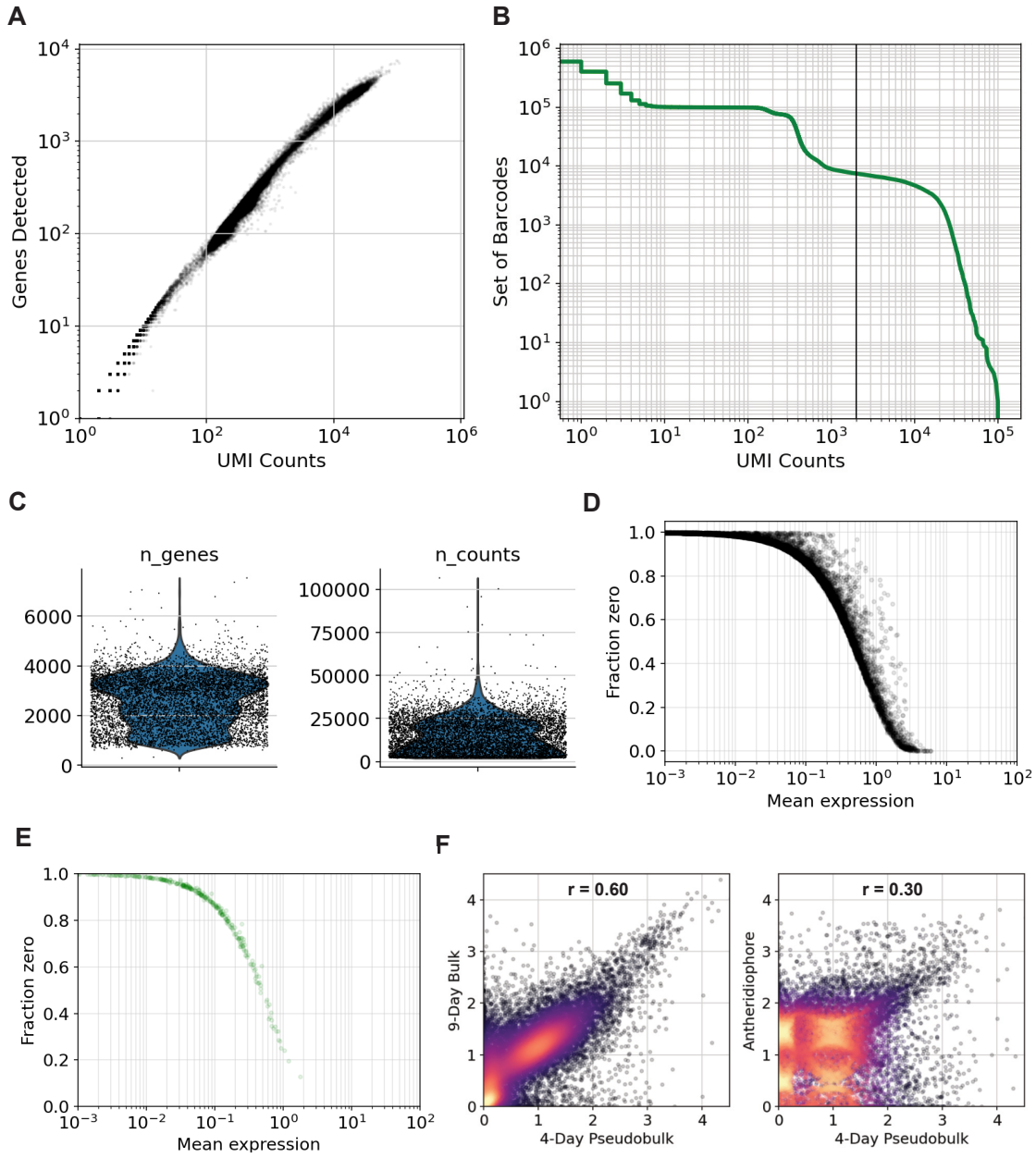

Fig. 4.2 Quality control metrics of single cell RNA-seq data. A) Kneeplot showing total UMI counts for each cell barcode in green. Cell barcodes with fewer than 2000 UMI (left of vertical black line) are filtered out. B) Number of genes detected per cell as a function of UMI counts. C) Violin-jitter plot, left showing the number of genes detected per cell (black dots) and the density of values (blue area). Right, same as left but showing the number of UMI detected per cell. D) Fraction of cells that do not express a gene plotted against the mean expression of each gene, each dot is a gene. E) Same as D but only showing transcription factor genes. F) Gene expression in bulk-RNA seq samples from similar (left) and dissimilar (right) tissues plotted against aggregate expression in the single cell dataset (pseudobulk). x-and y-axis are log10. Each dot represents a gene and is coloured by the density of dots in each area of the graph, r indicates the Pearson correlation coefficient.

factors validated in Chapter 3 and novel marker genes (Figure 4.2A-B). While these labels were chosen to indicate the most probable corresponding cell types for each group of single cell transcriptomes, based on all the information presented throughout this thesis, it is important to note that computationally defined clusters may not directly map to existing cell classifications or directly map to spatial domains. We employed SMALLCAPS typography throughout this thesis to differentiate when we refer to a computationally defined cluster of single cell transcriptomes as opposed to a cell type or tissue domain described in the literature, or defined by other observations. Based on the expression of published marker genes we grouped clusters into four broad categories, meristematic cells expressing Mp *TCP1*, Mp *SHI*, Mp *EF1A*, Mp *GCAM1* and Mp *PRR*, air chamber cells expressing Mp *WIP*, rhizoid cells expressing Mp *RSL1* and Mp *LOS1* and the remaining cells which were grouped as non-meristematic. Mp *TCP1* has been shown to be expressed in dividing cells of the meristem via *In situ* hybridisation, where the gene controls proliferation based on the cellular redox state [33]. Mp *SHI* has been shown to regulate auxin biosynthesis and is expressed in the very centre of the meristem, based on promoter GUS fusions of mature thallus [88]. Mp *EF1A* is a very highly expressed housekeeping gene with elevated expression in dividing cells of the meristem [6, 279]. Mp *GCAM1* is a positive regulator of cell proliferation and an essential gene for vegetative reproduction which has also been shown to be expressed in the meristem [354]. Mp *PRR* is a core regulator of the circadian clock in Marchantia and is expressed in the meristem and highly photosynthetic tissues [193]. Mp *WIP* is a regulator of air pore development with elevated expression in developing pores [166]. Mp *RSL1* regulates epidermal patterning and is essential for rhizoid development, it is expressed in the meristem and developing rhizoids [249, 274]. Using these markers we were to assign putative labels for most major cell lineages of gemmalings. However, we were unable to detect clear expression of any previously published oil body markers in any of our computational clusters [264, 167].

The transcription factor genes presented in Chapter 3 provide further support for the proposed cell type annotation, particularly for the meristem non-meristem boundary. I previously observed meristematic expression for transcriptional reporters of Mp *BHLH42*, Mp *BZR1*, Mp *BHLH29* and Mp *BHLH13* (Figure 3.4 and Figure 3.5), with Mp *BHLH42* showing the most specific expression in the centre of the meristem and the remaining promoters showing progressively more widespread expression. In our single cell data we observed similar trends (Figure 4.2B). Mp *BHLH42* expression was most abundant in the MERISTEM 1 cluster (Figure 4.2B). The transcriptional reporters for Mp *BZR1* and Mp *BHLH29* showed broader expression across the meristem (Figure 3.4) and in the single cell dataset these genes were most highly expressed in the MERISTEM 2 cluster. Reporters for Mp *BHLH13* marked meristem cells as well as other cell types (Figure 3.5) and we also

observed Mp *BHLH13* transcripts across multiple cell clusters (Figure 4.2B). For genes were we previously found reduced reporter expression in the meristem such as Mp *WOX*, Mp *ASLBD24*, Mp *NAC4* and Mp *NAC7* (Figure 3.6) we also find reduced expression in the MERISTEM 2 and particularly MERISTEM 1 clusters (Figure 4.2B). The expression of these markers supports the annotation of meristematic cells in our data and suggests that MERISTEM 1 cells may correspond to the apical most part of the meristem.

To support our annotation I additionally selected novel highly expressed marker genes for the putative meristem clusters and generated transcriptional reporters to validated their expression during gemmae development (Figure 4.3C, see Chapter 2.4.6). I observed distinct expression domains for all three genes. Mp4g01930 was selected as a marker gene for the MERSITEM 1 cluster and the expression of a transcriptional reporter for Mp4g01930 was restricted to the very centre of the meristem throughout gemma development (Figure 4.3C left). Mp2g25940 was selected as a MERISTEM 2 marker gene and the expression of a transcriptional reporter for this gene was localised around the meristem with no expression in the centre of the meristem or the central portion of the gemma (Figure 4.3C centre). Mp3g20970 was selected as a negative marker of both meristem populations and expression of a transcriptional reporter was indeed absent from the meristem of mature thalli, although we did not observe fluorescence in gemma (Figure 4.3C right). Taken together, the expression of existing and novel marker genes suggest that the MERISTEM 1 cluster may correspond to central stem cells, including the apical cell while the MERISTEM 2 cluster may consist of cells from the proliferation zone surrounding the meristem centre. We therefore propose to label the MERISTEM 1 population as CENTRAL STEM CELLS and the MERISTEM 2 population as PROLIFERATION ZONE (PZ) CELLS and will use these labels for the remainder of this thesis.

4.4 Dorso-ventral patterning

Next I investigated the establishment of dorso-ventral polarity. I selected two new marker genes for the putative VENTRAL (Mp3g11280) and DORSAL 1 (Mp1g15580) clusters (see Chapter 2.4.6). However, none of the marker gene candidates showed perfectly exclusive expression in the VENTRAL or DORSAL 1 cluster, consistent with the lack of clear cluster boundaries for non-meristematic cells (Figure 4.3A). To improve our ability to differentiate cell identities we focused on examining the relative expression of both gens. The expression for both genes was overlaid on a UMAP plot using a bivariate color scale mapped to the green and red components of the RGB space (Figure 4.4A). The color of each cell was controlled by RGB values, Mp3g11280 controled the value of red, while Mp1g15580 was mapped to green. Cells with minimal expression of both genes were coloured black, cells

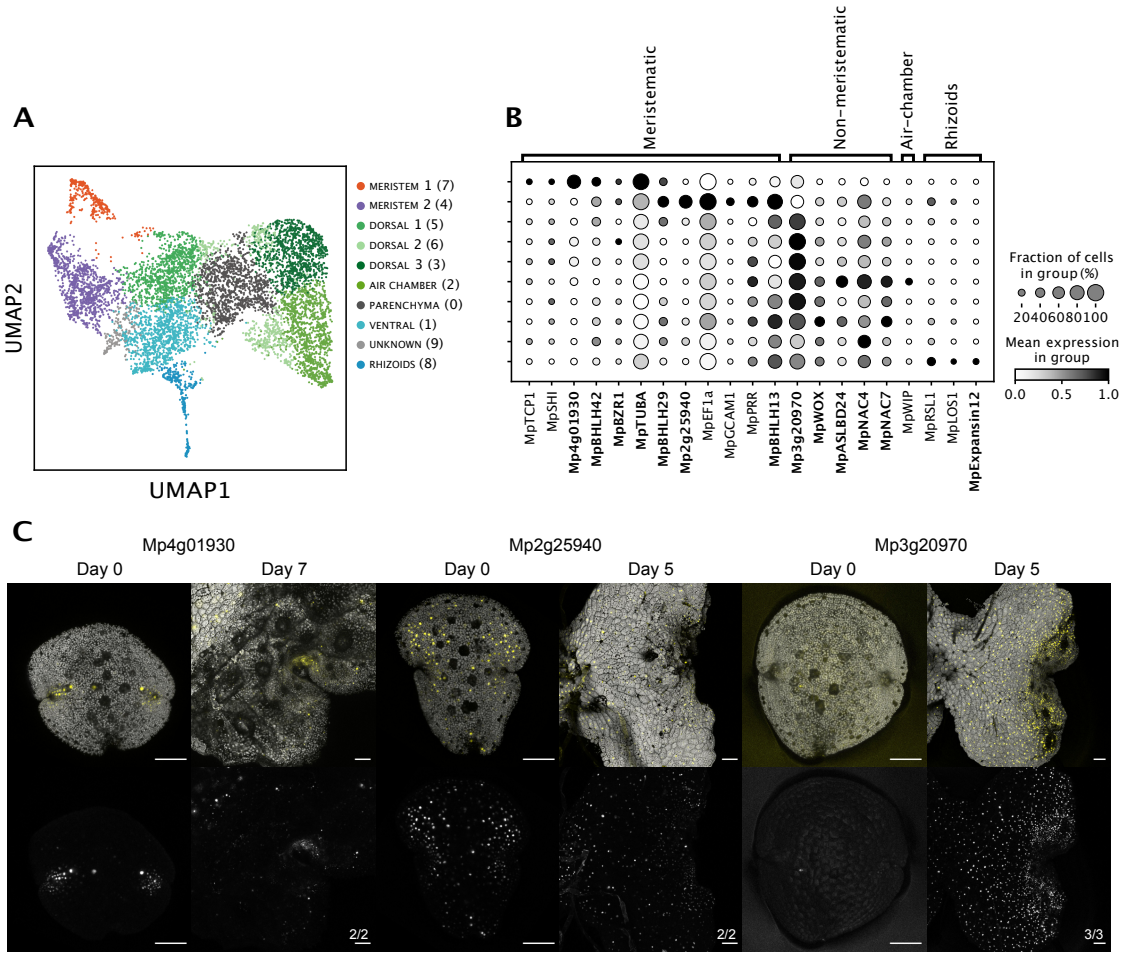

Fig. 4.3 **Cell type annotation** (A) UMAP plot of 7'456 single cell transcriptomes coloured according to leiden cluster. (B) Marker gene expression. Greyscale shows average gene expression across each cluster, re-scaled to the range 0-1 for each gene. Dot size corresponds to the percentage of cells in each cluster expressing the gene. Genes in bold font are validated in this thesis, others have been published previously as indicated in the text. (C) Expression patterns of promoter fusions for marker genes. Gene expression is shown in yellow (top) or greyscale (bottom) and chloroplast autofluorescence in grey (top). Plants were imaged straight after removal from gemma cups (Day 0) or after the indicated amount of days post germination. Scale bars 100µm

expressing only Mp3g11280 red, cells expressing only Mp1g15580 green and cells highly expressing both genes yellow. The resulting plot suggested a complex relationship between these markers (Figure 4.4A). Mp3g11280 expression appeared to be highest in meristematic cells and the VENTRAL cluster, but also increased in expression along the putative AIR CHAMBER cluster with high levels of expression in cells at the bottom right end of the cluster (Figure 4.4A). In contrast, Mp1g15580 expression was mainly detected in cells from the DORSAL 1 ,2 and 3 clusters and the AIR CHAMBER cluster. Based on these expression patterns both genes appeared to have largely complementary expression, but noticeably overlapped in expression in the bottom right end of the putative AIR CHAMBER cluster (Figure 4.4A). To validate these expression patterns, dual reporter construct were generated and transformed into Marchantia (Figure 4.4B). Nuclear localised mVenus was expressed from a Mp1g15580 promoter sequence while a Mp3g11280 promoter drove expression of nuclear localised mScarlet in the same plant. At early stages of gemma development (Day 0-2) we only observed mScarlet (Mp3g11280) fluorescence (Data not shown). Seven days after gemma germination, we observed mScarlet (Mp3g11280) expression across the ventral side of gemmalings but did not observe any mVenus (Mp1g15580) fluorescence on the ventral side (Figure 4.4B left). On the dorsal side, we observed expression for both reporters (Figure 4.4B right). However, when we generated composite image in which mVenus (Mp1g15580) fluorescent was shown in green and mScarlet (Mp3g11280) in red, distinct expression patterns were observed for both reporters (Figure 4.4B centre). As air chambers develop they are displaced away from the meristem and their developmental stage can be used as a marker of tissue maturity [9]. Air chambers were numbered from least to most mature based on pore size, to ease interpretation. In close proximity to the meristem (Air chambers 1-2) we observed mScarlet (Mp3g11280) expression in all epidermal cells, except air chamber pore cells which exclusively expressed mVenus (Mp1g15580). With increasing distance to the meristem (Air chambers 3-6), non-pore cells showed reduced expression of mScarlet (Mp3g11280) and increasing expression of mVenus (Mp1g15580), while pore cells retained mVenus (Mp1g15580) but also acquired mScarlet (Mp3g11280) as indicated by yellow nuclei in the composite image (Figure 4.4B centre). In mature air chambers (Air chambers 7-8) mScarlet (Mp3g11280) expression was only observed in the pore cells while mVenus (Mp1g15580) expression was present across epidermal cells and pore cells. These expression patterns suggest three distinct cell lineages for epidermal cells, a ventral lineage marked by Mp3g11280, a dorsal epidermis lineage where cells transition from Mp3g11280 expression to Mp1g15580 expression and an air pore cell lineage which is marked by Mp1g15580 expression in young pores and co-expression of Mp1g15580 and Mp3g11280 in mature pore cells (Figure 4.4B).

To further substantiate that these three lineages constitute functionally distinct cells, we generated gene expression scores for genes associated with specific biological processes (see Chapter 2.4.7). Photosynthesis genes showed low expression in meristematic cells, minimal expression in the VENTRAL cluster and highest expression in the DORSAL 1, 2 and 3 clusters (Figure 4.4C). In the AIR CHAMBER cluster expression of photosynthesis genes was also high, but we observed a decrease in expression in the cells toward the bottom right tip of the cluster which are marked by co-expression of Mp3g11280 and Mp1g15580 (Figure 4.4A). This is consistent with the phenotype of air chamber pore cells which appear to loose chloroplasts during their development, with mature pores showing near transparent morphology [152]. Interestingly, while investigating hormonal signals that may contribute to dorso-ventral polarity we noticed a strikingly clear inverse relationship between photosynthesis genes and ABA responsive genes [71]. While ABA is a well known stress signal and an inhibitor of germination in Marchantia, this suggests that ABA may also have a role during normal development, potentially promoting cellular dormancy and reducing expression of photosynthetic genes in ventral cells and maturing air pore cells. In summary, the expression of marker genes and genes associated with photosynthesis support our annotation of distinct ventral and dorsal cell clusters. Furthermore, the AIR CHAMBER cluster likely contains a sub-population of cells which represent developing air pore cells.

Given the presence of distinct dorsal and ventral cell populations we next turned to investigating the expression of genes thought to regulate the light response in Marchantia. Marchantia has a minimally complex phytochrome signaling pathway with a single phytochrome gene (Mp *PHY*) and a single phytochrome interacting factor (Mp *PIF*) regulating processes including gemma dormancy, meristem regeneration and sporeling development [228] based on the ratio of red to far-red light [143]. In Angiosperms, PIF genes are implicated in a more extensive light signaling regulatory module, with PIF activity restricted to the dark and HY5 promoting photomorphogenesis in the light [324]. While PIFs are directly regulated by phytochromes, HY5 is indirectly activated by phytochrome mediated repression of genes that promote rapid HY5 protein degradation in the dark, such as COP1 and related proteins [100, 371]. A putative PIF/H5 pathway for Marchantia is shown in Figure 4.5A. Based on our single cell data, most components of this putative light signaling pathway were expressed broadly across all cell types. We did find some evidence for higher Mp *PIF* expression in the VENTRAL cluster and reduced expression of Mp *COP1* and related proteins in the DORSAL 1 cluster, which may suggest higher Mp *HY5* activity along the dorsal lineage, however these were very subtle trends. Light dependent regulation Mp *PIF* and Mp *HY5* is thought to occur predominantly through the control of protein degradation [143, 359], which may explain the lack of clear of expression domains for the genes in this pathway.

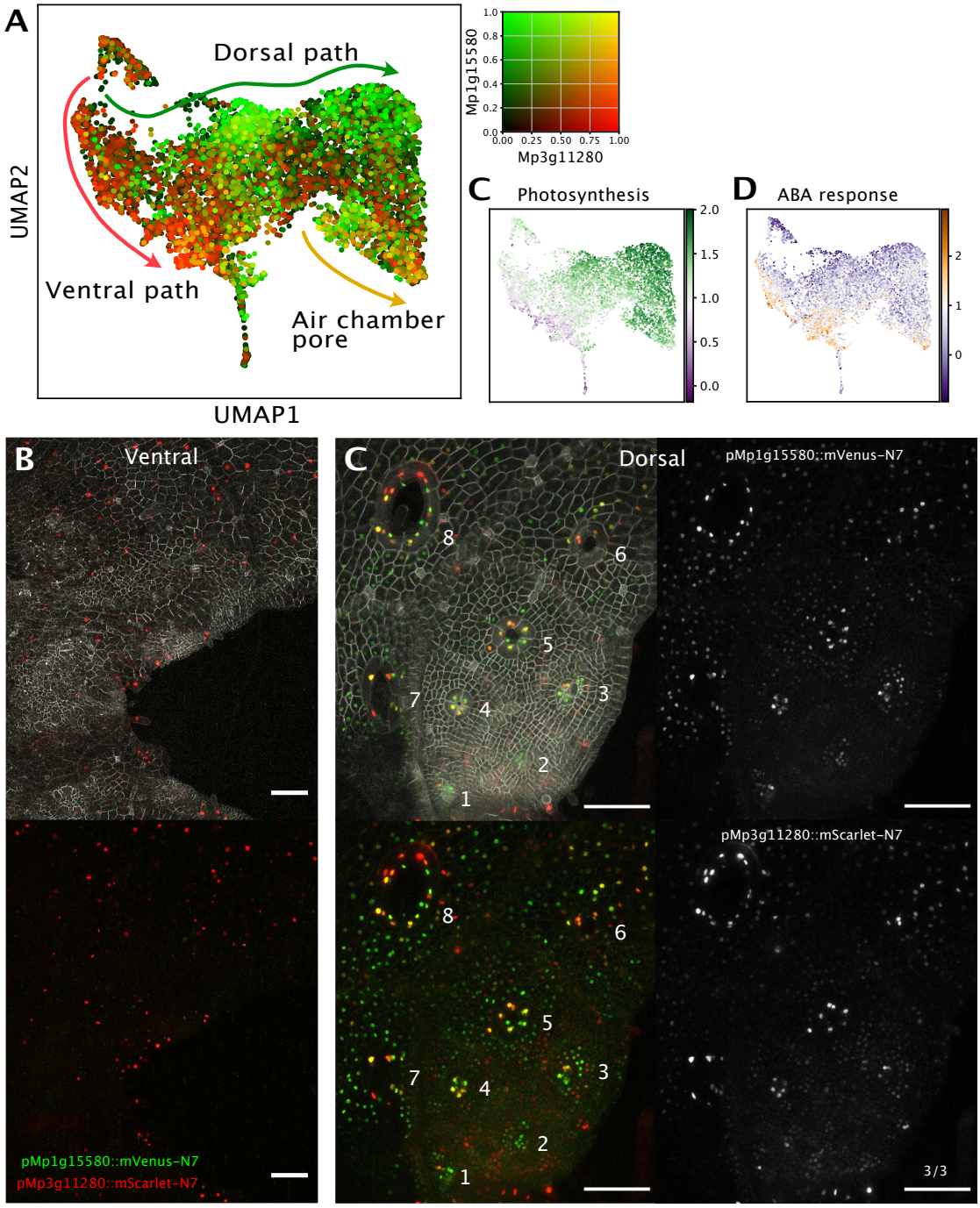

Fig. 4.4 **Dorso-Ventral differentiation** (**A**) UMAP plot showing expression of putative DORSAL 1 (Mp1g15580) and VENTRAL (Mp3g11280) marker genes. Gene expression for each gene is scaled to the range 0-1 and mapped to a bivariate color scale showing Mp1g15580 in green, Mp3g11280 expression in green and expression of both genes in yellow. Arrows indicate proposed developmental trajectories for ventral, dorsal and air chamber pore cells. (Continued on next page)

Fig. 4.4 (continued) (**B**) Confocal images of gemmalings 7 days post germination. Top: composite image showing pMpUBE2::eGFP-lti6b membrane marker in grey, pMp1g15580::mVenus-N7 expression in green and pMp3g11280::mScarlet-N7 expression in red. Bottom: same image without the membrane marker (**C**) Left: same as (**B**) but showing the dorsal surface. Air pores are numbered in order of developmental stage. Right: Individual fluorescence channels for pMp1g15580::mVenus-N7 and pMp3g11280::mScarlet-N7 shown in greyscale. All scale bars 100µM. (**C**) UMAP plot with cells coloured by gene expression scores for genes related to photosynthesis (see Chapter 2.4.7) (**D**) Same as (**C**) but scored for ABA response genes Eklund et al. [71]

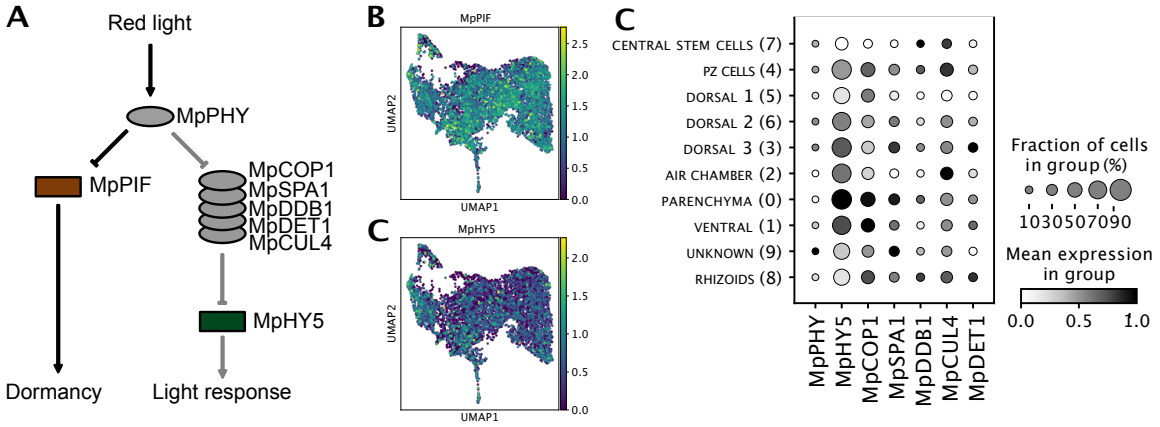

Fig. 4.5 **Putative Marchantia light response pathway** (**A**) Putative light response pathway in Marchantia. The single phytochrome Mp *PHY* is activated by a high Red/Far-red light ratio and Mp *PHY* activation inhibits Mp *PIF* function derepressing cell proliferation [228, 126]. Based on the function and regulation of *HY5* in Arabidopsis [347] the Marchantia ortholog Mp *HY5* may also be regulated by Mp *PHY* activity. Mp *PHY* may repress E3 ubiquitin ligase complexes which normally mediate rapid degradation of Mp *HY5*, permitting activation of light response genes. (**B**) UMAP projection of single cell data coloured by expression of Mp *PIF* (*C*) Same as (**B**) but showing expression of Mp *HY5*. (**D**) Dotplot heatmap showing expression of light response pathway genes across cell types. Greyscale shows average gene expression across each cluster, re-scaled to the range 0-1 for each gene. Dot size corresponds to the percentage of cells in each cluster that express the gene.

4.5 Rhizoid differentiation

Mature Marchantia thalli contain several morphologically distinct tip growing cells which are controlled by a common regulatory program [249]. On the ventral epidermis, smooth and pegged rhizoids develop to facilitate nutrient and water absorption, while unicellular mucilage papillae may form in the meristem and within gemma cups [290]. We were interested to see if the RHIZOID cluster we identified could be sub-divided into smaller clusters that

may correspond to some of these subsets of tip growing cells. We therefore re-embedded cells from the RHIZOID cluster in a new UMAP projection and annotated these subtypes using existing and novel marker genes (Figure 4.6A-B). On average, higher UMI counts were observed from rhizoid cells compared to other cell types (data not shown), which enabled us to apply RNA velocity to estimate the transcriptional trajectory of individual cells [182]. RNA-velocities can indicate developmental trajectory and suggest which cell cluster may correspond to precursors or terminal cell states. When applied to our data the trajectory of individual cells suggested a differentiation trajectory from the three rightmost cell clusters to the clusters in the bottom left of the umap graph (Figure 4.6A). Based on this information we assigned putative cell type labels to the RHIZOID PRECURSORS 1-3 clusters. Mp *RSL1* is a master regulator of epidermal cell patterning, including rhizoid development and was previously reported to be expressed in the meristem, rhizoids and other tip growing cells such as mucilage cells [249]. We observed Mp *RSL1* expression across most rhizoid sub-clusters, but observed the highest expression in a cluster which we provisionally labelled as COMMITED PRECURSOR. RNA-velocity suggested that cells from the RHIZOID PRECURSORS 1-3 clusters enter this COMMITED PRECURSOR cluster. The size of arrows indicates the magnitude of the predicted transcriptional changes which was markedly greater in the COMMITED PRECURSOR cluster compared to the RHIZOID PRECURSORS 1-3 clusters, which suggests rapid transcriptional changes. We observed expression of two additional published rhizoid markers Mp *LOS1* and Mp *NEK1*, a kinase required for directional tip growth of rhizoids [233], across rhizoid cell clusters, with Mp *NEK1* showing very similar expression compared to Mp *RSL1* (Figure 4.6B). Rhizoid outgrowth has been found to be orchestrated by microtubule organization Otani et al. [233]. In Chapter 3 we attempted to use a MpTUBA (Mp4g00550) promoter as a reference marker, but discarded its use after discovering that this promoter did not drive ubiquitous expression in gemma. Given the important role of microtubule organisation for tip growth we re-imaged this marker and observed high expression in meristematic cells as well as emerging rhizoids (Figure 4.6C). In the single cell data MpTUBA showed a gradual increase along the putative rhizoid trajectory, peaking in expression in a cluster which we provisionally labelled as ELONGATING RHIZOID (Figure 4.6B). Rhizoid elongation also likely requires cell wall loosening to accommodate expansion, which may be mediated by expansin genes [46]. We observed specific expression of an expansin gene MpExpansin12 (Mp2g18610) in the ELONGATING RHIZOID cluster and obtained a promoter sequence for validation. A transcriptional reporter for MpExpansin12 showed fluorescence exclusively in elongating rhizoids, with no detectable expression in any other cells including rhizoid precursors (Figure 4.6D). Finally, as part of the transcription factor screen (Chapter 3) we identified Mp *RSL2* as an exclusive marker of mucilage cells

(Figure 4.6E) and in the single cell dataset Mp *RSL2* expression was only detected in a small population of cells which were consequently annotated as MUCILAGE CELL. Mp *RSL1* has been previously shown to be essential for mucilage development [249]. We did not detect Mp *RSL1* expression in our MUCILAGE CELL cluster, but we speculate that this may simply be the result of the low expression of this gene and the very small number of cells captured in this cluster. While we did not obtain and validate marker genes for the two putative MATURE RHIZOID clusters, we did observe specific expression of cell death associated genes in the MATURE RHIZOID 2 cluster (data not shown). Mature Marchantia thalli contain two types of rhizoids, smooth rhizoids and pegged rhizoids, with pegged rhizoids thought to undergo apoptosis during maturation to facilitate water transport by capillarity [65]. While it is unclear when pegged rhizoids emerge during gemma development, our observation of a distinct cluster with expression of apoptosis genes combined with the low number of MATURE RHIZOID 2 cells we observe, suggests that this cluster may comprise developing pegged rhizoids, while the MATURE RHIZOID 1 cluster likely comprises mature smooth rhizoids.

To characterise the transcriptional changes that occur during rhizoid differentiation we used pseudotime analysis to order cells by their developmental stage. We calculated gene set scores for important hallmarks of rhizoid differentiation and visualised them along the rhizoid differentiation trajectory (Figure 4.6F). Consistent with microscopy observations, early stages of rhizoid development were marked by loss of expression of photosynthesis genes consistent with the loss of chlorophyll autofluorescence that can be observed in developing rhizoid precursors. Interestingly, we also found a concurrent decrease in the expression of ABA responsive genes. ABA promotes dormancy in Marchantia, suppressing cell divisions as well as rhizoid growth [71]. Our observations suggest that ABA response may also be an important signal during normal rhizoid development that antagonises commitment to rhizoid outgrowth. At the transition into the COMMITED PRECURSOR cluster we observed an increase in gene expression of auxin reponse genes, which is consistent with the role of auxins in Marchantia as a potent signal to promote rhizoid outgrowth [88]. At the transition from the COMMITED PRECURSOR to the ELONGATING RHIZOID stage we observed sharp consecutive increases in the expression of expansins, cytoskeleton genes and finally cell wall biogenesis genes. These results suggests that our datset captured cells along distinct stages of rhizoid development providing an unprecedented opportunity to probe gene expression along this developmental trajectory. We anticipate that this dataset will provide a rich resource for the Marchantia community to generate new hypotheses for the regulation of cell fate commitment.

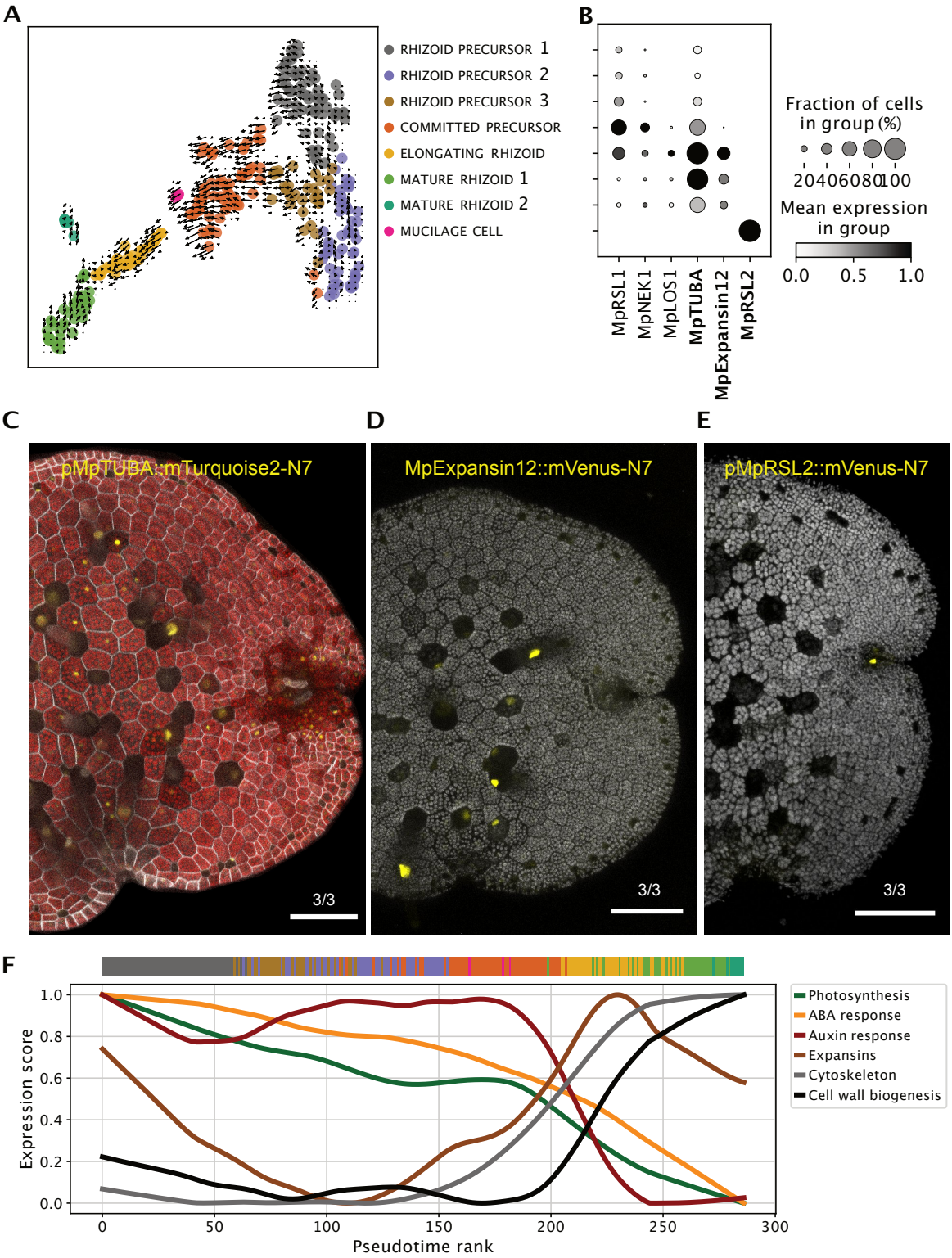

Fig. 4.6 **Rhizoid differentiation** (**A**) Re-embedded UMAP plot of rhizoid cluster revealing distinct sub-populations. Arrows show the RNA-velocity field [182], indicating the direction and speed (length of arrow) of individual cells averaged over a grid (Continued on next page)

Fig. 4.6 (continued) (**B**) Marker gene expression of existing rhizoid marker genes and novel markers (bold). (**C-E**) Validation of novel marker genes via promoter fusions for MpTUBA (pMpTUBA::mTurqouise2-N7) (**C**), MpExpansin12 (pMpExpansin12:mVenus-N7) (**D**) and MpRSL2 (pMpRSL2::mVenus-N7) (**E**). Fluorescence is shown in yellow, chlorophyll autofluorescence in red (**C**) or grey (**D-E**) and expression of the cell wall marker p35S::eGFP-lti6b in grey (**C**). Scale bars 100µM. (**F**) Smoothed normalised gene expression scores for genes associated with selected biological processes for each cell, plotted against cell pseudotime rank. Top bar shows cluster annotations for each cell, colors correspond to (**A**).

4.6 Discussion

In this chapter I present the analysis and validation of a single cell RNA-sequencing dataset of developing gemmalings. The dataset contains >7'000 single cell transcriptomes obtained from 4 day old gemmalings. Using dimensionality reduction and clustering I defined cell clusters with distinct transcriptional profiles in an unbiased manner, complementing previous work that has characterised Marchantia cell types based on morphology and a limited number of marker genes. I showed that these cell clusters correspond to distinct cell populations in gemma, which follow the major developmental axis of proximal-distal and dorso-ventral differentiation in Marchantia. Despite the sparse measurement of transcription factor expression I leveraged many of the marker lines from Chapter 3 to support this cell type annotation. I showed that the data captures large scale developmental gradients such as dorsal ventral patterning as well as distinct cell lineage differentiation such as air pore differentiation or rhizoid differentiation. For dorsal-ventral patterning I showed that components of the light signaling pathway were expressed broadly across all gemma cells consistent with the regulation of light signaling occurring predominantly on the post-transcriptional level. I described an intriguing strong negative association between the expression of photosynthesis genes and ABA response, suggesting that ABA may have a previously underappreciated role in regulating ventral cell dormancy. This may contribute to asymmetric cell proliferation which is observed predominantly on the dorsal side in mature thalli. I showed that the dataset contains rare rhizoid subtypes such as mucilage cells and that the data captured distinct stages of rhizoid differentiation with characteristic waves of gene expression associated with key morphological changes observed *in vivo*.

Oil body cells form the only major cell type that remains unidentified in this dataset. None of the previously published marker genes were detected in our datset [264, 167]. It is unclear whether this is the result of not capturing oil body cell transcriptomes or due to insufficient sensitivity of our dataset for detecting oil body marker gene expression. Oil

body cells may not have been captured as a result of the low abundance of oil body cells in Marchantia plants grown on agar [316], but a more probable explanation may be the inability to generate viable oil body protoplasts. RNA capture may also be inhibited by the diverse secondary metabolites stored in oil bodies [316]. We have not been able to verify the identity of one of our cell clusters which we labelled as UNKNOWN. It is possible that these cells could be oil body cells and could be validated as such by obtaining new maker genes from this cluster and validating their expression in gemma. Alternatively, additional oil body markers may be identified in the future which do show expression in this dataset.

For the meristem I identified two distinct cell populations which may correspond to the cells in the very centre of the meristem (CENTRAL STEM CELLS) and the dividing cells surrounding them (PZ CELLS). The functions of these meristem domains will be investigated in detail in chapter 5 and chapter 6 respectively.

Based on our rhizoid expression data, we propose a four stage model of rhizoid development. In stage one, Mp *RSL1* expression [249] and auxin signaling [70] may promote the differentiation of epidermal cells into rhizoid precursor cells, which are marked by a loss of chlorophyll. Rhizoid precursor fate at this stage is reversible and given favourable signals cells will revert back to chlorophyll rich epidermal cells (see e.g. Chapter 5 Figure 6.5). The second stage is marked by entry into the commited precursor state, which may be controlled by the balance of auxin and ABA signalling. Once committed, cells may enter stage three which is marked by the sequential upregulation of expansins, cytoskeleton genes and cell wall biogenesis, facilitating directional outgrowth of the rhizoid. Finally, cells may either mature into smooth rhizoids or enter the pegged rhizoid developmental trajectory ending in programmed cell death. Pegged rhizoids are closely associated with ventral scales and both structures have only been described in mature thalli [290]. For pegged rhizoids it is not known when these cells emerge during gemma development, but ventral scales have been shown to be fully formed as early as day 10 of gemma development [224]. Given our observations, we speculate that pegged rhizoids may emerge with the transition to mature thalli patterning, which occurs around day 4-5 of gemma development and our data provides a rich resource to obtain marker genes to investigate this hypothesis in the future.

The data presented in this chapter should serve as a rich resource to study the regulation of distinct cell type identities in Marchantia. While the data is currently limited to a single time-point during early thallus development, we anticipate that sampling of tissues from diverse stages of Marchantia development will follow in the near future. These datasets will form a critical part in generating a complete census of Marchantia cell types which will provide an valuable framework for future work in Marchantia.

Chapter 5

Central stem cells are tissue organisers

5.1 Introduction

Having established a new framework for classifying cell types in gemmae, I turned to auxin and cytokinin signalling which regulate diverse aspects of Marchantia development. Auxin is thought to be synthesized in the Marchantia apex and transported basipetally [23], establishing apical dominance by promoting cell expansion, differentiation and rhizoid elongation [208] in the central portion of Marchantia plants [70]. A series of studies in Marchantia have revealed the genetic components of the auxin signaling pathway, which contain all major components of auxin signaling known from Angiosperms, but with near minimal genetic redundancy (Figure 5.1A). Three publications identified the main components of the Marchantia auxin signaling pathway, comprising the auxin biosynthesis enzymes Mp *TAA* and Mp *YUC2*, auxin co-receptors Mp *IAA* and Mp *TIR*, the transcriptional co-repressor Mp *TPL* and the auxin response factors Mp *ARF1*, Mp *ARF2* and Mp *ARF3* [169, 88, 70]. Eklund et al. [70] showed that auxin in the Marchantia gametophyte is produced by the indole-3-pyruvic acid (IPyA) pathway in a two step reaction catalysed by Mp *TAA* and Mp *YUC2*. Mp *TAA* and Mp *YUC* gain of function mutations can phenocopy exogenous auxin application, resulting in cell expansion, inhibition of growth and ectopic rhizoid formation. Conversely, loss of function mutations or treatment with auxin synthesis inhibitors, resulted in undifferentiated tissue growth [70]. Flores-Sandoval et al. [88] identified Mp *IAA* and Mp *TPL* as negative regulators of auxin signaling. Kato et al. [169] investigated the transcriptional auxin response system, demonstrating protein-protein interactions between ARFs and MpIAA proteins and characterising MpARF1 as a transcriptional activator and MpARF2 as a transcriptional repressor, consistent with their phylogenetic classification as A and B class ARFs [101]. The class C ARF Mp *ARF3* has been found to antagonise cell differentiation, but is most likely not involved in auxin signaling [89, 171]. Mp *ARF1* loss of function resulted

in auxin insensitive plants with diverse developmental defects [170]. Gemma development in particular was disrupted in Mp *ARF1* loss of function plants, generating gemma with widened meristems, additional meristem and aberrant meristem positioning [170]. Mp *ARF1* overexpression induced auxin hypersensitivity, but also increased the number of meristems in adult thalli, possibly by promoting more frequent branching [88]. Recently, Kato et al. [171] further characterised the function of Marchantia ARFs showing that Mp *ARF1* and Mp *ARF2* directly compete for the same binding sites suggesting that ARF1/2 stoichiometry as well as auxin dependent derepression of Mp *ARF1* activity via Mp *IAA* determine auxin signaling output.

These results established auxin signaling as a major driver of Marchantia growth and as a key signal for maintaining apical dominance. Similar apical-distal auxin patterning has also been reported in Physcomitrium, suggesting an ancient conserved role of apical auxin in controlling meristem organisation [320]. While genetic and experimental perturbations point to an apical auxin source and distal auxin perception in Marchantia, the details of auxin patterning, particularly the relationship between auxin and distinct cell populations remains unknown. Given their position in the centre of the meristem and distinct morphology, central stem cells in particular have been suggested as possible auxin sources, but so far this has not been validated. Direct observation of auxin response has also been challenging, with attempts using the soybean GH3 promoter and GUS staining showing poor reporter signal and low resolution [154].

In this chapter I investigate how auxin may orchestrate gemma development and which role central stem cells may play in this process. I show that single cell RNA-seq data indicates CENTRAL STEM CELLS as auxin sources. I generated new fluorescent reporters for auxin biosynthesis (Mp *YUC2*), auxin transport (Mp *PIN1*) and auxin response (DR5v2 and Mp *ARF1-2* dual reporter) which enabled characterisation of auxin signaling in living plants with cellular resolution. The expression patterns for these reporters supported the characterisation of central stem cells as an auxin source in gemma and enabled direct visualisation of auxin response in the central portion of gemma. Finally, I identified an AP2/ERF transcription factor Mp *ERF20* as the first known direct regulator of apical cell fate and characterised its function. These results suggest that central stem cells may function as tissue organiser cells by acting as a strong auxin source, establishing auxin gradients which are critical for the control of tissue proliferation in gemma.

5.2 Central stem cells are auxin sources

To gain a more comprehensive view of how different parts of the auxin signaling pathway may be distributed across cell types I analysed the expression of the whole auxin signaling pathway across the single cell RNA-seq dataset (Figure 5.1B). The expression of auxin biosynthesis genes (Mp *TAA*, Mp *YUC2*) was highest in the CENTRAL STEM CELL cluster and dorsal cell clusters, consistent with previously reported GUS reporter expression in the marchantia meristem and photosynthetic tissues [70]. We observed similar expression pattern for Mp *PIN1* the only canonical auxin transporter [17], which showed maximal expression in the CENTRAL STEM CELL cluster. The auxin importer Mp *AUX1* showed a more even expression distribution across cell types. Mp *IAA* and Mp *TIR* are auxin co-receptor and their expression was also observed across most cell types with some differences in photosynthetic tissues. Mp *TPL* is a negative regulator of auxin signaling and our data suggests expression in the meristematic cell types. This is consistent with previously reported meristematic expression of a promoter fusion reporter for Mp *TPL* [88]. The two auxin response factors Mp *ARF1* and Mp *ARF2* were also expressed across most cell types but Mp *ARF2* showed similar expression trends compared to Mp *TPL*. Finally, we looked at the expression of three genes that have been used previously as reporters for auxin response in Marchantia [170, 221]. Expression for all three genes was detected across cell clusters, but we observed a clear expression minima in PZ CELLS and low expression in central stem cells for all three genes. This is consistent with previous reports suggesting low auxin signaling in the meristem [170]. In summary, our single cell expression data suggests auxin biosynthesis and export may occur predominantly in CENTRAL STEM CELLS. Most components of the signaling pathway may be broadly expressed across different cell types, with the exception of the negative regulators Mp *TPL* and Mp *ARF2* which showed elevated expression in the meristem. Finally, auxin response may be low in the meristem with a minimum in PZ CELLS.

I next aimed to generate transcriptional reporters for key aspects of the auxin signaling pathway to identify if auxin signaling components are specifically localised to tissue domains in living plants. To generate an auxin synthesis reporter I initially used a 2kb promoter fragment of the Mp *YUC2* promoter, which showed expression in the centre of the meristem as well as rhizoid precursors and oil body cells (Figure 5.2A). Using a longer promoter sequence (5.5kb), more specific expression in the centre of the meristem was observed for most lines (independent transformation events). In some lines, expression was restricted to just a crescent of cells in the centre of the meristem corresponding to the central stem cell population (Figure 5.2B) However, we did observe variability between lines and when using more sensitive imaging settings expression could be observed across the meristem in the least specific lines (Figure 5.2C)). We also generally observed expanding expression domains of

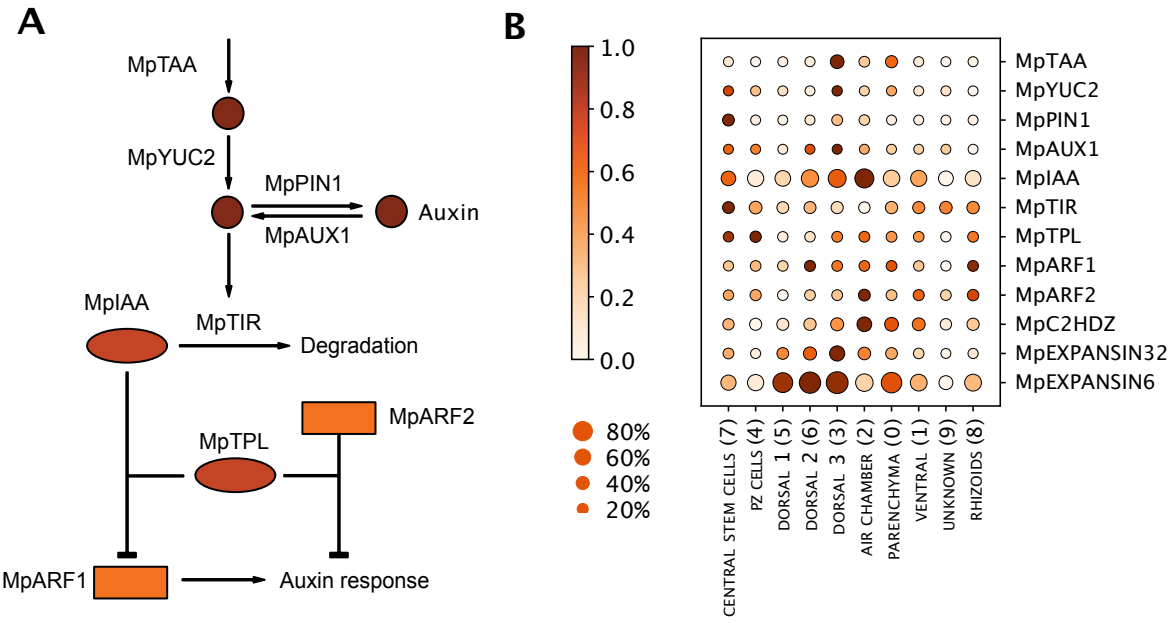

Fig. 5.1 **Auxin signaling pathway in Marchantia.** (**A**) Auxin signaling pathway for gametophyte development. Mp *TAA* and Mp *YUC2* catalyse a two step biosynthesis reaction, converting tryptophan to auxin (Indoleacetic Acid, IAA) [70] with the second step limiting the rate of the overall reaction [366]. Mp *PIN1* is thought to facilitate auxin export into surrounding cells [363] while Mp *AUX1* may promote auxin import into cells. Auxin promotes the assembly of co-receptor complexes of Mp *IAA* and Mp *TIR*, which result in ubiquitination mediated degradation of Mp *IAA* proteins [61]. In the absence of auxin Mp *IAA* can form a protein complex with Mp *ARF1* and Mp *TPL* proteins [171]. Mp *TPL* is a transcriptional co-repressor, preventing Mp *ARF1* from activating transcription at its target sites when bound. Mp *TPL* can also directly bind to Mp *ARF2* to repress transcription [171]. Mp *ARF1* and Mp *ARF2* bind to the same target sequences, suggesting that high levels of transcriptional activation by Mp *ARF1* may only occur in the presence of high levels of auxin and low levels of Mp *ARF2* [171]. (**B**) Dotplot heatmap of single cell gene expression. Color scale shows the average gene expression across each cluster, re-scaled to the range 0-1 for each gene. Dot size corresponds to the percentage of cells in each cluster expressing the gene.

our Mp *YUC2* reporters in older plants (Figure 5.2D)). These expression patterns suggest that while Mp *YUC2* may not be exclusively expressed in central stem cells, central stem cells appear to have very high levels of Mp *YUC2* expression. Our data is consistent with previous results from low resolution transcriptional reporters [70], which similarly observed maximum Mp *YUC2* expression in the centre most cells of the meristem.

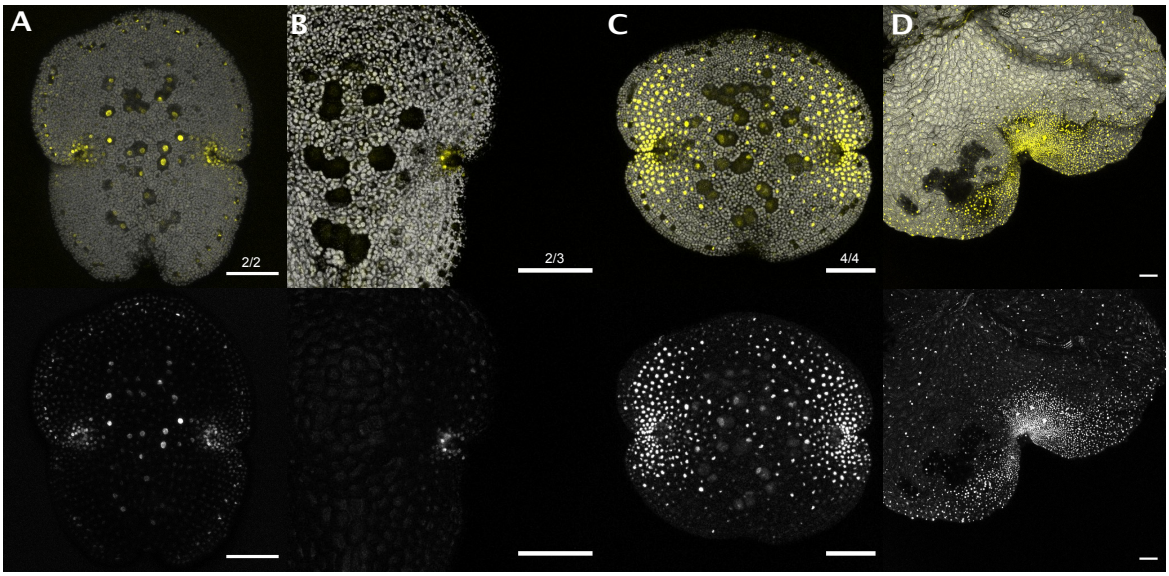

Fig. 5.2 **Expression of MpYUC2 reporters.** Confocal imaging of transcriptional reporter lines. Fluorescence for each reporter is shown in yellow (top) or greyscale (bottom) with chloroplast autofluorescence in grey (top). (**A**) pMpYUC2(2kb)::mScarletI-N7 expression in gemma. (**B**) pMpYUC2(5.5kb)::mTurqouise2-N7 expression in the gemma meristem. (**C**) Same as (**B**) but images of a different line using more sensitive imaging settings. (**D**) Same as (**C**) but imaged after four days of gemma growth on 0.5 Gamborg agar. Numbers above the scale bar indicate the number of independent transgenic lines imaged, which showed comparable expression. All scale bars 100µm.

Mp *PIN1* is the only canonical PIN auxin efflux carrier in Marchantia [17, 363]. When we generated fluorescent reporters for Mp *PIN* promoter activity, we observed fluorescence restricted to the very centre of the meristem (Figure 5.3A). Expression of the Mp *PIN* reporter was restricted to central stem cells and showing more restricted and consistent expression patterns than Mp *YUC2*. However, we observed very low levels of fluorescence using this reporter and were unable to follow Mp *PIN* expression through gemma development. To boost expression, we used a trans-activation system using the GAL4-VP16 transcriptional activator [271]. The Mp *PIN* promoter was used to drive expression of a GAL4-VP16 fusion protein and nuclear localised mVenus was expressed from the synthetic UAS promoter which contains multiple GAL4 binding sites [271]. This system is known to drive very high levels

of expression. Using this system we were able to generate bright fluorescent lines that showed fluorescence in the meristem, but also along the gemma edge (Figure 5.3B). in older plants expression was additionally observed in air chambers (Figure 5.3C). These observations suggest that Mp *PIN* expression is largely restricted to central stem cells. Lower levels of Mp *PIN* expression may additionally be present across other meristematic cells and along the gemma edge.

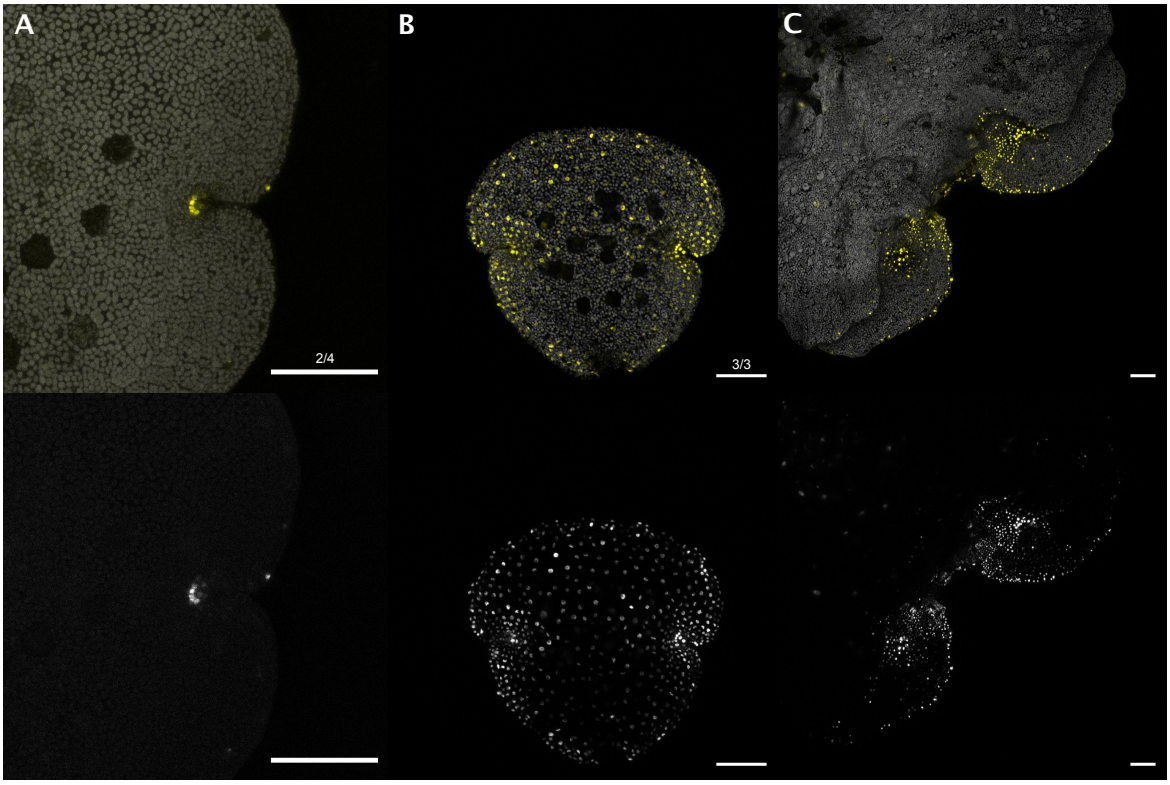

Fig. 5.3 **Expression of MpPIN1 reporters.** Confocal imaging of transcriptional reporter lines. Fluorescence for each reporter is shown in yellow (top) or greyscale (bottom) with chloroplast autofluorescence in grey (top). (**A**) pMpPIN1::mTurqouise2-N7 expression in the gemma meristem. (**B**) Transactivation reporter (pMpPIN1::GAL4-VP16, pUAS::mVenus-N7) expression in gemma. (**C**) Same as (**B**) but imaged after four days of gemma growth on 0.5 Gamborg agar. Numbers above the scale bar indicate the number of independent transgenic lines imaged, which showed comparable expression. All scale bars 100µm.

5.3 Auxin response is restricted to the central zone

5.3.1 Auxin reporter validation

There are previous reports of an auxin response reporter [154] using the soybean GH3 promoter [198, 190] which suggest that auxin response in Marchantia may be restricted to the central zone [170]. However, GUS staining using this reporter showed very faint signal and was only imaged with low magnification in older gemmalings [170]. Ishizaki et al. [154] also tested the use of a DR5 reporter [329] but were unable to detect any activity using their GUS reporter [154]. The DR5 reporter is based on a synthetic promoter sequence, comprising a minimal 35S promoter sequence and an upstream array of multiple ARF consensus binding sequences [329]. The expression of reporter constructs from this promoter should indicate the relative activity of the ARF signaling module which is govern but the relative activity of activating and repressing ARF proteins as well as co-regulators (Figure 5.1A). This readout can be used as a proxy of auxin signaling in the cell. I attempted to generate fluorescent auxin response reporters using the GH3 and DR5v2 [191] promoters, but was unable to detect expression for both constructs (data not shown). Based on the low levels of expression reported previously [154] we reasoned that the expression levels of these reporters may be below the detection threshold of fluorescence imaging. To explore this possibility we generated GAL4-VP16 transactivation reporters for GH3 and DR5v2. While we did see fluorescence in some pGH3::GAL4-VP16, pUAS::mVenus-N7 plants, expression was very patchy, often localised to oil body cells and was not clearly induced by exogenous application of 10µM NAA (data not shown). In contrast, the pDR5v2::GAL4-VP16, pUAS::mVenus-N7 reporter showed consistent fluorescence in developing gemma and a clear pattern of increased reporter activity in the central region of gemma was observed (Figure 5.4A). This is in line with the expected auxin signaling region in the central portion of the gemma. To test if the readout of this reporter does indeed correspond to auxin signaling, we grew gemma on agar supplemented with 10µM NAA and compared the reporter activity to control plants after four days. While control plant showed dim fluorescence in the central zone and emerging air chambers (Figure 5.4B), NAA treated plants showed very bright fluorescence in all cells (Figure 5.4C). These results demonstrate that the DR5v2 reporter is functional in Marchantia, but requires signal amplification to achieve sufficient expression for fluorescence imaging. The expression patterns from this reporter are in line with the expression patterns of auxin reporter genes in our single cell data (Figure 5.1B) suggesting that the Marchantia meristem in general and the proliferation zone in particular are characterised by low levels of auxin signaling.

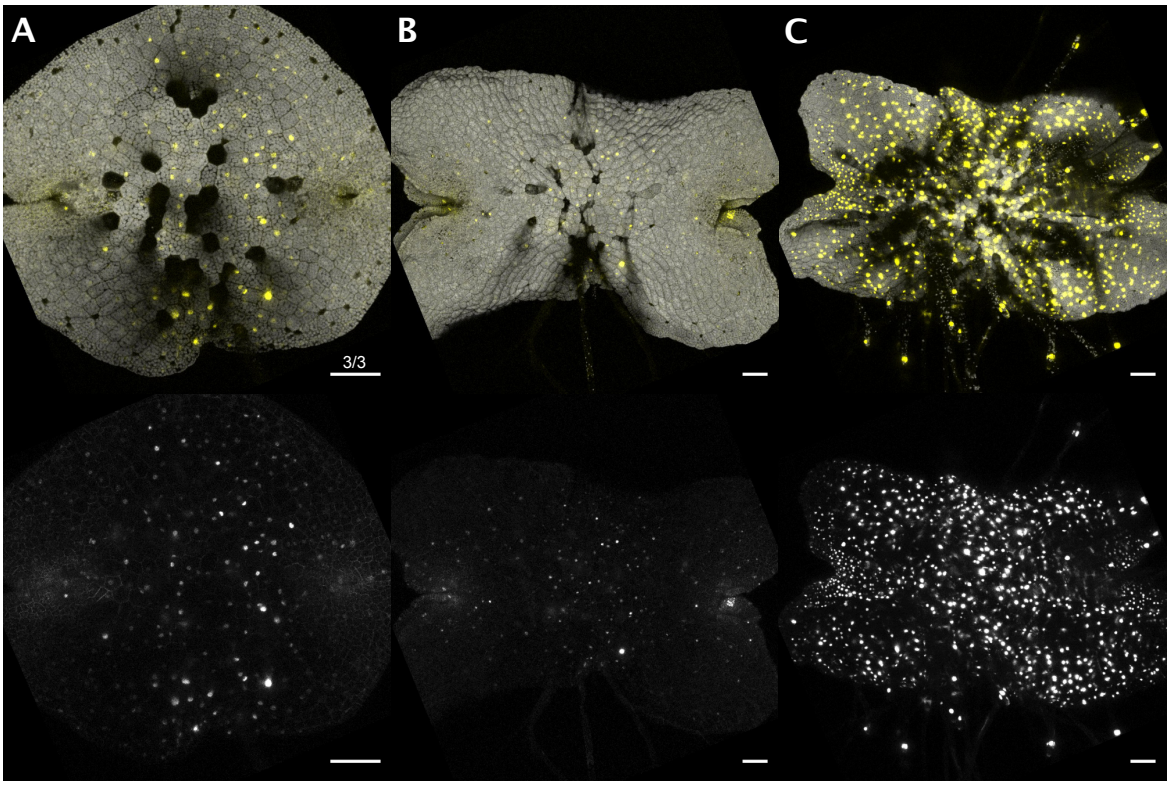

Fig. 5.4 **Validation of the DR5v2 reporter in Marchantia.** Confocal imaging of DR5v2 reporter lines. Fluorescence for each reporter is shown in yellow (top) or greyscale (bottom) with chloroplast autofluorescence in grey (top). (**A**) pDR5v2 transactivation reporter (pDR5v2::GAL4-VP16, pUAS::mVenus-N7) expression in gemma after one day of growth on 0.5 Gamborg agar. (**B**) Same plant as (**A**) imaged after four days of growth. (**C**) Same as (**B**) but 0.5 Gamborg agar was supplemented with 10µM NAA. Numbers above the scale bar indicate the number of independent transgenic lines imaged, which showed comparable expression. Experiments were repeated three times with similar results. All scale bars 100µm.

5.3.2 ARF stoichiometry contributes to the auxin response minima

Kato et al. [171] proposed a model for auxin signaling in Marchantia that emphasises the relative abundance of Mp *ARF1* and Mp *ARF2* as an important component of the overall transcriptional response. Kato et al. [171] characterised Mp *ARF1* and Mp *ARF2* abundance by tagging the genes with fluorescent proteins using genomic gene knock-in. The fluorescene of thesee knock-in lines suggested elevated Mp *ARF2* abundance in the meristem and along the gemma edge while Mp *ARF1* appeared to be ubiquitously expressed. However, since very low levels of fluorescence were observed for Mp *ARF2* and both genes were imaged in separate plants, the relative abundance of Mp *ARF1* and Mp *ARF2* at a cellular level remains unknown. To address this limitation, we aimed to generate dual-reporter lines for Mp *ARF1* and Mp *ARF2* that permit characterising their relative abundance with cellular resolution. A separate transcription unit for each promoter (pMpARF1::mVenus-N7 and pMpARF2::mScarletI-N7) was assembled and combined into a single L2 construct (see Methods 2.1.2). This construct was cloned and transformed into Marchantia by Mark Ball and Susana Sauret Gueto, all imaging was performed by the author. Broad expression was observed for the Mp *ARF1* reporter (Figure 5.5, middle), while the Mp *ARF2* reporter showed elevated expression levels in the meristem and in cells along the gemma edge (Figure 5.5, bottom). When we generated a composite image showing Mp *ARF1* reporter fluorescence in green and Mp *ARF2* reporter fluorescence activity in red we observed different relative activities of both reporters in different cells, suggesting changes in the relative abundance of Mp *ARF1* and Mp *ARF2* in different parts of the tissue (Figure 5.5, top). In day 0 gemma we observed high relative activity of the Mp *ARF2* reporter in rhizoid precursors and some cells along the gemma edge, while cells in the centre of the meristem showed high activity for both reporters, as indicated by bright yellow nuclei in the composite image (Figure 5.5, top). At day 2, we observed similar patterns, but by day four we observed a consistent zone of high Mp *ARF2* reporter activity relative to the Mp *ARF1* reporter expression (Figure 5.5). Based on the individual fluorescence channel intensity, this appeared to be driven by a reduction in Mp *ARF1* expression in the meristem of older plants (Figure 5.5). In summary, the expression of our ARF1/2 dual reporter in Marchantia is consistent with previously published expression patterns for individual genes [171] and suggests that ARF stoichiometry may gate auxin signaling output to maintain low levels of auxin response in the meristem.

5.4 MpERF20 regulates central stem cell fate

Our single cell gene expression data and the expression of our Mp *YUC2* and Mp *PIN1* reporters suggest that central stem cells may comprise a distinct cell population. However,

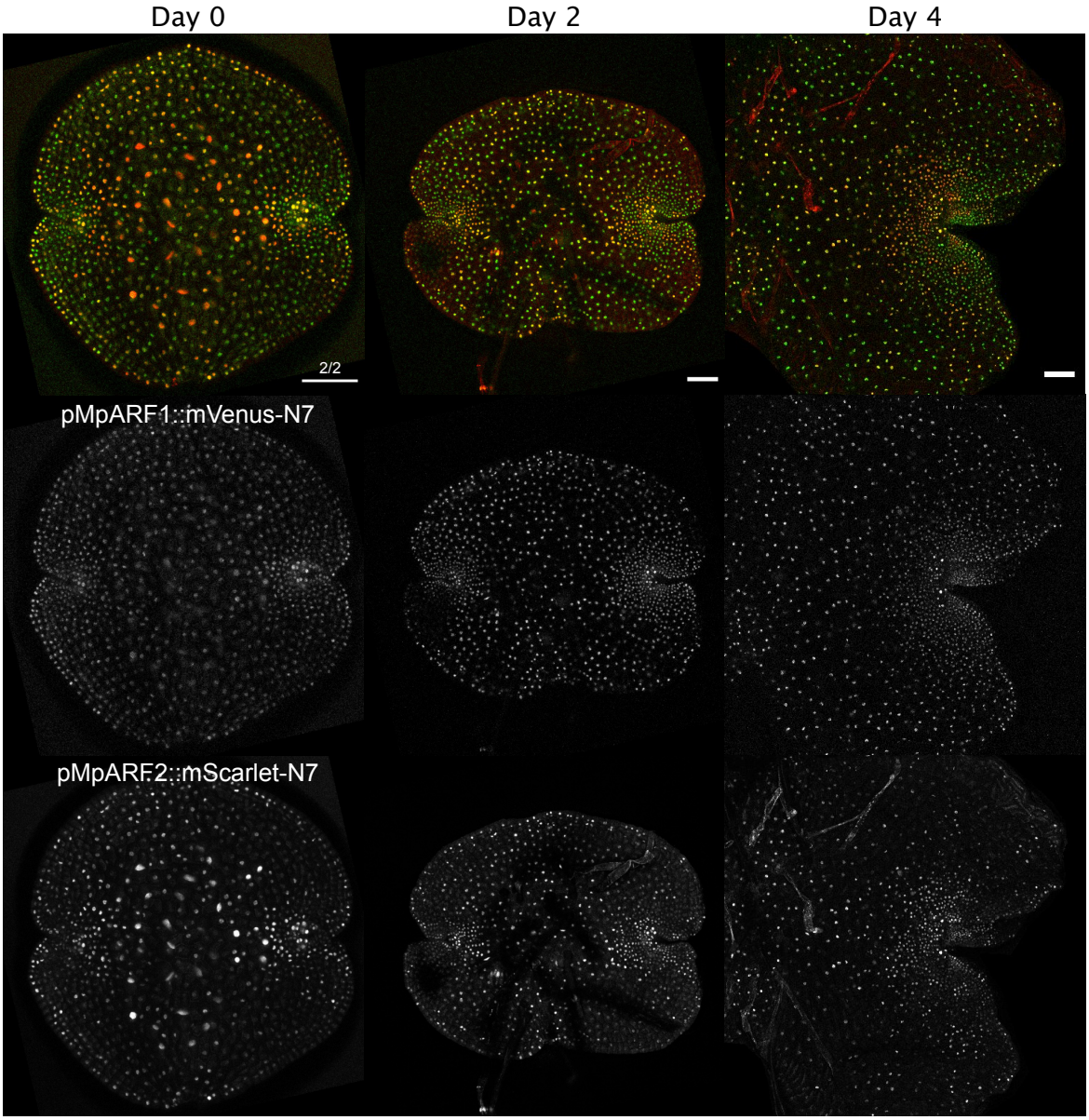

Fig. 5.5 **Expression of a multispectral MpARF1 and MpARF2 reporter.** Confocal time course series of a pMpARF1::mVenus-N7, pMpARF2::mScarletI-N7 gemma. Top row shows composite images of pMpARF1::mVenus-N7 in green and pMpARF2::mScarletI-N7 signal in red, middle and bottom row show the fluorescence of each reporter separately in greyscale. Plant was grown on on 0.5 Gamborg agar for the indicated amount of time before image acquisition. Numbers above the scale bar indicate the number of independent transgenic lines imaged, which showed comparable expression. All scale bars 100µm.

no direct genetic regulators of central stem cell fate or apical cell fate have been identified to date. During our transcription factor screening we observed faint expression of a proximal promoter for the ERF transcription factor Mp *ERF20* (Mp5g06970) in a very small number of cells in the centre of the meristem (Figure 5.6A). However, the expression levels were too low to follow expression of this reporter further. Mp *ERF20* is also very highly induced in a published RNA-seq dataset of regenerating gemma fragments [29, 90] suggesting a possible role in cell proliferation and organisation of the apex. We used GAL4-VP16 trans-activation to boost the expression of our Mp *ERF20* reporter. Using this transactivation reporter bright fluorescence was observed in a small population of cells in the centre of the gemma meristem, with additional reporter activity in some oil body cells (Figure 5.6B-C). We also included the 5.5kb Mp *YUC2* reporter we characterised earlier in these constructs to act as a reference for central stem cell expression. Mp *ERF20* and Mp *YUC2* reporter expression did overlap in apical cell and their direct derivatives, but Mp *YUC2* reporter expression extended further along the flanking region of the U-shaped central stem cell population (Figure 5.6C). At later stages of gemma development, Mp *ERF20* reporter expression was localised to clusters of cells across the meristem, but appeared to be absent from developing air chamber pores (Figure 5.6D). Having identified highly localised expression of Mp *ERF20* in early gemma we aimed to investigate Mp *ERF20* function by generating over-expression lines.

Based on the expression of our Mp *ERF20* reporter we suspected that this gene may play a role in stem cell regulation. Constitutive overexpression of stem cell regulators may result in severe developmental defects. We therefore aimed to build constructs that would enable inducible missexpression of Mp *ERF20*. We assembled a GAL4-VP16-GR fusion protein following previous work on inducible gene expression in plants [7]. In this system, the coding sequence of a gene can be placed under the control of the pUAS promoter which will drive very high expression of this gene if the system is induced. Trans-activation by GAL4-VP16 should not occur in the absence of dexamethasone as the GR domain will sequester the fusion protein from the nucleus [242]. In the presence of dexamethasone GAL4-VP16 will translocate to the nucleus, activating gene expression from the pUAS promoter. We generated two different constructs using different promoters to drive expression of the GAL4-VP16 trans-activator. For the first construct we used the Mp *YUC2* promoter to drive expression of this transactivation system in the meristem. Alternatively, we used a heat shock inducible promoter (pMpHSP18.7A1, 1.2kb upstream sequence of Mp7g07900) that was previously characterised as a highly inducible promoter in Marchantia [227]. Using the heat shock promoter we aimed to generate a double inducible system that could drive expression across all cells, if both signals are present, while hopefully reducing leaky expression. We first tested the function of these two induction systems, by trans-activating

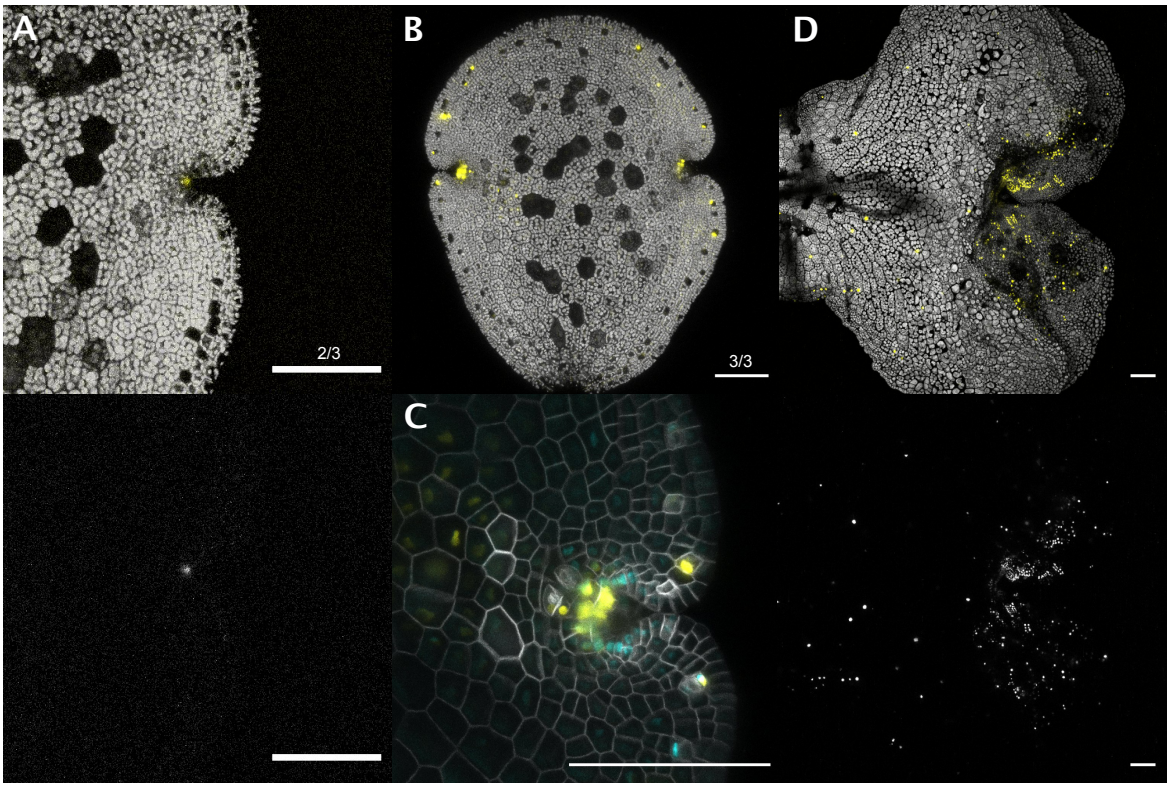

Fig. 5.6 **Expression of MpERF20 reporters.** Confocal imaging of transcriptional reporter lines. (**A**) pMpERF20::mVenus-N7 expression in the gemma meristem. Bottom shows reporter expression in greyscale, top is a composite image with reporter signal in yellow and chloroplast autofluorescence in grey. (**B**) Transactivation reporter (pMpERF20::GAL4-VP16, pUAS::mVenus-N7) expression in gemma. Composite image showing reporter signal in yellow and chloroplast autofluorescence in grey. (**C**) Zoomed in meristem view of (**B**). Composite image showing ERF20 reporter expression in yellow, pMpYUC2(5.5kb)::mTurqouise2-N7 in cyan and pMpUBE2::mScarletI-lti6b membrane marker in grey. (**D**) Same as (**B**) but imaged after five days of gemma growth on 0.5 Gamborg agar. Numbers above the scale bar indicate the number of independent transgenic lines imaged, which showed comparable expression. All scale bars 100µm.

expression of nuclear localised mVenus (Figure 5.7). The heat shock dexamethasone double induction system showed no detectable mVenus fluorescence in control conditions (Figure 5.7A). However when plants were incubated at 37°C for one hour and grown on media containing 10µM dexamethasone very bright fluorescence was observed across all cells (Figure 5.7B). Similalrly, when using the Mp *YUC2* promoter to drive expression of the GAL4-VP16-GR fusion protein, no detectable fluorescence was observed in the absence of dexamethasone (Figure 5.7C). After one day of growth on media supplemented with 10µM dexamethasone, bright mVenus expression was observed, with meristematic cells showing higher levels of fluorescence (Figure 5.7D). Having characterised the induction system, we assembled constructs to induce transactivation of a C-terminal translational fusion of Mp *ERF20* and mVenus. We decided to fuse mVenus to the Mp *ERF20* coding sequence to enable visualisation of Mp *ERF20* over-expression and identify the sub-cellular localisation of Mp *ERF20*.

We were able to transform both Mp *ERF20* over-expression constructs and obtain gemma from several independent lines. However, all gemma showed clear developmental defects in the absence of induction (Figure 5.8). Given that the induction system itself did not induce any developmental defects (Figure 5.7) we reasoned that Mp *ERF20* may be over-expressed even in control conditions, due to leakiness of the induction system. Indeed, while we mostly observed nuclear localised mVenus fluorescence after induction (Figure 5.8B, Day 2) we did also observe clusters of nuclear localised mVenus expression in non-induced controls (Figure 5.8A, Day 2) confirming leaky expression of the system. Despite our inability to precisely regulate Mp *ERF20* missexpression, we did observe a clear phenotype in all plants that contained either of the over-expression constructs. Gemma formed numerous ectopic notches along the gemma edge in addition to the normal pair of notches on either end of gemmae (Figure 5.8). Gemma notches are thought to form as a result of low rates of cell division and tissue expansion in the apex of the notch, which comprises the central stem cell population, compared to surrounding cells [299]. Most ectopic notches were already visible in gemma at the start of the experiment suggesting that they may have emerged during gemma development, but we did observe examples of notch formation (green asterisk) and loss (red asterisk) during our four day time course (Figure 5.8 C). This suggests that ectopic notch formation is not restricted to gemma development in the gemma cup, but can also occur after gemma germination (Figure 5.8). Wild type gemma show exponential growth during early development, doubling in area approximately every 3 days [299]. Gemma growth was severely retarded in our Mp *ERF20* overexpression lines, particularly in the heat shock and dexamethasone treated plants (Figure 5.8 B). Most notches appeared to be dormant over our time-course, with few signs of tissue expansion or cell divisions in surrounding

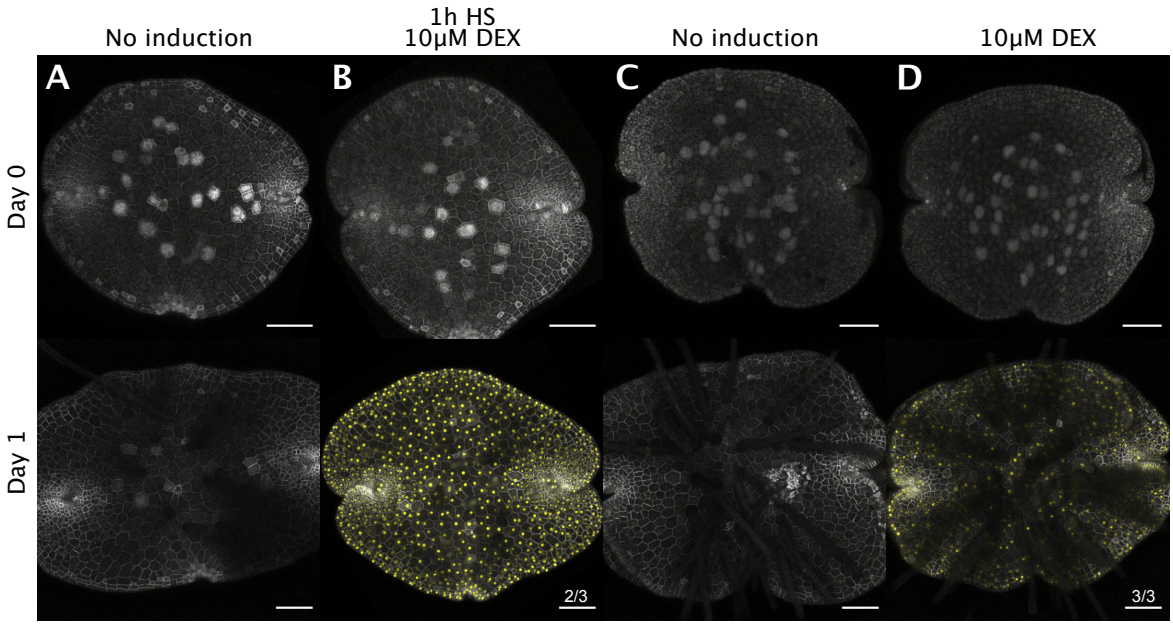

Fig. 5.7 **Inducible overexpression system** Confocal imaging of inducible transactivation constructs. (**A**) Composite image of a gemma showing pMpHSP18.7A1::GAL4-VP16-DEX, pUAS::mVenus-N7 fluorescence in yellow and pMpUBE2::mScarletI-lti6b membrane marker fluorescence in grey. Plant was grown on 0.5 Gamborg agar and imaged at the indicated timepoints. (**B**) Same as (**A**) but gemma was grown on 0.5 Gamborg agar supplemented with 10µM dexamethasone and placed in a 37°C incubator for 1h after acquisition of the Day 0 image (1h HS). The Day 1 image was acquired approximately 24 hours after the heat shock treatment. (**C**) Same as (**A**) but pMpYUC2::GAL4-VP16-DEX, pUAS::mVenus-N7 fluoresce is shown in yellow. (**D**) Same as (**C**) but plants were grown 0.5 gamborg agar supplemented with 10µM dexamethasone. Numbers above the scale bar indicate the number of independent transgenic lines imaged, which showed comparable expression. All scale bars 100µm.

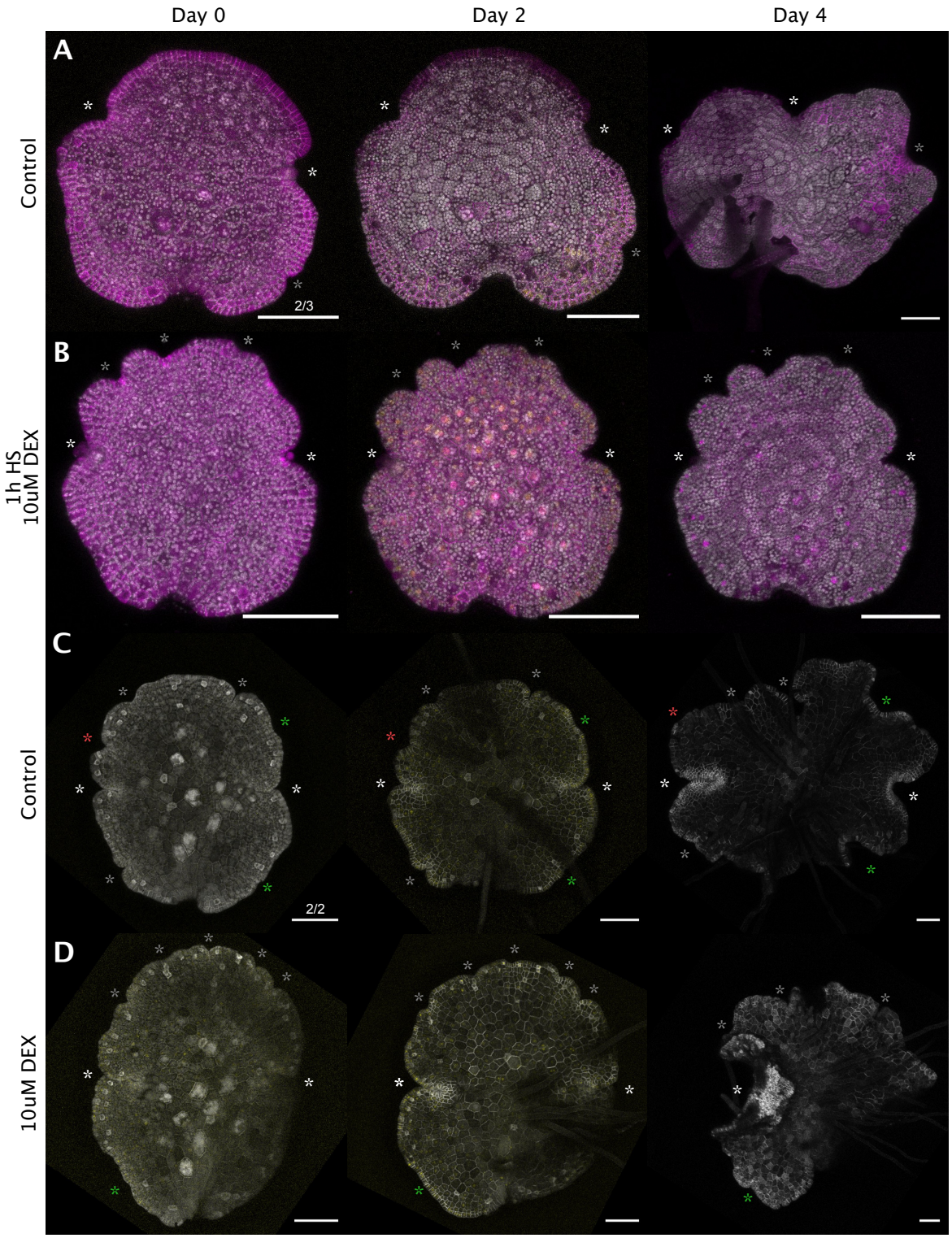

Fig. 5.8 **MpERF20 over-expression** (**A**) Time course confocal imaging of a MpERF20 overexpression gemma on 0.5 Gamborg agar. Composite images of maximum intensity projections showing pMpHSP18.7A1::GAL4-VP16-DEX, pUAS::MpERF20-mVenus expression in yellow, pMpUBE2::mScarletI-lti6b membrane marker expression in magenta and chloroplast autofluorescence in grey. Images were acquired at the indicated time-points. (Continued on next page)

Fig. 5.8 (continued) (**B**) Same as (**A**) but gemma was grown on agar supplemented with 10µM dexamethasone and moved to a 37°C incubator for 1h after acquisition of the first image (1h HS), before being returned to normal growth conditions. (**C**) Composite images showing pMpYUC2::GAL4-VP16-DEX, pUAS::MpERF20-mVenus expression in yellow and pMpUBE2::mScarletI-lti6b membrane marker expression in grey. (**D**) Same as (**C**) but gemma was grown on agar supplemented with 10µM dexamethasone. White asterisk indicate the normal pair of gemma meristems, grey asterisk denote ectopic meristems visible throughout the time course, green asterisk indicate ectopic meristems that form during the time course and red asterisk indicates ectopic meristems that disappear. Numbers above the scale bar indicate the number of independent transgenic lines imaged, which showed similar phenotypes. All scale bars 100µm.

cells. We typically observed only a single mitotically active notch in plants after four days, which is very uncommon in wild type plants where both notches always mark mitotically active meristems. We observed cases where one of the original notches showed meristematic activity (Figure 5.8 C-D) as well as cases where an ectopic notch became active while the original notch remained dormant (Figure 5.8 A). These results suggest that Mp *ERF20* over expression alone is sufficient to induce ectopic notch formation and that ectopic notches are functionally equivalent to the pair of notches that form during gemma development. The fact that the original pair of notches is still clearly visible and correctly positioned in our over-expression lines suggests that tissue patterning during gemma development in gemma cups is not disrupted by Mp *ERF20* activity. The slow growth of plants and small number of notches that become mitotically active could suggest competition between notches. Given our previous results, we suggest that ectopic Mp *ERF20* expression may induce apical cell fate resulting in notch formation. Ectopic apical cells may represent new centres of auxin production and export. Since there is very little space between notches, neighbouring notches may inhibit each other via auxin accumulation, while the strongest source of auxin production may eventually repress all other notches, permitting outgrowth of an active meristem.

5.4.1 MpERF20 over-expression overwrites auxin mediated inhibition of cell divisions

To further interrogate the relationship between central stem cells, Mp *ERF20* and auxin, we treated Mp *ERF20* overexpression plants with a high concentration of exogenous auxin. Plants without the overexpression construct that were treated with 10µM auxin showed rapid division arrest, cell expansion, ectopic rhizoid formation and rhizoid outgrowth (Figure 5.9 A). In contrast Mp *ERF20* overexpression lines did not show a clear rapid response to auxin

treatment over the first two days (Figure 5.9 C, centre). However, after four days of auxin treatment ectopic rhizoids did form, which are marked by loss of chlorophyll (Figure 5.9 C, right). All notches in auxin treated plants remained dormant in contrast to Mp *ERF20* overexpression plants that were grown in the absence of auxin, which showed clear signs of meristem activity after four days (Figure 5.9 B, right). Intriguingly, we did observe small clusters of dividing cells in auxin treated plants after fours days, which also showed Mp *ERF20* expression (Figure 5.9 C, right, white arrows). These observations suggest that Mp *ERF20* expression may promote auxin insensitivity, permitting slow rates of cell division even in the presence of high levels of exogenous auxin.

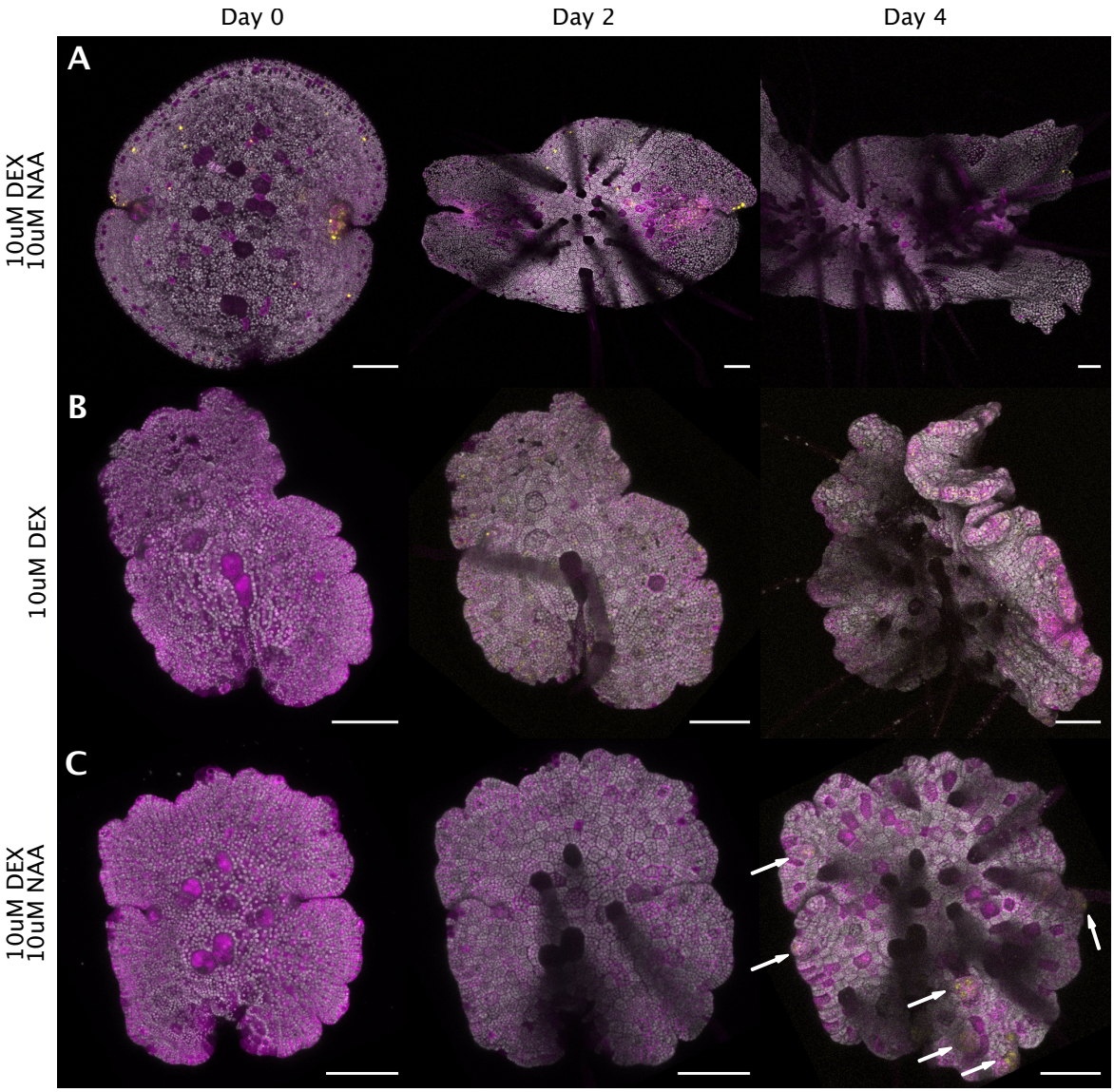

Fig. 5.9 **MpERF20 overexpression induces auxin insensitivity** (**A**) Time course confocal imaging of gemma gemma on 0.5 Gamborg agar supplemented with 10µM dexamethasone and 10µM naphthalene acetic acid (NAA). Gemma contains the MpERF20 transcriptional reporter pMpERF20::GAL4-VP16, pUAS::mVenus-N7 (shown in yellow) and a membrane marker pMpUBE2::mScarletI-lti6b (shown in magenta). Chlorophyll autofluorescence is shown in grey. Composite images of maximum intensity projections. Images were acquired at the indicated time-points. (**B**) Same as (**A**) but showing MpERF20 overexpression gemma (pMpYUC2::GAL4-VP16-DEX, pUAS::MpERF20-mVenus, fluorescence shown in yellow) on media containing only 10µM dexamethasone. (**C**) Same as (**B**) but agar was additionally supplemented with 10µM naphthalene acetic acid (NAA). White arrows indicate dividing cell clusters which also showed mVenus fluorescence. Numbers above the scale bar indicate the number of independent transgenic lines imaged, which showed similar phenotypes. All scale bars 100µm.

5.5 Discussion

In this chapter I investigated the role of auxin and the central stem cell population during gemma development. I showed that central stem cells are marked by Mp *YUC2* and Mp *PIN1* expression. I established a functional auxin response reporter based on the DR5v2 promoter, which demonstrated that auxin response in gemma is restricted to cells in the central portion. I imaged a dual transcriptional reporter for Mp *ARF1* and Mp *ARF2* during gemma development. The expression of this reporter supports the hypothesis that ARF stoichiometry may contribute to a low auxin signaling environment. I identified specific expression of the AP2/ERF transcription factor Mp *ERF20* in apical cells and demonstrated that Mp *ERF20* overexpression is sufficient to induce ectopic notches. Apical notches are comprised of central stem cells which are thought to be derived from the central apical cell, suggesting that Mp *ERF20* overexpression promotes apical cell fate. Mp *ERF20* overexpression also induced auxin insensitivity, delaying ectopic rhizoid formation and permitting slow cell divisions even in the presence of high concentrations of auxin.

The result presented in this chapter are consistent with previous work on auxin signaling in Marchantia and provide important new insights about the boundaries of meristem domains. Localised meristematic expression has been reported previously for Mp *YUC2* [70] as well as Mp *SHI* [88] which is thought to activate YUCCA gene expression [298, 72]. However, in both cases the use of GUS reporters and consequently low resolution imaging, prevented the determination of the exact cellular boundaries of YUCCA gene expression. Our results suggest that a single layer of cells in the centre of the meristem, forming a U-shaped population at edge of the tissue, is the likely source of apical auxin in Marchantia gemma. Apical auxin production and low auxin signaling in the meristem has also been reporter in Physcomitrium [320], supporting the role of auxin as a differentiation signal in Bryophytes.

We identified high expression of Mp *PIN1* in the CENTRAL STEM CELL population and observed highly localised fluorescence when imaging transcriptional reporters of Mp *PIN1* in the centre of the meristem. These observations suggest that auxin transport may be limited to the centre of the meristem. Given the long range auxin transport implied by previous experiments in Marchantia [70], as well as our own observation of localised auxin biosynthesis in the apex and auxin response in the central portion, we were surprised to observe Mp *PIN1* reporter expression specifically in central stem cells. Using our transactivation reporter, we observed more widespread expression, suggesting that lower levels of Mp *PIN1* expression may be present across the meristem. In addition, we only investigated Mp *PIN1* promoter activity. Cell to cell movement of mRNA and PIN1 proteins, could result in much more widespread PIN1 protein distribution. The Marchantia genome also contains four more PIN genes thought to regulate intracellular auxin homeostasis in bryophytes

[332, 363] as well as 3 PIN-LIKES (PILS) proteins which have been shown to perform similar functions in angiosperms [83]. We did find evidence for high expression of these genes in the PZ CELLS and DORSAL 1 clusters in our single cell data (Figure 5.10) suggesting that intracellular auxin sequestration may play a so far underappreciated role in maintaining low auxin signaling in the wider meristem. ARF stoichiometry and the broad meristematic expression of Mp *TPL* [88] also likely contribute to maintaining an auxin response minima in the meristem. Furthermore, in Arabidopsis, a detailed analysis of auxin response during shoot meristem organogenesis, showed that temporal integration of auxin concentration is required to induce auxin response [98]. This may be mediated by ARF dependent recruitment of histone deacetylases [345] including *TPL* [204] which may imprint genetic memory of low auxin signaling states via repressive chromatin marks. If this mechanisms is conserved in Marchantia, it is possible that auxin may indeed only be excluded from a small domain in the centre of the meristem, but surrounding cells only respond to auxin after prolonged exposure. Because the response is delayed cells may be displaced from the meristem before showing high levels of auxin response. This could explain the wider exclusion of auxin signaling from the meristem. The development of an auxin concentration reporter would be an important next advancement to uncover the dynamics of auxin distribution in Marchantia. Attempts have been made by us an others Delmans [52] to generate an auxin concentration reporter by adapting the R2D2 reporter Liao et al. [191] to Marchantia using the DII domain of Mp *IAA*. However, so far we have been unable to generate a reporter which showed a sensitive response to auxin. Alternative reporter systems such as a recently reporter auxin FRET sensor [127] could also be explored. We anticipate that auxin export, intracellular auxin sequestration, ARF/TPL stoichiometry and epigenetic memory all contribute to maintain a low auxin signaling output in the meristem and expect that the development of auxin concentration reporters for Marchantia may help to determine the relative contribution of each of these factors.

In this chapter I also identified Mp *ERF20* as regulator of apical cell fate. While Mp *ERF20* does not have clear orthologs in other species, numerous AP2/ERF transcription factors including *WIND1* [157, 156], *ESR1* [174, 155], *ERF115* [129] and PLT3/5/7 genes [168] are key regulators of shoot meristem regeneration in Arabidopsis. In Physcomitrium the STEMIN family of AP2/ERF transcription factors has also been implicated in stem cell regeneration following wounding and STEMIN overexpression has been shown to be sufficient to induce ectopic chloronema apical stem cells [149]. Orthologs of Arabidopsis *AINTEGUMENTA*, *PLETHORA* and *BABY BOOM* (*APB*) genes in Physcomitrium have also been shown to be essential for gametophore apical stem cell formation, suggesting a critical ancient role of this AP2/ERF family in specifying stem cell identity [8]. While a similar role

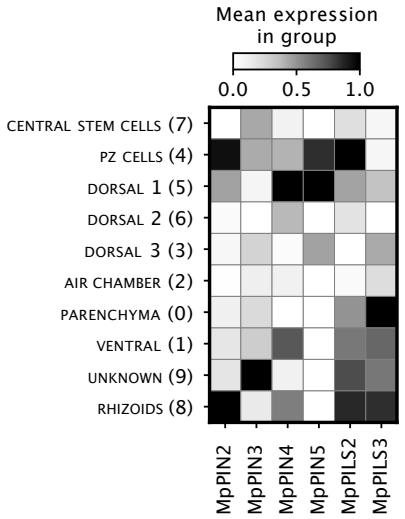

Fig. 5.10 **Non-canonical PIN expression** Heatmap of non-canonical PIN and PIN-LIKES genes expression across cell types. Greyscale scale shows the average gene expression across each cluster, re-scaled to the range 0-1 for each gene.

has been proposed for the only Marchantia *APB* ortholog [90, 122] the lack of meristematic expression of Mp *APB* (Figure 3.3) and our characterisation of Mp *ERF20* function, suggest that Mp *ERF20* may be the key regulator of apical stem cell fate in Marchantia. However, additional work will be required to uncover how Mp *ERF20* regulates stem cell fate and whether Mp *APB* is also involved in stem cell regulation in Marchantia. I have attempted to generate loss of function alleles of Mp *ERF20* to establish if Mp *ERF20* is required for apical cell formation, but was unable to obtain mutant alleles. During revisions of this thesis, Ishida et al. [147] characterised the function of Mp *ERF20* during Marchantia meristem regeneration, which is discussed further in Chapter 7. Ishida et al. [147] provided complementary data and observations that support the role of Mp *ERF20* as a stem cell regulator. They showed that Mp *ERF20* expression is repressed by auxin and that Mp *ERF20* knockout plants are viable, but show reduced proliferation during normal thallus growth and thallus regeneration. The authors also observed the formation of additional meristems in gemma of Mp *ERF20* overexpression lines, although the authors did not discuss these observations, focusing on the role of Mp *ERF20* during meristem regeneration instead. The high resolution time lapse imaging presented in this Chapter, strongly support our interpretation that Mp *ERF20* overexpression is sufficient to drive ectopic formation of apical cells. However, the results presented by Ishida et al. [147] suggest that Mp *ERF20* is not essential for apical cell fate. In summary, Mp *ERF20* appears to be a key regulator of apical cell fate in Marchantia and similarly to other angiosperm and bryophyte AP2/ERF transcription factors, it also plays a key role during tissue regeneration, which will be discussed further in Chapter 7.

Chapter 6

Regulation of the proliferation zone

6.1 Introduction

The rates of cell division, cell expansion, orientation of divisions and anisotropy of expansion at sites of tissue growth underpin plant morphogenesis [44]. The spatio-temporal control of cell division rates is one of the most important aspects of meristem function. Previous efforts to map tissue expansion and cell divisions during Marchantia gemma development [25, 250, 52] and thallus tissue growth models [299], suggest that the Marchantia meristem is comprised of a slowly dividing and expanding centre, surrounded by a zone of rapid cell division and expansion. This is reminiscent of the organisation of angiosperm shoot and root apical meristems, where a slowly dividing centre (central zone in the SAM, QC in the RAM) is surrounded by zones of rapid cell division (peripheral zone in the SAM, division zone in the RAM) [21, 312].

Cell division rates are determined by the frequency of cell cycle initiation and the speed of progression through the cell cycle, which are controlled by an array of cell cycle genes. The cell cycle includes DNA synthesis (S) and mitotic (M) phases separated by two gap phases (G1 and G2) (Figure 6.3 A). Progression through the cycle is thought to depend on the activity of cyclin-dependent kinases (CDKs) [270]. The main CDKs in plants are CDKAs, which are expressed throughout the cell cycle in all eukaryotes, and CDKBs which are plant specific and expressed during G2 and M phase [229]. CDK activity is dependent on a diverse array of cyclin genes which represent the important site of environmental and hormonal signal integration [291]. Most cell cycle regulation is clustered around the transitions from G1 to S phase and from G2 to M phase, representing the two major cell cycle checkpoints. The plant hormone cytokinin stimulates cell divisions [218] by promoting cell cycle progression through both the G1/S and G2/M phase transitions [280]. At the G1/S transition, cytokinin activates expression of D-type cyclins [260] promoting entry into the cell cycle [43]. At the

G2/M phase transition, cytokinin promotes MYB3R4 nuclear localization to activate mitosis [353].

Cytokinin signaling is mediated by a by a two component histidine kinase pathway (Figure 6.1 A). The dominant biosynthesis pathway for cytokinin is a two step reaction mediated by IPT and LOG genes, with the first step thought to limit the rate of overall reaction [238]. Cytokinin can be inactivated by cytokinin oxidases (CKX) and imported or exported from cells. Cytokinin is sensed by cytokinin receptor histidine kinases (CHK) [108] which auto-phosphorylate upon cytokinin binding before phosphorylating histidine-containing phosphotransfer (HPT) proteins. HPTs in turn phosphorylate type A (RRA) and type B response regulators (RRB). RRB proteins activate transcription at target sites when phosphorylated, while RRA proteins act as competitive inhibitors of RRB activation, by competing for phosphotransfer [238].

While the importance of cytokinin signaling for cell cycle regulation and meristem architecture is well established in Arabidopsis, less is known about cytokinin signaling in bryophytes. In Physcomitrium, exogenous cytokinin treatment induces bud formation, promoting the transition from filamentous growth to gametophore development [27, 258]. Conversely, disruption of cytokinin signaling reduces bud frequency and gametophore growth [333]. In Marchantia, Mp *RRB* knockdown and overexpression of Mp *RRA* causes defects in thallus development, generating smaller thalli with serrated margins and fewer gemma cups [87]. Aki et al. [4] further characterised the cytokinin signal transduction pathway, demonstrating that genetic manipulations that reduce cytokinin signalling, including overexpression of Mp *CKX* and Mp *RRA* or knockout of Mp *RRB*, shared phenotypes such as smaller thalli, inhibition of gemma cup formation, enhanced rhizoid formation and hyponastic thallus growth. Reduced cytokinin signaling also resulted in abnormal air pore morphology [5]. Conversely, Mp *RRA* knockout resulted in more gemma cups and epinastic thallus growth. These studies demonstrate that cytokinin is also an important regulator of bryophyte development and suggest that cytokinin may promote cell proliferation in shoot tissues of all land plants. However, how cytokinin signaling relates to cell type identity and whether cytokinin signaling directly controls cell proliferation in Marchantia remains unknown.

In this chapter I show that PZ CELLS are marked by cytokinin signaling and validate expression of new cytokinin markers in the proliferation zone of the Marchantia meristem. I investigate the expression of cell cycle genes, focusing on D-type cyclins. I show that Marchantia has only one canonical D-type cyclin gene, Mp *CYCD1*. I validate Mp *CYCD1* expression in dividing cells of the meristem and show that Mp *CYCD1* expression is sufficient to induce ectopic cell divisions. In contrast, Mp *CYCD2* is expressed at very low levels and does not affect cell cycle progression. These results suggest that cell cycle progression in

Marchantia is regulated by a near minimally complex cyclin repertoire, with a single D-type cyclin gating cell cycle entry in the proliferation zone of the gemma meristem.

6.2 The proliferation zone is associated with cytokinin signaling

Given the important role of cytokinin signaling in regulating cell divisions in flowering plants, I first investigated the expression of cytokinin genes in the single cell dataset to identify if cytokinin signaling was restricted to specific cell types in Marchantia (Figure 6.1 B). Despite observing very low expression for most genes in the pathway, I found evidence for preferential expression of genes in the PZ CELLS and photosynthetic clusters. For the steps in the pathway where there is genetic redundancy, we consistently observed one gene with high expression in the PZ CELLS cluster (Mp *IPT2* (Mp8g02960), Mp *CKX1* (Mp5g03090), Mp *CHK2* (Mp6g00310)) while the other gene showed highest expression in photosynthetic tissues (Mp *IPT1* (Mp1g16480), Mp *CKX2* (Mp5g10910), Mp *CHK1* (Mp2g03050)) suggesting two distinct cytokinin signaling modules which operate in different tissues. Conversely, Mp *LOG* (Mp1g00270) and genes that form the phosphorelay module at the end of the pathway (Mp *HPT* (Mp6g20830)), Mp *RRB* (Mp4g20600), Mp *RRA* (Mp3g03810)) were expressed at higher levels and more broadly across cell clusters. These expression patterns suggest that, similar to our observations for the auxin signaling pathway, biosynthesis of cytokinin may represent the tightest spatially controlled part of the pathway, while the signal transduction system may be present broadly across the tissue. This is consistent with previous reports of broad expression patterns for Mp *RRB* and Mp *RRA* [4].

We aimed to generated fluorescent reporters for genes along the cytokinin signaling pathway and successfully generated transcriptional reporter constructs for Mp *IPT1/2*, Mp *LOG*, Mp *CKX1/2* and Mp *CHK1/2*. However, we were unable to observe any fluorescence for Mp *IPT1*, Mp *LOG*, Mp *CKX2* and Mp *CHK2* (data not shown). Mp *IPT2* reporter expression was also not detectable, but we were able to generated a transactivation reporter which showed fluorescence (Figure 6.2 A). Mp *IPT2* expression was largely absent in gemma, with the exception of stalk cells, but after seven days of growth, expression was clearly localised to the meristem, matching the expression pattern predicted by scRNA-seq. Mp *CKX1* was expressed more broadly across the meristem in gemma and older plants, consistent with scRNA-seq data (Figure 6.2 B). Mp *CHK1* expression was barely detectable, but appeared to also be present across the meristem in older plants (Figure 6.2 C). While our validation of cytokinin signaling is incomplete, our data does suggest that the cells of the

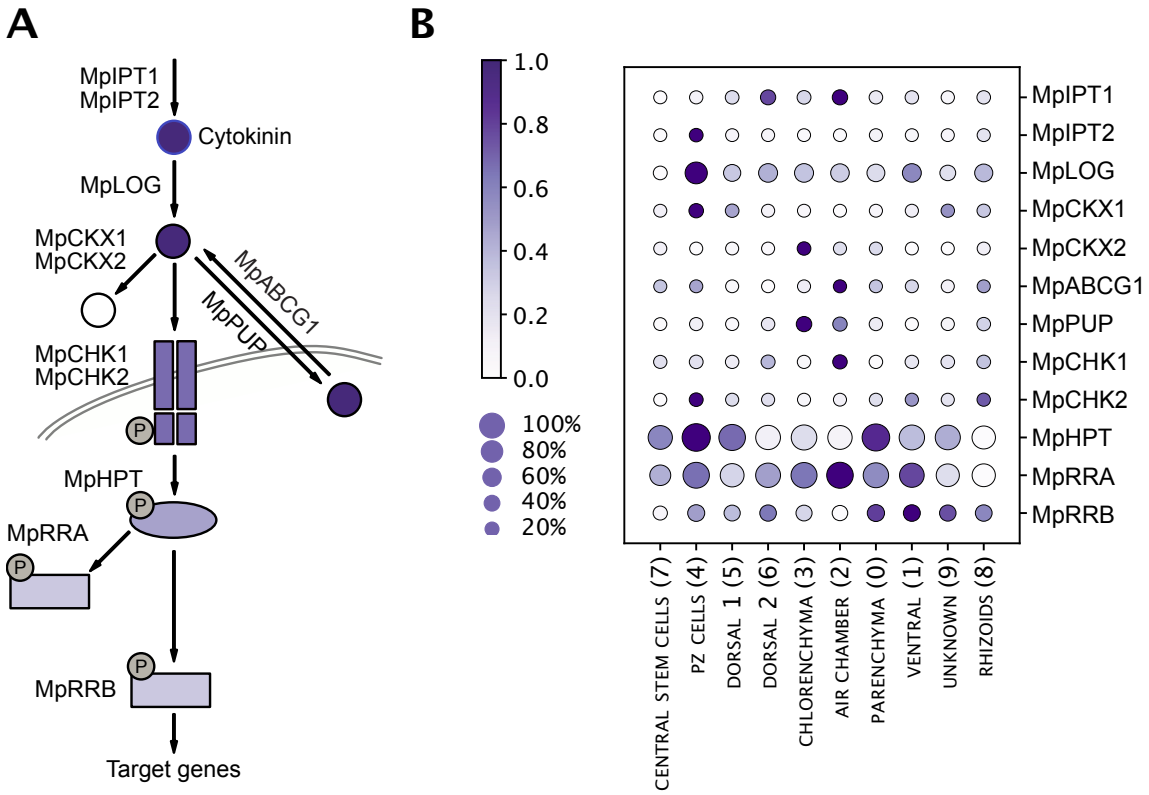

Fig. 6.1 **scRNA-seq expression of cytokinin signaling genes** (**A**) Cytokinin signaling pathway in Marchantia. Cytokinin biosynthesis is catalysed by a two step reaction, mediated by Mp *IPT1/2* and Mp *LOG* with the first step thought to be rate limiting for the overall reaction [238]. Mp *CKX1/2* genes can inactivate cytokinin [4, 285]. Mp *PUP* and Mp *ABCG1* may regulate cytokinin transport, with cell import inhibiting cytokinin signaling and export promoting it [66]. Cytokinins are perceived by Mp *CHK1/2* receptors [108] which auto-phosphorylate upon cytokinin binding and subsequently phosphorylate Mp *HPT* [132]. Mp *HPT* can phosphorylate Mp *RRB* converting it into a active form that can activate target gene expression, while Mp *RRA* competes for phosphorylation by Mp *HPT*, effectively inhibiting Mp *RRB* activation [238]. (**B**) Dotplot heatmap of single cell gene expression of cytokinin signaling genes. Color scale shows the average gene expression across each cluster, re-scaled to the range 0-1 for each gene. Dot size corresponds to the percentage of cells in each cluster expressing the gene.

proliferation zone in Marchantia are high in cytokinin signaling, consistent with the proposed role of cytokinin signaling in promoting cell divisions, particularly on the dorsal side of thalli [4].

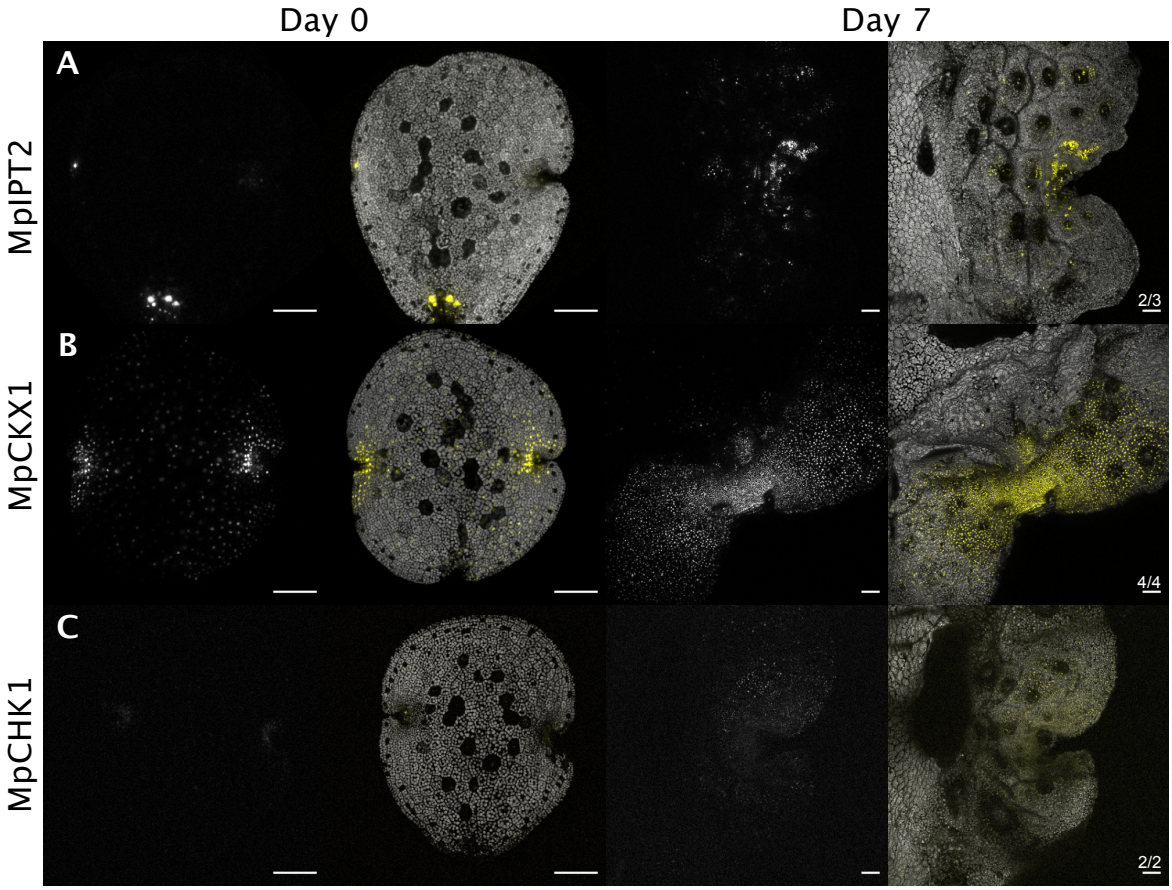

Fig. 6.2 **Cytokinin reporter gene expression** Confocal images of transcriptional reporters for selected cytokinin signaling genes. (**A**) pMpIPT2::GAL4-VP16, pUAS::mVenus-N7 transactivation reporter expression. Expression shown as greyscale or yellow in composite images. Images acquired at indicted time-points. (**B**) Same as (**A**) but showing expression of pMpCKX1::mVenus-N7. (**C**) Same as (**A**) but showing expression of pMpCHK1::mVenus-N7 expression. Numbers above scale bar indicate the number of independent transgenic lines imaged, which showed comparable expression. Numbers above the scale bar indicate the number of independent transgenic lines imaged, which showed comparable expression. All scale bars 100µm.

6.3 Expression of cell cycle related genes

Having found evidence to suggest high levels of cytokinin signaling in the proliferation zone, we next investigated whether cell cycle genes show similar expression patterns to

support PZ CELLS identity as rapidly cycling cells. Figure 6.3 A illustrates the function of key cell cycle regulators in Marchantia. We observed expression of Mp *CDKA* (Mp2g04270) across cell clusters, consistent with CDK presence at all cell cycle stages (Figure 6.3). For Mp *CDKB* (Mp5g19170), Mp *CYCA* (Mp2g25500), Mp *CYCB1* (Mp5g10030) and Mp *CYCD1* (Mp8g17230) we did not detect sufficient expression to infer any expression pattern (Figure 6.3). Mp *CYCD2* (Mp1g24670) expression marked the CENTRAL STEM CELL population, suggesting potential cell type specific cell cycle induction by this cyclin. Mp *RBR* (Mp8g18830), Mp *E2F* (Mp1g02890) and Mp *DP1* (Mp3g12060) were expressed across cell clusters, but we did observe increased expression of E2F-DP in the PZ CLUSTER (Figure 6.3). Mp *KRP* (Mp3g00300) expression marked CENTRAL STEM CELLS and the AIR CHAMBER cell cluster. Apical cells divide slowly [299] and air chamber pores do not divide at all at maturity [166, 152]. The specific expression of Mp *KRP* suggests it may play a role in repressing divisions in these cell types, similar to KRP expression repressing cell division rates in angiosperms [296]. Mp *SIM* (Mp1g14080) is another cell cycle inhibitor which showed broader expression, but also peaked in air chamber cells, but not CENTRAL STEM CELLS (Figure 6.3). Overall, we found widespread expression for most cell cycle genes, except D-type cyclins and their regulators. This is consistent with D-type cyclin expression and activity being tightly controlled by hormonal and environmental signals in Arabidopsis [291].

6.4 MpCYCD1 regulates cell divisions in the proliferation zone

6.4.1 MpCYCD1 is the only canonical D-type cyclin in Marchantia

Given the critical role of D-type cyclins in tuning cell division rates in meristematic tissues of angiosperms, we next focused on establishing whether CYCD function is conserved in Marchantia. The Marchantia genome contains only two D-type cyclins, Mp *CYCD1* and Mp *CYCD2* [29]. We first investigated how these two genes relate to other plant cyclins by searching for cyclin-D orthogroups using Orthofinder [74, 75]. Mp *CYCD1* was placed in an orthogroup with all Arabidopsis D-cyclins (Figure 6.4 A) except three genes which are known to regulate specific asymmetric division events rather than cell proliferation rates (*AtCYCD6;1*: cortex–endodermis lineage [301], *AtCYCD5;1* and *AtCYCD7;1*: stomata development [117, 339]). In contrast, Mp *CYCD2* only has one homologue in Physcomitrium (Pp3c22_17100), suggesting that this CYCD family may be bryophyte specific and not closely related to canonical D-cyclins. In addition, predicted protein domains suggest that

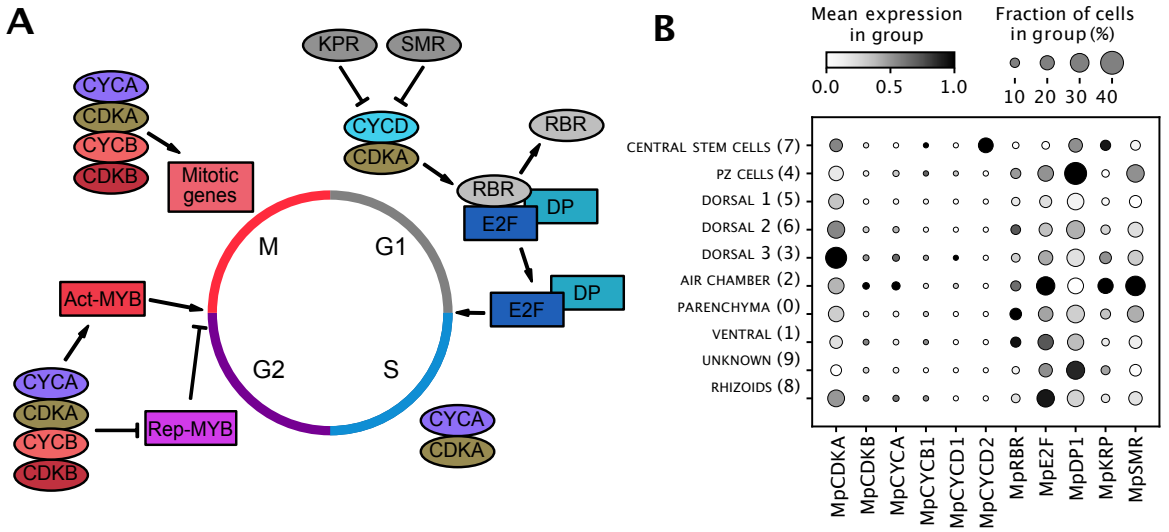

Fig. 6.3 **Expression of cell cycle related genes** (**A**) Schematic overview of cell cycle regulation in plants. Entry into a new cell cycle is regulated in G1 phase where the release of E2F-DP complexes triggers progression into S phase by inducing expression of replication genes [251]. E2F-DP complexes are usually bound and repressed by RBR proteins [55]. Phosphorylation of RBR by CYCD-CDKA complexes disrupts RBR binding, releasing E2F-DP inhibition [26]. CYCD genes themselves are repressed by KRP genes which act as an internal scale to adjust the length of the G1 phase based on cell size [67]. SMR genes form a second family of cell cycle repressors which inhibit CYCD/CDKA complexes [180]. After genome replication, G2/M specifc cell cycle genes including CYCB and CDK are expressed, forming CDKA/B-CYCA/B complexes. Entry into M phase is controlled by the activity of MYB3R transcription factors. Activating MYB3R genes (Act-MYB) can induce expression of mitosis genes [111, 112]. Meanwhile repressive MYB3R genes (Rep-MYB) can arrest cells in G2 phase [38]. The G2 phase CDKA/B-CYCA/B complex can phosphorylate MYB3R genes promoting activation of Act-MYB genes and degradation of Rep-MYB genes, thereby controlling the G2/M transition. (**B**) Dotplot heatmap of single cell gene expression for cell cycle genes. Greyscale shows the average gene expression across each cluster, re-scaled to the range 0-1 for each gene. Dot size corresponds to the percentage of cells in each cluster expressing the gene.

Mp *CYCD2* is lacking one of the conserved cyclin domains, retaining only the N-terminal domain (Figure 6.4 C), similarly to *AtCYCD5;1* in Arabidopsis [306]. These results suggest that Mp *CYCD1* may be the only canonical D-cyclin in Marchantia while Mp *CYCD2* may be part of a bryophyte specific clade, which shares characteristics with Arabidopsis D-cyclins involved in asymmetric cell divisions.

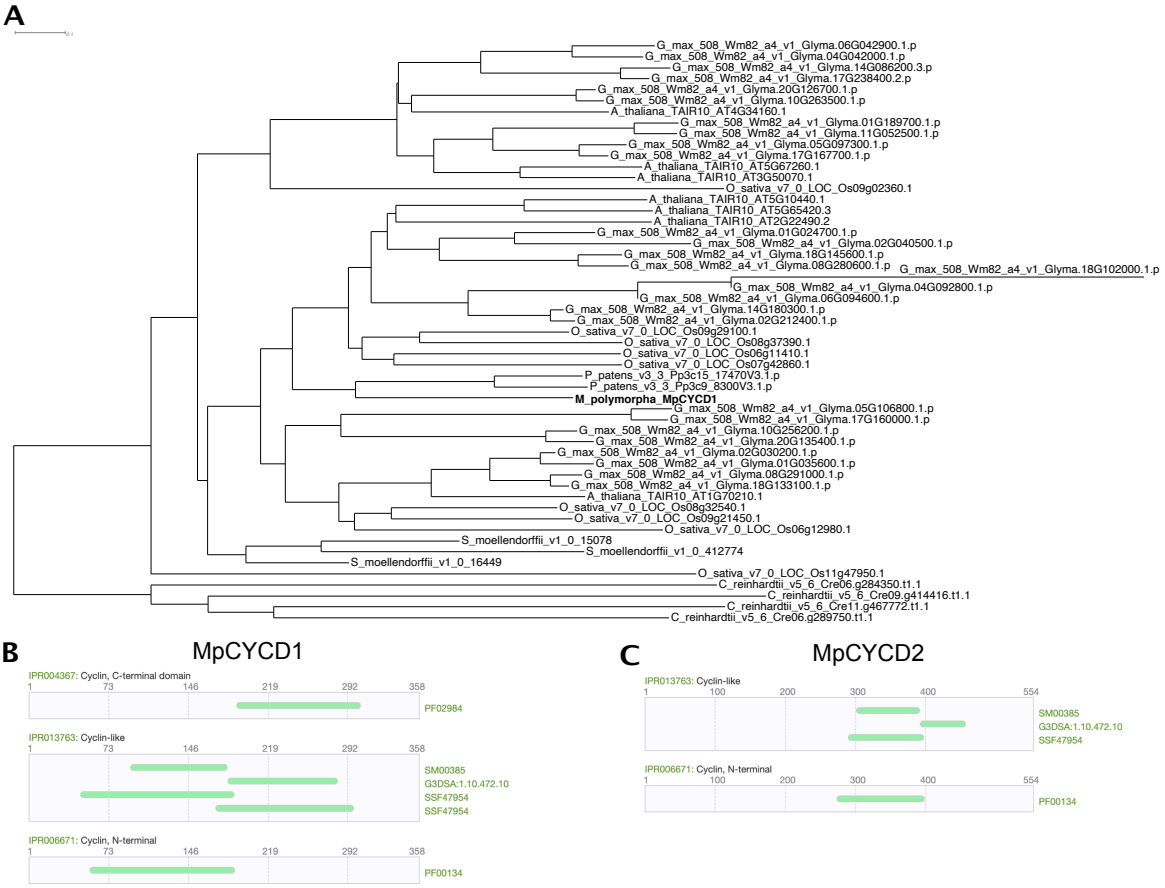

Fig. 6.4 **Orthogroups and protein domains of Marchantia D-type cyclins** (**A**) Rooted gene tree of Mp *CYCD1* homologues in *C. reinhardtii*, *P. patens*, *S. moellendorffii*, *A. thaliana*, *G. max* and *O. sativa* obtained using Orthofinder [74, 75]. Branch length is based on gene similarity scores. (**B**) Predicted protein domains for Mp *CYCD1* obtained from Phyotozome [104] (**C**) Same as (**B**) but for Mp *CYCD2*

6.4.2 MpCYCD1 expression is associated with cell divisions

Next, I aimed to validate the function of both CYCD genes, starting with investigating Mp *CYCD1* expression. Transcriptional reporters for Mp *CYCD1* were generated and their expression was imaged during gemma development (Figure 6.5). We observed bright Mp

CYCD1 expression in some rhizoid precursors and dim expression in the meristem of gemmae (Figure 6.5 A). Expression levels in the meristem increased throughout the time-course and we observed clear, widespread meristematic expression at four days (Figure 6.5 A, right). The expression of Mp *CYCD1* in rhizoid precursors was unexpected since these cells do not divide. However, rhizoid precursor fate is not terminal and cells may revert to chlorophyll rich epidermal cells, particularly on the dorsal site of developing gemmalings. Indeed, we found that many rhizoid precursors that expressed Mp *CYCD1* at the start of the experiment, acquired chlorophyll autofluorescence after two days, suggesting cell fate reversal. These cells underwent several rounds of divisions, forming Mp *CYCD1* expressing micro-sectors (Figure 6.5 B, arrows). Both the initial Mp *CYCD1* expression levels in rhizoid precursor and the frequency of rhizoid precursors reverting back to dividing epidermal cells, seemed to correlate with proximity to the meristem, with most central rhizoid precursors not expressing Mp *CYCD1* and remaining committed to rhizoid fate (Figure 6.5). These expression patterns support a role of Mp *CYCD1* in promoting cell divisions in the meristem in general and in reverting rhizoid precursors in particular.

6.4.3 MpCYCD1 overexpression is sufficient to induce cell divisions

Following these initial results, we generated inducible overexpression lines for Mp *CYCD1* using the heat shock dexamethasone-inducible trans-activation system introduced in chapter 5. We used C-terminal translational fusions with mVenus to enable tracking of Mp *CYCD1* overexpression. We did observe nuclear localised mVenus signal across all cells in gemmae one day after induction (Figure 6.6 C) but not in uninduced controls (Figure 6.6 B). However, despite the absence of mVenus signal, all plants containing the transactivation construct, regardless of the treatment, showed much smaller epidermal cell sizes and correspondingly much larger cell numbers compared induced plants containing a control construct (Figure 6.6 A). This suggested leakiness of our induction system, but confirmed that Mp *CYCD1* expression is sufficient to induce cell divisions in otherwise dormant cells. While there was clear evidence for ectopic epidermal cell divisions one day after induction, rhizoid precursor cells and oil body cells did not frequently express Mp *CYCD1* or show abnormal divisions one day after induction. However, when we followed rhizoid precursor cells for two days after induction we did observe divisions in some cells (Figure 6.6 D). Mature rhizoid precursors can be identified by a lack of chlorophyll autofluorescence and never divide in wild type gemma. The delayed response to Mp *CYCD1* over-expression suggests that rhizoid precursors may express inhibitors to promote Mp *CYCD1* degradation, explaining the initial lack of mVenus signal. Prolonged Mp *CYCD1* induction however did induce divisions even in rhizoid precursors that lack chlorophyll, generating micro-sectors which seem to retain

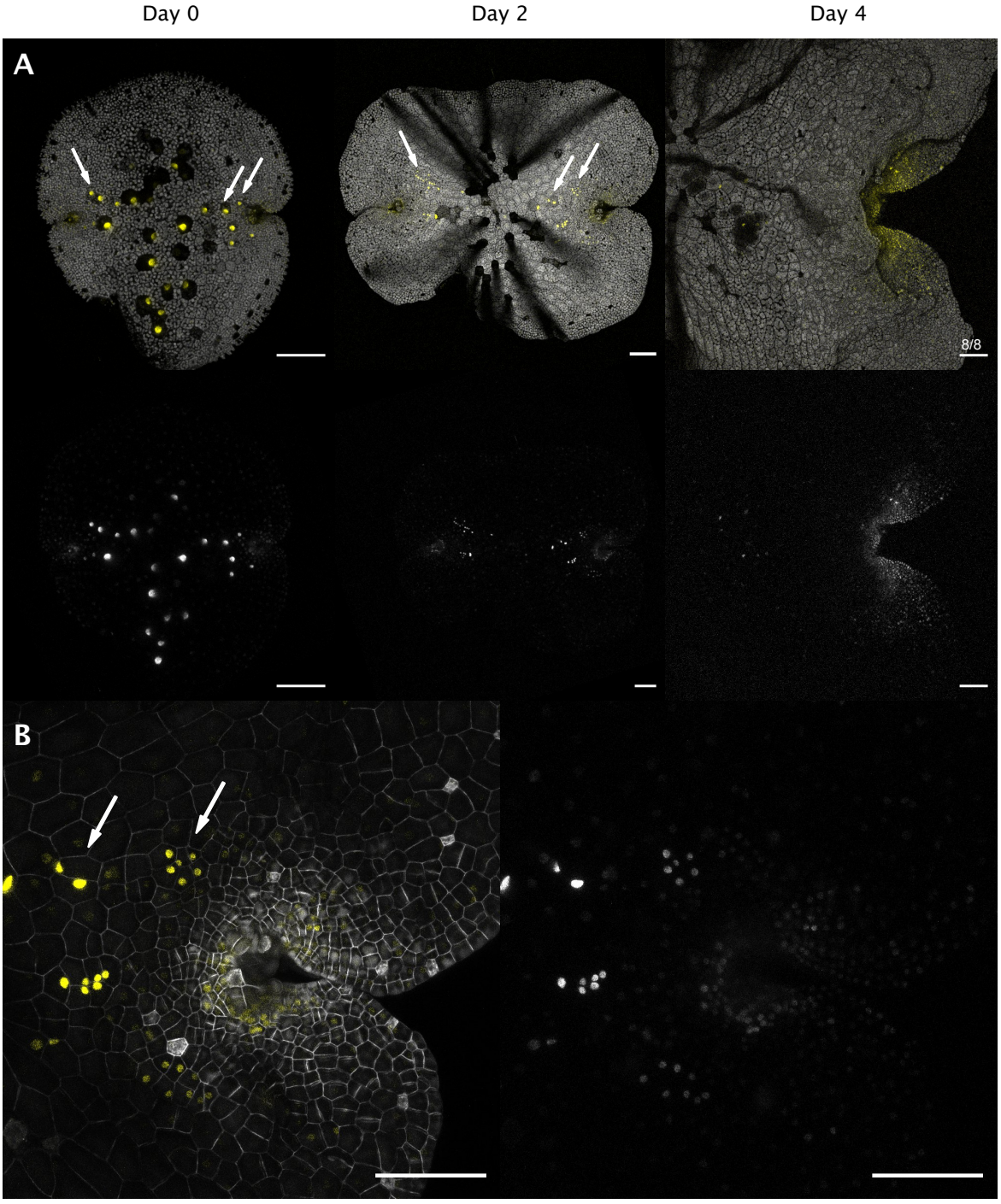

Fig. 6.5 **Expression of Mp *CYCD1*** (**A**) Confocal timecourse imaging of pMpCYCD1::mVenus-N7. Fluorescence is shown in yellow (top) or greyscale (bottom) with chloroplast autofluorescence in grey (top). Gemma was grown on 0.5 Gamborg agar and imaged at the indicated time-points. (continued on next page)

Fig. 6.5 (continued) (**B**) Magnified view of meristem at Day 2. Fluorescence is shown as grascale (right) or yellow (left) with pMpUBE2::mTurquoise2-lti6b membrane marker in grey (left). Arrows indicate Mp *CYCD1* expressing rhizoid precursors which reverted cell fate to epidermal cells forming rapidly dividing micro-sectors. Numbers above the scale bar indicate the number of independent transgenic lines imaged, which showed comparable expression. All scale bars 100µm.

rhizoid precursor fate (Figure 6.6 D, Day 2). Taken together with the high expression of Mp *CYCD1* in rhizoid precursors we observed earlier, we suggest a model where rhizoid precursors express Mp *CYCD1* during normal development, but repress Mp *CYCD1* through protein degradation. When precursor cells start reverting back to epidermal cell fate, Mp *CYCD1* may be released from inhibition and cells are permitted to cycle rapidly. Prolonged Mp *CYCD1* overexpression can overcome this inhibition and induce divisions even in cells that remain committed to rhizoid precursor fate. In contrast, we did not observe any oil body divisions, despite observing oil body cells with clear nuclear localised mVenus expression, suggesting that these cells are resistant to Mp *CYCD1* induced divisions (Figure 6.6 D). mVenus signal in oil body cells did not appear to be delayed compared to normal epidermal cells arguing against degradation based inhibition of Mp *CYCD1* in these cells. We instead propose that Mp *CYCD1* may not be able to induce divisions in oil body cells because of their small size. Epidermal cells in Mp *CYCD1* overexpression lines appear to reach a minimal size, which is comparable to cell sizes in the central portion of the meristem, as well as oil body cells. These cell sizes may represent a lower physical limit for cell sizes in Marchantia. Our results established Mp *CYCD1* as a key regulator of cell division rates in the Marchantia meristem and showed that Mp *CYCD1* miss-expression can be leveraged as a tool to induce ectopic divisions, irrespective of cell identity.

6.5 MpCYCD2 may not regulate cell cycle progression

Having established Mp *CYCD1* as a key regulator of cell division rates, I analysed Mp *CYCD2* function. A transcriptional reporter for Mp *CYCD2* showed very dim fluorescence in the centre of the meristem and oil body cells (Figure 6.7 A-B), consistent with the expression predicted by our transcriptomic analysis. A direct comparison with Mp *CYCD1* expression in the same plant, further supports distinct expression domains for both genes (Figure 6.7 B). We were unable to obtain high quality images of Mp *CYCD2* expression at later developmental stages due to the low expression levels. To overcome this limitation we built a transactivation reporter. Using this reporter we observed bright fluorescence in cells along

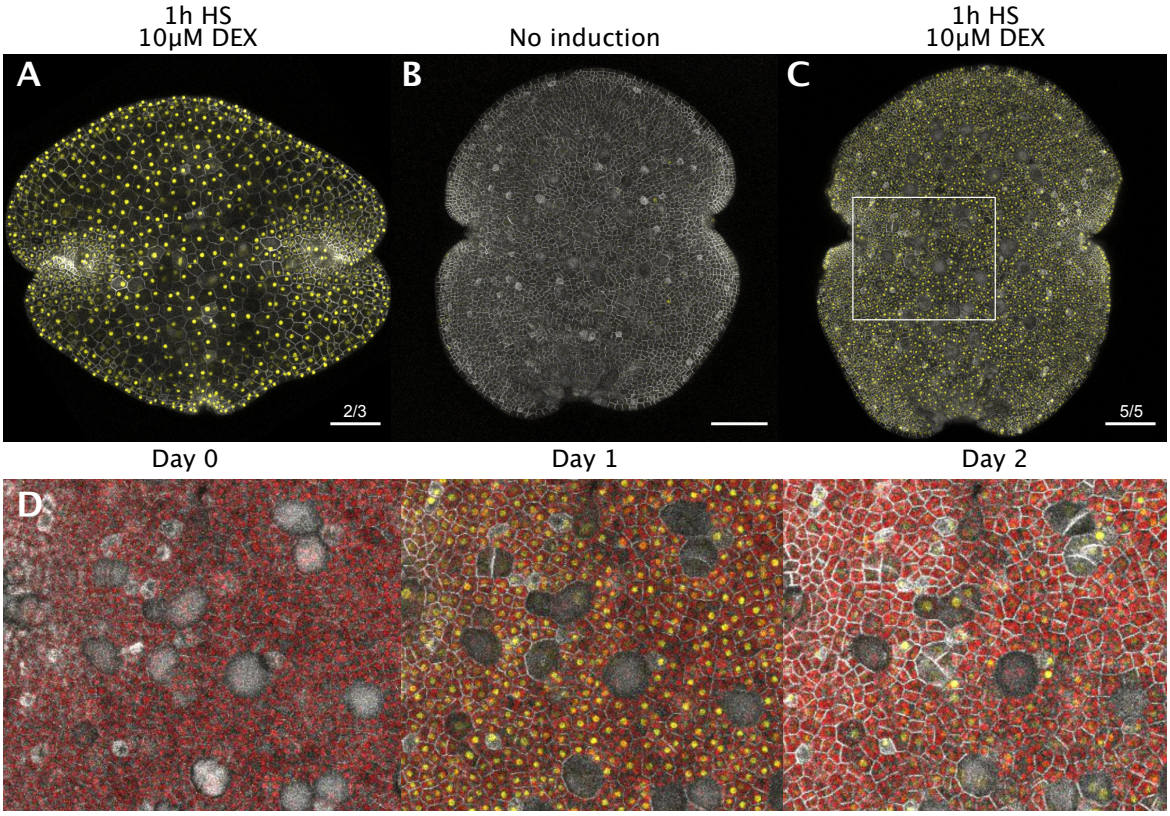

Fig. 6.6 **MpCYCD1 overexpression induces ectopic cell divisions** (**A**) pMpHSP18.7A1::GAL4-VP16-DEX, pUAS::mVenus-N7 gemma imaged one day after 1h heat shock treatment at 37°C and growth on 0.5 Gamborg media supplemented with 10µM dexamethasone. mVenus expression is shown in yellow, pMpUBE2::mScarletI-lti6b membrane marker expression in greyscale. (**B**) Un-induced pMpHSP18.7A1::GAL4-VP16-DEX, pUAS:MpCYCD1:mVenus gemma grown on 0.5 Gamborg media for one day. (**C**) pMpHSP18.7A1::GAL4-VP16-DEX, pUAS:MpCYCD1:mVenus gemma treated as in (**A**). (**D**) Time course of magnified view of (**C**). Centre image corresponds to the region outlined by the white rectangle in (**C**). Colours as in (**C**), with chlorophyll autofluorescence in red. Numbers above the scale bar indicate the number of independent transgenic lines imaged, which showed comparable phenotypes. All scale bars 100µm.

the tissue edge and the meristem centre in two day old plants (Figure 6.7 C) and preferential expression in air pore cells in five day old plants (Figure 6.7 D). These reporters suggest that Mp *CYCD2* expression is associated with slow, or non-dividing cells, in contrast to Mp *CYCD1* expression across the meristem. To interrogate Mp *CYCD2* function, we generated Mp *CYCD2* overexpression lines using the same construct design we used for Mp *CYCD1*. Mp *CYCD2* overexpression was clearly visible as nuclear localised mVenus fluorescence following induction (Figure 6.7 E). However, mVenus expression was absent in cells in the central portion of gemma, suggesting Mp *CYCD2* degradation in non-meristematic regions. Normal gemma development did not appear to be disrupted in Mp *CYCD2* overexpression lines, with plants showing normal tissue and cell morphology over the first four days of gemma development (Figure 6.7 F-G). These results suggest that Mp *CYCD2* may not have a direct role in regulating cell divisions in Marchantia meristems. The localised expression in non-dividing cells suggests Mp *CYCD2* may play a role in suppressing divisions and our analysis of Mp *CYCD2* overexpression does not rule out weak effects on gemma development. Overall, our analysis of D-type cyclins in Marchantia strongly suggests that Mp *CYCD1* is the only canonical D-type cyclin gene in Marchantia and plays a critical role in tuning cell division rates in the proliferation zone.

6.6 MYB3R function may be conserved in Marchantia

The G2/M phase transition represents the second major cell cycle checkpoint and is regulated by MYB3R transcription factors in plants and animals [270], suggesting deep evolutionary conservation. The Marchantia genome contains seven MYB3R genes [29], but Mp *3R-MYB1* is the only high confidence blast hit for *AtMYB3R1* and *AtMYB3R4*, the two activating MYB3R genes in Arabidopsis [111]. All genes except Mp *3R-MYB1* are also expressed at very low levels, only reaching comparable expression levels to Mp *3R-MYB1* in reproductive tissues, such as sporophytes (Figure 6.8 A-B). To investigate if Mp *3R-MYB1* could be involved in cell cycle regulation we aimed to generated transcriptional reporter constructs. We were unable to observe any fluorescence when we used a Mp *3R-MYB1* promoter to directly drive mVenus expresssion (data not shown), but we did observe fluorescence using a transcriptional transactivation reporter (pMp3R-MYB1::GAL4-VP16, pUAS::mVenus-N7) (Figure 6.8 C-E). Mp *3R-MYB1* expression was localised to the meristem during early gemma development, with similar expression compared to Mp *CYCD1* (Figure 6.8 C-D). After five days Mp *3R-MYB1* expression was more widespread across the meristem, but absent from air chamber pore cells (Figure 6.8 E). In Arabidopsis, MYB3R4 translocation to the nucleus is controlled by cytokinin, providing a molecular mechanisms for cytokinin mediated cell

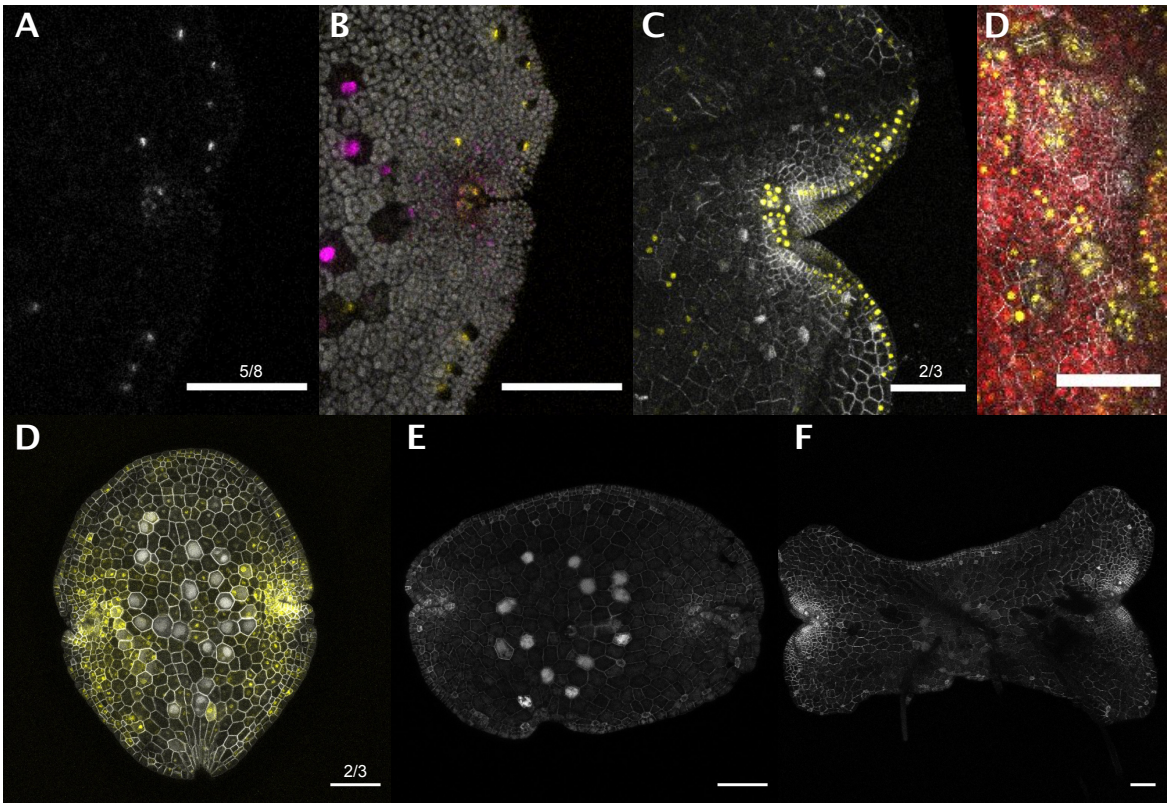

Fig. 6.7 **MpCYCD2 is not associated with dividing cells** (**A**) Confocal image of gemma meristem showing pMpCYCD2:mScarlet-N7 transcriptional reporter expression in greyscale. (**B**) Composite image of gemma meristem with (**A**) in yellow, pMpCYCD1:mVenus-N7 in magenta and chlorophyll autofluorescence in greyscale. (**C**) Expression of pMpCYCD2 transactivation reporter (pCYCD2::GAL4-VP16, pUAS::mVenus-N7) in gemmalings after two days of growth on 0.5 Gamborg agar. Reporter fluorescence in yellow, pMpUBE2::mScarletI-lti6b membrane marker expression in greyscale. (**D**) Same as (**C**) but imaged after five days of growth, showing developing air chambers. Chlorophyll autofluorescence is shown in red. (**E**) Mp *CYCD2* over-expresion gemma imaged one day after 1h heat shock treatment at 37°C and growth on 0.5 Gamborg media supplemented with 10µM dexamethasone. pMpHSP18.7A1::GAL4-VP16-DEX, pUAS:MpCYCD2:mVenus expression shown in yellow and pMpUBE2::mScarletI-lti6b membrane marker expression in greyscale. (**F**) pMpUBE2::mScarletI-lti6b membrane marker expression two days after induction. (**G**) Same as (**B**) but imaged four days after induction. Numbers above the scale bar indicate the number of independent transgenic lines imaged, which showed comparable expression/phenotypes. All scale bars 100µm.

division regulation [353]. We aimed to investigate whether this mechanisms is conserved in Marchantia by generating translational fusions of Mp *3R-MYB1* and mVenus, but we were unable to observe any fluorescence (data not shown). While we were unable to investigate if the nuclear translocation of Mp *3R-MYB1* is a conserved mechanisms of G2/M phase regulation, our results indicate that Mp *3R-MYB1* is a likely candidate for the regulation of the G2/M transition in Marchantia.

6.7 Cytokinin treatment alone may not affect gemmae development

Having established the proliferation zone of the Marchantia meristem as a region of high cytokinin signaling and revealed a conserved function of CYCDs in Marchantia, I next investigated whether cytokinin signaling can be directly linked to cell cycle regulation through the activation of Mp *CYCD1*. We grew gemma containing the pMpCYCD1::mVenus-N7 transcriptional reporter for two days on control media or media supplemented with 100µM kinetin, 100µM 6-Benzylaminopurine (BAP) or 1% (w/v) sucrose, which is also known to induce CYCD expression in angiosperms [261]. Surprisingly, we were unable to observe a clear increase in expression in any of the treatments, compared to control plants (Figure 6.9). We also did not observe any clear phenotypic changes for any of the treatments, suggesting that the tested concentrations may not be sufficient to illicit a response in Marchantia. Given the fast growth of gemma under our growth conditions, it is possible that our inability to induce a response to cytokinin or sucrose treatments may indicate saturation of cell cycle induction. Indeed, previous studies also did not observe clear phenotypic changes for cytokinin treatments [4] and 1% sucrose treatment did not affect cell cycle re-entry rates in regenerating thallus fragments grown under continuous light [228].

To investigate if cytokinin treatment can illicit a response under more repressive growth conditions, we performed co-treatment experiments with auxin and cytokinin. Gemma were grown on agar supplemented with 100µM kinetin as well as 1µM NAA or 10µM NAA and imaged after four days. Gemmalings treated with kinetin alone (Figure 6.10 bottom left) did not show a clear phenotype compared to controls (Figure 6.10 top left) while auxin treated plants showed no signs of growth and conversion of epidermal cells into rhizoids (Figure 6.10 top centre and right). However, co-treatment of auxin treated plants with cytokinin rescued growth defects, with plants grown on 1µM NAA and 100µM kinetin showing near wild type morphology (Figure 6.10 bottom centre). This suggests that exogenous cytokinin

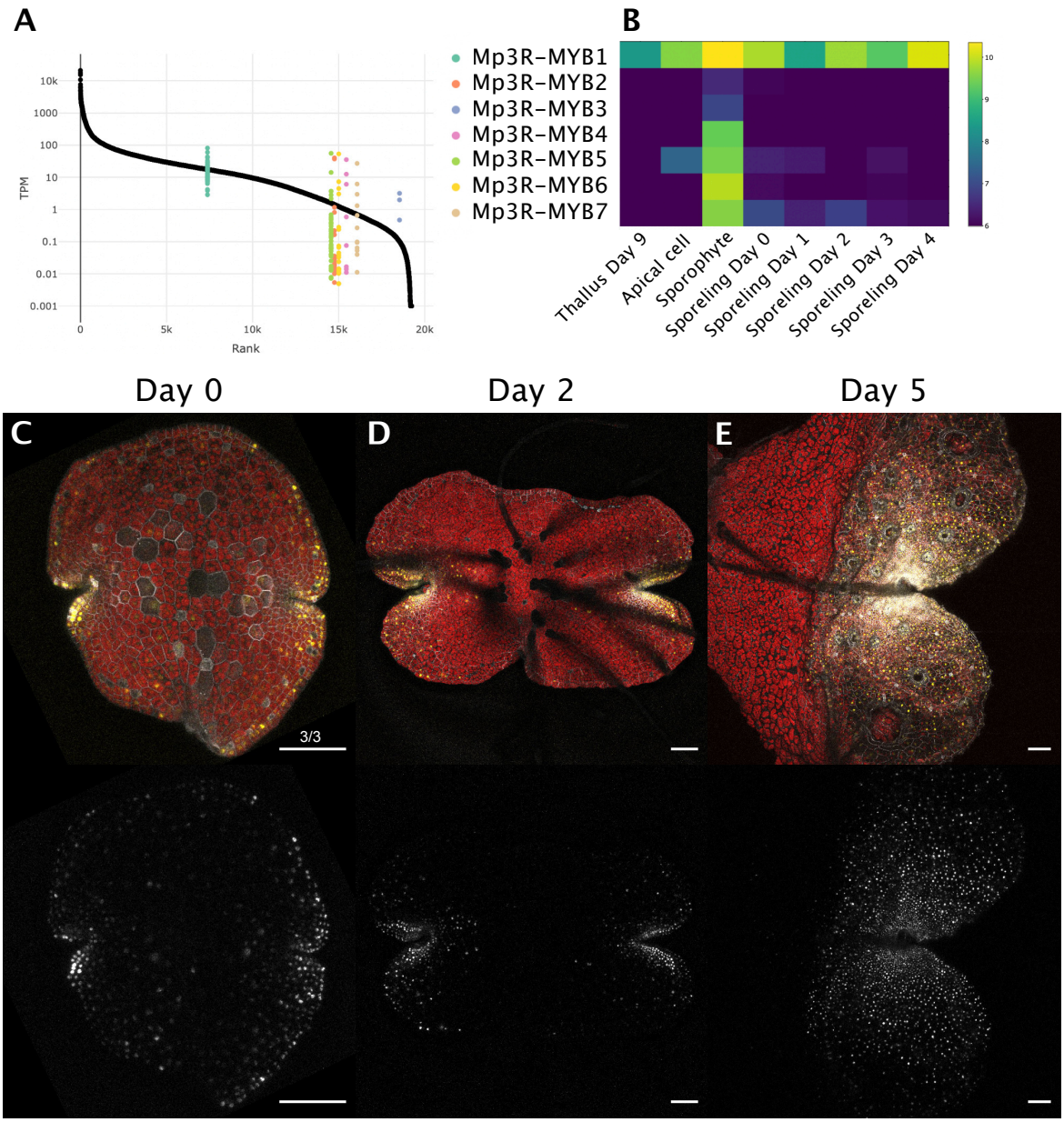

Fig. 6.8 **Mp3R-MYB1 expression in Marchantia** (**A**) Expression of Marchantia MYB3R genes relative to all genes in the Marchantia genome. Black dots show the average expression for each gene across a collection of bulk RNA-seq datasets [279] measured in transcripts per million (TPM) plotted against the rank of the average expression compared to all other genes. Coloured dots show the expression of selected genes across all experimental conditions. (**B**) Heatmap of Marchantia MYB3R gene expression across selected experimental conditions. Color scale shows variance stabilised gene expression per condition [203]. (**C**) Confocal images of Mp *3R-MYB1* transcriptional transactivation reporter (pMp3R-MYB1::GAL4-VP16, pUAS::mVenus-N7) expression in gemma. Top, composite image showing reporter expression in yellow, pMpUBE2::mScarletI-lti6b membrane marker expression in greyscale and chlorophyll autofluorescence in red. Bottom, reporter expression in greyscale. (**D**) Same as (**C**) but imaged after two days of growth on 0.5 Gamborg media. (**E**) Same as (**C**) but imaged after five days. Numbers above the scale bar indicate the number of independent transgenic lines imaged, which showed comparable expression. All scale bars 100µm.

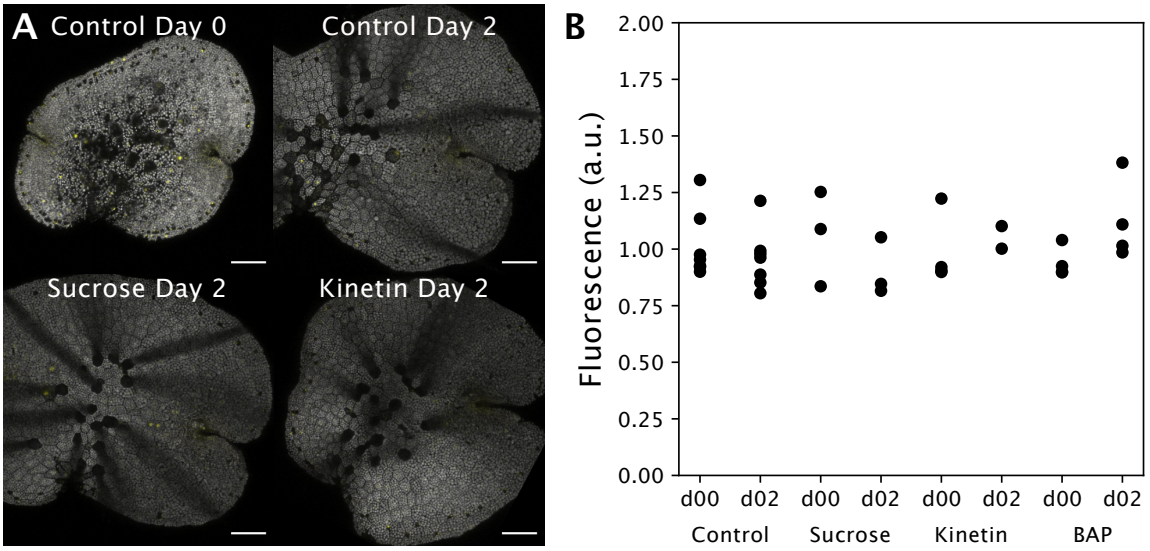

Fig. 6.9 **Response of CYCD1 reporter to cytokinins and sucrose** (**A**) Confocal images of gemma showing pMpCYCD1::mVenus-N7 fluorescence in yellow and chlorophyll autofluorescence in grey. Plants were imaged after the indicated time-points on control media or 0.5 Gamborg supplemented with 1% (w/v) sucrose (Sucrose), 100µM Kinetin (Kinetin) or 100µM 6-Benzylaminopurine (BAP). All scale bars 100µm. (**B**) Fluorescence quantification per gemma for each treatment. Fluorescence per gemma area was calculated and normalised to the average for each independent transgenic line and time-point (d00 = Day 0, d02 = Day 2). Each dot represents one plant, two independent transgenic lines were used.

treatment can affect gemma growth under certain conditions and supports the antagonistic relationship of auxin and cytokinin signaling during Marchantia development.

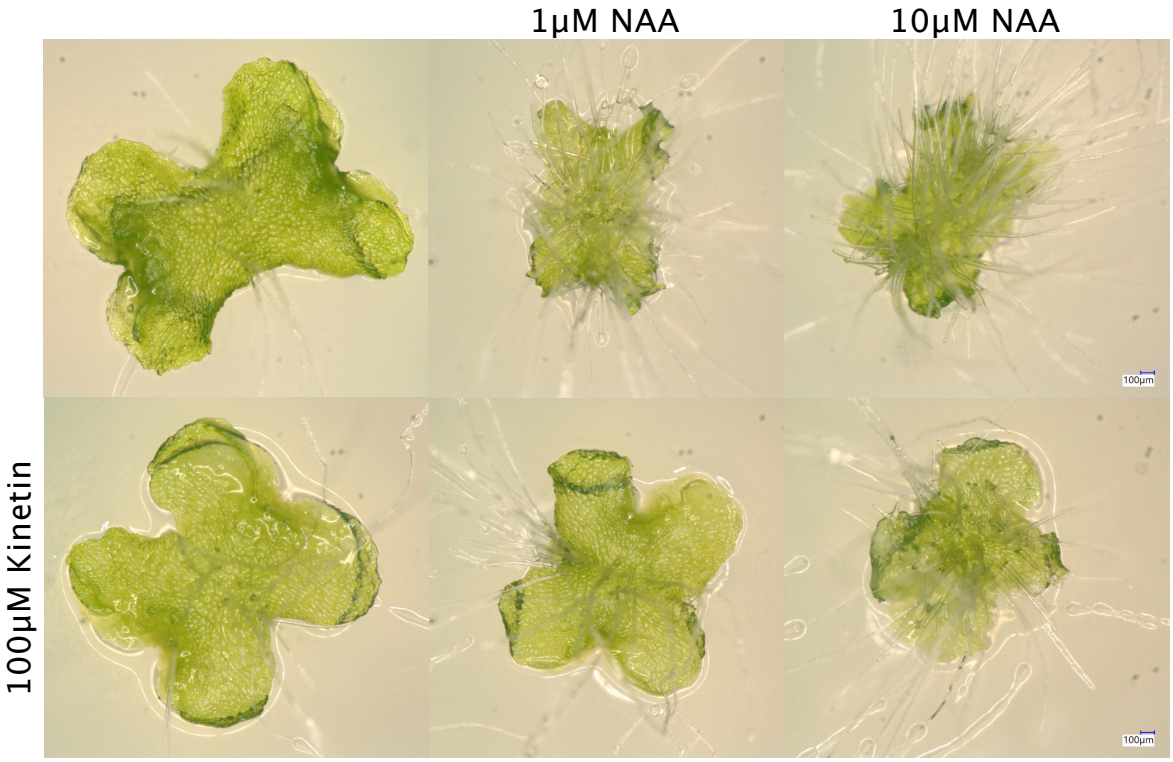

Fig. 6.10 **Cytokinin auxin cross-talk** Brightfield images of four day old Marchantia gemmalings grown 0.5 Gamborg agar supplemented with the indicated concentrations of auxin (NAA) or cytokinin (kinetin). Top left: Control, bottom left: cytokinin treatment only, top right: auxin treatment only, bottom right: auxin and cytokinin treatment. Eight plants were imaged for each condition and images show representative examples of the phenotypes.

6.8 Discussion

In this chapter I described the characterisation of the proliferation zone of the Marchantia meristem. I showed that PZ CELLS may display high levels of cytokinin signaling and observed expression of cytokinin signaling genes broadly across the meristem. I then focused on the regulation of division rates by investigating CYCD function in Marchantia. I showed that Mp *CYCD1* is related to canonical D-type cyclins, expressed in dividing cells and that Mp *CYCD1* overexpression is sufficient to induce ectopic cell divisions in any gemma cell except oil bodies. In contrast Mp *CYCD2* was expressed in dormant cells and overexpression of Mp *CYCD2* did not induce a clear developmental phenotype. In addition, I provided

evidence that supports Mp *3R-MYB1* as a likely regulator of the G2/M phase transition. Finally, I attempted to validate if the molecular mechanisms of cytokinin mediated regulation of the cell cycle are conserved, but I did not observe clear phenotypes for cytokinin treated plants.

Previous studies which treated Marchantia with exogenous cytokinins have not found clear effects on Marchantia growth at concentration ranges which are known to induce strong developmental responses in other plants [87, 4]. There are several possible explanations for the lack of disturbed phenotypes after treatment with exogenous cytokinin. The biologically active cytokinin species in Marchantia may differ from other plants. Examples of such differences have been reported in Marchantia. Jasmonic acid signaling in Marchantia is mediated by OPDA rather than jasmonoyl-isoleucine [219] and Marchantia shows distinct responses to ethylene and its precursor ACC [186]. However, measurements of endogenous cytokinins show that, while the relative abundance of some cytokinin species is different compared to Arabidopsis, Marchantia contains all common cytokinin species and accumulates cytokinins at much higher levels during thallus growth compared to Arabidopsis roots or shoots [4]. *In vitro* characterisation of CHK binding affinities also showed that Marchantia CHKs can bind common cytokinin species, however Marchantia CHKs showed much weaker responses to increasing cytokinin concentrations compared to Physcomitrium or Arabidopsis CHKs [108]. Given the high levels of endogenous cytokinins and low sensitivity of Marchantia CHKs, a second possibility is that the concentrations of exogenous cytokinins in our experiments was not sufficient to illicit a response. Very high concentrations of some cytokinins indeed result in growth retardation [4]. However, this does not mimic any phenotypes of genetic manipulations that increase cytokinin signaling, suggesting pleiotropic effects rather than increased cytokinin signaling. Finally, it is possible that the cytokinin signaling pathway rapidly adapts to maintain similar levels of cytokinin signaling despite greater abundance of cytokinins. Indeed, Aki et al. [4] showed that expression of the negative cytokinin response regulator Mp *RRA* nearly doubled within two hours of treatment with a cytokinin concentration that did not illicit any growth phenotype. It is likely that a combination of these factors enables Marchantia to buffer exogenous cytokinin application under the rapidly growing growth conditions we assayed. Our observation that cytokinin can partially rescue the growth arrest of auxin treated plants supports a view that cytokinin signaling may be saturated and buffered against excess cytokinins under normal growth conditions, while cytokinin concentration may be limiting under repressive growth conditions.

Our characterisation of cell cycle regulation in Marchantia is consistent with results from other plants [270]. Similar to other pathways, Marchantia appears to contain a near minimally complex set of cell cycle regulators, making it an exciting model system to study

cell cycle progression. For the G1/S transition our results suggest that only Mp *CYCD1* functions as a canonical D-type cyclin and that Mp *CYCD1* expression is critical for tuning division rates in Marchantia. CYCD function is generally not thought to be essential for cell cycle progression, but the generation of complete CYCD knockouts in other model species is challenging due to genetic redundancy. There is a report of CYCD knockout in Physcomitrium which suggested very limited disruption to development, with loss of CYCD mainly affecting the response to sugars [202]. At the time, Physcomitrium was thought to contain only one CYCD gene which was disrupted by the authors. However, the current version of the genome contains two CYCD genes which are homologues of Mp *CYCD1* and another CYCD gene which is a homologue of Mp *CYCD2*, suggesting that the minor CYCD knockout phenotype may be explained by genetic redundancy. The use of Marchantia as a model for cell cycle regulation represents a unique opportunity to study cell cycle components with near minimal redundancy, enabling more facile generation of true loss of function alleles.

While cell numbers in Mp *CYCD1* overexpression lines were greatly increased compared to wild-type gemma, there was no clear difference in the overall gemma size and plants were able to complete the full asexual life-cycle without clear sings of impairment. These observations are in line with results in angiosperms where some tissues do not show drastic changes in overall tissue size in response to increased or reduced cell cycle rates, but show altered average cell size across the tissue [56, 67]. Even CDKA knockouts are viable in Arabidopsis, despite greatly reduced cell cycle rates, resulting in abnormally enlarged cells [229]. The remarkable ability of plant organs to form properly across a large range of division rates makes sense given the rigid nature of plant tissues. Unlike soft tissues such as animal organs where cell divisions can push tissue outgrowth, plant cells are physically constrained. Plant organ growth requires tissue wide coordination of cell expansion and cell wall loosening to achieve expansion. Cell cycle regulation in growing tissues is therefore often tuned to maintain appropriate cell sizes [67] rather than being able to directly promote outgrowths.

6.8.1 Summary of the Marchantia meristem model

Based on the results presented in this chapter and chapter 5, I propose a model for Marchantia gemma meristems (Figure 6.11). In the centre of the meristem a small population of slowly dividing central stem cells acts as a dominant auxin source for the surrounding tissue. Central stem cell fate can be induced by Mp *ERF20*. Auxin is transported basipetally and promotes cell expansion, differentiation and dormancy in cells of the central zone. The low auxin signaling environment of the meristem permits cells surrounding central stem cells, to

enter the proliferation zone. Cells in the proliferation zone are characterised by cytokinin signaling and undergo rapid divisions which are tuned by Mp *CYCD1*. The overall growth of Marchantia likely requires a balance of auxin and cytokinin signaling to correctly tune cell expansion and division rates. Although some of the central angiosperm meristem regulators are not conserved in bryopyhtes, this model of the gemma meristem shares similarities with Arabidopsis shoot and root apical meristems. In all three systems populations of slowly dividing cells orchestrate meristem architecture by controlling signaling gradients, which include the establishment of distinct auxin and cytokinin signaling domains. While much work remains to be done to elucidate the regulation of the Marchantia meristem, we anticipate that the gemma meristem will represent an important model system for elucidating fundamental aspects of meristem regulation, by providing a system stripped of much of the complexity of vascular plants.

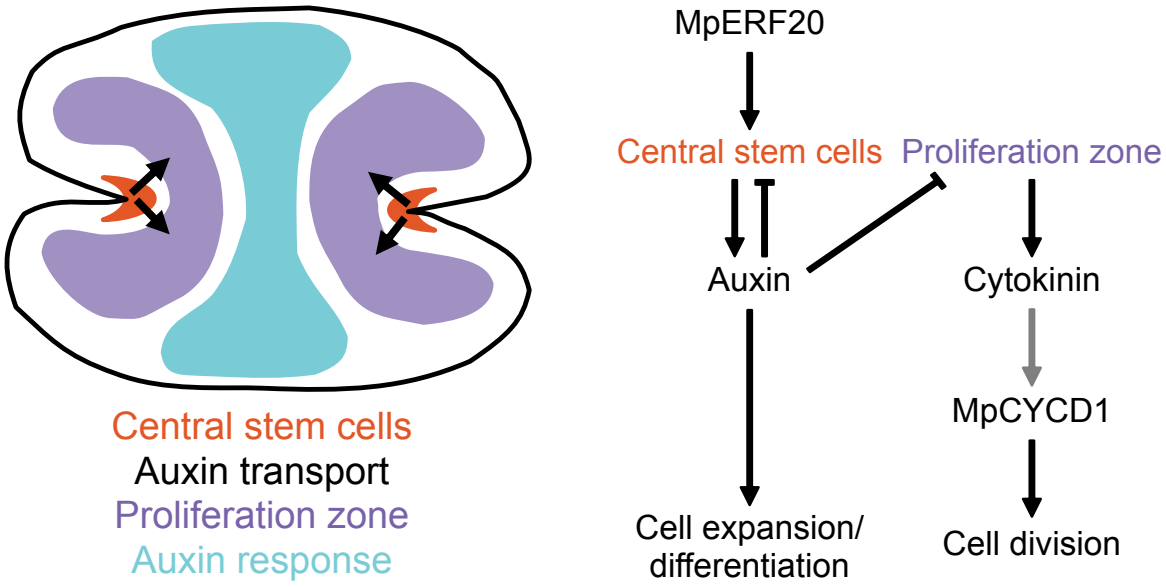

Fig. 6.11 **Gemma meristem model** Left: Spatial cell domains in gemmae, Right: Diagram of cell interactions. Central stem cells form a small population of cells in the meristem centre and central stem cell fate can be induced by Mp *ERF20*. Central stem cells maintain apical dominance by producing and exporting auxin. Auxin promotes cell expansion and differentiation in the central portion of gemma. The proliferation zone surround the central stem cell population. Auxin spatially restricts central stem cells and the proliferation zone by inhibiting both cell fates. Proliferation zone cells are cytokinin sources and their high mitotic activity is regulated by Mp *CYCD1*.

Chapter 7

Meristem regeneration

7.1 Introduction

In contrast to animals, plants generally possess a high degree of developmental plasticity, permitting regeneration of tissues, organs or whole plants following injury [141]. Plant meristems are typically formed during embryogenesis [235] but can also form *de novo* from different tissues, given appropriate signals. In Angiosperms however, meristems typically only regenerate from specific cell populations or indirectly through *in vitro* induction of callus tissue [141]. *In vitro* culture of plant tissue with exogenously supplied hormones, particularly auxin and cytokinin, can be used to induce callus tissue, which comprises a largely undifferentiated cell mass. Callus can be obtained from diverse tissues and subsequently undergo *de novo* shoot or root organogenesis, given appropriate hormonal cues [141]. Transcriptomic profiling of callus cells demonstrates that callus cells posses complex transcriptional identities, but share some similarities with meristematic cells in intact plant tissues [357]. AP2/ERF transcription factors including *WIND1* [157, 156], *ESR1* [174, 155], *ERF115* [129] and PLT3/5/7 genes [168] are key regulators of shoot meristem regeneration in Arabidopsis. While the molecular mechanisms vary for different genes and tissue contexts, stem cell induction is often accompanied by changes in the regulation of auxin and cytokinin response and the regulation of cell cycle genes.

Compared to angiosperms, early divergent land plants generally posses a much greater regenerative capacity. In Physcomitrium, both leaf explants [148] and individual leaf cells [278], regenerate chloronema apical stem cells within 24 hours of wounding without external hormone application. The regeneration of chloronema apical stem cells can be represented as a reversal to early stages of Physcomitrium development, where the tissue grows as tip-growing branching stem cells. At the cellular level, regeneration is marked by activation of cyclin-D genes which promote re-entry into the cell cycle in regenerating stem cells facing the

cut site [150]. The tip growth of regenerating cells requires WUSCHEL-related homeobox 13-like (PpWOX13L) genes, which are induced at the cut site [273]. A group of AP2/ERF transcription factors called STEM CELL-INDUCING FACTOR (STEMINs) regulate stem cell formation and STEMIN1 overexpression is sufficient to induce ectopic chloronema apical stem cells across gametophore leaves [149]. STEMIN1 induces epigentic changes which de-repress target genes including *PpCYCD1* to induce stem cell fate [149]. While STEMINs are not essential for stem cell reprogramming in general, STEMINs also mediate stem cell reprogramming in response to DNA-damage where they are indispensable [109]. The molecular characterisation of stem cell induction in Physcomitrium suggests that AP2/ERF transcription factors may be key regulators of stem cell regeneration processes in land plants. However, while Physcomitrium represents an excellent model to study reprogramming of individual cells, the filamentous growth of early physcomitrium development is very distinct from stem cell regeneration in other land plants, where cells are embedded in a tissue and cell fate dynamics are tightly linked to the re-establishment of morphogen gradients across the tissue.

Marchantia tissue explants from various tissue sources and protoplasts [231] readily regenerate thalli without any exogenous hormone application. Meristem regeneration in Marchantia is thought to resemble early sporeling development [176] where widespread rapid divisions are observed initially in explants lacking meristem, which become progressively restricted to specific domains of the tissue, culminating in establishment of apical cells and formation of a pro-thallus [175]. This makes Marchantia meristem regeneration an excellent model system to study the regeneration of meristems within an intact tissue, which could shed light on general principles of plant tissue regeneration. Studying the regeneration process may also improve our understanding of normal Marchantia meristem regulation. The re-establishment of morphogen gradients in particular, could reveal dynamics which are hard to observe in a steady state system. Early studies on meristem regeneration in Marchantia demonstrated that removal of the apical portion of thalli [334] or removal of a small area of tissue in the centre of the gemma meristem [60] is sufficient to induce meristem regeneration in the remaining tissue. More recent characterisation of auxin signaling in Marchantia suggests that auxin signaling is essential for the transition to ordered thallus growth, with disruptions to auxin signaling resulting in undifferentiated cell masses which resemble developing sporelings before the transition to pro-thalli [70, 88]. However, the re-establishment of phytohormone gradients and the regulation of cell reprogramming, cell divisions and cell differentiation during the regeneration process remain poorly understood.

In this Chapter, I characterize the process of meristem regeneration in Marchantia. Building on previous work [52], I have characterised three distinct stages of meristem regeneration:

widespread divisions (Stage 1), localised divisions (Stage 2) and fully regenerated meristems (Stage 3). I have established that removal of the central stem cell population is sufficient to induce regeneration, while meristems are maintained after partial ablation of different parts of the central stem cell population, affirming the view that central stem cells collectively functions as a tissue organiser, which is indispensable for meristem maintenance. I show that Stage 1 of meristem regeneration is characterised by tissue-wide initiation of cell divisions, mediated by upregulation of Mp *CYCD1*. The transition into Stage 1 is blocked by exogenous auxin treatment. I show that Mp *ERF20* and Mp *YUC2* are rapidly induced during stage one as a result of falling auxin concentrations in the tissue and their expression becomes progressively restricted to newly formed meristems during the regeneration process. I show that auxin transport is dynamically remodelled across the re-generating tissue and that inhibition of auxin transport or biosynthesis arrests regenerating fragments in Stage 2. Based on these results I propose a model for Marchantia meristem regeneration and maintenance which shares common themes with Arabidopsis meristem regeneration models, despite the vast differences between both species, hinting at conserved principles of meristem function in all land plants.

7.2 Stages of meristem regeneration

Previous detailed characterisation of the early stages of meristem regeneration after surgical removal of gemma meristematic notches, demonstrated a rapid onset of cell divisions in less than 24h, followed by progressively more restricted zones of cell divisions and finally full meristem regeneration [52]. We accordingly distinguish four phases of meristem regeneration which are shown in Figure 7.1. Within less than 24 hours, cells which would remain largely dormant in gemma with intact meristems, initiate rapid divisions across the tissue (Stage 1). Around two days after meristem removal, divisions become restricted to several clusters in the regenerating fragments (Stage 2). After five to seven days, fully regenerated, notch shaped meristems, with central stem cells emerge, indicating complete meristem regeneration (Stage 3).

7.3 Central stem cells are indispensable for meristem maintenance

Previous studies investigating meristem regeneration and apical dominance in Marchantia generally removed the entire meristematic region to trigger regeneration. Precise tissue

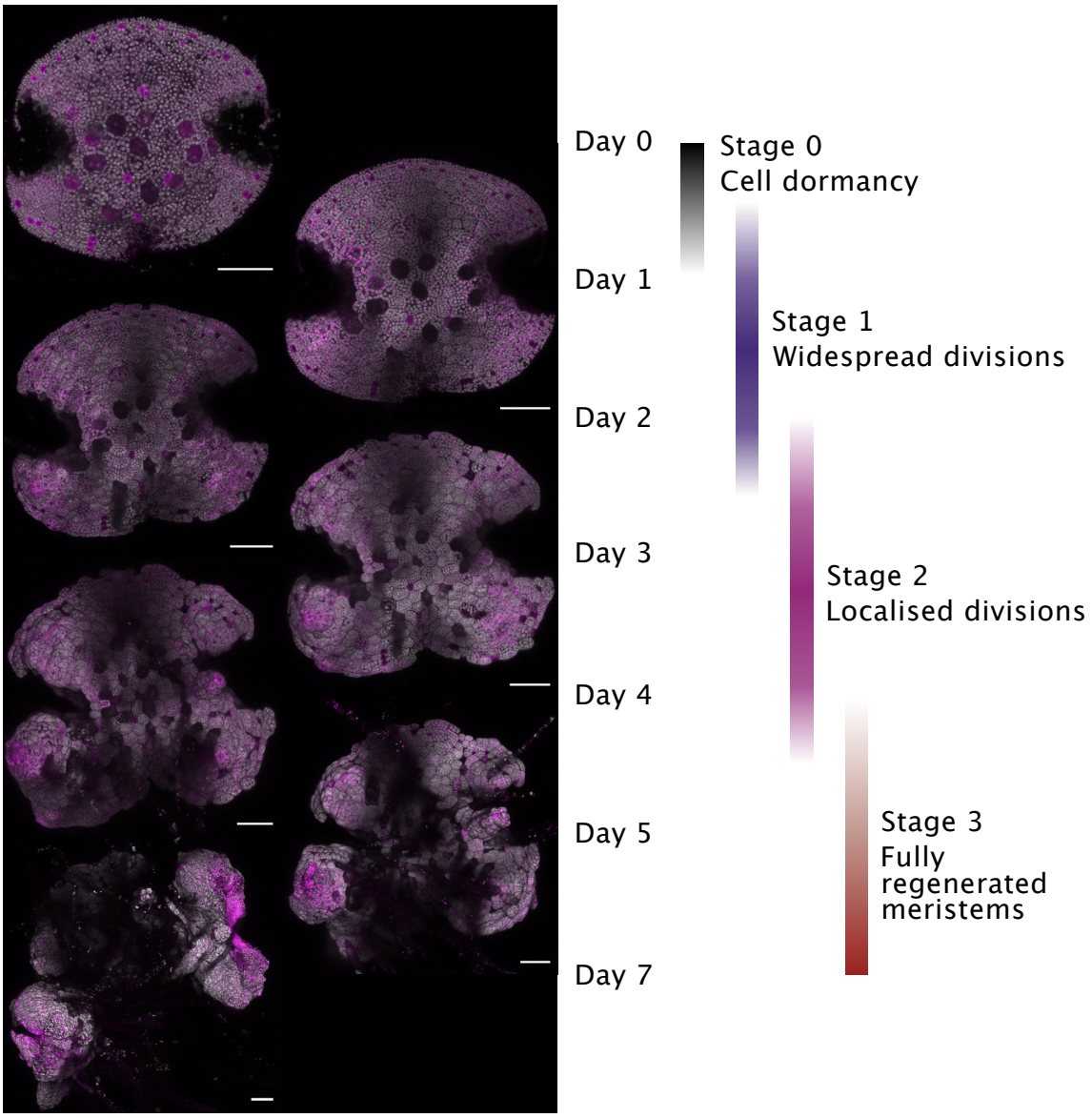

Fig. 7.1 **Stages of meristem regeneration** Left: Time-course of regeneration in a gemma fragment following laser ablation of the meristem. Composite images showing pMpUBE2::mScarletI-lti6b membrane marker expression in magenta and chlorophyll autofluorescence in grey. Images were acquired at the indicated time-points after meristem removal. All scale bars 100µm. Right: Stages of meristem regeneration, the overlap between stages and fading of stages indicates the uncertainty and variability of the timing of stage transitions

ablation, using tools such as laser microdissection, have not been applied in this context, but could help to clarify which specific cell populations in the meristem confer tissue organising properties. Our earlier characterisation of the central stem cell population suggested that central stem cells may function as tissue organisers by acting as auxin sources. If this function is unique to central stem cells, their removal should be sufficient to trigger meristem regeneration. To test this, we performed precise laser ablation experiments ablating only the central stem cell population of a gemma meristem, which comprises the first row of cells in the centre of the meristem, while leaving all other meristem cells intact (Figure 7.2 A-B). The second meristem was completely ablated to prevent any interference. Ablation of the central stem cell population was indeed sufficient to trigger meristem regeneration (Figure 7.2 C). Meristem organisation was disrupted following central stem cell ablation, with the notch of the gemma expanding outwards. A zone of cell division formed behind the ablated central stem cell population, in contrast to regeneration in fragments with completely ablated meristems were divisions are widespread across the tissue (Figure 7.1). This may be explained by the fact that cells of the proliferation zone were left intact in these experiments which are likely primed for high mitotic activity. There were no sign of notch re-establishment after 3 days of regeneration. These observations suggest that the central stem cell population is indispensable for meristem maintenance. However, gemma fragments which retain an intact proliferation zone appear to skip stage 1 of regeneration, as clusters of mitotically active cells are already present in the tissue.

The current Marchantia literature suggests a distinct identity for the central apical cell, compared to lateral cells Shimamura [290]. To test whether only the central apical cell is required for meristem maintenance, we performed targeted ablations, either destroying the flanking region of the central stem cell population, or the central region, while completely ablating the second meristem as before (Figure 7.3 A, C). In both cases, we observed no signs of meristem regeneration and gemma growth proceeded nearly undisturbed (Figure 7.3 B, D). Combined with our earlier characterisation of central stem cell transcriptomes and marker gene expression, these results suggest that central stem cells collectively function as tissue organisers and removal of the whole population is required to trigger regeneration. To simplify interpretation and experimental workflows, we ablated the entire gemma meristem for the remaining experiments.

7.3.1 MpCYCD1 expression is induced in regenerating fragments

Given our earlier characterisation of Mp *CYCD1* function we were first interested to see if the re-activation of divisions in regenerating fragments is associated with Mp *CYCD1* expression. We ablated meristems of gemma containing the pMpCYCD1::mVenus-N7

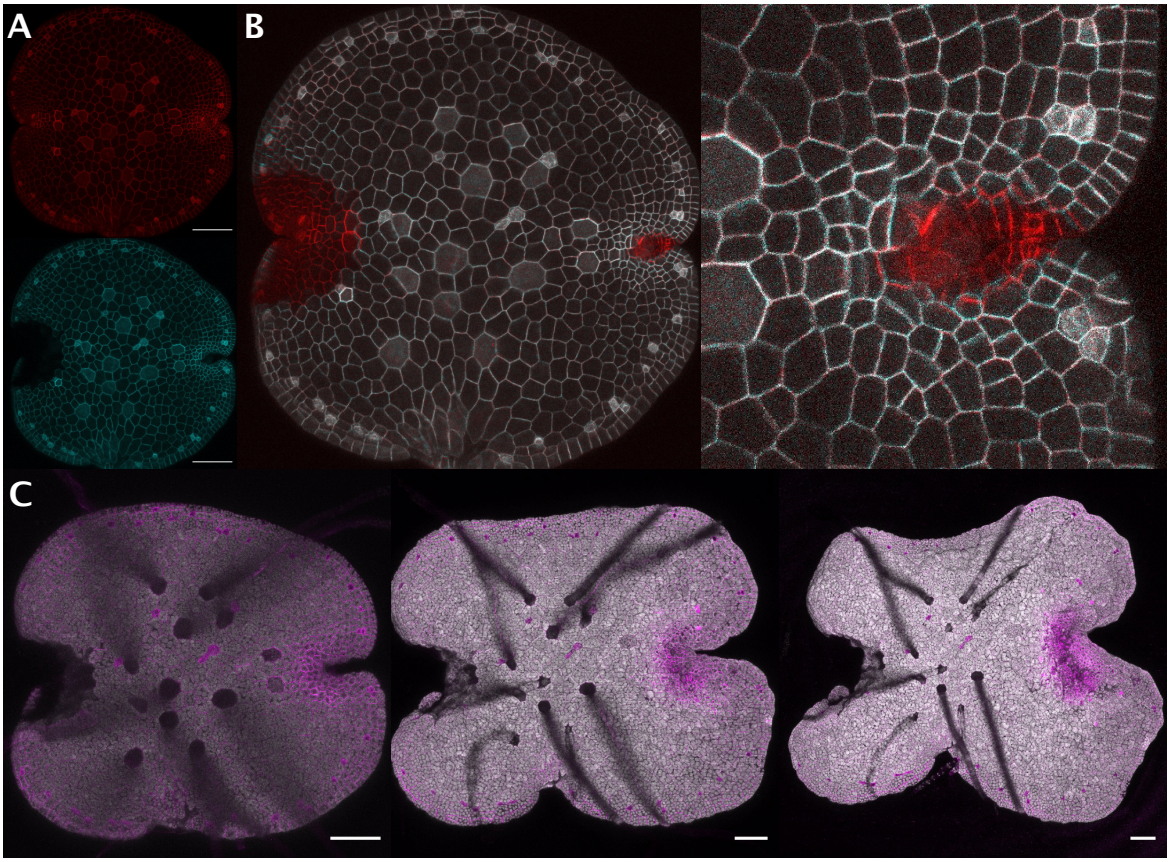

Fig. 7.2 **Precise ablation of the central stem cell population** (**A**) pMpUBE2::mScarletI-lti6b membrane marker expression before (top) and after (bottom) laser microdissection. (**B**) Composite image of (**A**), images were aligned using BUnwarpJ Arganda-Carreras et al. [10] to ensure correct overlap. Ablated cells can be seen in red. Right shows a magnified view of the meristem. (**C**) Confocal time course of regenerating fragments, showing membrane marker expression in magenta and chlorophyll chloroplast autofluorescence in grey. Images were acquired on Day 1, Day 2 and Day 3 after meristem removal. The experiment was repeated five times with similar results. All scale bars 100µm.

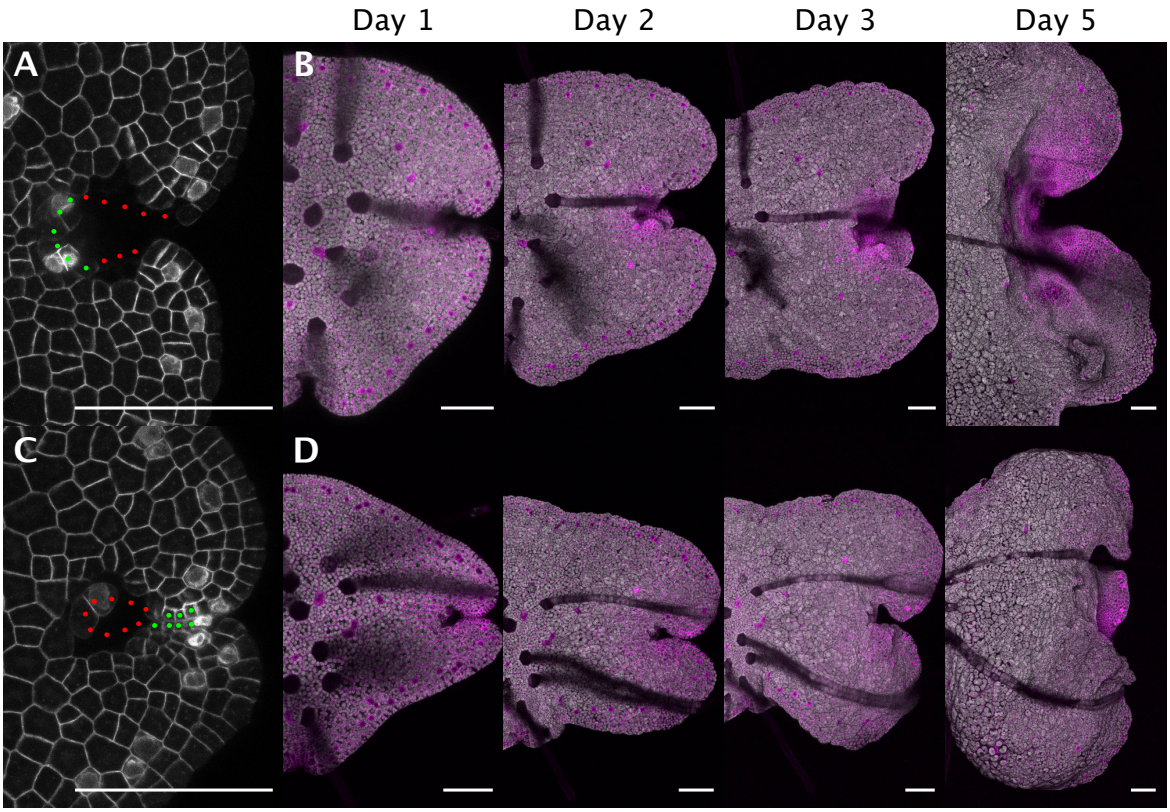

Fig. 7.3 **Partial ablation of the central stem cell population** (**A**) pMpUBE2::mScarletI-lti6b membrane marker expression of the right gemma meristem after cell ablation. The left meristem was completely ablated as in (Figure 7.2. The position of intact and removed central stem cells is indicated with green and red dots respectively. (**B**) Confocal time course of ablated gemma, showing membrane marker expression in magenta and chlorophyll chloroplast autofluorescence in grey. Images were acquired at the indicated time-points after meristem removal. (**C**) Same as (**A**) but central central stem cells (red dots) were ablated while flanking central stem cells remained intact (green dots). (**D**) Same as (**B**) but following development of (**C**). Each experiment was repeated two times with similar results. All scale bars 100µm.

transcriptional reporter and imaged regenerating fragments, focusing on the earlier stages of meristem regeneration (Figure 7.4). We indeed observed upregulation of Mp *CYCD1* as early as 24 hours after meristem removal (Figure 7.4B). After three days bright expression was observed in dividing cell clusters (Figure 7.4B). This suggests that upregulation of Mp *CYCD1* expression represents a likely molecular mechanisms of cycle re-entry in regenerating fragments, which is supported by our previous results and the the role of D-type cyclins during meristem regeneration in Physcomitrium [150] and Arabidopsis [237].

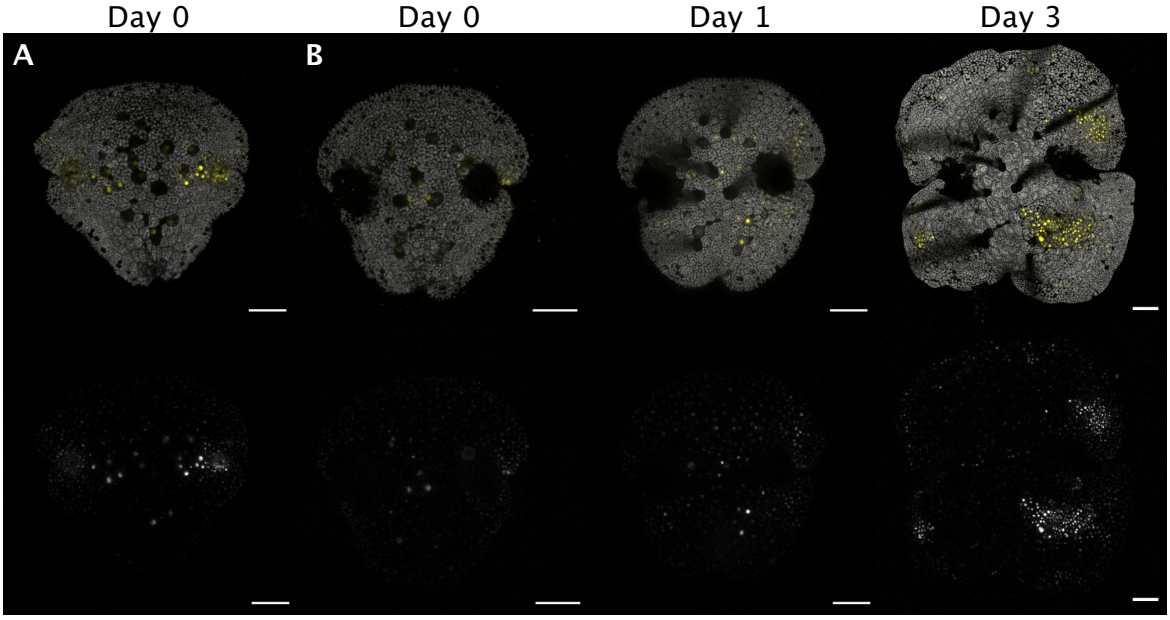

Fig. 7.4 **MpCYCD1 expression during meristem regeneration** (**A**) Confocal image of pMpCYCD1::mVenus-N7 gemma. Fluorescence is shown in yellow (top) or greyscale (bottom) with chloroplast autofluorescence in grey (top). (**B**) Same as (**A**) but showing a time course of gemma fragment regeneration on 0.5 Gamborg agar. Meristem cells were ablated using laser microdissection and the remaining fragment was imaged at the indicated time-points. The experiment was repeated four times with different independent transgenic lines, with similar results. All scale bars 100µm.

7.4 Auxin orchestrates regeneration

Previous work on meristem regeneration and apical dominance in Marchantia [23] as well as our own characterisation of auxin response and central stem cell function, suggest that auxin represses cell divisions in the central portion of gemma. Given that apex removal is sufficient to trigger regeneration, regeneration may be directly triggered by a drop in auxin concentration in the remaining tissue. Indeed, it has been shown that exogenous auxin

application is sufficient to completely block the regeneration of fragments [52]. However, how meristem markers respond to this loss of auxin concentration and how auxin signaling gradients are re-established during regeneration remains unknown.

7.4.1 MpERF20 and MpYUC2 are induced in regenerating fragments and repressed by auxin

Earlier we established Mp *ERF20* and Mp *YUC2* as central stem cell markers in intact meristems. Since apical cells only re-emerge at late stages of meristem regeneration we were interested to see how our marker lines for these genes respond to apex removal. In stark contrast to their restricted expression patterns in intact meristems, we observed widespread activation of Mp *YUC2* and particularly Mp *ERF20* within a day of meristem removal (Figure 7.5 A). After three days, Mp *YUC2* was largely restricted to dividing cell clusters, while Mp *ERF20* expression remained widespread. However, after seven days expression of both genes was again specifically localised to the centre of fully regenerated meristems (Figure 7.5 A). To test whether auxin can disrupt this response, we grew gemma fragments on media containing 10µM NAA, which completely blocked induction of Mp *YUC2* (Figure 7.5 B) or Mp *ERF20* expression (Figure 7.5 C). This suggests that both genes may be repressed by auxin. These observations are consistent with published RNA-seq data. Expression for both genes is elevated in thallus fragments after 24 hours of regeneration [29, 279], but repressed in response to a one hour auxin treatment [221, 279]. In fact the repression of YUCCA genes by auxin is a well known and conserved negative feedback loop of auxin signalling [221]. YUCCA gene expression is rapidly repressed in response to exogenous auxins in bryophytes and angiosperms [221]. Mp *YUC2* reporter expression during the early stages of meristem regeneration may therefore be directly inversely related to auxin concentration. Mp *YUC2* expression also closely tracks areas of cell division during early stages of regeneration, making it an excellent marker of reforming auxin gradients and the meristem regeneration process in general.

7.4.2 Auxin is required for the transition from Stage 2 to Stage 3

Since exogenous auxin application blocks the transition into Stage 1, we reasoned that inhibition of auxin biosynthesis should promote or prolong early stages of regeneration. To test this, we treated gemma fragments containing the Mp *YUC2* reporter with 100µM kynurenine, a competitive inhibitor of auxin biosynthesis [123]. Fragments showed brighter Mp *YUC2* fluorescence after two days of growth on kynurenine (Figure 7.6 B) compared to controls (Figure 7.6 A). At two days, Mp *YUC2* reporter fluorescence was localised to

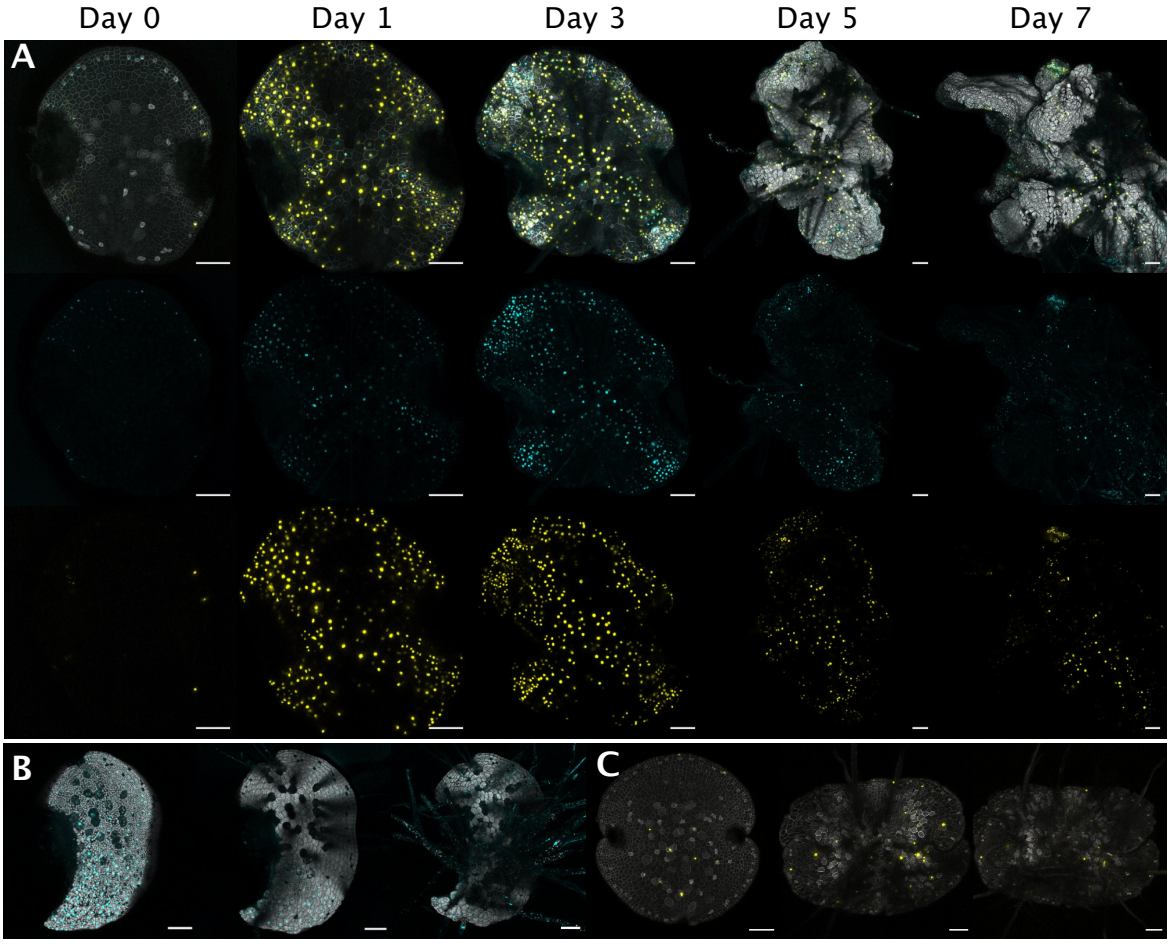

Fig. 7.5 **MpERF20 and MpYUC2 are induced during meristem regeneration** (**A**) Confocal images of regenerating gemma fragments, imaged at indicated time-points following meristem ablation, day 0 image was acquired within 1 hour of meristem ablation. Top: composite images showing ERF20 transactivation reporter (pMpERF20::GAL4-VP16, pUAS::mVenus-N7) expression in yellow, pMpYUC2(5.5kb)::mTurqouise2-N7 expression in cyan and pMpUBE2::mScarletI-lti6b membrane marker (Day 0-3) or chlorophyll autofluorescence (Day 5-7) in grey. (**B**) pMpYUC2(5.5kb)::mTurqouise2-N7 expression (cyan) in regenerating gemmae fragments grown on agar supplemented with 10µM NAA, chlorophyll autofluorescence shown in grey. Images were acquired at Day 0 (left), Day 2 (centre) and Day 4 (right). (**C**) Same as (B) but showing expression of the ERF20 transactivation reporter (pMpERF20::GAL4-VP16, pUAS::mVenus-N7) in yellow and the pMpUBE2::mScarletI-lti6b membrane marker in grey. Each experiment was repeated four times using at least two different independent transgenic lines, with similar results. All scale bars 100µm.

cell clusters in treated fragments and controls, suggesting successful progression to Stage 2. However, while meristem regeneration was completed by day 7 in control plants, kynurenine treated fragments still displayed expression patterns characteristic of Stage 2 of regeneration, with no signs of increasingly specific Mp *YUC2* expression. Kynurenine treatment at this concentration may not abolish the establishment of division zones, but it may block the transition to Stage 3, suggesting that auxin is required for the re-establishment of mature meristems containing apical cells. This is consistent with the phenotypes of strong genetic perturbations to auxin signaling [88] and treatment of gemma with very high concentrations of kynurenine [70], both result in callus like growth devoid of patterning, resembling the early stages of meristem regeneration. The fact that kynurenine treated fragments are still able to establish division zones could be explained by incomplete inhibition of auxin synthesis which is probable given the competitive nature of kynurenine inhibition He et al. [123].

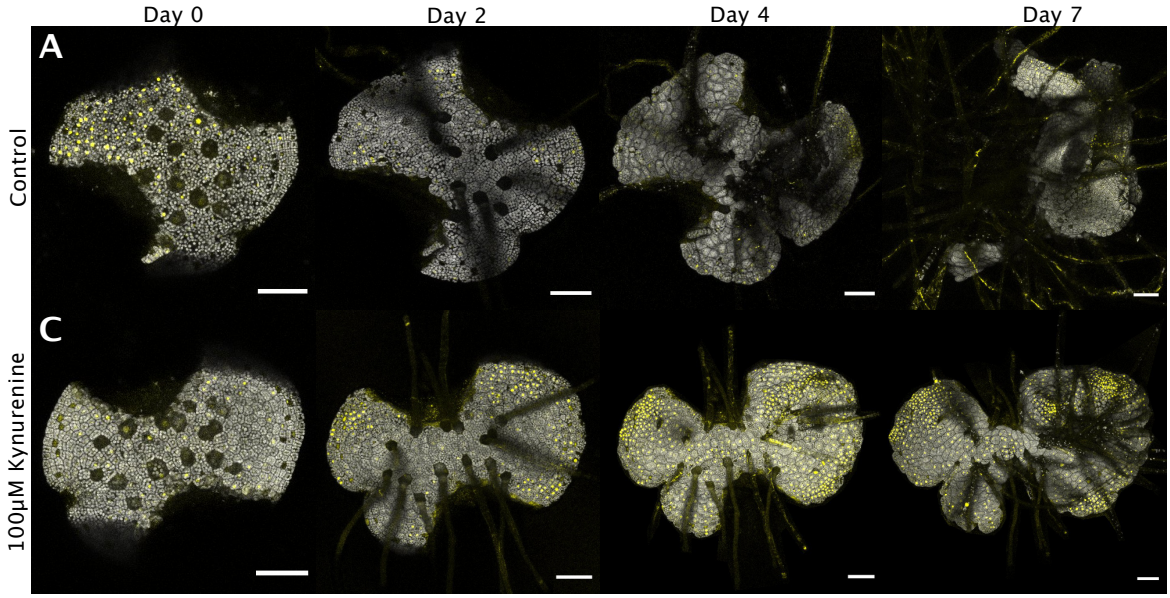

Fig. 7.6 **Inhibition of auxin biosynthesis during meristem regeneration** (**A**) Confocal time course of pMpYUC2::mTurquoise2-N7 gemma fragment regeneration on 0.5 Gamborg agar. Fluorescence is shown in yellow and chloroplast autofluorescence in grey. Meristem cells were ablated using laser microdissection and the remaining fragment was imaged at the indicated time-points, day 0 image was acquired within 1 hour of meristem ablation. (**B**) Same as (**A**) but media was supplemented with 100µM kynurenine (auxin biosynthesis inhibitor). Each experiment was repeated twice using independent transgenic lines, with similar results. All scale bars 100µm.

7.4.3 Regeneration is driven by auxin transport reorganisation rather than auxin signaling genes

In chapter 5, I investigated the roles of ARF stoichiometry and auxin transport in intact meristems. The results presented in chapter 5 suggested that both auxin transport and ARF1/2 stoichiometry contribute to the auxin response minima in the meristem. However, whether these processes also act synergistically during meristem regeneration is unknown.

I first investigated the response of the ARF1/2 dual reporter (see chapter 5.3.2) to meristem removal, to determine if the expression of ARF genes displays a dynamic response during the regeneration process. There was no indication for preferential abundance of ARF1 or ARF2 in the gemma fragment one hour after meristem removal (Figure 7.7, Day 0). However, after four days, at the transition from Stage 2 to Stage 3, we observed a clear excess of Mp *ARF1* expression compared to Mp *ARF2* in clusters of dividing cells. This is the opposite pattern we observed earlier in the division zone of intact meristems (Figure 5.5). Mp *ARF2* expression was elevated along the newly forming thallus edge (Figure 7.7, Day 4 zoom) which is similar to our observations in intact meristems (Figure 5.5) and consistent with previously reported higher expression of Mp *ARF2* along the gemma edge [171]. Even at earlier stages (Day 2) Mp *ARF1* appeared to be expressed to a greater extent in dividing cells (Figure 7.7). The high relative abundance of Mp *ARF1* compared to Mp *ARF2* suggested that auxin producing, dividing cells may actually be hyper-sensitive to auxin signaling, during Stage 2 and 3 of meristem regeneration. This argues against a role of ARF stoichiometry in stabilising localised auxin biosynthesis.

To test whether localised auxin biosynthesis may be stabilised by auxin transport, we imaged our Mp *PIN1* transactivation reporter during meristem regeneration. As shown previously Mp *PIN1* was expressed in central stem cells of intact gemma and we detected almost no expression one hour after meristem ablation (Figure 7.8 A). However, after two days, very bright expression was detected across the regenerating tissue. After four days, expression was again localised to a small number of cells at the edge of the dividing cell clusters (Figure 7.8 A). The expression of Mp *PIN1* at the edge of dividing cell clusters during stage 2 was different compared to Mp *YUC2*, which was expressed across all dividing cells at this stage, suggesting that specific Mp *PIN1* expression precedes specific Mp *YUC2* expression. The strong initial upregulation of Mp *PIN1* and rapid restriction to emerging meristems, strongly suggested that auxin transport re-orientation is a key driver of the regeneration process. Indeed, inhibition of auxin transport by treatment with 2,3,5-triiodobenzoic acid (TIBA) [57] blocked full meristem regeneration (Figure 7.8 B). Clusters of dividing cells marked by Mp *YUC2* expression did form, but full meristems did not regenerate after seven days, suggesting that transition into Stage 3 of regeneration requires auxin transport. These results suggest

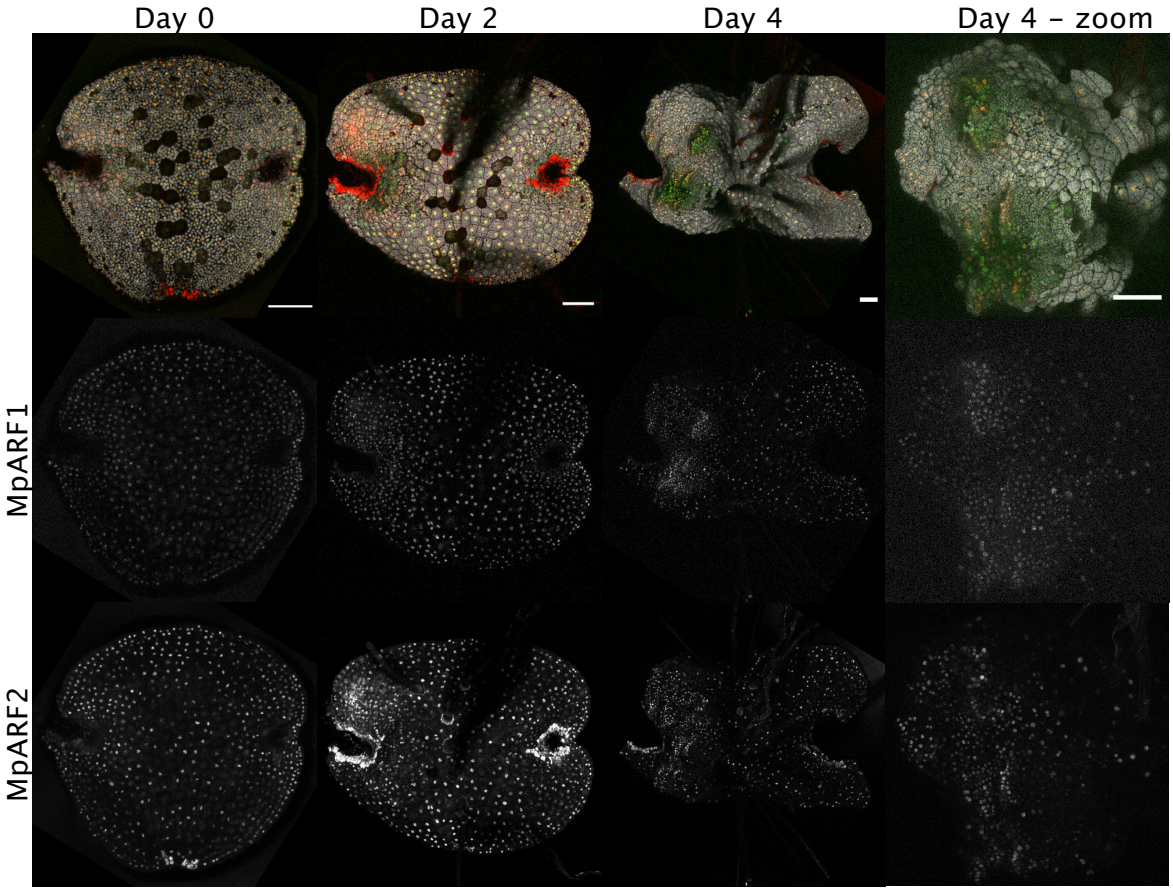

Fig. 7.7 **ARF stoichiometry during regeneration** Confocal time course series of a pMpARF1::mVenus-N7, pMpARF2::mScarletI-N7 gemma fragment. Top row shows composite images of pMpARF1::mVenus-N7 in green, pMpARF2::mScarletI-N7 signal in red and chloroplast autofluorescence in grey, middle and bottom row show the fluorescence of each reporter separately in greyscale. The meristem was removed via laser ablation and the fragment was grown on 0.5 Gamborg agar for the indicated amount of time before image acquisition, day 0 image was acquired within 1 hour of meristem ablation. The rightmost image is a magnified view of Day 4. The experiment was repeated three times with similar results. All scale bars 100µm.

that the meristem regeneration process is driven by the re-establishment of auxin producing and exporting cell clusters which is mediated by the re-orientating auxin transport, rather than localised expression of auxin response genes.

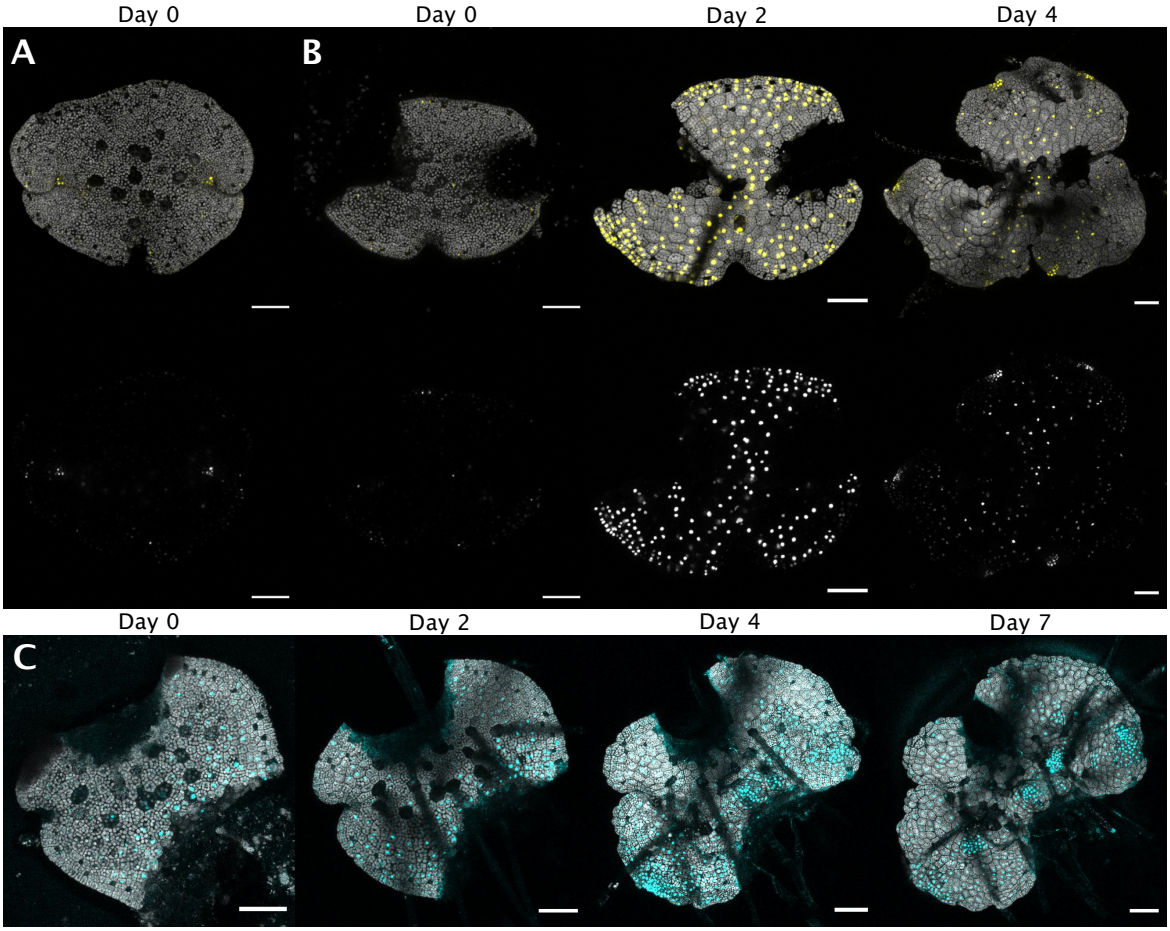

Fig. 7.8 **Auxin transport re-organisation during meristem regeneration** (**A**) Mp *PIN1* transactivation reporter (pMpPIN1::GAL4-VP16, pUAS::mVenus-N7) expression in gemma. Top: composite image of reporter expression in yellow and chloroplast autofluorescence in grey, bottom reporter expression in greyscale. (**B**) same as (**A**) but showing a regenerating gemma fragment imaged at the indicated time-points, day 0 image was acquired within 1 hour of meristem ablation. The experiment was repeated three times with similar results. (**C**) pMpYUC2::mTurquoise2-N7 gemma fragment regeneration on 0.5 Gamborg agar supplemented with 100µM 2,3,5-triiodobenzoic acid (TIBA). pMpYUC2::mTurquoise2-N7 expression shown in cyan, chloroplast autofluorescence in grey. Plants were imaged at the indicated time-points. The experiment was repeated twice with similar results. All scale bars 100µm.

7.5 Regeneration model

Based on our observations, we propose a model of meristem regeneration and meristem maintenance which is illustrated in Figure 7.9. Key observations that underpin this model are summarised below:

- Central stem cells are sites of auxin production and export (Figure 5.2, 5.3).
- Auxin promotes cell expansion and antagonises cell proliferation. The gemma meristem is characterised by an auxin response minima, permitting cell proliferation, while cell divisions in the central zone of gemmae are repressed by high auxin response (Figure 5.4).
- Central stem cell removal is sufficient to trigger meristem regeneration (Figure 7.2, 7.3)
- Mp *CYCD1* is a key regulator of cell divisions in the proliferation zone of intact meristems (Figure 6.5, 6.6), but following meristem removal Mp *CYCD1* is up regulated across cells in the regenerating fragment (Figure 7.4).
- After meristem removal, the central stem cells markers Mp *YUC2*, Mp *PIN1* and Mp *ERF20* are rapidly up-regulated across all cells (Stage 1) and this induction is blocked by exogenous auxin (Figure 7.5, 7.8).
- Mp *PIN1* and Mp *YUC2* expression become progressively restricted to cell clusters which retain high rates of cell prolifeartion while divisions elsewhere cease (Stage 2), suggesting re-establishment of auxin source-sink domains (Figure 7.5, 7.8).
- Reformation of a notch shaped meristem (Stage 3) is blocked by auxin synthesis and transport inhibitors (Figure 7.6, 7.8)

These results suggest that meristem regeneration is primarily driven by the re-establishment of auxin patterning (Figure 7.9). I propose that following meristem removal (Stage 0), auxin concentration drops rapidly across the tissue. This alleviates the repression of cell divisions, but also permits induction of auxin biosynthesis across the tissue (Stage 1). Exogenous application of auxin completely blocks this induction, arresting fragments at Stage 0. Cells simultaneously up-regulate auxin transport, converting every cell into a small separate auxin source (Stage 1). As cells export auxin to their neighbours they may inhibit auxin biosynthesis in surrounding cells, creating a competitive environment to establish a new dominant auxin source. Re-alignment of auxin transport polarity likely also plays an important role

in this process, but this is beyond the scope of the work presented here. Eventually, auxin biosynthesis is again restricted to small domains of the tissue where auxin biosynthesis is stabilised by sufficient export of auxin (Stage 2). These emerging meristems retain high rates of cell division while cell divisions in the remaining tissue cease, suggesting the re-establishment of auxin source-sink dynamics. Auxin appears to be required for successful completion meristem regeneration (Stage 3) as fragments treated with auxin biosynthesis or transport inhibitors do not progress past Stage 2, but it is unclear why auxin appears to be required for the re-emergence of central stem cells.

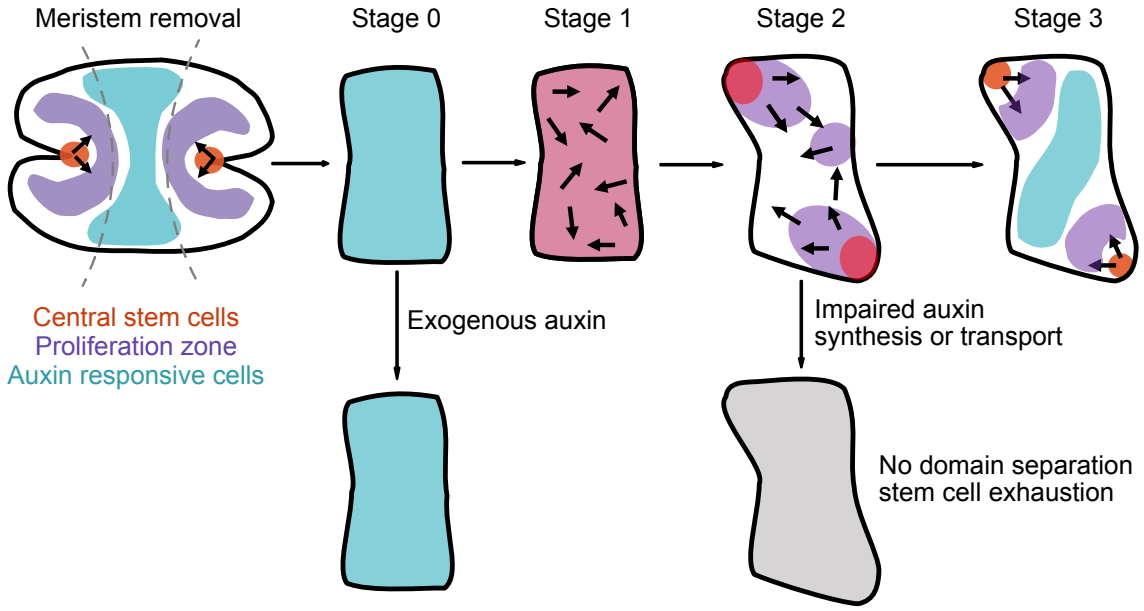

Fig. 7.9 **Meristem regeneration model** Gemmae contain a small population of central stem cells surrounded by a proliferation zone which contains rapidly dividing cells. Cells in the central portion show high levels of auxin response which represses cell divisions. Removal of the meristematic region, isolates this repressed cell population (Stage 0). If the fragment is treated with exogenous auxin, cells will remain repressed and commit to rhizoid fate. Without exogenous auxin, cells will rapidly initiate cell divisions (Stage 1) and up-regulate auxin biosynthesis and transport (marked by black arrows). At this stage, cells express marker genes for both central stem cells and proliferation zone cells, suggesting a complex, mixed stem cell identity. With time, cell divisions, auxin biosynthesis and export become restricted to multiple cell clusters (Stage 2) while cells in the remaining tissue stop dividing and convert to rhizoid fate, indicating rising auxin signaling in the remaining tissue. At Stage 3, central stem cells are fully reformed and divisions occur predominantly in surrounding cells, indicating complete reformation of meristem domains. Inhibition of auxin biosynthesis or transport prevents the transition into Stage 3, indicating that auxin signaling gradients are essential for the re-establishment of the central stem cell population

7.6 Discussion

Our proposed regeneration model shares common features with angiosperm meristem regeneration models. In the root apical meristem, removal of the entire root tip [265] or specific ablation of the QC population [330] triggers meristem regeneration by disrupting existing patterning mechanisms including the distribution of hormones such as auxin [348]. During regeneration, markers and functions of the QC cell population are distributed across different cell populations and root cell fates are dynamically remodelled following an embryo like sequence [69]. QC identity appears to only reform at late stages of regeneration, when hormone signalising domains have re-stabilised, mirroring the relatively late emergence of the QC domain during embryo development [209]. In callus tissue, cells initially show broad expression of diverse meristem markers and signaling pathways, but the emergence of shoot initials is preceded by the establishment of new spatially restricted auxin and cytokinin signaling domains, which enable the subsequent re-specification of distinct cell fates [236]. We similarly observe expression of central stem cell and proliferation zone markers across the regenerating tissue at early stages and our results strongly suggest that the re-establishment of distinct hormone signaling domains drives the regeneration process.

Some of the AP2/ERF transcription factors which are implicated in Angiosperm meristem regeneration have roles restricted to specific cell types during normal development. For instance, in Arabidopsis ERF115 controls division rates in QC cells in intact root meristems [130], but is induced more broadly in response to wounding to grant regenerative competency to surrounding cells [129]. ERF115 and auxin signaling act synergistically in this process [34]. We similarly observed a very strong induction of Mp *ERF20* during regeneration which closely tracked auxin gradients, suggesting a broader role of Mp *ERF20* in promoting stem cell fate. In chapter 5 I showed that Mp *ERF20* overexpression induced ectopic notch formation, presumably by promoting apical cell fate. However, despite the early upregulation of Mp *ERF20* in regenerating fragments apical cells only reform at late stages of regeneration. One possible explanation for these different observations could be that the induction of apical cell fate by Mp *ERF20* is dependent on the re-establishment of auxin signaling gradients. A recent study [147] characterised the role of auxin and Mp *ERF20* during Marchantia meristem regeneration in adult thalli fragments, rather than gemmae. Multiple observations in this study provide further support for our model. Ishida et al. [147] measured auxin concentration in thalli fragments, demonstrating a rapid drop in auxin concentration following meristem removal. Ishida et al. [147] confirmed our observations that exogenous auxin application is sufficient to block meristem regeneration and that Mp *ERF20* and Mp *CYCD1* expression is induced in fragments within a day of meristem removal in an auxin dependent manner. Crucially, the authors were also able to obtain loss of function alleles

of Mp *ERF20* demonstrating that Mp *ERF20* knockout impairs regeneration competency, but is not essential for regeneration. Future work will be required to discern the targets of Mp *ERF20* and further delineate its role during meristem regeneration and meristem maintenance.

In our model we suggest that cells acquire a proliferation zone like state during early stages of regeneration based on the high rates of division and lack of auxin signaling we observed, which mimics some aspects of the proliferation zone in intact meristems. I was unable to fully explore the response of cytokinin markers introduced in chapter 6 due to time constrains. It would be interesting to see if the early stages of meristem regeneration are marked by an upregulation of cytokinin biosynthesis or cytokinin response which would support a proliferation zone like cell identity during Stage 1 of regeneration. However, given that many of the central stem cell markers are also broadly expressed during the early stages of development characterising cells during Stage 1 of regeneration as proliferation zone like cells likely represents an oversimplified view of cell identity during this stage. Single cell profiling of regenerating Marchantia tissue fragments could help to shed light on cell identity during regeneration and we expect that regenerating cells will display complex mixed meristematic identities, similarly to reports on the transcriptional identity of callus cells in Arabidopsis [357].

Tracking of cell identities with scRNA-seq during the regeneration process may also help to elucidate how central stem cells reform in the regenerating tissue. In our experience it has been very challenging to directly observe the re-emergence of central stem cells in regenerating fragments. This is in part a result of technical issues such as variability in the timing of regeneration stages, rhizoid emergence and disorganised growth which often obscure the view of the centre of the emerging meristems. However, it is very likely that central stem cell emergence, similarly to QC formation during embryo development and regeneration, represents a gradual process. Central stem cells may be very hard to distinguish from other meristematic cells at early stages and only appear as a clearly identifiable population long after their fate was specified. Our observations that auxin biosynthesis and transport inhibitors appear to prevent central stem cell reformation suggest that auxin may be an important signal for central stem cell re-specification. However, very little is known about central stem cell specification and it is therefore very difficult to speculate what the role of auxin in this process may be. Quantification of auxin levels in different parts of the Marchantia thallus suggest that, apart from the high levels of auxin in the central portion, auxin levels may also be relatively high in the apical most portion [70], hinting at a possible role of auxin for the maintenance of central stem cells. This would be consistent with our observations that inhibition of auxin biosynthesis may inhibit central stem cell formation in

regenerating fragments and previous observation which showed strong disruptions to auxin biosynthesis result in callus like tissue [70]. We were unable to observe any fluorescence for our DR5 reporter in central stem cells (Figure 5.4) but it is possible that the sensitivity of this reporter may be too low to detect low levels of auxin response. Inducible expression of dominant negative regulators of auxin response such as fusion proteins of TPL and partial IAA proteins [313] or auxin insensitive IAA mutants [115], from a central stem cell specific promoter such as Mp *YUC2*, Mp *PIN1* or Mp *ERF20* could help to establish if auxin signaling is required to maintain central stem cell fate.

Meristem regeneration in Marchantia is rapid, can be initiated from any source tissue, shares key similarities with angiosperm meristem regeneration and does not require the application of exogenous hormones, making it an excellent model system to study the dynamics of morphogen gradients and the re-establishment of cell fates. Future work on bryophyte meristem regeneration may help to elucidate fundamental mechanisms of meristem regeneration which are harder to observe in plants with limited regeneration competency and high levels of genetic redundancy.

Chapter 8

General discussion

8.1 Summary

This dissertation describes a framework for the cellular composition and genetic interactions during Marchantia gemma meristem maintenance and regeneration. Single cell RNA-seqeuncing and tissue specific fluorescent reporters were used to establish a provisional cell type map of gemmalings. I developed novel fluorescent reporters to interrogate auxin source sink relationships. High resolution imaging of theses reporters suggested that central stem cells are an auxin source and that auxin represses cell proliferation in cells of the central zone. I identified Mp *ERF20* as a positive regulator of apical cell fate, demonstrating that ectopic Mp *ERF20* expression is sufficient to trigger notch formation. I investigated the regulation of cells in the proliferation zone which surrounds the central stem cell population. I presented results that suggest high levels of cytokinin signaling in this cell population. I further interrogated cell cycle regulation, demonstrating that Mp *CYCD1* is a positive regulator of cell cycle entry and that Mp *CYCD1* overexpression can be leveraged as a tool to induce ectopic cell divisions across cell types. Given these results, I proposed a two domain meristem model which shares similarities with tissue domains in the SAM and RAM of angiosperms. Finally, I investigated the cellular responses to ablation of the meristematic regions. I showed that meristem ablation alleviates auxin mediated repression of cell divisions, triggering cell proliferation across the remaining tissue. My results suggest that meristem regeneration is driven by the re-establishment of auxin signaling gradients via re-orientation of auxin transport dynamics across the tissue. In combination, these results significantly advance our understanding of meristem regulation in Marchantia, provide a framework for the cellular architecture of the meristem and identified novel tools to support future attempts to engineer growth in this simple morphogenetic system.

8.2 Screening of a proximal promoter library for all transcription factors in Marchantia

The Marchantia genome contains a remarkably low number of transcription factors, but very few of these genes have been characterised so far. Transcriptional reporters of transcription factors could provide useful tools to define cellular domains in the Marchantia meristem and identify potential meristem regulators. Given the low number of transcription factors in Marchantia a lab-wide effort was initiated to comprehensively screen the expression patterns of proximal promoter sequences for all 400 transcription factors. I presented the initial results of this screen in Marchantia gemmae. So far, 79 promoter reporter constructs were generated and transformed into Marchantia. Transgenic plants were imaged during gemma development and 51 promoters showed expression, providing a rich source of promoter activities. I focused on the characterisation of reporters which displayed differential expression in meristematic regions. Transcriptional reporters for Mp *WOX* and Mp *APB*, two homologues of core meristem regulators of angiopsperms, unexpectedly did not show signs of meristematic expression in Marchantia, suggesting differences in the regulation of meristematic cell fates between angiosperms and Marchantia. I identified numerous new positive and negative markers of meristematic cells which represent promising targets for future functional validation. Some of these genes, including Mp *GRAS1*, Mp *NAC1* and Mp *NAC2* may be related to angiosperm meristem regulators, hinting at potentially conserved elements of meristem regulation. One of the genes we identified as a marker of meristematic cells (Mp *BZR1*), has been validated as a regulator of cell proliferation [215], supporting the utility of this approach for the identification of candidate meristem regulators. However, the main outcome of this work was the generation of marker lines that can be used to distinguish distinct cell domains in gemmae. Most genes showed proximal distal gradients of expression suggesting that the Marchantia meristem may not be sharply spatially delineated from the remaining tissue, but rather comprise a gradient of cell proliferation and differentiation. Similar graded domain transitions are present in the SAM of angiosperms, however in the SAM key marker genes provide a robust framework to categorise cell domains. We anticipate that completion of the transcription factor screen and functional characterisation of genes with meristematic expression will result in the identification of genes that can be used to define distinct meristematic domains. Given that CLE peptide signaling is important for Marchantia meristem organisation but WOX protein function is not conserved [134, 133, 314], the identification of transcription factors which may act upstream or downstream of CLE signalling could be particularly useful to establish a common framework between angiosperm and bryophyte meristems.

8.3 Charting a cell type map for Marchantia

The development of high throughput single cell RNA-seqeuncing technologies has transformed our ability to profile cell identities and expanded opportunities for data driven cell type classification in diverse organisms. However, so far scRNA-seq has not been applied to non-vascular plants. I presented the analysis and validation of a single cell RNA-sequencing dataset of developing gemmalings which comprised >7'000 single cell transcriptomes. Using dimensionality reduction and clustering I defined cell clusters with distinct transcriptional profiles. I leveraged published marker genes, transcriptional reporters from the transcription factor screen and novel marker genes to identify tissue domains and cell types which likely correspond to cells from these computationally defined clusters. I identified two distinct populations of meristematic cells which likely correspond to the cells at the centre of the meristem and the surrounding tissue. These clusters were accordingly labelled as CENTRAL STEM CELLS and PROLIFERATION ZONE CELLS and their distinct transcriptional identity support a functional distinction for the corresponding cells in gemma. I identified novel marker genes which defined distinct dorso-ventral cell lineages for ventral epidermal cells, dorsal epidermal cells and air pore cells. I described an intriguing strong negative association between the expression of photosynthesis genes and ABA response, suggesting that ABA may have a previously underappreciated role in regulating ventral cell dormancy. I speculated that this may contribute to the patterns of asymmetric cell proliferation observed in mature thalli, where dorsal cells proliferate more rapidly. I showed that rhizoid cells can be sub-divided into distinct rhizoid sub types such as mucilage cells and distinct developmental stages of rhizoid development. I identified Mp *Expansin12* as a novel cell type marker which specifically labels elongating rhizoids. Finally, I characterised the transcriptional changes which occur along the putative rhizoid differentiation trajectory. I identifying loss of chlorophyll biosynthesis in RHIZOID PRECURSORS, decreased expression of ABA responsive genes and increased expression of auxin response genes in COMMITTED PRECURSORS and upregulation of expansin genes, cytoskeletal genes and genes related to cell wall biogenesis in ELONGATING RHIZOIDS and MATURE RHIZOIDS.

While the annotation of this dataset is preliminary and some cell populations remain poorly defined owing to a lack of published marker genes, we anticipate that this dataset will provide a valuable resource for the Marchantia community. Since this dataset was obtained from a single sample of four day old gemmalings there are limitations on the cell types profiled and the ability to translate insights to different stages of Marchantia development. However, I anticipate that publication of this dataset, which demonstrates the feasibility and value of applying scRNA-seq to bryophytes, will inspire efforts to sample other tissues. Initiatives such as the plant cell atlas [259, 162] may catalyse the systematic

and comprehensive categorisation of cell types across plants and this dataset represents an important first step to capture the cellular diversity of bryophytes.

8.4 Central stem cells and auxin

Previous research on the role of auxin in Marchantia points to an apical source of auxin which promotes cell proliferation in the central portion of gemmma [70]. However, tools to directly visualise this presumed auxin gradient have been limited and little is known about the cellular source of apical auxin, or the spatial distribution of auxin signaling components in Marchantia. I developed novel fluorescent reporters for auxin biosynthesis, signaling and response to enable characterisation of the spatial organisation of auxin signaling. I showed that central stem cells are marked by Mp *YUC2* and Mp *PIN1* expression, suggesting that these cells constitute the apical auxin source. I established a functional auxin response reporter based on the DR5v2 promoter, which demonstrated that auxin response in gemma is restricted to cells in the central portion. I imaged a dual transcriptional reporter for Mp *ARF1* and Mp *ARF2* during gemma development which supported ARF stoichiometry as a potential component of maintaining a low auxin signaling environment in the meristem. I identified specific expression of the AP2/ERF transcription factor Mp *ERF20* in the central stem cell population and demonstrated that Mp *ERF20* overexpression is sufficient to induce ectopic notches. Apical notches are comprised of central stem cells, suggesting that Mp *ERF20* overexpression promotes central stem cell or apical cell fate. Mp *ERF20* overexpression also induced auxin insensitivity, delaying ectopic rhizoid formation and permitting slow cell divisions even in the presence of high concentrations of auxin.

These results represent an important addition to the existing literature on auxin signaling in Marchantia. My observations complement previous work which has focused on validating the function of components of the auxin signaling pathway. Crucially, the development of fluorescent reporters and high resolution imaging in gemma enabled the identification of central stem cells as auxin sources and the visualisation of auxin response with cellular resolution. The role of central stem cells as auxin sources was suspected based on previous results, but methods employed previously, lacked the necessary resolution to establish the cellular boundaries of auxin signaling. Future work will be needed to reconcile the localised expression of Mp *YUC2* and Mp *PIN1* with the low levels of auxin signaling across the meristem. The development of a translational fusion for Mp *PIN1* or labeling of Mp *PIN1* via immunofluorescence would be particularly important to establish the contribution of polar auxin transport in Marchantia. The results of this dissertation and the existing literature hint at the presence of polar auxin transport in Marchantia, but alternative mechanism may be

present. For instance, Physcomitrium gametophore development shares similarities with the Marchantia gametophyte, but has been shown to be orchestrated by apolar auxin transport [48]

Mp *ERF20* is the first gene reported in Marchantia that can induce ectopic formation of apical cells. However, it is not clear how Mp *ERF20* itself may be regulated. Previous work on CLE signaling in Marchantia has demonstrated that Mp *CLE2* is a positive regulator of the central stem cell population [133]. Characterisation of Mp *CLE2* signaling targets could therefore be a promising avenue for future research, to reveal if Mp *ERF20* is a target of CLE peptide signaling in Marchantia, or if these pathways act independently to promote central stem cell or apical cell fate.

8.5 Regulation of the proliferation zone

The Marchantia meristem contains a distinct region of rapidly dividing cells which I termed the proliferation zone. Cell divisions in plants are regulated by cell cycle genes. In angiosperms cytokinin promotes cell cycle progression by inducing expression of D-type cylins which promote cell cycle entry and nuclear translocation of Act-Myb genes to regulate the commitment to mitosis. I described the characterisation of the proliferation zone of the Marchantia meristem. PZ CELLS were found to show high levels of expression for cytokinin signaling genes and I validated expression of cytokinin signaling genes in the gemma meristem. I investigated D-type cyclin function in Marchantia. I showed that Mp *CYCD1* is related to canonical D-type cyclins, expressed in dividing cells and that Mp *CYCD1* overexpression is sufficient to induce ectopic cell divisions. I provided evidence that suggests Mp *3R-MYB1* as a very likely regulator of the G2/M phase transition. I also investigated if exogenous cytokinin treatment induced Mp *CYCD1* expression, but I did not observe clear phenotypes for cytokinin treated plants. Cytokinin treatment did however rescue growth repression by exogenous auxin treatment in a co-treatment experiment, suggesting that exogenous cytokinin can promote cell divisions in repressive growth conditions.

The main outcomes of this part of my work was the identification of conserved cell cycle regulators, in particularly the identification of a single canonical cyclin-D gene in Marchantia. The presence of a single D-type cyclin opens up exciting opportunities for dissecting the roles of distinct cell cycle regulators with minimal genetic redundancy. The generation of a loss of function allele for Mp *CYCD1* would be particularly interesting to establish if D-type cyclins are indeed not essential for plant cell division, as has been suggested previously [202]. The regulation of Mp *CYCD1* by environmental signals could also an important future research direction as cyclin-D gene expression is thought to be tuned by environmental

signals. Given the presence of a single cyclin-D genes such experiments would be greatly simplified compared to the potential for redundant activation of different cyclin-D genes in other plant models. Further characterisation of Mp *3R-MYB1*, in particular successful generation of a fluorescent protein fusion for Mp *3R-MYB1* could help to identify if the regulation of the G2/M transition is also conserved across land plants. Given the simplicity of cell cycle regulation in Marchantia we anticipate that experiments in Marchantia may help shed light on fundamental aspects of cell cycle regulation in all plants.

While the work presented in this thesis extends the characterisation of cytokinin signaling in Marchantia this work remains incomplete and we anticipate that future work in Marchantia will aim to close the gaps in our understanding of the roles of cytokinin in Marchantia. An important first step could be the development of high resolution cytokinin response reporters, for instance using the synthetic TCS promoter [372], to establish the spatial domains of cytokinin signaling in Marchantia.

8.6 Meristem regeneration

Plants display a remarkable ability to regenerate tissues following injury, but the regeneration process can be challenging to dissect in angiosperm model systems owing to genetic complexity and the requirement for *in vitro* culture of explants in the presence of exogenous hormones for some regeneration processes. Meristem regeneration in Marchantia represents a very accessible system which enables direct observation of regeneration processes in a tissue without the need for exogenous hormone application. In this thesis, I established a framework for the regeneration process in Marchantia by developing a four stage model. I showed that apex removal (Stage 0) triggers upregulation of cell cycle regulators (Mp *CYCD1*), auxin biosynthesis (Mp *YUC2*) and auxin transport (Mp *PIN1*) across the remaining tissue (Stage 1). I suggested that the regeneration process is driven by cell-cell competition to re-establish auxin source sink dynamics. The upregulation of auxin biosynthesis and transport convert cells into auxin sources, but auxin accumulation inhibits auxin biosynthesis [221] creating a competitive environment between auxin sources. As a result of this competition, auxin biosynthesis (Mp *YUC2*) and transport (Mp *PIN1*) are progressively restricted to distinct clusters of cells which remain mitotically active, while the remaining tissue becomes a sink for auxin where cell division is repressed (Stage 2). Once the auxin source-sink dynamics are fully established, notch shaped meristems with apical cells re-form within the (Mp *YUC2*) expressing cell clusters, completing the regeneration process.

There are several aspects of this model that will require future investigation. I suggested that the regeneration process is driven by auxin transport re-polarisation. The development

and detailed imaging of a Mp *PIN1* fusion during the regeneration process could reveal if this is a plausible mechanism.

The relationship between Mp *ERF20* expression, auxin signaling and central stem cell fate during meristem regeneration appears to be complex. During regeneration, Mp *ERF20* is very rapidly up-regulated, but apical cells do not emerge until late stages of regeneration when auxin signaling gradients are fully restored. While these results suggest that Mp *ERF20* and auxin signaling are required for apical cell re-specification it is not clear how these processes interact. We showed that Mp *ERF20* overexpression may induce auxin insensitivity and up-regulation of Mp *ERF20* in regenerating fragments is blocked by exogenous auxin. Previous work on auxin signaling in Marchantia suggest that auxin response factor signaling may not be required for apical cell specification as Mp *ARF1* loss of function plants were able to form meristems with apical cells [170]. However, *Mparf1* plants displayed aberrant meristem positioning, suggesting that auxin signaling may act as a positional cue for apical cell formation. Future work may reveal how Mp *ERF20* connects to auxin signaling by investigating the targets of Mp *ERF20* and Mp *ARF1* activation or exploring Mp *ERF20* expression and function in auxin signaling mutants.

I have not been able to explore cytokinin signaling during the regeneration process which may have an important role in this process. As a starting point, imaging of the cytokinin reporters introduced in chapter 6 during the regeneration process could shed light on whether cytokinin production or signaling shows a dynamic response during the regeneration process. Treatment of regenerating fragments with exogenous cytokinins or cytokinin inhibitors may also help to reveal if cytokinin signaling has an important role during the regenration process.

8.7 Novel tools for meristem engineering

The application of synthetic biology approaches to the engineering of multi-cellular development, remains in its infancy [283, 68]. In order to enable targeted control of tissue proliferation, tools need to be identified that can control aspects of tissue proliferation in tissues of interest. For plant development, we anticipate that tools to manipulate the relative rates of cell division and tissue expansion will be critical to achieve the goal of rationally manipulating plant growth. This may be achieved through targeted changes in upstream regulators, such hormone gradients, or direct manipulation of genes which control cell expansion and division. The work presented in this thesis provides a framework to conceptualise distinct tissue domains in Marchantia and their relationship with hormonal interactions, which could serve as a starting point to engineer Marchantia growth. We also identified a number of tools which could be valuable for future work in this area. The promoter collection screened in

chapter 3, has already identified many regulatory sequences that can be used to drive gene expression in distinct domains of the Marchantia gemma and we anticipate that completion of this screen will yield a large repertoire of sequences to drive tissue specific expression. The identification of Mp *CYCD1* as a potent regulator of cell cycle entry opens up possibilities to directly manipulate cell cycle rates. Miss-expression Mp *CYCD1* in distinct tissue domains could boost division rates in tissues of interest, potential driving tissue outgrowth. In the future, characterisation of putative negative regulators of Mp *CYCD* such as Mp *KRP* could enable targeting of counter-acting processes to balance division rates.

8.8 Conclusions

The work described in this thesis establishes a framework for meristem regulation in Marchantia, emphasising the importance of two distinct cellular domains of the meristem, central stem cells and the proliferation zone. These domains are characterised by distinct domains of auxin and cytokinin signaling. My results show that auxin in particular is a critical signal for meristem organisation and regeneration. The findings of this thesis represent important advancements in our understanding of gemma meristem regulation and point to common themes in plant meristem organisation. The framework introduced by this thesis will be critical for future attempts to explore Marchantia as a testbed for morphogenetic engineering of growth.

References

[1] Abràmoff, M. D., Magalhães, P. J., and Ram, S. J. (2004). Image processing with imagej. Biophotonics international, 11(7):36–42.

[2] Aida, M., Beis, D., Heidstra, R., Willemsen, V., Blilou, I., Galinha, C., Nussaume, L., Noh, Y.-S., Amasino, R., and Scheres, B. (2004). The plethora genes mediate patterning of the arabidopsis root stem cell niche. Cell, 119(1):109–120.

[3] Aida, M., Ishida, T., Fukaki, H., Fujisawa, H., and Tasaka, M. (1997). Genes involved in organ separation in arabidopsis: an analysis of the cup-shaped cotyledon mutant. The plant cell, 9(6):841–857.

[4] Aki, S. S., Mikami, T., Naramoto, S., Nishihama, R., Ishizaki, K., Kojima, M., Takebayashi, Y., Sakakibara, H., Kyozuka, J., Kohchi, T., et al. (2019a). Cytokinin signaling is essential for organ formation in marchantia polymorpha. Plant and Cell Physiology, 60(8):1842–1854.

[5] Aki, S. S., Nishihama, R., Kohchi, T., and Umeda, M. (2019b). Cytokinin signaling coordinates development of diverse organs in marchantia polymorpha. Plant signaling & behavior, 14(11):1668232.

[6] Althoff, F., Kopischke, S., Zobell, O., Ide, K., Ishizaki, K., Kohchi, T., and Zachgo, S. (2014). Comparison of the mpef1α and camv35 promoters for application in marchantia polymorpha overexpression studies. Transgenic research, 23(2):235–244.

[7] Aoyama, T. and Chua, N.-H. (1997). A glucocorticoid-mediated transcriptional induction system in transgenic plants. The Plant Journal, 11(3):605–612.

[8] Aoyama, T., Hiwatashi, Y., Shigyo, M., Kofuji, R., Kubo, M., Ito, M., and Hasebe, M. (2012). Ap2-type transcription factors determine stem cell identity in the moss physcomitrella patens. Development, 139(17):3120–3129.

[9] Apostolakos, P., Galatis, B., and Mitrakos, K. (1982). Studies on the development of the air pores and air chambers of marchantia paleacea: 1. light microscopy. Annals of Botany, 49(3):377–396.

[10] Arganda-Carreras, I., Sorzano, C. O., Marabini, R., Carazo, J. M., Ortiz-de Solorzano, C., and Kybic, J. (2006). Consistent and elastic registration of histological sections using vector-spline regularization. In International Workshop on Computer Vision Approaches to Medical Image Analysis, pages 85–95. Springer.

[11] Arsuffi, G. and Braybrook, S. A. (2018). Acid growth: an ongoing trip. Journal of Experimental Botany, 69(2):137–146.

[12] Ashton, N., Grimsley, N., and Cove, D. (1979). Analysis of gametophytic development in the moss, physcomitrella patens, using auxin and cytokinin resistant mutants. Planta, 144(5):427–435.

[13] Bar-On, Y. M., Phillips, R., and Milo, R. (2018). The biomass distribution on earth. Proceedings of the National Academy of Sciences, 115(25):6506–6511.

[14] Barnes, C. R. and Land, W. J. G. (1908). Bryological papers. ii. the origin of the cupule of marchantia. Botanical Gazette, 46(6):401–409.

[15] Benfey, P. N., Linstead, P. J., Roberts, K., Schiefelbein, J. W., Hauser, M.-T., and Aeschbacher, R. A. (1993). Root development in arabidopsis: four mutants with dramatically altered root morphogenesis. Development, 119(1):57–70.

[16] Benková, E., Michniewicz, M., Sauer, M., Teichmann, T., Seifertová, D., Jürgens, G., and Friml, J. (2003). Local, efflux-dependent auxin gradients as a common module for plant organ formation. Cell, 115(5):591–602.

[17] Bennett, T., Brockington, S. F., Rothfels, C., Graham, S. W., Stevenson, D., Kutchan, T., Rolf, M., Thomas, P., Wong, G. K.-S., Leyser, O., et al. (2014a). Paralogous radiations of pin proteins with multiple origins of noncanonical pin structure. Molecular Biology and Evolution, 31(8):2042–2060.

[18] Bennett, T. A., Liu, M. M., Aoyama, T., Bierfreund, N. M., Braun, M., Coudert, Y., Dennis, R. J., O'Connor, D., Wang, X. Y., White, C. D., et al. (2014b). Plasma membrane-targeted pin proteins drive shoot development in a moss. Current Biology, 24(23):2776–2785.

[19] Bergen, V., Lange, M., Peidli, S., Wolf, F. A., and Theis, F. J. (2020). Generalizing rna velocity to transient cell states through dynamical modeling. Nature biotechnology, 38(12):1408–1414.

[20] Berleth, T. and Jurgens, G. (1993). The role of the monopteros gene in organising the basal body region of the arabidopsis embryo. Development, 118(2):575–587.

[21] Besnard, F., Vernoux, T., and Hamant, O. (2011). Organogenesis from stem cells in planta: multiple feedback loops integrating molecular and mechanical signals. Cellular and Molecular Life Sciences, 68(17):2885–2906.

[22] Bezrutczyk, M., Zöllner, N. R., Kruse, C. P., Hartwig, T., Lautwein, T., Köhrer, K., Frommer, W. B., and Kim, J.-Y. (2021). Evidence for phloem loading via the abaxial bundle sheath cells in maize leaves. The Plant Cell, 33(3):531–547.

[23] Binns, A. and Maravolo, N. (1972). Apical dominance, polarity, and adventitious growth in marchantia polymorpha. American Journal of Botany, 59(7):691–696.

[24] Blilou, I., Xu, J., Wildwater, M., Willemsen, V., Paponov, I., Friml, J., Heidstra, R., Aida, M., Palme, K., and Scheres, B. (2005). The pin auxin efflux facilitator network controls growth and patterning in arabidopsis roots. Nature, 433(7021):39–44.

[25] Boehm, C. R., Pollak, B., Purswani, N., Patron, N., and Haseloff, J. (2017). Synthetic botany. Cold Spring Harbor perspectives in biology, 9(7):a023887.

[26] Boniotti, M. B. and Gutierrez, C. (2001). A cell-cycle-regulated kinase activity phosphorylates plant retinoblastoma protein and contains, in arabidopsis, a cdka/cyclin d complex. The Plant Journal, 28(3):341–350.

[27] Bopp, M. and Brandes, H. (1964). Versuche zur analyse der protonemaentwicklung der laubmoose: Ii. über den zusammenhang zwischen protonemadifferenzierung und kinetinwirkung bei der bildung von moosknospen. Planta, 62(2. H):116–136.

[28] Bowman, J. L. (2016). A brief history of marchantia from greece to genomics. Plant and Cell Physiology, 57(2):210–229.

[29] Bowman, J. L., Kohchi, T., Yamato, K. T., Jenkins, J., Shu, S., Ishizaki, K., Yamaoka, S., Nishihama, R., Nakamura, Y., Berger, F., et al. (2017). Insights into land plant evolution garnered from the marchantia polymorpha genome. Cell, 171(2):287–304.

[30] Brand, U., Fletcher, J. C., Hobe, M., Meyerowitz, E. M., and Simon, R. (2000). Dependence of stem cell fate in arabidopsis on a feedback loop regulated by clv3 activity. Science, 289(5479):617–619.

[31] Bray, N. L., Pimentel, H., Melsted, P., and Pachter, L. (2016). Near-optimal probabilistic rna-seq quantification. Nature biotechnology, 34(5):525–527.

[32] Breuninger, H., Rikirsch, E., Hermann, M., Ueda, M., and Laux, T. (2008). Differential expression of wox genes mediates apical-basal axis formation in the arabidopsis embryo. Developmental cell, 14(6):867–876.

[33] Busch, A., Deckena, M., Almeida-Trapp, M., Kopischke, S., Kock, C., Schüssler, E., Tsiantis, M., Mithöfer, A., and Zachgo, S. (2019). Mp tcp 1 controls cell proliferation and redox processes in marchantia polymorpha. New Phytologist, 224(4):1627–1641.

[34] Canher, B., Heyman, J., Savina, M., Devendran, A., Eekhout, T., Vercauteren, I., Prinsen, E., Matosevich, R., Xu, J., Mironova, V., et al. (2020). Rocks in the auxin stream: Wound-induced auxin accumulation and erf115 expression synergistically drive stem cell regeneration. Proceedings of the National Academy of Sciences, 117(28):16667–16677.

[35] Cao, Y., Kitanovski, S., Küppers, R., and Hoffmann, D. (2021). Umi or not umi, that is the question for scrna-seq zero-inflation. Nature Biotechnology, 39(2):158–159.

[36] Chalfie, M., Tu, Y., Euskirchen, G., Ward, W. W., and Prasher, D. C. (1994). Green fluorescent protein as a marker for gene expression. Science, 263(5148):802–805.

[37] Chen, L.-G., Gao, Z., Zhao, Z., Liu, X., Li, Y., Zhang, Y., Liu, X., Sun, Y., and Tang, W. (2019). Bzr1 family transcription factors function redundantly and indispensably in br signaling but exhibit bri1-independent function in regulating anther development in arabidopsis. Molecular plant, 12(10):1408–1415.

[38] Chen, P., Takatsuka, H., Takahashi, N., Kurata, R., Fukao, Y., Kobayashi, K., Ito, M., and Umeda, M. (2017). Arabidopsis r1r2r3-myb proteins are essential for inhibiting cell division in response to dna damage. Nature communications, 8(1):1–12.

[39] Chen, Y., Tong, S., Jiang, Y., Ai, F., Feng, Y., Zhang, J., Gong, J., Qin, J., Zhang, Y., Zhu, Y., et al. (2021). Transcriptional landscape of highly lignified poplar stems at single-cell resolution. Genome biology, 22(1):1–22.

[40] Chickarmane, V. S., Gordon, S. P., Tarr, P. T., Heisler, M. G., and Meyerowitz, E. M. (2012). Cytokinin signaling as a positional cue for patterning the apical–basal axis of the growing arabidopsis shoot meristem. Proceedings of the National Academy of Sciences, 109(10):4002–4007.

[41] Chiyoda, S., Yamato, K. T., and Kohchi, T. (2014). Plastid transformation of sporelings and suspension-cultured cells from the liverwort marchantia polymorpha l. In Chloroplast Biotechnology, pages 439–447. Springer.

[42] Clowes, F. (1954). The promeristem and the minimal constructional centre in grass root apices. New Phytologist, 53(1):108–116.

[43] Cockcroft, C. E., den Boer, B. G., Healy, J. S., and Murray, J. A. (2000). Cyclin d control of growth rate in plants. Nature, 405(6786):575–579.

[44] Coen, E., Rolland-Lagan, A.-G., Matthews, M., Bangham, J. A., and Prusinkiewicz, P. (2004). The genetics of geometry. Proceedings of the National Academy of Sciences, 101(14):4728–4735.

[45] Colangelo, E. P. and Guerinot, M. L. (2004). The essential basic helix-loop-helix protein fit1 is required for the iron deficiency response. The Plant Cell, 16(12):3400–3412.

[46] Cosgrove, D. J. (2000). Loosening of plant cell walls by expansins. Nature, 407(6802):321–326.

[47] Coudert, Y., Novák, O., and Harrison, C. J. (2019). A knox-cytokinin regulatory module predates the origin of indeterminate vascular plants. Current Biology, 29(16):2743–2750.

[48] Coudert, Y., Palubicki, W., Ljung, K., Novak, O., Leyser, O., and Harrison, C. J. (2015). Three ancient hormonal cues co-ordinate shoot branching in a moss. Elife, 4:e06808.

[49] Cutler, S. R., Ehrhardt, D. W., Griffitts, J. S., and Somerville, C. R. (2000). Random gfp cdna fusions enable visualization of subcellular structures in cells of arabidopsis at a high frequency. Proceedings of the National Academy of Sciences, 97(7):3718–3723.

[50] Daum, G., Medzihradszky, A., Suzaki, T., and Lohmann, J. U. (2014). A mechanistic framework for noncell autonomous stem cell induction in arabidopsis. Proceedings of the National Academy of Sciences, 111(40):14619–14624.

[51] de Vries, J., Fischer, A. M., Roettger, M., Rommel, S., Schluepmann, H., Bräutigam, A., Carlsbecker, A., and Gould, S. B. (2016). Cytokinin-induced promotion of root meristem size in the fern azolla supports a shoot-like origin of euphyllophyte roots. New Phytologist, 209(2):705–720.

[52] Delmans, M. (2020). Engineering morphogenesis of Marchantia polymorpha gemmae. PhD thesis, University of Cambridge.

[53] Delmans, M., Pollak, B., and Haseloff, J. (2017). Marpodb: an open registry for marchantia polymorpha genetic parts. Plant and Cell Physiology, 58(1):e5–e5.

[54] Denyer, T., Ma, X., Klesen, S., Scacchi, E., Nieselt, K., and Timmermans, M. C. (2019). Spatiotemporal developmental trajectories in the arabidopsis root revealed using high-throughput single-cell rna sequencing. Developmental cell, 48(6):840–852.

[55] Desvoyes, B. and Gutierrez, C. (2020). Roles of plant retinoblastoma protein: Cell cycle and beyond. The EMBO Journal, 39(19):e105802.

[56] Dewitte, W., Scofield, S., Alcasabas, A. A., Maughan, S. C., Menges, M., Braun, N., Collins, C., Nieuwland, J., Prinsen, E., Sundaresan, V., et al. (2007). Arabidopsis cycd3 d-type cyclins link cell proliferation and endocycles and are rate-limiting for cytokinin responses. Proceedings of the National Academy of Sciences, 104(36):14537–14542.

[57] Dhonukshe, P., Grigoriev, I., Fischer, R., Tominaga, M., Robinson, D. G., Hašek, J., Paciorek, T., Petrášek, J., Seifertová, D., Tejos, R., et al. (2008). Auxin transport inhibitors impair vesicle motility and actin cytoskeleton dynamics in diverse eukaryotes. Proceedings of the National Academy of Sciences, 105(11):4489–4494.

[58] Di Laurenzio, L., Wysocka-Diller, J., Malamy, J. E., Pysh, L., Helariutta, Y., Freshour, G., Hahn, M. G., Feldmann, K. A., and Benfey, P. N. (1996). The scarecrow gene regulates an asymmetric cell division that is essential for generating the radial organization of the arabidopsis root. Cell, 86(3):423–433.

[59] Diamond, J. (2002). Evolution, consequences and future of plant and animal domestication. Nature, 418(6898):700–707.

[60] DICKSON, H. (1932). Polarity and the production of adventitious growing points in marchantia polymorpha. Annals of Botany, 46(183):683–701.

[61] Dinesh, D. C., Villalobos, L. I. A. C., and Abel, S. (2016). Structural biology of nuclear auxin action. Trends in Plant Science, 21(4):302–316.

[62] Ding, Z. and Friml, J. (2010). Auxin regulates distal stem cell differentiation in arabidopsis roots. Proceedings of the National Academy of Sciences, 107(26):12046–12051.

[63] Dolan, L., Janmaat, K., Willemsen, V., Linstead, P., Poethig, S., Roberts, K., and Scheres, B. (1993). Cellular organisation of the arabidopsis thaliana root. Development, 119(1):71–84.

[64] Dorrity, M. W., Alexandre, C. M., Hamm, M. O., Vigil, A.-L., Fields, S., Queitsch, C., and Cuperus, J. T. (2021). The regulatory landscape of arabidopsis thaliana roots at single-cell resolution. Nature communications, 12(1):1–12.

[65] Duckett, J. G., Ligrone, R., Renzaglia, K. S., and Pressel, S. (2014). Pegged and smooth rhizoids in complex thalloid liverworts (marchantiopsida): structure, function and evolution. Botanical Journal of the Linnean Society, 174(1):68–92.

[66] Durán-Medina, Y., Díaz-Ramírez, D., and Marsch-Martínez, N. (2017). Cytokinins on the move. Frontiers in Plant Science, 8:146.

[67] D'Ario, M., Tavares, R., Schiessl, K., Desvoyes, B., Gutierrez, C., Howard, M., and Sablowski, R. (2021). Cell size controlled in plants using dna content as an internal scale. Science, 372(6547):1176–1181.

[68] Ebrahimkhani, M. R. and Ebisuya, M. (2019). Synthetic developmental biology: build and control multicellular systems. Current opinion in chemical biology, 52:9–15.

[69] Efroni, I., Mello, A., Nawy, T., Ip, P.-L., Rahni, R., DelRose, N., Powers, A., Satija, R., and Birnbaum, K. D. (2016). Root regeneration triggers an embryo-like sequence guided by hormonal interactions. Cell, 165(7):1721–1733.

[70] Eklund, D. M., Ishizaki, K., Flores-Sandoval, E., Kikuchi, S., Takebayashi, Y., Tsukamoto, S., Hirakawa, Y., Nonomura, M., Kato, H., Kouno, M., et al. (2015). Auxin produced by the indole-3-pyruvic acid pathway regulates development and gemmae dormancy in the liverwort marchantia polymorpha. The Plant Cell, 27(6):1650–1669.

[71] Eklund, D. M., Kanei, M., Flores-Sandoval, E., Ishizaki, K., Nishihama, R., Kohchi, T., Lagercrantz, U., Bhalerao, R. P., Sakata, Y., and Bowman, J. L. (2018). An evolutionarily conserved abscisic acid signaling pathway regulates dormancy in the liverwort marchantia polymorpha. Current Biology, 28(22):3691–3699.

[72] Eklund, D. M., Thelander, M., Landberg, K., Ståldal, V., Nilsson, A., Johansson, M., Valsecchi, I., Pederson, E. R., Kowalczyk, M., Ljung, K., et al. (2010). Homologues of the arabidopsis thaliana shi/sty/lrp1 genes control auxin biosynthesis and affect growth and development in the moss physcomitrella patens. Development, 137(8):1275–1284.

[73] Elowitz, M. B. and Leibler, S. (2000). A synthetic oscillatory network of transcriptional regulators. Nature, 403(6767):335–338.

[74] Emms, D. M. and Kelly, S. (2015). Orthofinder: solving fundamental biases in whole genome comparisons dramatically improves orthogroup inference accuracy. Genome biology, 16(1):1–14.

[75] Emms, D. M. and Kelly, S. (2019). Orthofinder: phylogenetic orthology inference for comparative genomics. Genome biology, 20(1):1–14.

[76] Endrizzi, K., Moussian, B., Haecker, A., Levin, J. Z., and Laux, T. (1996). The shoot meristemless gene is required for maintenance of undifferentiated cells in arabidopsis shoot and floral meristems and acts at a different regulatory level than the meristem genes wuschel and zwille. The plant journal, 10(6):967–979.

[77] Engler, C., Kandzia, R., and Marillonnet, S. (2008). A one pot, one step, precision cloning method with high throughput capability. PloS one, 3(11):e3647.

[78] Engstrom, E. M., Andersen, C. M., Gumulak-Smith, J., Hu, J., Orlova, E., Sozzani, R., and Bowman, J. L. (2011). Arabidopsis homologs of the petunia hairy meristem gene are required for maintenance of shoot and root indeterminacy. Plant physiology, 155(2):735–750.

[79] Etchells, J. P., Smit, M. E., Gaudinier, A., Williams, C. J., and Brady, S. M. (2016). A brief history of the tdif-pxy signalling module: balancing meristem identity and differentiation during vascular development. New Phytologist, 209(2):474–484.

[80] Farmer, A., Thibivilliers, S., Ryu, K. H., Schiefelbein, J., and Libault, M. (2021). Single-nucleus rna and atac sequencing reveals the impact of chromatin accessibility on gene expression in arabidopsis roots at the single-cell level. Molecular Plant, 14(3):372–383.

[81] Federici, F., Dupuy, L., Laplaze, L., Heisler, M., and Haseloff, J. (2012). Integrated genetic and computation methods for in planta cytometry. nature methods, 9(5):483–485.

[82] Fendrych, M., Leung, J., and Friml, J. (2016). Tir1/afb-aux/iaa auxin perception mediates rapid cell wall acidification and growth of arabidopsis hypocotyls. elife, 5:e19048.

[83] Feraru, E., Vosolsobě, S., Feraru, M. I., Petrášek, J., and Kleine-Vehn, J. (2012). Evolution and structural diversification of pils putative auxin carriers in plants. Frontiers in plant science, 3:227.

[84] Ferreira-Guerra, M., Marquès-Bueno, M., Mora-García, S., and Caño-Delgado, A. I. (2020). Delving into the evolutionary origin of steroid sensing in plants. Current Opinion in Plant Biology, 57:87–95.

[85] Fleming, A. J., McQueen-Mason, S., Mandel, T., and Kuhlemeier, C. (1997). Induction of leaf primordia by the cell wall protein expansin. Science, 276(5317):1415–1418.

[86] Fletcher, J. C., Brand, U., Running, M. P., Simon, R., and Meyerowitz, E. M. (1999). Signaling of cell fate decisions by clavata3 in arabidopsis shoot meristems. Science, 283(5409):1911–1914.

[87] Flores-Sandoval, E., Dierschke, T., Fisher, T. J., and Bowman, J. L. (2016). Efficient and inducible use of artificial micrornas in marchantia polymorpha. Plant and Cell Physiology, 57(2):281–290.

[88] Flores-Sandoval, E., Eklund, D. M., and Bowman, J. L. (2015). A simple auxin transcriptional response system regulates multiple morphogenetic processes in the liverwort marchantia polymorpha. PLoS genetics, 11(5):e1005207.

[89] Flores-Sandoval, E., Eklund, D. M., Hong, S.-F., Alvarez, J. P., Fisher, T. J., Lampugnani, E. R., Golz, J. F., Vázquez-Lobo, A., Dierschke, T., Lin, S.-S., et al. (2018a). Class c arf s evolved before the origin of land plants and antagonize differentiation and developmental transitions in marchantia polymorpha. New Phytologist, 218(4):1612–1630.

[90] Flores-Sandoval, E., Romani, F., and Bowman, J. L. (2018b). Co-expression and transcriptome analysis of marchantia polymorpha transcription factors supports class c arfs as independent actors of an ancient auxin regulatory module. Frontiers in plant science, 9:1345.

[91] Frank, M. H. and Scanlon, M. J. (2015). Transcriptomic evidence for the evolution of shoot meristem function in sporophyte-dominant land plants through concerted selection of ancestral gametophytic and sporophytic genetic programs. Molecular Biology and Evolution, 32(2):355–367.

[92] Friml, J., Vieten, A., Sauer, M., Weijers, D., Schwarz, H., Hamann, T., Offringa, R., and Jürgens, G. (2003). Efflux-dependent auxin gradients establish the apical–basal axis of arabidopsis. Nature, 426(6963):147–153.

[93] Fuchs, M. and Lohmann, J. U. (2020). Aiming for the top: non-cell autonomous control of shoot stem cells in arabidopsis. Journal of plant research, 133(3):297–309.

[94] Fuller, D. Q., Denham, T., Arroyo-Kalin, M., Lucas, L., Stevens, C. J., Qin, L., Allaby, R. G., and Purugganan, M. D. (2014). Convergent evolution and parallelism in plant domestication revealed by an expanding archaeological record. Proceedings of the National Academy of Sciences, 111(17):6147–6152.

[95] Furumizu, C. and Sawa, S. (2021). Insight into early diversification of leucine-rich repeat receptor-like kinases provided by the sequenced moss and hornwort genomes. Plant Molecular Biology, pages 1–17.

[96] Gala, H. P., Lanctot, A., Jean-Baptiste, K., Guiziou, S., Chu, J. C., Zemke, J. E., George, W., Queitsch, C., Cuperus, J. T., and Nemhauser, J. L. (2021). A single-cell view of the transcriptome during lateral root initiation in arabidopsis thaliana. The Plant Cell, 33(7):2197–2220.

[97] Galinha, C., Hofhuis, H., Luijten, M., Willemsen, V., Blilou, I., Heidstra, R., and Scheres, B. (2007). Plethora proteins as dose-dependent master regulators of arabidopsis root development. Nature, 449(7165):1053–1057.

[98] Galvan-Ampudia, C. S., Cerutti, G., Legrand, J., Brunoud, G., Martin-Arevalillo, R., Azais, R., Bayle, V., Moussu, S., Wenzl, C., Jaillais, Y., et al. (2020). Temporal integration of auxin information for the regulation of patterning. Elife, 9:e55832.

[99] Gälweiler, L., Guan, C., Müller, A., Wisman, E., Mendgen, K., Yephremov, A., and Palme, K. (1998). Regulation of polar auxin transport by atpin1 in arabidopsis vascular tissue. Science, 282(5397):2226–2230.

[100] Gangappa, S. N. and Botto, J. F. (2016). The multifaceted roles of hy5 in plant growth and development. Molecular plant, 9(10):1353–1365.

[101] Gao, B., Wang, L., Oliver, M., Chen, M., and Zhang, J. (2020). Phylogenomic synteny network analyses reveal ancestral transpositions of auxin response factor genes in plants. Plant methods, 16:1–13.

[102] Gasiunas, G., Barrangou, R., Horvath, P., and Siksnys, V. (2012). Cas9–crrna ribonucleoprotein complex mediates specific dna cleavage for adaptive immunity in bacteria. Proceedings of the National Academy of Sciences, 109(39):E2579–E2586.

[103] Gelvin, S. B. (2021). Plant dna repair and agrobacterium t- dna integration. International Journal of Molecular Sciences, 22(16):8458.

[104] Goodstein, D. M., Shu, S., Howson, R., Neupane, R., Hayes, R. D., Fazo, J., Mitros, T., Dirks, W., Hellsten, U., Putnam, N., et al. (2012). Phytozome: a comparative platform for green plant genomics. Nucleic acids research, 40(D1):D1178–D1186.

[105] Gordon, S. P., Chickarmane, V. S., Ohno, C., and Meyerowitz, E. M. (2009). Multiple feedback loops through cytokinin signaling control stem cell number within the arabidopsis shoot meristem. Proceedings of the National Academy of Sciences, 106(38):16529–16534.

[106] Grieneisen, V. A., Xu, J., Marée, A. F., Hogeweg, P., and Scheres, B. (2007). Auxin transport is sufficient to generate a maximum and gradient guiding root growth. Nature, 449(7165):1008–1013.

[107] Gruel, J., Landrein, B., Tarr, P., Schuster, C., Refahi, Y., Sampathkumar, A., Hamant, O., Meyerowitz, E. M., and Jönsson, H. (2016). An epidermis-driven mechanism positions and scales stem cell niches in plants. Science advances, 2(1):e1500989.

[108] Gruhn, N., Halawa, M., Snel, B., Seidl, M. F., and Heyl, A. (2014). A subfamily of putative cytokinin receptors is revealed by an analysis of the evolution of the two-component signaling system of plants. Plant Physiology, 165(1):227–237.

[109] Gu, N., Tamada, Y., Imai, A., Palfalvi, G., Kabeya, Y., Shigenobu, S., Ishikawa, M., Angelis, K. J., Chen, C., and Hasebe, M. (2020). Dna damage triggers reprogramming of differentiated cells into stem cells in physcomitrella. Nature plants, 6(9):1098–1105.

[110] Ha, C. M., Jun, J. H., and Fletcher, J. C. (2010). Shoot apical meristem form and function. Current topics in developmental biology, 91:103–140.

[111] Haga, N., Kato, K., Murase, M., Araki, S., Kubo, M., Demura, T., Suzuki, K., Muller, I., Voß, U., Jurgens, G., et al. (2007). R1r2r3-myb proteins positively regulate cytokinesis through activation of knolle transcription in arabidopsis thaliana.

[112] Haga, N., Kobayashi, K., Suzuki, T., Maeo, K., Kubo, M., Ohtani, M., Mitsuda, N., Demura, T., Nakamura, K., Jürgens, G., et al. (2011). Mutations in myb3r1 and myb3r4 cause pleiotropic developmental defects and preferential down-regulation of multiple g2/m-specific genes in arabidopsis. Plant Physiology, 157(2):706–717.

[113] Haghverdi, L., Buettner, F., and Theis, F. J. (2015). Diffusion maps for high-dimensional single-cell analysis of differentiation data. Bioinformatics, 31(18):2989–2998.

[114] Haig, D. (2008). Homologous versus antithetic alternation of generations and the origin of sporophytes. The Botanical Review, 74(3):395–418.

[115] Hamann, T., Mayer, U., and Jurgens, G. (1999). The auxin-insensitive bodenlos mutation affects primary root formation and apical-basal patterning in the arabidopsis embryo. Development, 126(7):1387–1395.

[116] Han, H., Yan, A., Li, L., Zhu, Y., Feng, B., Liu, X., and Zhou, Y. (2020). A signal cascade originated from epidermis defines apical-basal patterning of arabidopsis shoot apical meristems. Nature communications, 11(1):1–17.

[117] Han, S.-K., Qi, X., Sugihara, K., Dang, J. H., Endo, T. A., Miller, K. L., Kim, E.-D., Miura, T., and Torii, K. U. (2018). Mute directly orchestrates cell-state switch and the single symmetric division to create stomata. Developmental cell, 45(3):303–315.

[118] Hanahan, D., Jessee, J., and Bloom, F. R. (1991). [4] plasmid transformation of escherichia coli and other bacteria. Methods in enzymology, 204:63–113.

[119] Hardtke, C. S. and Berleth, T. (1998). The arabidopsis gene monopteros encodes a transcription factor mediating embryo axis formation and vascular development. The EMBO journal, 17(5):1405–1411.

[120] Harris, B. J., Harrison, C. J., Hetherington, A. M., and Williams, T. A. (2020a). Phylogenomic evidence for the monophyly of bryophytes and the reductive evolution of stomata. Current Biology, 30(11):2001–2012.

[121] Harris, C. R., Millman, K. J., van der Walt, S. J., Gommers, R., Virtanen, P., Cournapeau, D., Wieser, E., Taylor, J., Berg, S., Smith, N. J., et al. (2020b). Array programming with numpy. Nature, 585(7825):357–362.

[122] Hata, Y. and Kyozuka, J. (2021). Fundamental mechanisms of the stem cell regulation in land plants: lesson from shoot apical cells in bryophytes. Plant Molecular Biology, pages 1–13.

[123] He, W., Brumos, J., Li, H., Ji, Y., Ke, M., Gong, X., Zeng, Q., Li, W., Zhang, X., An, F., et al. (2011). A small-molecule screen identifies l-kynurenine as a competitive inhibitor of taa1/tar activity in ethylene-directed auxin biosynthesis and root growth in arabidopsis. The Plant Cell, 23(11):3944–3960.

[124] Heisler, M. G., Ohno, C., Das, P., Sieber, P., Reddy, G. V., Long, J. A., and Meyerowitz, E. M. (2005). Patterns of auxin transport and gene expression during primordium development revealed by live imaging of the arabidopsis inflorescence meristem. Current biology, 15(21):1899–1911.

[125] Helariutta, Y., Fukaki, H., Wysocka-Diller, J., Nakajima, K., Jung, J., Sena, G., Hauser, M.-T., and Benfey, P. N. (2000). The short-root gene controls radial patterning of the arabidopsis root through radial signaling. Cell, 101(5):555–567.

[126] Hernández-García, J., Sun, R., Serrano-Mislata, A., Inoue, K., Vargas-Chávez, C., Esteve-Bruna, D., Arbona, V., Yamaoka, S., Nishihama, R., Kohchi, T., et al. (2021). Coordination between growth and stress responses by della in the liverwort marchantia polymorpha. bioRxiv.

[127] Herud-Sikimić, O., Stiel, A. C., Kolb, M., Shanmugaratnam, S., Berendzen, K. W., Feldhaus, C., Höcker, B., and Jürgens, G. (2021). A biosensor for the direct visualization of auxin. Nature, 592(7856):768–772.

[128] Hetherington, A. J. and Dolan, L. (2018). Stepwise and independent origins of roots among land plants. Nature, 561(7722):235–238.

[129] Heyman, J., Cools, T., Canher, B., Shavialenka, S., Traas, J., Vercauteren, I., Van den Daele, H., Persiau, G., De Jaeger, G., Sugimoto, K., et al. (2016). The heterodimeric transcription factor complex erf115–pat1 grants regeneration competence. Nature plants, 2(11):1–7.

[130] Heyman, J., Cools, T., Vandenbussche, F., Heyndrickx, K. S., Van Leene, J., Vercauteren, I., Vanderauwera, S., Vandepoele, K., De Jaeger, G., Van Der Straeten, D., et al. (2013). Erf115 controls root quiescent center cell division and stem cell replenishment. Science, 342(6160):860–863.

[131] Higo, A., Niwa, M., Yamato, K. T., Yamada, L., Sawada, H., Sakamoto, T., Kurata, T., Shirakawa, M., Endo, M., Shigenobu, S., et al. (2016). Transcriptional framework of male gametogenesis in the liverwort marchantia polymorpha l. Plant and Cell Physiology, 57(2):325–338.

[132] Higuchi, M., Pischke, M. S., Mähönen, A. P., Miyawaki, K., Hashimoto, Y., Seki, M., Kobayashi, M., Shinozaki, K., Kato, T., Tabata, S., et al. (2004). In planta functions of the arabidopsis cytokinin receptor family. Proceedings of the National Academy of Sciences, 101(23):8821–8826.

[133] Hirakawa, Y., Fujimoto, T., Ishida, S., Uchida, N., Sawa, S., Kiyosue, T., Ishizaki, K., Nishihama, R., Kohchi, T., and Bowman, J. L. (2020). Induction of multichotomous branching by clavata peptide in marchantia polymorpha. Current Biology, 30(19):3833–3840.

[134] Hirakawa, Y., Uchida, N., Yamaguchi, Y. L., Tabata, R., Ishida, S., Ishizaki, K., Nishihama, R., Kohchi, T., Sawa, S., and Bowman, J. L. (2019). Control of proliferation in the haploid meristem by cle peptide signaling in marchantia polymorpha. PLoS genetics, 15(3):e1007997.

[135] Hou, Z., Liu, Y., Zhang, M., Zhao, L., Jin, X., Liu, L., Su, Z., Cai, H., and Qin, Y. (2021). High-throughput single-cell transcriptomics reveals the female germline differentiation trajectory in arabidopsis thaliana. Communications biology, 4(1):1–16.

[136] Hughes, R. A. and Ellington, A. D. (2017). Synthetic dna synthesis and assembly: putting the synthetic in synthetic biology. Cold Spring Harbor perspectives in biology, 9(1):a023812.

[137] Hughes, S. J. (1971). On conidia of fungi, and gemmae of algae, bryophytes, and pteridophytes. Canadian Journal of Botany, 49(8):1319–1339.

[138] Hunter, J. D. (2007). Matplotlib: A 2d graphics environment. Computing in science & engineering, 9(03):90–95.

[139] Huson, D. H., Richter, D. C., Rausch, C., Dezulian, T., Franz, M., and Rupp, R. (2007). Dendroscope: An interactive viewer for large phylogenetic trees. BMC bioinformatics, 8(1):1–6.

[140] Huson, D. H. and Scornavacca, C. (2012). Dendroscope 3: an interactive tool for rooted phylogenetic trees and networks. Systematic biology, 61(6):1061–1067.

[141] Ikeuchi, M., Ogawa, Y., Iwase, A., and Sugimoto, K. (2016). Plant regeneration: cellular origins and molecular mechanisms. Development, 143(9):1442–1451.

[142] Inoue, K., Nishihama, R., Araki, T., and Kohchi, T. (2019). Reproductive induction is a far-red high irradiance response that is mediated by phytochrome and phytochrome interacting factor in marchantia polymorpha. Plant and Cell Physiology, 60(5):1136–1145.

[143] Inoue, K., Nishihama, R., Kataoka, H., Hosaka, M., Manabe, R., Nomoto, M., Tada, Y., Ishizaki, K., and Kohchi, T. (2016). Phytochrome signaling is mediated by phytochrome interacting factor in the liverwort marchantia polymorpha. The Plant Cell, 28(6):1406–1421.

[144] Ioio, R. D., Galinha, C., Fletcher, A. G., Grigg, S. P., Molnar, A., Willemsen, V., Scheres, B., Sabatini, S., Baulcombe, D., Maini, P. K., et al. (2012). A phabulosa/cytokinin feedback loop controls root growth in arabidopsis. Current Biology, 22(18):1699–1704.

[145] Ioio, R. D., Linhares, F. S., Scacchi, E., Casamitjana-Martinez, E., Heidstra, R., Costantino, P., and Sabatini, S. (2007). Cytokinins determine arabidopsis root-meristem size by controlling cell differentiation. Current biology, 17(8):678–682.

[146] Ioio, R. D., Nakamura, K., Moubayidin, L., Perilli, S., Taniguchi, M., Morita, M. T., Aoyama, T., Costantino, P., and Sabatini, S. (2008). A genetic framework for the control of cell division and differentiation in the root meristem. Science, 322(5906):1380–1384.

[147] Ishida, S., Suzuki, H., Iwaki, A., Kawamura, S., Yamaoka, S., Kojima, M., Takebayashi, Y., Yamaguchi, K., Shigenobu, S., Sakakibara, H., et al. (2022). Diminished auxin signaling triggers cellular reprogramming by inducing a regeneration factor in the liverwort marchantia polymorpha. Plant and Cell Physiology, 63(3):384–400.

[148] Ishikawa, M. and Hasebe, M. (2022). Molecular mechanisms of reprogramming of differentiated cells into stem cells in the moss physcomitrium patens. Current Opinion in Plant Biology, 65:102123.

[149] Ishikawa, M., Morishita, M., Higuchi, Y., Ichikawa, S., Ishikawa, T., Nishiyama, T., Kabeya, Y., Hiwatashi, Y., Kurata, T., Kubo, M., et al. (2019). Physcomitrella stemin transcription factor induces stem cell formation with epigenetic reprogramming. Nature plants, 5(7):681–690.

[150] Ishikawa, M., Murata, T., Sato, Y., Nishiyama, T., Hiwatashi, Y., Imai, A., Kimura, M., Sugimoto, N., Akita, A., Oguri, Y., et al. (2011). Physcomitrella cyclin-dependent kinase a links cell cycle reactivation to other cellular changes during reprogramming of leaf cells. The Plant Cell, 23(8):2924–2938.

[151] Ishizaki, K., Chiyoda, S., Yamato, K. T., and Kohchi, T. (2008). Agrobacterium-mediated transformation of the haploid liverwort marchantia polymorpha l., an emerging model for plant biology. Plant and cell physiology, 49(7):1084–1091.

[152] Ishizaki, K., Mizutani, M., Shimamura, M., Masuda, A., Nishihama, R., and Kohchi, T. (2013). Essential role of the e3 ubiquitin ligase nopperabo1 in schizogenous intercellular space formation in the liverwort marchantia polymorpha. The Plant Cell, 25(10):4075–4084.

[153] Ishizaki, K., Nishihama, R., Yamato, K. T., and Kohchi, T. (2016). Molecular genetic tools and techniques for marchantia polymorpha research. Plant and Cell Physiology, 57(2):262–270.

[154] Ishizaki, K., Nonomura, M., Kato, H., Yamato, K. T., and Kohchi, T. (2012). Visualization of auxin-mediated transcriptional activation using a common auxin-responsive reporter system in the liverwort marchantia polymorpha. Journal of plant research, 125(5):643–651.

[155] Iwase, A., Harashima, H., Ikeuchi, M., Rymen, B., Ohnuma, M., Komaki, S., Morohashi, K., Kurata, T., Nakata, M., Ohme-Takagi, M., et al. (2017). Wind1 promotes shoot regeneration through transcriptional activation of enhancer of shoot regeneration1 in arabidopsis. The Plant Cell, 29(1):54–69.

[156] Iwase, A., Kondo, Y., Laohavisit, A., Takebayashi, A., Ikeuchi, M., Matsuoka, K., Asahina, M., Mitsuda, N., Shirasu, K., Fukuda, H., et al. (2021). Wind transcription factors orchestrate wound-induced callus formation, vascular reconnection and defense response in arabidopsis. The New Phytologist.

[157] Iwase, A., Mitsuda, N., Koyama, T., Hiratsu, K., Kojima, M., Arai, T., Inoue, Y., Seki, M., Sakakibara, H., Sugimoto, K., et al. (2011). The ap2/erf transcription factor wind1 controls cell dedifferentiation in arabidopsis. Current Biology, 21(6):508–514.

[158] Jägermeyr, J., Müller, C., Ruane, A. C., Elliott, J., Balkovic, J., Castillo, O., Faye, B., Foster, I., Folberth, C., Franke, J. A., et al. (2021). Climate impacts on global agriculture emerge earlier in new generation of climate and crop models. Nature Food, pages 1–13.

[159] Jasinski, S., Piazza, P., Craft, J., Hay, A., Woolley, L., Rieu, I., Phillips, A., Hedden, P., and Tsiantis, M. (2005). Knox action in arabidopsis is mediated by coordinate regulation of cytokinin and gibberellin activities. Current Biology, 15(17):1560–1565.

[160] Jean-Baptiste, K., McFaline-Figueroa, J. L., Alexandre, C. M., Dorrity, M. W., Saunders, L., Bubb, K. L., Trapnell, C., Fields, S., Queitsch, C., and Cuperus, J. T. (2019). Dynamics of gene expression in single root cells of arabidopsis thaliana. The Plant Cell, 31(5):993–1011.

[161] Jeong, S., Trotochaud, A. E., and Clark, S. E. (1999). The arabidopsis clavata2 gene encodes a receptor-like protein required for the stability of the clavata1 receptor-like kinase. The Plant Cell, 11(10):1925–1933.

[162] Jha, S. G., Borowsky, A. T., Cole, B. J., Fahlgren, N., Farmer, A., Huang, S.-s. C., Karia, P., Libault, M., Provart, N. J., Rice, S. L., et al. (2021). Science forum: Vision, challenges and opportunities for a plant cell atlas. Elife, 10:e66877.

[163] Jiang, W., Zhou, H., Bi, H., Fromm, M., Yang, B., and Weeks, D. P. (2013). Demonstration of crispr/cas9/sgrna-mediated targeted gene modification in arabidopsis, tobacco, sorghum and rice. Nucleic acids research, 41(20):e188–e188.

[164] Jinek, M., Chylinski, K., Fonfara, I., Hauer, M., Doudna, J. A., and Charpentier, E. (2012). A programmable dual-rna–guided dna endonuclease in adaptive bacterial immunity. science, 337(6096):816–821.

[165] Jones, V. A. and Dolan, L. (2012). The evolution of root hairs and rhizoids. Annals of botany, 110(2):205–212.

[166] Jones, V. A. and Dolan, L. (2017). Mp wip regulates air pore complex development in the liverwort marchantia polymorpha. Development, 144(8):1472–1476.

[167] Kanazawa, T., Morinaka, H., Ebine, K., Shimada, T. L., Ishida, S., Minamino, N., Yamaguchi, K., Shigenobu, S., Kohchi, T., Nakano, A., et al. (2020). The liverwort oil body is formed by redirection of the secretory pathway. Nature communications, 11(1):1–11.

[168] Kareem, A., Durgaprasad, K., Sugimoto, K., Du, Y., Pulianmackal, A. J., Trivedi, Z. B., Abhayadev, P. V., Pinon, V., Meyerowitz, E. M., Scheres, B., et al. (2015). Plethora genes control regeneration by a two-step mechanism. Current Biology, 25(8):1017–1030.

[169] Kato, H., Ishizaki, K., Kouno, M., Shirakawa, M., Bowman, J. L., Nishihama, R., and Kohchi, T. (2015). Auxin-mediated transcriptional system with a minimal set of components is critical for morphogenesis through the life cycle in marchantia polymorpha. PLoS Genetics, 11(5):e1005084.

[170] Kato, H., Kouno, M., Takeda, M., Suzuki, H., Ishizaki, K., Nishihama, R., and Kohchi, T. (2017). The roles of the sole activator-type auxin response factor in pattern formation of marchantia polymorpha. Plant and Cell Physiology, 58(10):1642–1651.

[171] Kato, H., Mutte, S. K., Suzuki, H., Crespo, I., Das, S., Radoeva, T., Fontana, M., Yoshitake, Y., Hainiwa, E., van den Berg, W., et al. (2020). Design principles of a minimal auxin response system. Nature plants, 6(5):473–482.

[172] Kenrick, P. (2018). Changing expressions: a hypothesis for the origin of the vascular plant life cycle. Philosophical Transactions of the Royal Society B: Biological Sciences, 373(1739):20170149.

[173] Kim, J.-Y., Symeonidi, E., Pang, T. Y., Denyer, T., Weidauer, D., Bezrutczyk, M., Miras, M., Zöllner, N., Hartwig, T., Wudick, M. M., et al. (2021). Distinct identities of leaf phloem cells revealed by single cell transcriptomics. The Plant Cell, 33(3):511–530.

[174] Kirch, T., Simon, R., Grunewald, M., and Werr, W. (2003). The dornroschen/enhancer of shoot regeneration1 gene of arabidopsis acts in the control of meristem cell fate and lateral organ development. The Plant Cell, 15(3):694–705.

[175] Kohchi, T., Yamato, K. T., Ishizaki, K., Yamaoka, S., and Nishihama, R. (2021). Development and molecular genetics of marchantia polymorpha. Annual Review of Plant Biology, 72.

[176] Kreh, W. (1909). Über die Regeneration der Lebermoose, volume 90. Dt. Akademie der Naturforscher.

[177] Kremers, G.-J., Goedhart, J., van Munster, E. B., and Gadella, T. W. (2006). Cyan and yellow super fluorescent proteins with improved brightness, protein folding, and fret förster radius. Biochemistry, 45(21):6570–6580.

[178] Kubo, H., Nozawa, S., Hiwatashi, T., Kondou, Y., Nakabayashi, R., Mori, T., Saito, K., Takanashi, K., Kohchi, T., and Ishizaki, K. (2018). Biosynthesis of riccionidins and marchantins is regulated by r2r3-myb transcription factors in marchantia polymorpha. Journal of plant research, 131(5):849–864.

[179] Kubota, A., Ishizaki, K., Hosaka, M., and Kohchi, T. (2013). Efficient agrobacterium-mediated transformation of the liverwort marchantia polymorpha using regenerating thalli. Bioscience, biotechnology, and biochemistry, 77(1):167–172.

[180] Kumar, N., Harashima, H., Kalve, S., Bramsiepe, J., Wang, K., Sizani, B. L., Bertrand, L. L., Johnson, M. C., Faulk, C., Dale, R., et al. (2015). Functional conservation in the siamese-related family of cyclin-dependent kinase inhibitors in land plants. The Plant Cell, 27(11):3065–3080.

[181] Kwon, C.-T., Heo, J., Lemmon, Z. H., Capua, Y., Hutton, S. F., Van Eck, J., Park, S. J., and Lippman, Z. B. (2020). Rapid customization of solanaceae fruit crops for urban agriculture. Nature biotechnology, 38(2):182–188.

[182] La Manno, G., Soldatov, R., Zeisel, A., Braun, E., Hochgerner, H., Petukhov, V., Lidschreiber, K., Kastriti, M. E., Lönnerberg, P., Furlan, A., et al. (2018). Rna velocity of single cells. Nature, 560(7719):494–498.

[183] Leibfried, A., To, J. P., Busch, W., Stehling, S., Kehle, A., Demar, M., Kieber, J. J., and Lohmann, J. U. (2005). Wuschel controls meristem function by direct regulation of cytokinin-inducible response regulators. Nature, 438(7071):1172–1175.

[184] Lemmon, Z. H., Reem, N. T., Dalrymple, J., Soyk, S., Swartwood, K. E., Rodriguez-Leal, D., Van Eck, J., and Lippman, Z. B. (2018). Rapid improvement of domestication traits in an orphan crop by genome editing. Nature plants, 4(10):766–770.

[185] Lenhard, M., Jurgens, G., and Laux, T. (2002). The wuschel and shootmeristemless genes fulfil complementary roles in arabidopsis shoot meristem regulation.

[186] Li, D., Flores-Sandoval, E., Ahtesham, U., Coleman, A., Clay, J. M., Bowman, J. L., and Chang, C. (2020a). Ethylene-independent functions of the ethylene precursor acc in marchantia polymorpha. Nature Plants, 6(11):1335–1344.

[187] Li, F.-W., Nishiyama, T., Waller, M., Frangedakis, E., Keller, J., Li, Z., Fernandez-Pozo, N., Barker, M. S., Bennett, T., Blázquez, M. A., et al. (2020b). Anthoceros genomes illuminate the origin of land plants and the unique biology of hornworts. Nature plants, 6(3):259–272.

[188] Li, H., Dai, X., Huang, X., Xu, M., Wang, Q., Yan, X., Sederoff, R. R., and Li, Q. (2021a). Single-cell rna sequencing reveals a high-resolution cell atlas of xylem in populus. Journal of Integrative Plant Biology.

[189] Li, L., Verstraeten, I., Roosjen, M., Takahashi, K., Rodriguez, L., Merrin, J., Chen, J., Shabala, L., Smet, W., Ren, H., et al. (2021b). Cell surface and intracellular auxin signalling for h+ fluxes in root growth. Nature, pages 1–5.

[190] Li, Y., Wu, Y. H., Hagen, G., and Guilfoyle, T. (1999). Expression of the auxin-inducible gh3 promoter/gus fusion gene as a useful molecular marker for auxin physiology. Plant and cell physiology, 40(7):675–682.

[191] Liao, C.-Y., Smet, W., Brunoud, G., Yoshida, S., Vernoux, T., and Weijers, D. (2015). Reporters for sensitive and quantitative measurement of auxin response. Nature methods, 12(3):207–210.

[192] Lin, W., Zhou, X., Tang, W., Takahashi, K., Pan, X., Dai, J., Ren, H., Zhu, X., Pan, S., Zheng, H., et al. (2021). Tmk-based cell-surface auxin signalling activates cell-wall acidification. Nature, pages 1–5.

[193] Linde, A.-M., Eklund, D. M., Kubota, A., Pederson, E. R., Holm, K., Gyllenstrand, N., Nishihama, R., Cronberg, N., Muranaka, T., Oyama, T., et al. (2017). Early evolution of the land plant circadian clock. New Phytologist, 216(2):576–590.

[194] Liu, L., Gallagher, J., Arevalo, E. D., Chen, R., Skopelitis, T., Wu, Q., Bartlett, M., and Jackson, D. (2021a). Enhancing grain-yield-related traits by crispr–cas9 promoter editing of maize cle genes. Nature Plants, 7(3):287–294.

[195] Liu, Q., Liang, Z., Feng, D., Jiang, S., Wang, Y., Du, Z., Li, R., Hu, G., Zhang, P., Ma, Y., et al. (2021b). Transcriptional landscape of rice roots at the single-cell resolution. Molecular Plant, 14(3):384–394.

[196] Liu, Z. and Karmarkar, V. (2008). Groucho/tup1 family co-repressors in plant development. Trends in plant science, 13(3):137–144.

[197] Liu, Z., Zhou, Y., Guo, J., Li, J., Tian, Z., Zhu, Z., Wang, J., Wu, R., Zhang, B., Hu, Y., et al. (2020). Global dynamic molecular profiling of stomatal lineage cell development by single-cell rna sequencing. Molecular Plant, 13(8):1178–1193.

[198] Liu, Z.-B., Ulmasov, T., Shi, X., Hagen, G., and Guilfoyle, T. J. (1994). Soybean gh3 promoter contains multiple auxin-inducible elements. The Plant Cell, 6(5):645–657.

[199] Lo, J.-C., Tsednee, M., Lo, Y.-C., Yang, S.-C., Hu, J.-M., Ishizaki, K., Kohchi, T., Lee, D.-C., and Yeh, K.-C. (2016). Evolutionary analysis of iron (fe) acquisition system in marchantia polymorpha. New Phytologist, 211(2):569–583.

[200] Long, J. A., Moan, E. I., Medford, J. I., and Barton, M. K. (1996). A member of the knotted class of homeodomain proteins encoded by the stm gene of arabidopsis. Nature, 379(6560):66–69.

[201] Lopez-Anido, C. B., Vatén, A., Smoot, N. K., Sharma, N., Guo, V., Gong, Y., Gil, M. X. A., Weimer, A. K., and Bergmann, D. C. (2021). Single-cell resolution of lineage trajectories in the arabidopsis stomatal lineage and developing leaf. Developmental Cell, 56(7):1043–1055.

[202] Lorenz, S., Tintelnot, S., Reski, R., and Decker, E. L. (2003). Cyclin d-knockout uncouples developmental progression from sugar availability. Plant molecular biology, 53(1):227–236.

[203] Love, M. I., Huber, W., and Anders, S. (2014). Moderated estimation of fold change and dispersion for rna-seq data with deseq2. Genome biology, 15(12):1–21.

[204] Ma, Y., Miotk, A., Šutiković, Z., Ermakova, O., Wenzl, C., Medzihradszky, A., Gaillochet, C., Forner, J., Utan, G., Brackmann, K., et al. (2019). Wuschel acts as an auxin response rheostat to maintain apical stem cells in arabidopsis. Nature communications, 10(1):1–11.

[205] Macosko, E. Z., Basu, A., Satija, R., Nemesh, J., Shekhar, K., Goldman, M., Tirosh, I., Bialas, A. R., Kamitaki, N., Martersteck, E. M., et al. (2015). Highly parallel genome-wide expression profiling of individual cells using nanoliter droplets. Cell, 161(5):1202–1214.

[206] Mähönen, A. P., Ten Tusscher, K., Siligato, R., Smetana, O., Díaz-Triviño, S., Salojärvi, J., Wachsman, G., Prasad, K., Heidstra, R., and Scheres, B. (2014). Plethora gradient formation mechanism separates auxin responses. Nature, 515(7525):125–129.

[207] Marand, A. P., Chen, Z., Gallavotti, A., and Schmitz, R. J. (2021). A cis-regulatory atlas in maize at single-cell resolution. Cell, 184(11):3041–3055.

[208] Maravolo, N. C. and Voth, P. D. (1966). Morphogenic effects of three growth substances on marchantia gemmalings. Botanical Gazette, 127(2/3):79–86.

[209] Matosevich, R. and Efroni, I. (2021). The quiescent center and root regeneration. Journal of Experimental Botany, 72(19):6739–6745.

[210] Maugarny, A., Gonçalves, B., Arnaud, N., and Laufs, P. (2016). Cuc transcription factors: to the meristem and beyond. In Plant Transcription Factors, pages 229–247. Elsevier.

[211] Mayer, K. F., Schoof, H., Haecker, A., Lenhard, M., Jürgens, G., and Laux, T. (1998). Role of wuschel in regulating stem cell fate in the arabidopsis shoot meristem. Cell, 95(6):805–815.

[212] McInnes, L., Healy, J., and Melville, J. (2018). Umap: Uniform manifold approximation and projection for dimension reduction. arXiv preprint arXiv:1802.03426.

[213] McKinney, W. et al. (2010). Data structures for statistical computing in python. In Proceedings of the 9th Python in Science Conference, volume 445, pages 51–56. Austin, TX.

[214] McQueen-Mason, S., Durachko, D. M., and Cosgrove, D. J. (1992). Two endogenous proteins that induce cell wall extension in plants. The Plant Cell, 4(11):1425–1433.

[215] Mecchia, M. A., García-Hourquet, M., Lozano-Elena, F., Planas-Riverola, A., Blasco-Escamez, D., Marquès-Bueno, M., Mora-García, S., and Caño-Delgado, A. I. (2021). The bes1/bzr1-family transcription factor mpbes1 regulates cell division and differentiation in marchantia polymorpha. Current Biology, 31(21):4860–4869.

[216] Melsted, P., Booeshaghi, A. S., Liu, L., Gao, F., Lu, L., Min, K. H. J., da Veiga Beltrame, E., Hjörleifsson, K. E., Gehring, J., and Pachter, L. (2021). Modular, efficient and constant-memory single-cell rna-seq preprocessing. Nature biotechnology, pages 1–6.

[217] Milla, R. and Osborne, C. P. (2021). Crop origins explain variation in global agricultural relevance. Nature Plants, 7(5):598–607.

[218] Miller, C. O., Skoog, F., Von Saltza, M. H., and Strong, F. (1955). Kinetin, a cell division factor from deoxyribonucleic acid1. Journal of the American Chemical Society, 77(5):1392–1392.

[219] Monte, I., Ishida, S., Zamarreño, A. M., Hamberg, M., Franco-Zorrilla, J. M., García-Casado, G., Gouhier-Darimont, C., Reymond, P., Takahashi, K., García-Mina, J. M., et al. (2018). Ligand-receptor co-evolution shaped the jasmonate pathway in land plants. Nature chemical biology, 14(5):480–488.

[220] Muller, R., Bleckmann, A., and Simon, R. (2008). The receptor kinase coryne of arabidopsis transmits the stem cell–limiting signal clavata3 independently of clavata1. The Plant Cell, 20(4):934–946.

[221] Mutte, S. K., Kato, H., Rothfels, C., Melkonian, M., Wong, G. K.-S., and Weijers, D. (2018). Origin and evolution of the nuclear auxin response system. Elife, 7:e33399.

[222] Nakajima, K., Sena, G., Nawy, T., and Benfey, P. N. (2001). Intercellular movement of the putative transcription factor shr in root patterning. Nature, 413(6853):307–311.

[223] Naramoto, S., Hata, Y., Fujita, T., and Kyozuka, J. (2021). The bryophytes physcomitrium patens and marchantia polymorpha as model systems for studying evolutionary cell and developmental biology in plants. The Plant Cell.

[224] Naramoto, S., Jones, V. A. S., Trozzi, N., Sato, M., Toyooka, K., Shimamura, M., Ishida, S., Nishitani, K., Ishizaki, K., Nishihama, R., et al. (2019). A conserved regulatory mechanism mediates the convergent evolution of plant shoot lateral organs. PLoS biology, 17(12):e3000560.

[225] Nasu, M., Tani, K., Hattori, C., Honda, M., Shimaoka, T., Yamaguchi, N., and Katoh, K. (1997). Efficient transformation of marchantia polymorpha that is haploid and has very small genome dna. Journal of fermentation and bioengineering, 84(6):519–523.

[226] Negin, B., Shemer, O., Sorek, Y., and Eshed Williams, L. (2017). Shoot stem cell specification in roots by the wuschel transcription factor. PLoS One, 12(4):e0176093.

[227] Nishihama, R., Ishida, S., Urawa, H., Kamei, Y., and Kohchi, T. (2016). Conditional gene expression/deletion systems for marchantia polymorpha using its own heat-shock promoter and cre/lox p-mediated site-specific recombination. Plant and Cell Physiology, 57(2):271–280.

[228] Nishihama, R., Ishizaki, K., Hosaka, M., Matsuda, Y., Kubota, A., and Kohchi, T. (2015). Phytochrome-mediated regulation of cell division and growth during regeneration and sporeling development in the liverwort marchantia polymorpha. Journal of plant research, 128(3):407–421.

[229] Nowack, M. K., Harashima, H., Dissmeyer, N., Bouyer, D., Weimer, A. K., De Winter, F., Yang, F., Schnittger, A., et al. (2012). Genetic framework of cyclin-dependent kinase function in arabidopsis. Developmental cell, 22(5):1030–1040.

[230] O'Hanlon, M. E. (1926). Germination of spores and early stages in development of gametophyte of marchantia polymorpha. Botanical Gazette, 82(2):215–222.

[231] Ono, K., Ohyama, K., and Gamborg, O. L. (1979). Regeneration of the liverwort marchantia polymorpha l. from protoplasts isolated from cell suspension culture. Plant Science Letters, 14(3):225–229.

[232] Ortiz-Ramírez, C., Guillotin, B., Xu, X., Rahni, R., Zhang, S., Yan, Z., Coqueiro Dias Araujo, P., Demesa-Arevalo, E., Lee, L., Van Eck, J., et al. (2021). Ground tissue circuitry regulates organ complexity in maize and setaria. Science, 374(6572):1247–1252.

[233] Otani, K., Ishizaki, K., Nishihama, R., Takatani, S., Kohchi, T., Takahashi, T., and Motose, H. (2018). An evolutionarily conserved nima-related kinase directs rhizoid tip growth in the basal land plant marchantia polymorpha. Development, 145(5):dev154617.

[234] Overvoorde, P. J., Okushima, Y., Alonso, J. M., Chan, A., Chang, C., Ecker, J. R., Hughes, B., Liu, A., Onodera, C., Quach, H., et al. (2005). Functional genomic analysis of the auxin/indole-3-acetic acid gene family members in arabidopsis thaliana. The Plant Cell, 17(12):3282–3300.

[235] Palovaara, J., de Zeeuw, T., and Weijers, D. (2016). Tissue and organ initiation in the plant embryo: a first time for everything. Annual Review of Cell and Developmental Biology, 32:47–75.

[236] Perez-Garcia, P. and Moreno-Risueno, M. A. (2018). Stem cells and plant regeneration. Developmental biology, 442(1):3–12.

[237] Perianez-Rodriguez, J., Manzano, C., and Moreno-Risueno, M. A. (2014). Post-embryonic organogenesis and plant regeneration from tissues: two sides of the same coin? Frontiers in plant science, 5:219.

[238] Perilli, S., Moubayidin, L., and Sabatini, S. (2010). The molecular basis of cytokinin function. Current opinion in plant biology, 13(1):21–26.

[239] Petersson, S. V., Johansson, A. I., Kowalczyk, M., Makoveychuk, A., Wang, J. Y., Moritz, T., Grebe, M., Benfey, P. N., Sandberg, G., and Ljung, K. (2009). An auxin gradient and maximum in the arabidopsis root apex shown by high-resolution cell-specific analysis of iaa distribution and synthesis. The Plant Cell, 21(6):1659–1668.

[240] Petricka, J. J., Winter, C. M., and Benfey, P. N. (2012). Control of arabidopsis root development. Annual review of plant biology, 63:563–590.

[241] Pi, L., Aichinger, E., van der Graaff, E., Llavata-Peris, C. I., Weijers, D., Hennig, L., Groot, E., and Laux, T. (2015). Organizer-derived wox5 signal maintains root columella stem cells through chromatin-mediated repression of cdf4 expression. Developmental cell, 33(5):576–588.

[242] Picard, D., Salser, S. J., and Yamamoto, K. R. (1988). A movable and regulable inactivation function within the steroid binding domain of the glucocorticoid receptor. Cell, 54(7):1073–1080.

[243] Pien, S., Wyrzykowska, J., McQueen-Mason, S., Smart, C., and Fleming, A. (2001). Local expression of expansin induces the entire process of leaf development and modifies leaf shape. Proceedings of the National Academy of Sciences, 98(20):11812–11817.

[244] Poethig, R. S. (1987). Clonal analysis of cell lineage patterns in plant development. American Journal of Botany, 74(4):581–594.

[245] Pollak, B., Cerda, A., Delmans, M., Álamos, S., Moyano, T., West, A., Gutiérrez, R. A., Patron, N. J., Federici, F., and Haseloff, J. (2019). Loop assembly: a simple and open system for recursive fabrication of dna circuits. New Phytologist, 222(1):628–640.

[246] PRESCOTT-ALLEN, R. and PRESCOTT-ALLEN, C. (1990). How many plants feed the world? Conservation Biology, 4(4):365–374.

[247] Prigge, M. J., Lavy, M., Ashton, N. W., and Estelle, M. (2010). Physcomitrella patens auxin-resistant mutants affect conserved elements of an auxin-signaling pathway. Current Biology, 20(21):1907–1912.

[248] Prigge, M. J., Otsuga, D., Alonso, J. M., Ecker, J. R., Drews, G. N., and Clark, S. E. (2005). Class iii homeodomain-leucine zipper gene family members have overlapping, antagonistic, and distinct roles in arabidopsis development. The Plant Cell, 17(1):61–76.

[249] Proust, H., Honkanen, S., Jones, V. A., Morieri, G., Prescott, H., Kelly, S., Ishizaki, K., Kohchi, T., and Dolan, L. (2016). Rsl class i genes controlled the development of epidermal structures in the common ancestor of land plants. Current Biology, 26(1):93–99.

[250] Purswani Ramchandani, N. (2015). Introducing the gemma of the liverwort Marchantia polymorpha L. as a simple morphogenetic system. PhD thesis, University of Cambridge.

[251] Ramirez-Parra, E., Fründt, C., and Gutierrez, C. (2003). A genome-wide identification of e2f-regulated genes in arabidopsis. The Plant Journal, 33(4):801–811.

[252] Raven, J. (1975). Transport of indoleacetic acid in plant cells in relation to ph and electrical potential gradients, and its significance for polar iaa transport. New Phytologist, 74(2):163–172.

[253] Regev, A., Teichmann, S. A., Lander, E. S., Amit, I., Benoist, C., Birney, E., Bodenmiller, B., Campbell, P., Carninci, P., Clatworthy, M., et al. (2017). Science forum: the human cell atlas. elife, 6:e27041.

[254] Reinhardt, D., Mandel, T., and Kuhlemeier, C. (2000). Auxin regulates the initiation and radial position of plant lateral organs. The Plant Cell, 12(4):507–518.

[255] Reinhardt, D., Pesce, E.-R., Stieger, P., Mandel, T., Baltensperger, K., Bennett, M., Traas, J., Friml, J., and Kuhlemeier, C. (2003). Regulation of phyllotaxis by polar auxin transport. Nature, 426(6964):255–260.

[256] Reinhardt, D., Wittwer, F., Mandel, T., and Kuhlemeier, C. (1998). Localized upregulation of a new expansin gene predicts the site of leaf formation in the tomato meristem. The Plant Cell, 10(9):1427–1437.

[257] Rensing, S. A., Lang, D., Zimmer, A. D., Terry, A., Salamov, A., Shapiro, H., Nishiyama, T., Perroud, P.-F., Lindquist, E. A., Kamisugi, Y., et al. (2008). The physcomitrella genome reveals evolutionary insights into the conquest of land by plants. Science, 319(5859):64–69.

[258] Reski, R. and Abel, W. O. (1985). Induction of budding on chloronemata and caulonemata of the moss, physcomitrella patens, using isopentenyladenine. Planta, 165(3):354–358.

[259] Rhee, S. Y., Birnbaum, K. D., and Ehrhardt, D. W. (2019). Towards building a plant cell atlas. Trends in plant science, 24(4):303–310.

[260] Riou-Khamlichi, C., Huntley, R., Jacqmard, A., and Murray, J. A. (1999). Cytokinin activation of arabidopsis cell division through a d-type cyclin. Science, 283(5407):1541–1544.

[261] Riou-Khamlichi, C., Menges, M., Healy, J. S., and Murray, J. A. (2000). Sugar control of the plant cell cycle: differential regulation of arabidopsis d-type cyclin gene expression. Molecular and cellular biology, 20(13):4513–4521.

[262] Rodríguez-Leal, D., Lemmon, Z. H., Man, J., Bartlett, M. E., and Lippman, Z. B. (2017). Engineering quantitative trait variation for crop improvement by genome editing. Cell, 171(2):470–480.

[263] Rojo, E., Sharma, V. K., Kovaleva, V., Raikhel, N. V., and Fletcher, J. C. (2002). Clv3 is localized to the extracellular space, where it activates the arabidopsis clavata stem cell signaling pathway. The Plant Cell, 14(5):969–977.

[264] Romani, F., Banić, E., Florent, S. N., Kanazawa, T., Goodger, J. Q., Mentink, R. A., Dierschke, T., Zachgo, S., Ueda, T., Bowman, J. L., et al. (2020). Oil body formation in marchantia polymorpha is controlled by mpc1hdz and serves as a defense against arthropod herbivores. Current Biology, 30(14):2815–2828.

[265] ROST, T. L. and JONES, T. J. (1988). Pea root regeneration after tip excisions at different levels: polarity of new growth. Annals of botany, 61(4):513–523.

[266] Rubery, P. H. and Sheldrake, A. R. (1974). Carrier-mediated auxin transport. Planta, 118(2):101–121.

[267] Ryu, K. H., Huang, L., Kang, H. M., and Schiefelbein, J. (2019). Single-cell rna sequencing resolves molecular relationships among individual plant cells. Plant physiology, 179(4):1444–1456.

[268] Ržička, K., Šimášková, M., Duclercq, J., Petrášek, J., Zažímalová, E., Simon, S., Friml, J., Van Montagu, M. C., and Benková, E. (2009). Cytokinin regulates root meristem activity via modulation of the polar auxin transport. Proceedings of the National Academy of Sciences, 106(11):4284–4289.

[269] Sabatini, S., Heidstra, R., Wildwater, M., and Scheres, B. (2003). Scarecrow is involved in positioning the stem cell niche in the arabidopsis root meristem. Genes & development, 17(3):354–358.

[270] Sablowski, R. and Gutierrez, C. (2021). Cycling in a crowd: coordination of plant cell division, growth, and cell fate. The Plant Cell.

[271] Sadowski, I., Ma, J., Triezenberg, S., and Ptashne, M. (1988). Gal4-vp16 is an unusually potent transcriptional activator. Nature, 335(6190):563–564.

[272] Sakakibara, K., Nishiyama, T., Deguchi, H., and Hasebe, M. (2008). Class 1 knox genes are not involved in shoot development in the moss physcomitrella patens but do function in sporophyte development. Evolution & development, 10(5):555–566.

[273] Sakakibara, K., Reisewitz, P., Aoyama, T., Friedrich, T., Ando, S., Sato, Y., Tamada, Y., Nishiyama, T., Hiwatashi, Y., Kurata, T., et al. (2014). Wox13-like genes are required for reprogramming of leaf and protoplast cells into stem cells in the moss physcomitrella patens. Development, 141(8):1660–1670.

[274] Sakamoto, Y., Ishimoto, A., Sakai, Y., Sato, M., Nishihama, R., Abe, K., Sano, Y., Furuichi, T., Tsuji, H., Kohchi, T., et al. (2021). Improved clearing method contributes to deep imaging of plant organs.

[275] Sarkar, A. K., Luijten, M., Miyashima, S., Lenhard, M., Hashimoto, T., Nakajima, K., Scheres, B., Heidstra, R., and Laux, T. (2007). Conserved factors regulate signalling in arabidopsis thaliana shoot and root stem cell organizers. Nature, 446(7137):811–814.

[276] Sassi, M. and Vernoux, T. (2013). Auxin and self-organization at the shoot apical meristem. Journal of experimental botany, 64(9):2579–2592.

[277] Satija, R., Farrell, J. A., Gennert, D., Schier, A. F., and Regev, A. (2015). Spatial reconstruction of single-cell gene expression data. Nature biotechnology, 33(5):495–502.

[278] Sato, Y., Sugimoto, N., Hirai, T., Imai, A., Kubo, M., Hiwatashi, Y., Nishiyama, T., and Hasebe, M. (2017). Cells reprogramming to stem cells inhibit the reprogramming of adjacent cells in the moss physcomitrella patens. Scientific reports, 7(1):1–12.

[279] Sauret-Gueto, S., Frangedakis, E., Silvestri, L., Rebmann, M., Tomaselli, M., Markel, K., Delmans, M., West, A., Patron, N. J., and Haseloff, J. (2020). Systematic tools for reprogramming plant gene expression in a simple model, marchantia polymorpha. ACS synthetic biology, 9(4):864–882.

[280] Schaller, G. E., Street, I. H., and Kieber, J. J. (2014). Cytokinin and the cell cycle. Current opinion in plant biology, 21:7–15.

[281] Schindelin, J., Arganda-Carreras, I., Frise, E., Kaynig, V., Longair, M., Pietzsch, T., Preibisch, S., Rueden, C., Saalfeld, S., Schmid, B., et al. (2012). Fiji: an open-source platform for biological-image analysis. Nature methods, 9(7):676–682.

[282] Schlegel, J., Denay, G., Pinto, K. G., Stahl, Y., Schmid, J., Blümke, P., and Simon, R. (2021). Control of arabidopsis shoot stem cell homeostasis by two antagonistic cle peptide signalling pathways. bioRxiv.

[283] Schlissel, G. and Li, P. (2020). Synthetic developmental biology: understanding through reconstitution. Annual review of cell and developmental biology, 36:339–357.

[284] Schmid, M. W., Giraldo-Fonseca, A., Rövekamp, M., Smetanin, D., Bowman, J. L., and Grossniklaus, U. (2018). Extensive epigenetic reprogramming during the life cycle of marchantia polymorpha. Genome biology, 19(1):1–17.

[285] Schmülling, T., Werner, T., Riefler, M., Krupková, E., and y Manns, I. B. (2003). Structure and function of cytokinin oxidase/dehydrogenase genes of maize, rice, arabidopsis and other species. Journal of plant research, 116(3):241–252.

[286] Schoof, H., Lenhard, M., Haecker, A., Mayer, K. F., Jürgens, G., and Laux, T. (2000). The stem cell population of arabidopsis shoot meristems is maintained by a regulatory loop between the clavata and wuschel genes. Cell, 100(6):635–644.

[287] Shan, Q., Wang, Y., Li, J., Zhang, Y., Chen, K., Liang, Z., Zhang, K., Liu, J., Xi, J. J., Qiu, J.-L., et al. (2013). Targeted genome modification of crop plants using a crispr-cas system. Nature biotechnology, 31(8):686–688.

[288] Sharma, N., Bhalla, P. L., and Singh, M. B. (2013). Transcriptome-wide profiling and expression analysis of transcription factor families in a liverwort, marchantia polymorpha. BMC genomics, 14(1):1–17.

[289] Shi, B. and Vernoux, T. (2022). Hormonal control of cell identity and growth in the shoot apical meristem. Current opinion in plant biology, 65:102111.

[290] Shimamura, M. (2016). Marchantia polymorpha: taxonomy, phylogeny and morphology of a model system. Plant and Cell Physiology, 57(2):230–256.

[291] Shimotohno, A., Aki, S. S., Takahashi, N., and Umeda, M. (2021). Regulation of the plant cell cycle in response to hormones and the environment. Annual Review of Plant Biology, 72.

[292] Shimotohno, A., Heidstra, R., Blilou, I., and Scheres, B. (2018). Root stem cell niche organizer specification by molecular convergence of plethora and scarecrow transcription factor modules. Genes & development, 32(15-16):1085–1100.

[293] Shulse, C. N., Cole, B. J., Ciobanu, D., Lin, J., Yoshinaga, Y., Gouran, M., Turco, G. M., Zhu, Y., O'Malley, R. C., Brady, S. M., et al. (2019). High-throughput single-cell transcriptome profiling of plant cell types. Cell reports, 27(7):2241–2247.

[294] Silverman, J. D., Roche, K., Mukherjee, S., and David, L. A. (2020). Naught all zeros in sequence count data are the same. Computational and structural biotechnology journal, 18:2789.

[295] Sister Ellen, O. (1926). Germination of the Spores and Early Stages in the Development of the Gametophyte of Marchantia Polymorpha. University of Chicago Press.

[296] Sizani, B. L., Kalve, S., Markakis, M. N., Domagalska, M. A., Stelmaszewska, J., AbdElgawad, H., Zhao, X., De Veylder, L., De Vos, D., Broeckhove, J., et al. (2019). Multiple mechanisms explain how reduced krp expression increases leaf size of arabidopsis thaliana. New Phytologist, 221(3):1345–1358.

[297] Skoog, F. and Thimann, K. V. (1934). Further experiments on the inhibition of the development of lateral buds by growth hormone. Proceedings of the National Academy of Sciences of the United States of America, 20(8):480.

[298] Sohlberg, J. J., Myrenås, M., Kuusk, S., Lagercrantz, U., Kowalczyk, M., Sandberg, G., and Sundberg, E. (2006). Sty1 regulates auxin homeostasis and affects apical–basal patterning of the arabidopsis gynoecium. The Plant Journal, 47(1):112–123.

[299] Solly, J. E., Cunniffe, N. J., and Harrison, C. J. (2017). Regional growth rate differences specified by apical notch activities regulate liverwort thallus shape. Current Biology, 27(1):16–26.

[300] Soyk, S., Lemmon, Z. H., Oved, M., Fisher, J., Liberatore, K. L., Park, S. J., Goren, A., Jiang, K., Ramos, A., van der Knaap, E., et al. (2017). Bypassing negative epistasis on yield in tomato imposed by a domestication gene. Cell, 169(6):1142–1155.

[301] Sozzani, R., Cui, H., Moreno-Risueno, M., Busch, W., Van Norman, J., Vernoux, T., Brady, S., Dewitte, W., Murray, J. A. H., and Benfey, P. (2010). Spatiotemporal regulation of cell-cycle genes by shortroot links patterning and growth. Nature, 466(7302):128–132.

[302] Spartz, A. K., Ren, H., Park, M. Y., Grandt, K. N., Lee, S. H., Murphy, A. S., Sussman, M. R., Overvoorde, P. J., and Gray, W. M. (2014). Saur inhibition of pp2c-d phosphatases activates plasma membrane h+-atpases to promote cell expansion in arabidopsis. The Plant Cell, 26(5):2129–2142.

[303] Stahl, Y., Grabowski, S., Bleckmann, A., Kühnemuth, R., Weidtkamp-Peters, S., Pinto, K. G., Kirschner, G. K., Schmid, J. B., Wink, R. H., Hülsewede, A., et al. (2013). Moderation of arabidopsis root stemness by clavata1 and arabidopsis crinkly4 receptor kinase complexes. Current Biology, 23(5):362–371.

[304] Stahl, Y., Wink, R. H., Ingram, G. C., and Simon, R. (2009). A signaling module controlling the stem cell niche in arabidopsis root meristems. Current biology, 19(11):909–914.

[305] Stewart, R. and Dermen, H. (1975). Flexibility in ontogeny as shown by the contribution of the shoot apical layers to leaves of periclinal chimeras. American Journal of Botany, 62(9):935–947.

[306] Strzalka, W. K., Aggarwal, C., Krzeszowiec, W., Jakubowska, A., Sztatelman, O., and Banas, A. K. (2015). Arabidopsis pcnas form complexes with selected d-type cyclins. Frontiers in plant science, 6:516.

[307] Su, D., Yang, L., Shi, X., Ma, X., Zhou, X., Hedges, S. B., and Zhong, B. (2021). Large-scale phylogenomic analyses reveal the monophyly of bryophytes and neoproterozoic origin of land plants. Molecular Biology and Evolution.

[308] Sugano, S. S., Shirakawa, M., Takagi, J., Matsuda, Y., Shimada, T., Hara-Nishimura, I., and Kohchi, T. (2014). Crispr/cas9-mediated targeted mutagenesis in the liverwort marchantia polymorpha l. Plant and Cell Physiology, 55(3):475–481.

[309] Svensson, V. (2020). Droplet scrna-seq is not zero-inflated. Nature Biotechnology, 38(2):147–150.

[310] Svensson, V., Vento-Tormo, R., and Teichmann, S. A. (2018). Exponential scaling of single-cell rna-seq in the past decade. Nature protocols, 13(4):599–604.

[311] Svitashev, S., Schwartz, C., Lenderts, B., Young, J. K., and Cigan, A. M. (2016). Genome editing in maize directed by crispr–cas9 ribonucleoprotein complexes. Nature communications, 7(1):1–7.

[312] Svolacchia, N., Salvi, E., and Sabatini, S. (2020). Arabidopsis primary root growth: let it grow, can't hold it back anymore! Current Opinion in Plant Biology, 57:133–141.

[313] Szemenyei, H., Hannon, M., and Long, J. A. (2008). Topless mediates auxin-dependent transcriptional repression during arabidopsis embryogenesis. Science, 319(5868):1384–1386.

[314] Takahashi, G., Betsuyaku, S., Okuzumi, N., Kiyosue, T., and Hirakawa, Y. (2021). An evolutionarily conserved coreceptor gene is essential for clavata signaling in marchantia polymorpha. Frontiers in plant science, 12:624.

[315] Tanaka, D., Ishizaki, K., Kohchi, T., and Yamato, K. T. (2016a). Cryopreservation of gemmae from the liverwort marchantia polymorpha l. Plant and Cell Physiology, 57(2):300–306.

[316] Tanaka, M., Esaki, T., Kenmoku, H., Koeduka, T., Kiyoyama, Y., Masujima, T., Asakawa, Y., and Matsui, K. (2016b). Direct evidence of specific localization of sesquiterpenes and marchantin a in oil body cells of marchantia polymorpha l. Phytochemistry, 130:77–84.

[317] Tang, F., Barbacioru, C., Wang, Y., Nordman, E., Lee, C., Xu, N., Wang, X., Bodeau, J., Tuch, B. B., Siddiqui, A., et al. (2009). mrna-seq whole-transcriptome analysis of a single cell. Nature methods, 6(5):377–382.

[318] Teague, B. P., Guye, P., and Weiss, R. (2016). Synthetic morphogenesis. Cold Spring Harbor perspectives in biology, 8(9):a023929.

[319] ten Hove, C. A., Lu, K.-J., and Weijers, D. (2015). Building a plant: cell fate specification in the early arabidopsis embryo. Development, 142(3):420–430.

[320] Thelander, M., Landberg, K., and Sundberg, E. (2019). Minimal auxin sensing levels in vegetative moss stem cells revealed by a ratiometric reporter. New Phytologist, 224(2):775–788.

[321] Thimann, K. V. and Skoog, F. (1933). Studies on the growth hormone of plants: Iii. the inhibiting action of the growth substance on bud development. Proceedings of the National Academy of Sciences of the United States of America, 19(7):714.

[322] Tian, C., Du, Q., Xu, M., Du, F., and Jiao, Y. (2020a). Single-nucleus rna-seq resolves spatiotemporal developmental trajectories in the tomato shoot apex. bioRxiv.

[323] Tian, F., Yang, D.-C., Meng, Y.-Q., Jin, J., and Gao, G. (2020b). Plantregmap: charting functional regulatory maps in plants. Nucleic acids research, 48(D1):D1104–D1113.

[324] Toledo-Ortiz, G., Johansson, H., Lee, K. P., Bou-Torrent, J., Stewart, K., Steel, G., Rodríguez-Concepción, M., and Halliday, K. J. (2014). The hy5-pif regulatory module coordinates light and temperature control of photosynthetic gene transcription. PLoS genetics, 10(6):e1004416.

[325] Tomaselli, M. (2021). Cell markers for air chamber development in Marchantia polymorpha. PhD thesis, University of Cambridge.

[326] Traag, V. A., Waltman, L., and Van Eck, N. J. (2019). From louvain to leiden: guaranteeing well-connected communities. Scientific reports, 9(1):1–12.

[327] Tsuboyama, S. and Kodama, Y. (2014). Agartrap: a simplified agrobacterium-mediated transformation method for sporelings of the liverwort marchantia polymorpha l. Plant and Cell Physiology, 55(1):229–236.

[328] Tsuboyama-Tanaka, S. and Kodama, Y. (2015). Agartrap-mediated genetic transformation using intact gemmae/gemmalings of the liverwort marchantia polymorpha l. Journal of plant research, 128(2):337–344.

[329] Ulmasov, T., Murfett, J., Hagen, G., and Guilfoyle, T. J. (1997). Aux/iaa proteins repress expression of reporter genes containing natural and highly active synthetic auxin response elements. The Plant Cell, 9(11):1963–1971.

[330] Van den Berg, C., Willemsen, V., Hage, W., Weisbeek, P., and Scheres, B. (1995). Cell fate in the arabidopsis root meristem determined by directional signalling. Nature, 378(6552):62–65.

[331] Vernoux, T., Kronenberger, J., Grandjean, O., Laufs, P., and Traas, J. (2000). Pin-formed 1 regulates cell fate at the periphery of the shoot apical meristem. Development, 127(23):5157–5165.

[332] Viaene, T., Landberg, K., Thelander, M., Medvecka, E., Pederson, E., Feraru, E., Cooper, E. D., Karimi, M., Delwiche, C. F., Ljung, K., et al. (2014). Directional auxin transport mechanisms in early diverging land plants. Current Biology, 24(23):2786–2791.

[333] von Schwartzenberg, K., Lindner, A.-C., Gruhn, N., Šimura, J., Novák, O., Strnad, M., Gonneau, M., Nogué, F., and Heyl, A. (2016). Chase domain-containing receptors play an essential role in the cytokinin response of the moss physcomitrella patens. Journal of experimental botany, 67(3):667–679.

[334] Vöchting, H. (1885). Über die regeneration der marchantieen. Jahrbücher für wissenschaftliche Botanik, 16:367–414.

[335] Wang, Y., Huan, Q., Li, K., and Qian, W. (2021a). Single-cell transcriptome atlas of the leaf and root of rice seedlings. Journal of Genetics and Genomics.

[336] Wang, Z., Cheng, D., Fan, C., Zhang, C., Zhang, C., and Liu, Z. (2021b). Cell type-specific differentiation between indica and japonica rice root tip responses to different environments based on single-cell rna sequencing. Frontiers in Genetics, 12:635.

[337] Wang, Z.-Y., Nakano, T., Gendron, J., He, J., Chen, M., Vafeados, D., Yang, Y., Fujioka, S., Yoshida, S., Asami, T., et al. (2002). Nuclear-localized bzr1 mediates brassinosteroid-induced growth and feedback suppression of brassinosteroid biosynthesis. Developmental cell, 2(4):505–513.

[338] Weijers, D., Schlereth, A., Ehrismann, J. S., Schwank, G., Kientz, M., and Jürgens, G. (2006). Auxin triggers transient local signaling for cell specification in arabidopsis embryogenesis. Developmental cell, 10(2):265–270.

[339] Weimer, A. K., Matos, J. L., Sharma, N., Patell, F., Murray, J. A., Dewitte, W., and Bergmann, D. C. (2018). Lineage-and stage-specific expressed cycd7; 1 coordinates the single symmetric division that creates stomatal guard cells. Development, 145(6):dev160671.

[340] Wendrich, J. R., Möller, B. K., Li, S., Saiga, S., Sozzani, R., Benfey, P. N., De Rybel, B., and Weijers, D. (2017). Framework for gradual progression of cell ontogeny in the arabidopsis root meristem. Proceedings of the National Academy of Sciences, 114(42):E8922–E8929.

[341] Werner, T., Motyka, V., Laucou, V., Smets, R., Van Onckelen, H., and Schmulling, T. (2003). Cytokinin-deficient transgenic arabidopsis plants show multiple developmental alterations indicating opposite functions of cytokinins in the regulation of shoot and root meristem activity. The Plant Cell, 15(11):2532–2550.

[342] Whitewoods, C. D., Cammarata, J., Venza, Z. N., Sang, S., Crook, A. D., Aoyama, T., Wang, X. Y., Waller, M., Kamisugi, Y., Cuming, A. C., et al. (2018). Clavata was a genetic novelty for the morphological innovation of 3d growth in land plants. Current Biology, 28(15):2365–2376.

[343] Wilhelmsson, P. K., Mühlich, C., Ullrich, K. K., and Rensing, S. A. (2017). Comprehensive genome-wide classification reveals that many plant-specific transcription factors evolved in streptophyte algae. Genome Biology and Evolution, 9(12):3384–3397.

[344] Wolf, F. A., Angerer, P., and Theis, F. J. (2018). Scanpy: large-scale single-cell gene expression data analysis. Genome biology, 19(1):1–5.

[345] Wu, M.-F., Yamaguchi, N., Xiao, J., Bargmann, B., Estelle, M., Sang, Y., and Wagner, D. (2015). Auxin-regulated chromatin switch directs acquisition of flower primordium founder fate. Elife, 4:e09269.

[346] Xie, Y., Jiang, S., Li, L., Yu, X., Wang, Y., Luo, C., Cai, Q., He, W., Xie, H., Zheng, Y., et al. (2020). Single-cell rna sequencing efficiently predicts transcription factor targets in plants. Frontiers in plant science, 11:1946.

[347] Xu, D. (2020). Cop1 and bbxs-hy5-mediated light signal transduction in plants. New Phytologist, 228(6):1748–1753.

[348] Xu, J., Hofhuis, H., Heidstra, R., Sauer, M., Friml, J., and Scheres, B. (2006). A molecular framework for plant regeneration. Science, 311(5759):385–388.

[349] Xu, X., Crow, M., Rice, B. R., Li, F., Harris, B., Liu, L., Demesa-Arevalo, E., Lu, Z., Wang, L., Fox, N., et al. (2021). Single-cell rna sequencing of developing maize ears facilitates functional analysis and trait candidate gene discovery. Developmental cell, 56(4):557–568.

[350] Yadav, R. K., Perales, M., Gruel, J., Girke, T., Jönsson, H., and Reddy, G. V. (2011). Wuschel protein movement mediates stem cell homeostasis in the arabidopsis shoot apex. Genes & development, 25(19):2025–2030.

[351] Yamaoka, S., Nishihama, R., Yoshitake, Y., Ishida, S., Inoue, K., Saito, M., Okahashi, K., Bao, H., Nishida, H., Yamaguchi, K., et al. (2018). Generative cell specification requires transcription factors evolutionarily conserved in land plants. Current Biology, 28(3):479–486.

[352] Yanai, O., Shani, E., Dolezal, K., Tarkowski, P., Sablowski, R., Sandberg, G., Samach, A., and Ori, N. (2005). Arabidopsis knoxi proteins activate cytokinin biosynthesis. Current Biology, 15(17):1566–1571.

[353] Yang, W., Cortijo, S., Korsbo, N., Roszak, P., Schiessl, K., Gurzadyan, A., Wightman, R., Jönsson, H., and Meyerowitz, E. (2021). Molecular mechanism of cytokinin-activated cell division in arabidopsis. Science, 371(6536):1350–1355.

[354] Yasui, Y., Tsukamoto, S., Sugaya, T., Nishihama, R., Wang, Q., Kato, H., Yamato, K. T., Fukaki, H., Mimura, T., Kubo, H., et al. (2019). Gemma cup-associated myb1, an ortholog of axillary meristem regulators, is essential in vegetative reproduction in marchantia polymorpha. Current Biology, 29(23):3987–3995.

[355] Yin, Y., Wang, Z.-Y., Mora-Garcia, S., Li, J., Yoshida, S., Asami, T., and Chory, J. (2002). Bes1 accumulates in the nucleus in response to brassinosteroids to regulate gene expression and promote stem elongation. Cell, 109(2):181–191.

[356] Zhai, H., Zhang, X., You, Y., Lin, L., Zhou, W., and Li, C. (2020). Seuss integrates transcriptional and epigenetic control of root stem cell organizer specification. The EMBO journal, 39(20):e105047.

[357] Zhai, N. and Xu, L. (2021). Pluripotency acquisition in the middle cell layer of callus is required for organ regeneration. Nature Plants, 7(11):1453–1460.

[358] Zhang, J., Fu, X.-X., Li, R.-Q., Zhao, X., Liu, Y., Li, M.-H., Zwaenepoel, A., Ma, H., Goffinet, B., Guan, Y.-L., et al. (2020a). The hornwort genome and early land plant evolution. Nature plants, 6(2):107–118.

[359] Zhang, L., Li, T., Su, S., Peng, H., Li, S., Li, K., Ji, L., Xing, Y., Zhang, J., Du, X., et al. (2021a). Functions of cop1/spa e3 ubiquitin ligase mediated by mpcry in the liverwort marchantia polymorpha under blue light. International journal of molecular sciences, 23(1):158.

[360] Zhang, M. J., Ntranos, V., and Tse, D. (2020b). Determining sequencing depth in a single-cell rna-seq experiment. Nature communications, 11(1):1–11.

[361] Zhang, T.-Q., Chen, Y., Liu, Y., Lin, W.-H., and Wang, J.-W. (2021b). Single-cell transcriptome atlas and chromatin accessibility landscape reveal differentiation trajectories in the rice root. Nature communications, 12(1):1–12.

[362] Zhang, T.-Q., Xu, Z.-G., Shang, G.-D., and Wang, J.-W. (2019). A single-cell rna sequencing profiles the developmental landscape of arabidopsis root. Molecular plant, 12(5):648–660.

[363] Zhang, Y., Hartinger, C., Wang, X., and Friml, J. (2020c). Directional auxin fluxes in plants by intramolecular domain–domain coevolution of pin auxin transporters. New Phytologist, 227(5):1406–1416.

[364] Zhang, Y., Jiao, Y., Jiao, H., Zhao, H., and Zhu, Y.-X. (2017a). Two-step functional innovation of the stem-cell factors wus/wox5 during plant evolution. Molecular biology and evolution, 34(3):640–653.

[365] Zhang, Z., Tucker, E., Hermann, M., and Laux, T. (2017b). A molecular framework for the embryonic initiation of shoot meristem stem cells. Developmental Cell, 40(3):264–277.

[366] Zhao, Y., Christensen, S. K., Fankhauser, C., Cashman, J. R., Cohen, J. D., Weigel, D., and Chory, J. (2001). A role for flavin monooxygenase-like enzymes in auxin biosynthesis. Science, 291(5502):306–309.

[367] Zhao, Z., Andersen, S. U., Ljung, K., Dolezal, K., Miotk, A., Schultheiss, S. J., and Lohmann, J. U. (2010). Hormonal control of the shoot stem-cell niche. Nature, 465(7301):1089–1092.

[368] Zheng, G. X., Terry, J. M., Belgrader, P., Ryvkin, P., Bent, Z. W., Wilson, R., Ziraldo, S. B., Wheeler, T. D., McDermott, G. P., Zhu, J., et al. (2017). Massively parallel digital transcriptional profiling of single cells. Nature communications, 8(1):1–12.

[369] Zhou, Y., Liu, X., Engstrom, E. M., Nimchuk, Z. L., Pruneda-Paz, J. L., Tarr, P. T., Yan, A., Kay, S. A., and Meyerowitz, E. M. (2015). Control of plant stem cell function by conserved interacting transcriptional regulators. Nature, 517(7534):377–380.

[370] Zhou, Y., Yan, A., Han, H., Li, T., Geng, Y., Liu, X., and Meyerowitz, E. M. (2018). Hairy meristem with wuschel confines clavata3 expression to the outer apical meristem layers. Science, 361(6401):502–506.

[371] Zhu, L., Bu, Q., Xu, X., Paik, I., Huang, X., Hoecker, U., Deng, X. W., and Huq, E. (2015). Cul4 forms an e3 ligase with cop1 and spa to promote light-induced degradation of pif1. Nature communications, 6(1):1–10.

[372] Zürcher, E., Tavor-Deslex, D., Lituiev, D., Enkerli, K., Tarr, P. T., and Müller, B. (2013). A robust and sensitive synthetic sensor to monitor the transcriptional output of the cytokinin signaling network in planta. Plant physiology, 161(3):1066–1075.

Appendix A

List of plasmids

Table A.1 List of L2 plasmids

Figure	Plasmid_ID	Description
3.3	L2_1068	p5-35S-BP:HygR2, p5-MpWOX:mVenus-N7, p5-o941:mTurq-N7, p5-o941:mScar-Lti6b
3.3	L2_328	35SBP:HygR2, p5-MpAPB::mVen-N7, o941:mScar-Lti6b,
3.3	L2_1031	35S-BP:HygR2, p5-MpGRAS1:mVen-N7, Tuba:mTurq-N7, 35S-BP:eGFP-Lti6b
3.4	L2_1009	35S-BP-HygR, p5_MpBHLH42:mVenus-N7, MpTuba:mTur-N7, 35S-BP-eGFP-Lti6b
3.4	L2_1052	35S-BP:HygR2, p5-MpBZR1:mVen-N7, Tuba:mTurq-N7, 35S-BP:eGFP-Lti6b
3.4	L2_1057	35S-BP:HygR2, p5-MpWRKY11:mVen-N7, Tuba:mTurq-N7, 35S-BP:eGFP-Lti6b
3.4	L2_1000	35S-BP-HygR, p5_MpBHLH29:mVenus-N7, MpTuba:mTur-N7, 35S-BP-eGFP-Lti6b
3.5	L2_1041	35S-BP-HygR, p5_MpNAC1:mVenus-N7, MpTuba:mTur-N7, 35S-BP-eGFP-Lti6b
3.5	L2_1008	35S-BP-HygR, p5_MpBHLH13:mVenus-N7, MpTuba:mTur-N7, 35S-BP-eGFP-Lti6b
3.6	L2_1055	35S-BP-HygR, p5_MpASLBD24:mVenus-N7, MpTuba:mTur-N7, 35S-BP-eGFP-Lti6b
3.6	L2_1042	35S-BP-HygR, p5_MpNAC4:mVenus-N7, MpTuba:mTur-N7, 35S-BP-eGFP-Lti6b
3.6, 4.6	L2_1064	35S-BP-HygR, p5_MpNAC2:mVenus-N7, MpNOP1:mTur-N7, 35S-BP-eGFP-Lti6b
4.3	L2_337	35SBP:HygR2, o941:eGFP-Lti6b, p5-Mp8g17780:mVen-N7, p5-Mp3g20570:mTurq2-N7, p5-Mp4g01930:mScar-N7
4.3	L2_338	35SBP:HygR2, o941:eGFP-Lti6b, p5-Mp8g13430:mVen-N7, p5-Mp4g09230:mTurq2-N7, p5-Mp2g25940:mScar-N7
4.3	L2_341	35SBP:HygR2, o941:eGFP-Lti6b, p5-MpCKX1:mVenus-N7, p5-Mp3g20970-AntiTA:mTurq2-N7, p5-Mp2g25940-TA:mScar-N7
4.4	L2_342	35SBP:HygR2, o941:eGFP-Lti6b, p5-Mp1g15580-Dors:mVen-N7, p5-Mp4g17680-unkn:mTurq2-N7, p5-Mp3g11280-Vent:mScar-N7
4.6	L2_266	35SBP:HygR2, p5-Mapoly0137s0020:mVen-N7, p5-o941:mScar-N7, o941:eGFP-Lti6b
4.6	L2_1023	35S-BP-HygR, p5_MpRSL2:mVenus-N7, MpTuba:mTur-N7, 35S-BP-eGFP-Lti6b
5.2A	L2_289	35SBP:HygR2, o941:DII-mVen-N7, p5-YUC2(2kb)::mScar-N7, p5-PIN1:PIN1-eGFP
5.2B, 5.6A	L2_295	35S:HygR, p5-ERF20:mVen-N7, p5-YUC2(5.5kb):mTurq-N7, p5-o941:mScar-Lti6b
5.2C-D, 7.5B, 7.6, 7.8C	L2_283	35SBP:HygR2, p5-YUC2(5.5kb):mVen-N7, o941:mScar-lti6b, p5-PIN1:PIN1-eGFP
5.3A, 7.1, 7.2, 7.3	L2_267	35SBP:HygR2, o941:eGFP-Lti6b, p5-GH3:mVen-N7, p5-DR5v2:mScar-N7, p5-PIN1:mTurq2
5.3B-C, 7.8A-B	L2_268	35SBP:HygR2, p5-PIN1:GAL4-VP16, p5-UAS-GAL4:mVen-N7, o941:eGFP-Lti6b
5.4	L2_270	35SBP:HygR2, p5-DR5v2_MR:GAL4-VP16, p5-UAS-GAL4:mVen-N7, o941:eGFP-Lti6b
5.5, 7.7	L2_225	35S-BP-HygR, p5-ARF1:mVenus-N7, p5-p5-ARF3:mTurq2-N7, p5-MpARF2:mScarlet-N7
5.6B-D, 5.9A, 7.5A, 7.5C	L2_324	35SBP:HygR2, o941:mScar-Lti6b, p5-ERF20:GAL4-VP16, p5-UAS-GAL4:mVen-N7, p5-MpYUC2(5.5kb):Turq2-N7
5.7A-B, 6.6A	L2_758	35SBP:HygR2, o941:mScar-Lti6b, p5-MpHSP18.7:GAL4-VP16-GR, p5-UAS-GAL4:mVen-N7, p5-MpYUC2(5.5kb):Turq2-N7
5.7C-D	L2_759	35SBP:HygR2, o941:mScar-Lti6b, p5-SN-MpYUC2:GAL4-VP16-GR, p5-UAS-GAL4:mVen-N7, p5-Mapoly0048s0099:Turq2-N7
5.8A-B	L2_347	35SBP:HygR2, o941:mScar-Lti6b, p5-MpHSP18.7:GAL4-VP16, p5-UAS-GAL4:CDS-ERF20-mVen, p5-MpYUC2(5.5kb):Turq2-N7
5.8C-D, 5.9B-C	L2_754	35SBP:HygR2, o941:mScar-Lti6b, p5-MpYUC2(5.5kb):GAL4-VP16-GR, p5-UAS-GAL4:CDS-MpERF20-mVen, p5-Mapoly0048s0099:Turq2-N7
6.2A	L2_334	35SBP:HygR2, p5_MpIPT2:GAL4-VP16, p5-UAS-GAL4:mVen-N7, o941:mScar-Lti6b
6.2B	L2_331	35SBP:HygR2, p5-MpCKX1:mVenus-N7, p5-UBE2-o941:mTurq-Lti6b, p5-MpCKX2:mScar-N7
6.2C	L2_333	35SBP:HygR2, p5-MpCHK1:mVenus-N7, p5-UBE2-o941:mTurq-Lti6b, p5-MpCHK2:mScar-N7
6.5, 6.7A-B, 7.4	L2_329	35SBP:HygR2, p5-CYCD;1:mVenus-N7, p5-UBE2-o941:mTurq-Lti6b, p5-CYCD;2:mScar-N7
6.6B-D	L2_345	35SBP:HygR2, o941:mScar-Lti6b, p5-MpHSP18.7:GAL4-VP16, p5-UAS-GAL4:CDS-MpCYCD;1-mVen, p5-MpYUC2(5.5kb):Turq2-N7
6.7C-D	L2_788	35SBP:HygR2, p5-CYCD;2:GAL4-VP16, p5-UAS-GAL4;mVen-N7, o941;mScar-Lti6b
6.7E	L2_346	35SBP:HygR2, o941:mScar-Lti6b, p5-MpHSP18.7:GAL4-VP16, p5-UAS-GAL4:CDS-MpCYCD;2-mVen, p5-MpYUC2(5.5.kb):Turq2-N7
6.8	L2_766	35SBP:HygR2, p5-Mp3R-MYB1:GAL4-VP16, p5-UAS-GAL4:mVen-N7, o941:mScar-Lti6b